Universitat Autònoma de Barcelona

Oxidoreductive bioprocess intensification through reaction engineering and enzyme immobilization

Jordi Solé Ferré

ADVERTIMENT. L'accés als continguts d'aquesta tesi queda condicionat a l'acceptació de les condicions d'ús establertes per la següent llicència Creative Commons: http://cat.creativecommons.org/?page id=184

ADVERTENCIA. El acceso a los contenidos de esta tesis queda condicionado a la aceptación de las condiciones de uso establecidas por la siguiente licencia Creative Commons: http://es.creativecommons.org/blog/licencias/

WARNING. The access to the contents of this doctoral thesis it is limited to the acceptance of the use conditions set by the following Creative Commons license: https://creativecommons.org/licenses/?lang=en

Universitat Autònoma de Barcelona

Escola d’Enginyeria

Departament d’Enginyeria Química, Biològica i Ambiental

Oxidoreductive bioprocess intensification through reaction engineering and enzyme immobilization

Memòria per optar al grau de Doctor Internacional per la Universitat Autònoma de Barcelona, sota la dirección de la Dra. Marina Guillén Montalbán i Dra. Glòria Caminal Saperas

per

Jordi Solé Ferré

Bellaterra, Octubre 2019

La Dra. Marina Guillén Montalbán, professora del Departament d'Enginyeria Química, Biològica i Ambiental de la Universitat Autònoma de Barcelona i la Dra. Glòria Caminal Saperas, investigadora científica de l'Institut de Química Avançada de Catalunya (IQAC) i professora del Departament d'Enginyeria Química, Biològica i Ambiental de la Universitat Autònoma de Barcelona,

Certifiquem:

Que el graduat en Biotecnologia Jordi Solé Ferré ha dut a terme al Departament d'Enginyeria Química, Biològica i Ambiental de la Universitat Autònoma de Barcelona i sota la nostra dirección, la tesi doctoral titulada **Oxidoreductive bioprocess intensification through reaction engineering and enzyme immobilization**. La mateixa, es presenta en aquesta memòria i constitueix el manuscrit per optar al Grau de Doctor en Biotecnologia per la Universitat Autònoma de Barcelona.

I per tal que se'n prengui coneixement i consti als efectes oportuns, signem la present declaració a Bellaterra, a 25 de juliol de 2019.

Jordi Solé Ferré Dra. Marina Guillén Montalbán Dra. Glòria Caminal Saperas

Resum

La investigació plasmada en aquesta tesi doctoral tracta l'aplicació dels principis d'enginyeria de reacció i immobilització enzimàtica per a la millora de reaccions d'oxidoreducció biocatalitzades.

Els enzims, com a catalitzadors naturals, ofereixen una sèrie d'avantatges sobre les rutes químiques clàssiques com: l'acceptació d'un únic substrat (especificitat), la producció exclusiva d'un sol producte (selectivitat) i la capacitat de treballar en condicions suaus tant de temperatura, de pressió i/o de reactius. Un cop demostrada l'eficàcia d'un enzim per a una reacció, s'ha de demostrar que aquest és realment rentable, és a dir, s'ha d'intentar portar la reacció fins a les més òptimes condicions. Per a això, s'han d'eliminar els factors limitants de la mateixa i es poden utilitzar tècniques com la immobilització, per millorar les prestacions del biocatalitzador.

En una primera part de la tesi, es va estudiar la co-immobilització de la monooxigenasa P450 BM3 juntament amb un enzim regenerador del cofactor NADPH, la glucosa deshidrogenasa (GDH-Tac). Els millors derivats es van obtenir utilitzant dos suports d'agarosa, un funcionalitzat amb grups epoxy (83% i 20% activitats retingudes respectivament) i l'altre amb grups amino (28% i 25% activitats retingudes respectivament). Posteriorment es va provar de re-utilitzar aquests enzims immobilitzats en diferents cicles de reacció utilitzant un dels substrats naturals de la P450 BM3, el laurat de sodi.

Un cop demostrat que ambdós enzims immobilitzats podien ser reciclats, es va estudiar l'aplicació d'aquests en dues reaccions d'interès industrial, la hidroxilació de la α-isoforona i la hidroxilació del diclofenac. En el primer cas, va fer falta optimitzar certs paràmetres de la reacció abans d'aplicar els derivats. Un cop es van tenir unes condicions acceptables, es va comprovar que els resultats obtinguts anteriorment amb el laurat de sodi, no podien ser extrapolats. La reutilització no va ser possible. En quant al diclofenac, es van obtenir resultats similars. En ambdós casos però, l'aplicació dels enzims en la seva forma soluble, va permetre obtenir conversions altes: 86.2% per a la α-isoforona (50 mM inicial) i 100% per al diclofenac (3.5 mM inicial).

El producte hidroxilat de l'α-isoforona, la 4-hidroxi-isoforona, ha de ser oxidat en un segon pas per arribar a l'intermediari desitjat, la keto-isoforona. Aquesta segona reacció es duu a terme amb una alcohol deshidrogenasa, la qual també necessita un regenerador de cofactor, la NADPH oxidasa. Al aplicar els dos enzims en la seva forma soluble, al cap de 24h, es va aconseguir un 95.7% de rendiment i una productivitat de 6.52 g L^{-1} dia^{-1}. A part, l'enzim diana, l'alcohol

deshidrogenasa, es va poder immobilitzar en epoxy-agarosa obtenint una activitat retinguda del 58.2%. Al intentar re-utilitzar-lo, es va poder operar durant 96h (4 cicles) millorant el rendiment del biocatalitzador fins a 2.5 vegades comparat amb la reacció en soluble.

La reacció d'hidrogenació de la α-isoforona, per altre banda, resulta en la 3,3,5-trimetilciclohexanona, un substrat amb interès industrial per a l'obtenció de polímers. En aquest cas, es va utilitzar la Baeyer-Villiger ciclohexanona monooxigenasa juntament amb una glucosa deshidrogenasa comercial (GDH-01) per a realitzar la reacció d'inserció d'un àtom d'oxigen en l'anell de carbonis. Es van optimitzar diferents paràmetres de la reacció com la formulació del biocatalitzador, la velocitat d'adició de substrat i la quantitat d'enzim afegida. Un cop optimitzada la reacció es va escalar primer a 1 litre i finalment a 100 litres. En aquesta última reacció a escala pre-industrial, es va obtenir una conversió del 85%, una productivitat de 2.7 g L^{-1} h^{-1} i un rendiment del biocatalitzador de 0.83 g g^{-1}_{cww}.

Finalment aquesta mateixa reacció es va realitzar utilitzant els enzims immobilitzats i reciclant-os. Tant la ciclohexanona monooxigenasa com la glucosa deshidrogenasa (GDH-01) es van poder immobilitzar en agarosa funcionalitzada amb grups amino. En el primer cas es va obtenir una activitat retinguda del 62.4% (mètode obtingut de la bibliografia) i en el segon cas del 62.6%. En reacció, els dos enzims immobilitzats van ser utilitzats tant per separat com conjuntament. Al cap de sis cicles de reacció (132.5 mM de substrat inicial), es va assolir un rendiment de biocatalitzador 3.6 vegades superior per a la monooxigenasa i 1.9 vegades superior per a la GDH-01 comparat amb la reacció en soluble.

En definitiva, es pot afirmar que aquesta tesi ha servit per oferir nous mecanismes d'immobilització de les oxidoreductases estudiades així com noves condicions optimitzades per a realitzar les reaccions dianes. En el cas de la 3,3,5-trimetilciclohexanona, el treball realitzat ha arribat a superar els objectius marcats pel projecte i per tant, es valora la seva producció industrial per part de les empreses interessades.

Abstract

The research performed and disclosed in this thesis deals with the reaction engineering and the enzyme immobilization principles as tools to improve biocatalyzed oxidoreductive reactions.

The enzymes, considered “natural catalysts”, confer some advantages over tradition chemical routes: specificity for a single substrate, selectivity for one target reaction and the intrinsic property to perform in mild conditions in terms of temperature, pressure and/or harsh reagents. Once an enzyme is selected to catalyze a desired reaction, the conditions must be optimized in order to prove its potential profitability. Furthermore, enzyme immobilization can serve as a powerful tool to improve the biocatalyst capabilities.

On a first stage, the co-immobilization of the P450 BM3 monooxygenase together with a NADPH cofactor regeneration enzyme, the glucose dehydrogenase (GDH-Tac), was studied. The best derivates were obtained when using two agarose supports, an epoxy functionalized (83% and 20% retained activity respectively) and an amino functionalized (28% and 25% retained activity respectively). Later on, the re-cycling of the immobilized enzymes was tested in reaction cycles using one of the natural substrates of the P450 BM3, the sodium laurate.

Once it could be demonstrated that re-cycling of both P450 BM3 and GDH-Tac was possible, both enzymes were studied in two of the project’s target reactions, the hydroxylation of α-isophorone and the hydroxylation of diclofenac. In the first case, the optimization of the reaction conditions had to be performed prior to the reaction cycles. The reactor configuration, the oxygen income or the glucose concentration were adjusted. However, when the reaction was performed using the co-immobilized enzymes, the P450 BM3 was deactivated and it could not be re-used. The same happened with the hydroxylation of diclofenac. On the other hand, the reaction using soluble enzymes, resulted in 86.2% conversion for the α-isophorone (50 mM initial concentration) and 100% for the diclofenac (3.5 mM initial concentration).

The product resulting from the hydroxylation of α-isophorone, the 4-hydroxy-isophorone, can be further oxidized to keto-isophorone, an intermediary for the synthesis of carotenoids and vitamin E. In order to enzymatically perform this step, an alcohol dehydrogenase and a NADPH oxidase, as a cofactor regenerator, were employed. When used in their soluble form, after 24 hours, 95.7% yield and a space time yield of 6.52 g L^{-1} day^{-1} were achieved. Moreover, the alcohol dehydrogenase was immobilized on epoxy-agarose and 58.2% retained activity was obtained. When re-used, the derivate could operate for 96h (4 cycles) improving the biocatalyst yield 2.5-fold compared with the reaction with soluble enzymes.

The hydrogenation of α-isophorone results in 3,3,5-trimethylcyclohexanone, an industrial interesting substrate due to the polymers that can be obtained from its oxidized product, the trimethyl-ε-caprolactone. This compound is obtained by the Baeyer-Villiger insertion of an oxygen atom into the carbon ring. For this purpose, a cyclohexanone monooxygenase together with a commercial glucose dehydrogenase (GDH-01) were used. Different parameters of the reaction were optimized such as the biocatalyst formulation, the substrate addition rate or the biocatalyst loading. Afterwards, the reaction was scaled up to 1 liter first and then up to 100 liters. In this last pre-industrial reaction, 85% conversion, a space time yield of 2.7 g L^{-1} h^{-1} and a biocatalyst yield of 0.83 g g^{-1}_{cww} could be obtained.

Finally, this same reaction was performed using both enzymes immobilized and re-cycling was intended. The cyclohexanone monooxygenase could be immobilized following a previously described method and 62.4% retained activity was achieved. In the GDH-01 case, different supports were screened albeit at the end, it was also the amino functionalized agarose that resulted successful. A retained activity of 62.6% was obtained. In the reaction cycles, the immobilized enzymes were used either separately or both together. In the best case scenario, after six cycles of reaction (132.5 mM initial substrate) 3.6-fold and 1.9-fold higher biocatalysts yields were obtained for the monooxygenase and the GDH-01, respectively.

As a conclusion, this thesis has served to broaden the enzyme immobilization portfolio and it has conferred new optimized conditions to perform oxidoreductive reactions. In the case of the 3,3,5-trimethylcyclohexanone, the results reported have exceeded the target metrics set by the project partners. Its implementation at industrial scale is feasible.

Abbreviations

$[S]_0$: initial substrate concentration

µSCALE: micro-capillary single-cell analysis and laser extraction

ADH: alcohol dehydrogenase

ADHaa: alcohol dehydrogenase from *Artemisia annua*

AOX: alcohol oxidase

API: active pharmaceutical ingredient

BSA: bovine serum albumin

BVMO: Baeyer-Villiger monooxygenase

CAGR: compound annual growth rate

CFE: cell free extract

CHL: trimethyl-ε-caprolactone

CHMO: cyclohexanone monooxygenase

CLEA: cross-linked enzyme aggregate

Cww: cell wet weight

CYP: cytochrome P450

DIF: diclofenac

DOE: design of experiment

DSP: downstream processing

E. coli*: Escherichia coli*

EC: Enzyme Commission

EC: extraction coefficient

EDC: *N*-(3-dimethylaminopropyl)-*N*′-ethylcarbodiimide

FAD^+: flavin adenine dinucleotide oxidized form

FMN: flavin mononucleotide

GC: gas chromatograph

GC-FID: gas cromatograph equipped with a flame ionization detector

GDH: glucose dehydrogenase

GDH-01: commercial glucose dehydrogenase from InnoSyn B.V.

GDH-105: commercial glucose dehydrogenase from Codexis

GDH-Tac: glucose dehydrogenase from *Thermoplasma acidophilus*

Glu: D-(+)-glucose

HDI: 4′/5′-hydroxy-diclofenac

HID: 4-hydroxy-isophorone

HPLC: high performance liquid chromatograph

HPLC-RID: high performance liquid chromatograph equipped with a refractive index detector

HPLC-UV: high performance liquid chromatograph equipped with a ultra-violet detector

IS: internal standard

ISO: α-isophorone

IUBMB: Union of Biochemistry and Molecular Biology

IUPAC: Union for Pure and Applied Chemistry

IY: immobilization yield

KET: keto-isophorone

KPi: potassium phosphate buffer

LB: Luria-Bertani medium

LF: liquid formulation

Mana: monoaminoethyl-*N*-aminoethyl

NAD$^+$: nicotinamide adenine dinucleotide oxidated form

NADH: nicotinamide adenine dinucleotide reduced form

NADP$^+$: nicotinamide adenine dinucleotide phosphate oxidated form

NADPH: nicotinamide adenine dinucleotide phosphate reduced form

NaPi: sodium phosphate buffer

NOX: NADPH oxidase

P450: cytochrome P450

P450 BM3: cytochrome P450 from *Bacillus megaterium*

P450 BM3 M22C02: cytochrome P450 from *Bacillus megaterium* mutant M22C02

P450 BM3 WT: cytochrome P450 from Bacillus megaterium wild type

PCR: polymerase chain reaction

RA: retained activity

ROBOX: European Union Project, grant agreement n° 635734. It sands for *"Expanding the industrial use of Robust Oxidative Biocatalysts for the conversion and production of alcohols"*

ROS: reactive oxygen species

SDS-PAGE: sodium dodecyl sulphate polyacrylamide gel electrophoresis

SFPR: substrate feed product removal

STY: space time yield

TB: terrific broth medium

TMCH: 3,3,5-trimethylcyclohexanone

TmCHMO: cyclohexanone monooxygenase from *Thermocrispum municipale*

TTN: total turnover number

U: unit of activity

V_T: total working volume

WC: whole cell formulation

WP: work package

WT: wild type

Contents

Resum 05

Abstract 07

Abbreviations 09

1. Introduction 15
    - 1.1 General aspects: 15
        - 1.1.1 Principles of biocatalysis 15
        - 1.1.2 History of industrial bio-transformations 15
        - 1.1.3 Enzyme classification 17
            - 1.1.3.1 Oxidoreductases 18
        - 1.1.4 Enzyme discovery, engineering and modification 19
    - 1.2 Immobilization 21
        - 1.2.1 Support features and considerations 22
        - 1.2.2 Immobilization methods 22
    - 1.3 Bioprocess design and engineering 24
        - 1.3.1 Process aims 24
        - 1.3.2 Catalyst characteristics 25
        - 1.3.3 Reaction engineering 25
        - 1.3.4 Reactor design 26
        - 1.3.5 Process implementation 26
    - 1.4 ROBOX project 27
        - 1.4.1 Objectives 28
        - 1.4.2 Target enzymes and reaction of the ROBOX project 29
    - 1.5 Enzymes employed in this thesis 30
    - 1.6 Target reactions of this thesis 30
        - 1.6.1 Hydroxylation of sodium laurate 30
        - 1.6.2 Hydroxylation of α-isophorone 31
        - 1.6.3 Hydroxylation of diclofen 32
        - 1.6.4 Baeyer-Villiger oxidation of 3,3,5-trimethylcyclohexanone ... 32
2. Objectives 35
3. Experimental: Materials & Methods 37
    - 3.1 Materials and supports 37
    - 3.2 Commercial enzymes 38
    - 3.3 Recombinant expression of enzymes 38
    - 3.4 Total protein and enzyme content 39
    - 3.5 Active P450 BM3 determination 40
    - 3.6 Enzyme activity measurements 40
    - 3.7 Summary of the characterized enzymes 42
    - 3.8 Stability studies 43
    - 3.9 Immobilization metrics 43
    - 3.10 Immobilization studies 44

3.11 Oxidoreductive reactions 46
3.12 Reaction progress determination - sampling 54
3.13 Substrates and products analysis 55
3.14 Isolation and purification of trimethyl-ε-caprolactone 56
4 Co-immobilization of P450 BM3 and glucose dehydrogenase on different supports for application as a self-sufficient oxidative biocatalyst 59
4.1 Introduction 61
4.2 Results and discussion 63
4.2.1 Characterization of the *E. coli* lysate containing P450 BM3 and GDH 63
4.2.2 Screening of supports for the immobilization of P450 BM3 – Purolite® 65
4.2.3 Immobilization of P450 BM3 onto different functionalized agaroses 68
4.2.4 Co-immobilization of P450 BM3 and glucose dehydrogenase 71
4.2.5 Co-immobilization of P450 BM3 and GDH into polyvinyl alcohol particles – Entrapment 72
4.2.6 Reusability of the biocatalyst using sodium laurate as substrate 73
4.3 Conclusions 75
5 Process intensification of P450 BM3-mediated reactions of industrial interest: hydroxylation of α-isophorone and diclofenac 77
5.1 Introduction 79
5.2 Results and discussion 80
5.2.1 Hydroxylation of α-isophorone 80
5.2.2 Reaction with low substrate concentration ([S] = 2 mM, V_T = 30 mL) 81
5.2.3 Tackling the mass imbalance 83
5.2.4 Reactions with 10 mM substrate concentration and soluble enzymes (V_T = 5 mL) 84
5.2.5 Reactions with Mana- and epoxy-agarose immobilized enzymes ([S] = 10 mM, V_T = 5 mL) 87
5.2.6 Addition of catalase as hydrogen peroxide scavenger 88
5.2.7 Reactions with 50 mM substrate concentration and soluble enzymes (V_T = 10 mL) 90
5.2.8 Reactions with additional pulses of 5% (v/v) P450 BM4 WT CFE ([S] = 50 mM, V_T = 10 mL) 92
5.2.9 Hydroxylation of diclofenac 94
5.2.10 Immobilization of a P450 BM3 mutant (M22C02) onto Mana-agarose and epoxy-agarose 94
5.2.11 Hydroxylation of diclofenac with P450 BM3 M22C02 ([S] = 3.5 mM, V_T = 5 mL) 96
5.3 Conclusions 98
6 Synthesis of keto-isophorone with an immobilized alcohol dehydrogenase 101

- 6.1 Introduction ... 103
- 6.2 Results and discussion ... 105
  - 6.2.1 Characterization of the cell lysates ... 105
  - 6.2.2 Immobilization of ADHaa onto methacrylate/styrene supports ... 106
  - 6.2.3 Immobilization of ADHaa onto epoxy- and amino functionalized agaroses ... 107
  - 6.2.4 Immobilization of ADHaa on epoxy-agarose-M1 and M2 applying high loads of enzyme ... 110
  - 6.2.5 Oxidation of 4-hydroxy-isophorone to keto-isophorone: soluble and immobilized biocatalysts ... 110
- 6.3 Conclusions ... 115
- 6.4 Supporting information ... 116

7 Enzymatic synthesis of trimethyl-ε-caprolactone: process intensification and demonstration at 100 liter scale ... 119

- 7.1 Introduction ... 121
- 7.2 Results and discussion ... 122
  - 7.2.1 Process development on 30 mL scale ... 122
    - 7.2.1.1 Control experiments for substrate and product solubility and background titration ... 122
    - 7.2.1.2 Variation of the applied TmCHMO enzyme formulation ... 123
    - 7.2.1.3 Variation of the applied GDH source for cofactor regeneration ... 124
    - 7.2.1.4 Variation of the applied substrate dosing rate ... 125
    - 7.2.1.5 Variation of the applied TmCHMO loading ... 126
    - 7.2.1.6 Variation of the applied GDH loading ... 127
    - 7.2.1.7 Variation of the applied methanol amount ... 128
  - 7.2.2 Scale-up to 1 L scale ... 129
    - 7.2.2.1 Scale-up of the optimized conditions and application of pure oxygen ... 129
    - 7.2.2.2 Final conditions under application of the fermented material for the demonstration ... 131
    - 7.2.2.3 Development of an adequate downstream processing procedure ... 133
  - 7.2.3 Demonstration on 100 L pilot plant scale ... 133
    - 7.2.3.1 Reaction ... 133
    - 7.2.3.2 Downstream processing ... 135
- 7.3 Conclusions ... 136

8 Synthesis of trimethyl-ε-caprolactone with a novel immobilized glucose dehydrogenase and an immobilized thermostable cyclohexanone monooxygenase 139
  8.1 Introduction 141
  8.2 Results and discussion 143
    8.2.1 Stability of GDH-01 in different pH values and concentrations 143
    8.2.2 Immobilization of GDH-01. Characterization of different supports 145
      8.2.2.1 Methacrylate/styrene based supports 145
      8.2.2.2 Agarose based matrices: epoxy- and Mana-agarose 147
    8.2.3 Immobilization of GDH-01 and TmCHMO on Mana-agarose. Maximum loading capacity 149
    8.2.4 Synthesis of trimethyl-ε-caprolactone 150
      8.2.4.1 Soluble enzymes 150
      8.2.4.2 Immobilized enzymes 151
  8.3 Conclusions 156
  8.4 Supporting information 158
9 Overall conclusions 159
10 Acknowledgements 161
11 Scientific contributions 163
12 References 165

1. Introduction

1.1 General aspects

1.1.1 Principles of biocatalysis [1]

Enzymes are present in every living organism and are responsible for the reactions going on in every cell and so, in every bio-transformation. Reactions going on inside organisms are called, bio-chemical reactions, and each of them is catalyzed by an enzyme, a bio-catalyst. Enzymes are proteins, often conjugated with other molecules (metal ions, carbohydrates, lipids or DNA/RNA) that are able to reduce the free energy barrier that every substrate must overcome to become a product. By doing this, enzymes accelerate reactions that otherwise would proceed at very low rates. Their catalytic activity lies on its three dimensional structure and they act on substrates transition states by different means [2], [3]: (i) complementary charge distribution, (ii) formation of covalent intermediate/s, (iii) reduction of the reaction's entropy change. Thus, creating an activated transition complex that has the required energy state to start the reaction. Enzymes, theoretically, as every catalyst, do not suffer any change after the reaction is completed and they could be used infinite times. However, this is not the case and every enzyme has its limited amount of substrate that it can convert, its own total turnover number (TTN). Moreover, from a different perspective, every enzyme has its total amount of time that it can remain active, its stability value [4]. Anyhow, after certain use or time, enzymes eventually get deactivated by undefined irreversible processes. The unfolding of its weak spots on the surface of the protein is considered to play a crucial role [5].

As well as enzymes are used in nature to catalyse all sorts of reactions, they can also be used to catalyse chemical reactions of industrial interest.

1.1.2 History of industrial bio-transformations [6], [7]

The use of microorganisms or isolated enzymes to modify certain molecules and obtain desired products is what it is now known as, bio-transformations. However, these bio-based processes were present in ancient societies long before enzymes or even cells were described. Sumerians and Babylonians practised the art of brewing before 6000 BC and Egyptians, for example, used wild yeast for baking bread made from emmer wheat or barley [8]. In this same line, the production of vinegar dates back to 2000 BC [9]. All these operations had something in common though, few was known about the intrinsic organisms and reactions that were involved in the transformations.

It was not until Antony von Leeuwenhoek (1632 – 1723) invented the first microscope, that the small world, hidden from the naked eye, could be unravelled [10]. He built more than 400 of these instruments during his lifetime and still now, microscope is considered one of the greatest impacts in the history of science. Thanks to the microscope, in 1665 Hooke (1635 – 1703) could lay the foundations of the cell theory, eventually formulated in 1839 [11], [12]. The cell biology research and experimentation had started and it was not meant to stop.

Further contributions came, for example, from Payen who in 1833 isolated an enzymatic complex from malt and named it “diastase” [13]. It catalyzed the breakdown of starch into glucose and it is considered to be the first enzyme ever discovered. In 1862, Pasteur studied the bio-transformation of alcohol into acetic acid (vinegar) concluding that the pellicle, so-called “the flower of vinegar”, “served as a method of transport for the oxygen in air to a multitude of organic substances” [14]. The names used at that time to describe such substances were “organized ferment” (intracellular enzymes) and “unorganized ferment” (extracellular enzymes). It was not until 1876 that Kühne proposed the name *enzyme*, from the Greek “in yeast” or “leavened” [15]. The use of resting cells and cell free extracts to catalyse bio-reactions was initiated by a report presented in 1897 by Buchner who stated that broken yeast cells, grinded with sand, could still perform the alcoholic fermentation, from glucose to ethanol [16].

More recent investigations on enzyme technology, were carried out by the German biochemist Leonor Michaelis and his Canadian assistant Maud Leonara Menten. In 1913, they disclosed the enzyme-substrate complex theory that led to the formulation of the Michaelis-Menten equation [17]. They observed that an enzymatically catalyzed reaction rate is proportional to the substrate concentration until a maximum limit is reached. With the first protein crystallization studies in 1920, further details on protein structure and enzyme-substrate complex could be envisaged. In 1926, Sumner crystallized and structurally characterized a urease from jack bean (*Canavalia ensiformis*), meriting for this the Nobel prize in 1946 [18]. However, it was in 1966 with the introduction of X-ray crystallography when the first tertiary structure could be defined, the lysozyme [19]. Nowadays, several thousands of enzymes crystal structures are available through the ExPASy server (http://www.expasy.org/enzyme/).

In between the last century breakthroughs in synthetic biology, there is the publication in 1950, of the double helix and chemical nature of RNA and DNA by Watson and Crick [20]. Essential work this, for the later discovery in 1941 (Nobel Prize 1958) by Beadle and Tatum, who concluded that each gen present in DNA controls the synthesis of a particular enzyme, the one gene-one enzyme hypothesis [21]. It was not late after these findings that, Cohen and Boyer discovered the artificial recombinant DNA technology (1973) [22]. They found that genes from an organism could be transferred and propagated into a different host if inserted in DNA molecules with replicative capacity. The gate for recombinant protein production was open. The production of small molecules started in 1983 [23]. In 1984, for the starch industry, Novozymes commercialized a maltogenic amylase (Maltogenase®) from the first genetically modified organism [24].

Nowadays, enzymes either in free formulation or over-expressed in host organisms are used in a broad range of applications. The food industry has traditionally been the most prominent sector that makes use of bio-transformations. The dairy companies, for example, use acid proteinases for milk coagulation, lipases for cheese ripening or transglutaminases for protein cross-linking [8]. The baking industry has incorporated new enzymes like xylanases for dough conditioning or glucose oxidases for dough strengthening. In a different sector, in the production of polymers, enzymes can be used as polymerization agents like laccases with bisphenol A or as ring-openers like Lipases in the polymerization of lactones [25]. Another industry that has benefited from enzyme technology is the detergent's one, with the use of amylases for carbohydrate stain removal or cellulases for color clarification [26]. Many are the examples currently present in other sectors like the beverage, leather, cosmetics, organic synthesis, waste management and pharmaceuticals among others [8].

Global market for enzymes in industrial application was estimated about $5.5 billion in 2018 and expected to proceed at a compound annual growth rate (CAGR) of about 4.9% over the period of 2018 and 2023 to reach approximately $7.0 billion [27].

1.1.3 Enzyme classification

Back in the XVIII century when the role of enzymes started to be disclosed, arbitrary names were given to each enzyme. It did not take long until two different names were given to the same enzyme or the other way around. Classification and standardization of naming was highly required. In 1961, the Nomenclature Committee of the International Union of Biochemistry and Molecular Biology (IUBMB) in collaboration with the International Union for Pure and Applied Chemistry (IUPAC), published a report classifying enzymes in six families according to the type of reaction they catalyzed (Table 1.1) [28]. At the same time, two standardized names were set to be used for each enzyme: the recommended name (daily use) and the systematic name (includes the substrate converted). The source organism was not included in either nomenclature and it is usually added following the name. Furthermore, following the guidelines of the Enzyme Commission (EC), integrated in the IUBMB, a four-digit number was assigned to each enzyme. This number stands first for the type of reaction catalyzed, second for the chemical group upon which it acts, third for the chemical groups involved in the reaction and fourth for the identification number within the third group [6].

Table 1.1. Classification of the different enzyme classes, the catalyzed reactions and some examples.

Enzyme class	Catalyzed reaction	Reaction scheme	Examples
1. Oxidoreductases	Electron transfer	AH2 + 1/2O2 → A + H2O	Dehydrogenases, oxidases, peroxidases, oxygenases, hydroxilases and reductases
2. Transferases	Functional group transfer	AB + C → A + CB	Mono-carbon group, aldehyde/keto residues, acyltransferases, glycosyltransferases, alkyl/aryltransferases, aitrogenous groups, etc.
3. Hydrolases	Hydrolysis	AB + H2O → AH + BOH	Esterases, glycosidases, ether hydrolases, peptidases, carbon-nitrogen hydrolases, etc.
4. Lyases	Group elimination with double bond/ring formation	AB → A + B	Acting on C-C, C-O, C-N, C-S, C-X, P-O, etc.
5. Isomerases	Isomerization	ABC → ACB	Racemases/epimerases, cis-trans isomerases, intramolecular oxidoreductases, intramolecular transferases, etc.
6. Ligases	Bond formation with triphosphate cleavage	A + B + XTP → AB + XDP + Pi	Creating C-O, C-S, C-N, C-C, phosphoric esters, N-metal, etc.

This thesis has focused on the application of oxidoreductases to target reactions of industrial interest.

1.1.3.1 Oxidoreductases

Oxidoreductases represent approximately one third of all the enzymes classified so far. Among them, around 50% make use of the NAD(P)H/NAD(P)$^+$ co-factor (co-substrate) as electron donor/acceptor, the so-called NAD(P)H-dependent oxidoreductases [29]. In the best case scenario, this co-factor is stoichiometrically consumed at the same rate as the substrate does. Due to its elevated cost, if industrial feasibility is considered, these molecules have to be re-generated somehow. In this thesis, enzymatic re-generation has been employed [30]. A second enzyme consuming a sacrificial substrate performs the inverse reaction to re-generate the NAD(P)H/NAD(P)$^+$. An added issue to this regeneration though, is that oxidoreductases often exhibit an uncoupling effect, an unproductive use of NAD(P)H to form by-products [31]. Moreover, these by-products are usually reactive oxygen species that, into the bargain, inactivate the enzyme.

NAD(P)H-dependent oxidoreductases catalyse a broad variety of substrates and reactions, covering the whole spectrum of oxidoreductases sub-classes (EC 1.1 to EC 1.23) [32]. Among them, the transfer of electrons from the co-factor to the substrate is not always direct and it differs depending on the sub-class [33]. Amino-acid side chains or other co-factors such as flavins or metallic ions are often required.

This thesis has focused on the utilization of four different types of NADPH-dependent oxidoreductases:

- Dehydrogenases (EC 1.1): they catalyse the transfer of hydrogen atoms to NAD$^+$, NADP$^+$, FAD$^+$ and/or FMN [34].
- Oxidases (EC 1.6): they catalyse an oxidation/reduction reaction by using O_2 as an electron acceptor [35].
- Monooxygenases (EC 1.14): these enzymes cover a major part of the thesis. Monooxygenases are able to insert an oxygen atom into a non-activated carbon present in an organic molecule. The donor is molecular oxygen which has to be activated by the electrons transferred, usually, from the enzyme's cofactor [36].

Furthermore a peroxidase was also used as a hydrogen peroxide scavenger (catalase). Further details about each enzyme are disclosed at the end of this section and throughout this thesis.

1.1.4 Enzyme discovery, engineering and modification

The time pressures from industry and the long lead times required to stablish an optimal bio-catalyzed process, hurdled the implementation of enzymes as a first choice in the manufacture plants. Enzymes were usually relegated as the last option once all chemical trials failed. However, the increasing interest of industry on bio-based transformations, fuelled the research on the field and major advances were made on this direction.

Nowadays, a bio-catalyzed process is specially interesting when high specificity/selectivity is required, when the reaction must be carried on in mild conditions, when there are some environmental restrictions or when the natural label is a major advantage for the product to be sold [37]. On the other hand, enzymes often come with some major drawbacks that hinder their application in industry: inexistence of the adequate enzyme, high degree of instability, very complex interactions to maintain the three dimensional structure or production issues among others [38]. These downsides of biocatalysis are tackled by four main approaches [39]: i) enzyme discovery, ii) enzyme engineering, iii) physicochemical modification of known enzymes and iv) reaction engineering.

- *Enzyme discovery:* founding new enzymes either in nature [40] or artificially designed by computational methods [41], always encounters the tedious and time-consuming labour of screening the pools of variants. In these sense, new methodologies with significant higher throughputs have been developed. Robotics, electronics, chemical analysis and biotechnology have merged to create, what it is known as ultrahigh-throughput platforms [42]. These platforms enable the screening of up to 10^6 – 10^9 variants day^{-1}. High performing flow cytometers [43], [44], micro-capillary single-cell analysis and laser extraction (µSCALE) [45], lithographic microchips [46] or droplet-based screening [47] are some of these modern platforms.
- *Enzyme engineering:* once an enzyme that suits a target reaction is found, modifications on its primary sequence, to improve its stability, selectivity or activity, are often required. In order to fulfil this task, two strategies are followed: directed evolution and rational design. In the first case, the encoding DNA sequence is modified either by recombination with related sequences (gene shuffling) or by randomly introducing mutations (error-prone PCR) [48]. This strategy, also makes use of the aforementioned ultrahigh-throughput platforms for screening of the variants. The second case, the rational design, relies on the study of the three-dimensional structure of the protein by computational methods [49], [50]. Biochemical data and molecular modelling data [51] are assessed to propose a concrete change in the sequence that is carried on by site-specific mutagenesis [52]. Both techniques can be combined to perform an enzyme engineering in a semi-rational manner.
- *Physicochemical modifications:* in order to enhance enzyme properties, its primary sequence does not always need to be altered, modifications can be performed directly on the folded protein [53]. Even though the main goal of these modifications is usually to improve stability, other properties of the enzyme might also be altered. In this sense,

different chemicals are used: site-directed reagents that target only a specific amino-acid, non-specific reagents [54], affinity labels that bind to a specific site of the enzyme, cross-linkers to generate enzyme aggregates (CLEAs) [55], [56], crystallization techniques [57], [58], auxiliary molecules that non-covalently bind the active site and modify its specificity [59]; and several supports and techniques for immobilization [60]–[62]. Among all these modifications, this thesis has focused on immobilization, which will be further explained later on.

- *Reaction engineering:* taking an enzyme from its natural environment and placing it, for instance, in a bio-reactor with totally different conditions, can be a severe factor favouring enzyme instability. At the same time, several enzymatic substrates are poorly soluble in water so that the presence of organic solvents is required. Reaction engineering, deals with the different variables affecting both the enzyme and the optimal reaction conditions, trying to find a consensus and maximize the throughput [63]. Temperature, salinity, pH, aeration, stirring, substrate/product concentration, co-factors, surfactants, co-solvents or biphasic media are some of the common variables dealt with. Part of this thesis has made use of the reaction engineering principles to intensify oxido-reductive bioprocesses [64]. Further on, a section is dedicated to it.

1.2 Immobilization

In 1916, the first evidence of enzyme immobilization was reported [65]. Studies performed on an invertase showed that the enzyme, adsorbed on charcoal or aluminium hydroxide, exhibited the same activity as soluble. Later on, in the first Enzyme Engineering Conference (1971) immobilization was defined as “enzymes physically confined or localized in a certain defined region of space with retention of their catalytic activity, and which can be used repeatedly and continuously” [66].

Immobilization often confers extra rigidity to biocatalysts and so it results in improved operational and storage stability [67], [68]. It also allows an easy separation of the enzyme-support derivate from the rest of the reactor content and makes re-usability possible [69]. Immobilization is especially appropriate in a bioprocess when the downstream process requires less unit operations or a free allergen product [70]; and when the enzyme production represents a significant cost to the process. Whilst a homogeneous catalyzed reaction operate mainly in stirred tank reactors (batch or fed-batch) [71], immobilization makes possible the operation in continuous reactors, packed bed reactors, plug-flow reactors or fluidized bed reactors among others [72], [73]. On the downsides of immobilization, there is the loss of total or partial enzymatic activity during the attachment of the biocatalyst and the added cost that the carrier and the immobilization process represents [60]. Furthermore, placing the enzymes in confined regions of space, as it is a small pore, entails that the substrate/s transport is governed by diffusional phenomena. Reaction rate is then limited by the concentration gradient and catalytic activity can get significantly reduced [74], [75].

1.2.1 Support features and considerations

A golden rule that always allows optimal immobilization of a given enzyme, does not exist. However, in order to address the possible hurdles that might appear during immobilization, some considerations can be taken into account beforehand regarding both the enzyme and the support. Protein molecular mass, surface functional groups, specific activity, enzyme stability against pH, melting point or sensibility in front of reagents are important enzyme parameters that should match with the matrix features and the immobilization protocol [76], [77]. On the support's side, the affordability, the chemical composition, the mechanical strength, the hydrophilicity, the functional group and activation degree; the pore size, the particle size, the maximal enzyme load, the internal morphology and the spacer length are crucial features to be taken into consideration [78], [79]. As stated above, no rational approach exists that always yields a successful immobilization. Trial and error is the common strategy followed .

The available set of materials for enzyme immobilization is vast and new carriers with modern functionalities continuously appear. For example, smart polymers or magnetic nanoparticles have gained interest in last decades. The most commonly used materials can be divided in three groups and are summarized below these lines [80]:

- *Natural polymers*: alginate, chitosan and chitin; collagen, carrageenan, cellulose, starch, pectin, sepharose, etc.
- *Inorganic polymers*: zeolites, ceramics, celite, silica, glass, activated carbon, etc.
- *Synthetic polymers*: polyvinyl chloride, polyurethane, polyvinyl alcohol, polymethacrylate, polystyrene, polyaniline, nylon, etc.

This thesis has focused on the utilization of methacrylate/styrene, agarose and polyvinyl alcohol supports for the immobilization of oxidoreductases. The carriers employed presented a broad variety of features and functionalities in order to cover as much different support's characteristics as possible.

1.2.2 Immobilization methods

Once a candidate enzyme is chosen and all the potential carriers have been evaluated, the immobilization method has to be addressed. Each support's configuration (material, linker and functional group) is designed to bind to the enzyme in a certain way. At the same time, every immobilization method entails a protocol and conditions that must be adequate for the enzyme. A compilation of immobilization methods with its main characteristics is presented below these lines [60]:

Table 1.2. The different immobilization methods divided by the physical/chemical interaction that exists between the enzyme and the carrier.

Method	Scheme	Principle	Types of interactions	Considerations
Adsorption	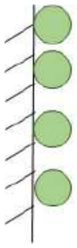	Non-specific physical interactions	Ionic, van der Wals, hydrophobic, deposition, hydrogen bonding, etc.	Reversible and weak. Usually entails high retained activity.
Affinity	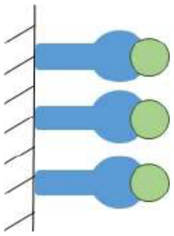	Complementary biomolecules or metal chelation	Antibody-antigen, protein-protein interaction, Ni-His tag, aptamers, etc.	Reversible and stronger than adsorption.
Covalent binding	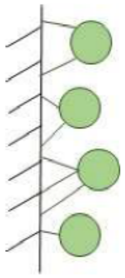	Covalent bonds formed between the enzyme and the support	Carboxyl-amino, epoxy-amino, CNBr-amino, aldehyde-amino, etc.	Strong, irreversible and often multipoint attached (increased stability). Low retained activities.
Entrapment	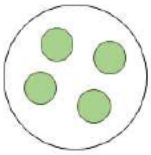	Caging the enzymes within gels or fibres	Inclusion into polymer networks, sol-gels, membranes, etc.	Easy, fast and cheap to use but leakage often observed.
Cross-linking	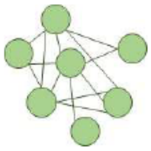	Enzymes are braced with cross-linkers. Carrier-less.	Cross-linked crystals (CLECs) and corss-linked aggregates (CLEAs)	Simple and inexpensive but often encompass diffusional limitations.

This thesis has dealt with the immobilization of oxidoreductases following different methods: ionic adsorption, hydrophobic interaction, covalent bonding and entrapment.

1.3 Bioprocess design and engineering

Rational process design and optimization of the variables affecting the reaction throughput are crucial steps in the planning and implementation of an industrial transformation. Both technical and economical feasibility are to be considered. In general terms, any process aims to maximize selectivity, yield, purity and most important, profitability. At the same time, it also tends to minimize the catalyst consumption, the energy use and the raw materials and solvents involved [81], [82]. The flowchart commonly followed from the first evaluations and up to large-scale production, is shown below these lines:

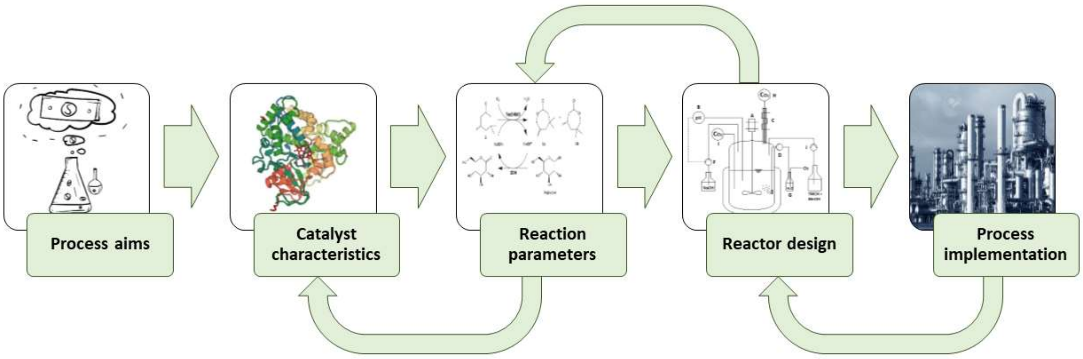

Figure 1.1. The flowchart that defines the different steps usually followed in the implementation of a biocatalyzed reaction.

1.3.1 **Process aims:** once the product to be synthesized has been set and its potential market studied, some process metrics must be defined taking into account the potential final product value [83]:

- *a.* *Conversion:* defined as the number of converted molecules per number of starting molecules. It takes into consideration the substrate and product value as well as the future complications that could arise when purifying.
- *b.* *Yield:* defined as the number of synthesized molecules of product per number of starting molecules of substrate. The by-products generated and the mass balance inconsistencies are directly related with the yield.
- *c.* *Space Time Yield (STY):* defined as the amount of product generated per unit of volume and unit of time. It is also known as volumetric productivity or reactor productivity. The substrate solubility and concentration; the yield and the reaction kinetics govern the final STY value.

d. *Purity:* defined as the ratio or concentration of the desired product at each stage of the process. The reaction yield, the product concentration and the efficiency of all the downstream unit operations are related to it.

e. *Bio-catalyst yield:* defined as the amount of product generated per gram of enzyme or biomass. It is directly dependent on the biocatalyst production cost and stability.

f. *Environmental aspects:* legislation is to be taken into account from the first stage of the process. Environmental laws and possible process restrictions must be evaluated and addressed.

1.3.2 Catalyst characteristics: the bio-catalyst selection is of crucial importance in the process definition. An enzyme/s able to catalyse the desired reaction and as easier as possible to be produced are minimums required. As stated in the previous sections, many modifications are possible to alter the bio-catalyst characteristics. The important features that the final candidate should maximize are summarized below:

a. *Activity:* defined as the reaction rate per mass of catalyst. The STY directly depends on the activity of the bio-catalyst. NADPH-dependent oxidoreductases activity can be measured spectrophotometrically following the consumption or generation of NADPH.

b. *Selectivity:* defined as the number of product molecules synthesized per number of substrate molecules converted. It is usually an intrinsic property of the enzyme, altered only by active-site modifications. It can be divided in chemo-, regio- and enantio-selectivity. Performing preliminary reactions with the target substrate can provide a good insight in the enzyme's selectivity.

c. *Stability:* inverse of the deactivation degree of the catalyst in front of temperature, mechanical stress, organic solvents, pH, etc. Among others, previously explained, stability can be altered by changing the enzyme formulation: cell free extract, whole cell, broth, etc. Following the activity decay of the enzyme in defined conditions gives an indication of the enzyme's stability. The total turnover number (mol of product mol^{-1} of enzyme) and the half-life (time in which the activity is halved) are two metrics used to evaluate the stability of an enzyme.

1.3.3 Reaction engineering: once the process aims are disclosed and the main characteristics of the catalyst have been studied, the reaction parameters have to be adjusted. The variables affecting both the reaction throughput and the enzyme have to be optimized: buffer, salinity, pH, temperature, organic solvents, etc. Moreover, at this point, the substrate/product inhibition issues, often observed in oxidoreductases such as Baeyer-Villiger monooxygenases, have to be addressed as well [63], [84]. The use of specialized software may help in the Design of Experiments (DOE), reducing significantly the number of experiments required to achieve an optimum state. Another element of interest, at this point, might be the construction of a kinetic model of the reaction [85]. It is a mathematical equation able to predict the system response to a given alteration. The reaction engineering and the reactor design are in a closed loop, continuously influencing one another.

1.3.4 **Reactor design:** the presence of soluble catalyst in the reaction hinders the operation in continuous mode (membranes required). The type of reactor often observed in bio-catalyzed processes is the stirred tank reactor operated in a batch mode. It is a simple and robust model of reactor, however, depending on the reaction needs, the tank has to incorporate some additional inputs and/or controls:

a. *Inputs:* in oxidation/reduction processes, oxygen is often a co-substrate of the reaction and so, aeration is required. Thus, an air inlet and a condenser on top of the reactor are necessary. Apart from this, dosing of substrate, product removal, sampling, co-solvent addition or biomass additions are possible needs from the reaction that could involve configurational changes on the vessel [86].

b. *Controls:* the temperature (e.g. jacketed reactor), the pH or the dissolved oxygen are common variables controlled in oxido-reductive reactions. This implies the use of probes and controlling equipment, adding like this an extra cost to the process [87].

The use of immobilized enzymes allows the easy implementation of continuous operating modes and reactors such as the continuous stirred tank or the plug-flow reactor.

1.3.5 **Process implementation:** the final steps, before a given reaction is taken to an industrial plant, are the downstream processing of the product and the scale-up of the reaction volume:

a. *Downstream processing (DSP):* it serves as a method to isolate the product from the rest of the reactor content. The finalization of a bio-catalyzed reaction is usually followed by a liquid-liquid extraction. A secondary liquid, often an organic solvent, is used to dissolve as much product as possible. The selection of a proper secondary liquid is important to obtain high extraction coefficients. Filtration is another unit operation usually employed. It makes use of filters in order to clarify the reaction liquid or to recover solids present in the reactor [88].

In biotechnology membranes are also applied and they are divided according to the molecular weight of the compound they retain. Other examples are precipitation and crystallization, which are based on the intrinsic properties of the product to become insoluble. Heat, solvents, salts or derivatization reactions are methods to make it possible [89]. Another case, extensively used in in-situ product removal, is the adsorption of the product on selective resins. It is widely used as well for purification of proteins by using activated carbon, ion-exchange or metal chelated resins [90]. Finally, the last method is chromatography. The difference in equilibrium constants for components placed in a biphasic systems, allows its separation.

b. *Scale-up:* the design and optimization of a reaction from scratch, is usually pursued at bench-scale (≈ 100 mL). Thus, scale-up is necessary to achieve large-scale production. Increasing the volume handled though, implies a decrease in the surface to volume ratio meaning that, mass and energy transport limitations arise [91]. Scaling up, requires engineering and economic considerations in addition to expertise. Some of the issues found when increasing the reaction volume are: i) when mixing, the tip speed of the stirrer is higher and creates higher shear stress, ii) the aeration, depending on the sparger design and the bubbles size might become less efficient, iii) the heat transfer is poorer due to the reduced surface area available in comparison with the increased volume, iv) equipment size, power consumption and safety have to be adapted to the new scale, v) rheology alterations, due to heat and mass transfer changes and vi) unexpected metabolic changes of the microorganisms [92].

The process implementation is directly influenced and in continuous closed loop with both, the reaction parameters and the reactor design. Economic evaluation, on the other hand, is supposed to be included in every stage of the process design.

In this thesis, the optimization and scale-up of the Baeyer-Villiger oxidation of the 3,3,5-trimethylcyclohexanone (TMCH) to trimethyl-ε-caprolactone (CHL) was performed. The optimization was carried out at 30 mL scale and the reaction was scaled up to 100 L.

1.4 ROBOX project

The research performed along this PhD thesis has been led and financed by the European Union project ROBOX (grant agreement n˚ 635734). ROBOX stands for *Expanding the industrial use of Robust Oxidative Biocatalysts for the conversion and production of alcohols* and it was initially conformed by a consortium of 19 partners from different countries all over Europe. As its name clearly states, from the beginning, it was an industrially focused proposal. Both scientific and advisory companies were involved and the Dutch multinational company DSM Chemical Technology R&D B.V. initially served as coordinator.

1.4.1 Objectives

The general aim of the project is the evaluation and comparison of the technologies and platforms that enable a rapid implementation of robust oxidative bio-catalysts in industrial scales and timelines. The enzyme classes selected for this purpose were: the cytochromes P450, the Baeyer-Villiger monooxygenases (BVMOs), the alcohol dehydrogenases (ADHs) and the alcohol oxidases (AOXs). The target reactions proposed to be catalyzed by these enzyme involve the oxygenation of non-activated carbons into the form of alcohols or esters; and the transformation of the alcohol groups into the corresponding aldehyde, ketone or carboxylic acid groups. The target reactions studied were 11 and the obtained products were thought to be commercialized in different industrial areas: pharma, nutrition, fine/specialty chemicals and materials.

The specific objectives of the project were divided into 5 Work packages (WP):

- *Enzyme engineering & identification*: was dedicated to the identification of novel oxidoreductases within the four selected groups and further engineering of the best hits. The final candidates should feature higher robustness in terms of activity, stability and selectivity. The methods used for this purpose include both principles: the directed evolution (SeSam, OmniChange, MAP, FACS, TLC spotter, etc.) and the rational design (the novel approach FRESCO).
- *Enzyme production*: was focused on stablishing robust recombinant hosts and fermentative processes for high density enzyme production. The goal was the creation of robust and affordable platforms that would allow the production of any of the oxidative enzymes at large scales and high densities. Different hosts were evaluated: bacteria like *Escherichia coli (E. coli)*, yeast like *Pichia Pastoris* or *Schizosaccharomyces pombe* and hyphal fungi such as *Myceliophthora thermophile*.
- *Biocatalytic process design & validation*: worked on the application and optimization of the enzyme's performance in the conversion of the target substrates. Reaction engineering, reactor design, storage conditions and transport conditions were all part of the package. The reactions were optimized in terms of pH, temperature, buffer

composition, co-solvents and substrate/product concentration. Moreover, new reactor configurations with novel aeration strategies were tested.

- *Demonstration:* dedicated to bridge the gap between the recently discovered enzymes and optimized reactions; and the final industrial application. This package was basically devoted to scale-up the target reactions that fulfilled the pre-stablished metrics in the bench-scale. All the efforts were put in overcoming the issues arising when enlarging the reaction volume, explained in the previous section.
- *Process benchmarking & evaluation:* performed the evaluation of the bioprocesses that reached the final stages and also of the ones that did not. All the generated data, environmental impact and energetic performance of reactions was gathered to set up a framework. The aim was to pave the way of the technologies investigated for further replications in new. Furthermore, the analysis of faults and errors from the end perspective allows the subsequent learning for future projects.

1.4.2 Target enzymes and reactions of the ROBOX project

The companies involved in the ROBOX project proposed a set of target reactions with industrial interest to be studied by the consortium. The target reactions and their corresponding target enzymes are represented in the figure below (Figure 1.2):

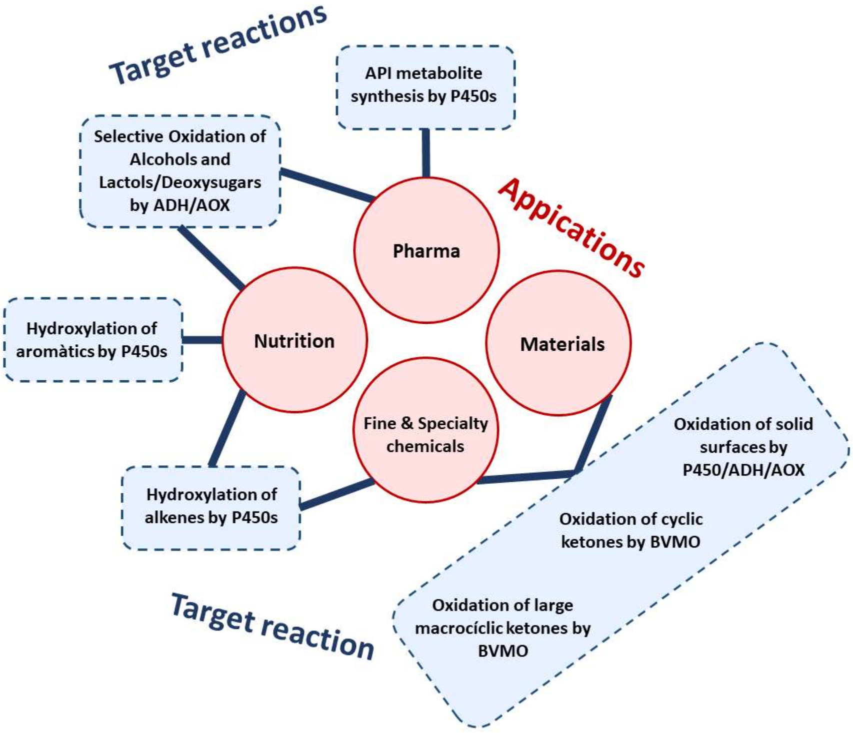
Target reactions
API metabolite synthesis by P450s
Selective Oxidation of Alcohols and Lactols/Deoxysugars by ADH/AOX
Appications
Pharma
Nutrition
Materials
Hydroxylation of aromàtics by P450s
Fine & Specialty chemicals
Oxidation of solid surfaces by P450/ADH/AOX
Hydroxylation of alkenes by P450s
Oxidation of cyclic ketones by BVMO
Oxidation of large macrocíclic ketones by BVMO
Target reaction

Figure 1.2. Graphical abstract of the target reactions (blue) and their application in the market (red).

1.5 Enzymes employed in this thesis

The enzymes used throughout this thesis are:

- Dehydrogenases (EC 1.1): an alcohol dehydrogenase from *Artemisia annua* (ADHaa; EC 1.1.1.1) was used for the oxidation of 4-hydroxy-isophorone to keto-isophorone [93]. Additionally, three glucose dehydrogenases (EC 1.1.1.47) were used as co-factor regeneration enzymes, coupled with oxygenation reactions [94], [95].
- Oxidases (EC 1.6): also used as a co-factor regeneration enzyme, an NADPH-oxidase (NOX; EC 1.6.3.1) was coupled with the ADHaa reaction mentioned above [35].
- Peroxidases (EC 1.11): not considered an NADPH-dependent enzyme but indirectly related to it, bovine liver catalase (EC 1.11.1.6) was used as a scavenger for the elimination of hydrogen peroxide, the uncoupling by-product of a P450-mediated reaction [96].
- Monooxygenases (EC 1.14): two monooxygenases were studied, covering the major part of the thesis: i) the cyclohexanone monooxygenase from *Thermocrispum municipale* (TmCHMO; EC 1.14.13.22) was used for the Baeyer-Villiger oxidation of trimethyl-ε-caprolactone [97] and ii) the cytochrome P450 from *Bacillus megaterium* (P450 BM3; EC 1.14.14.1), either the wild type (WT) or mutated (M22C02), was used for the hydroxylation of two target substrates: α-isophorone and diclofenac [98]–[100].

1.6 Target reactions of this thesis

Among all reaction proposed by the ROBOX consortium, three of them were investigated by the group and are presented in this thesis. Additionally, the hydroxylation of sodium laurate was chosen as a model reaction for the investigation of P450 BM3.

1.6.1 Hydroxylation of sodium laurate

In nature, P450 BM3 catalyses the hydroxylation of medium to long-chain fatty acids in the ω-1, ω-2 and ω-3 position [98]. The P450-associated uncoupling is less prominent when employing native substrates. That is why, sodium laurate (C12) was used to test the re-cycling capacity of this enzyme. According to Nobel *et al.* the amount of NADPH utilized in the uncoupled reactions when laurate is used as substrate is 3.8% [31]. Laurate was also chosen due to its higher solubility compared with the longer-chain fatty acids (C13 to C22).

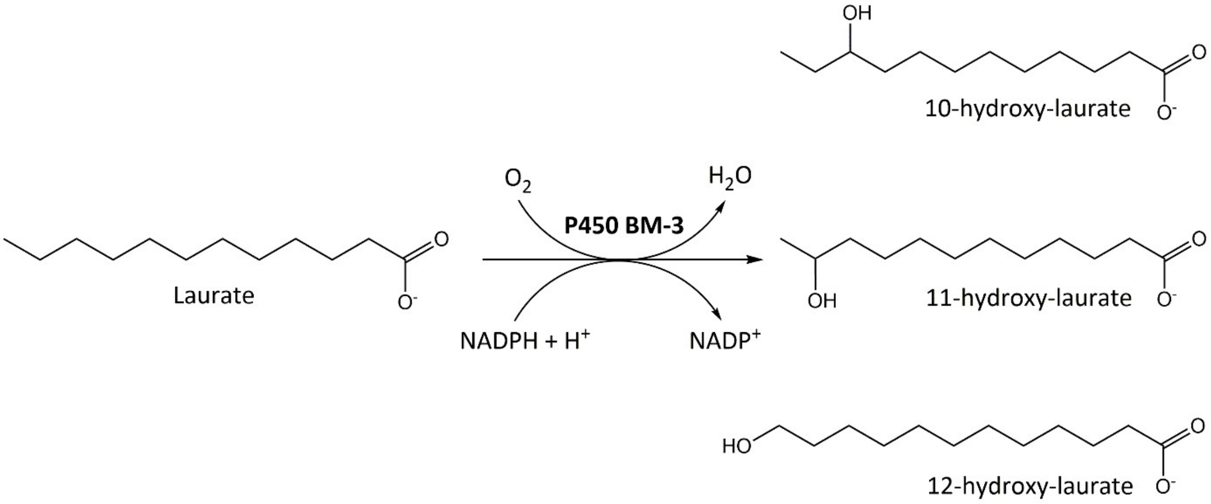
O$_2$
H$_2$O
P450 BM-3
NADPH + H$^+$
NADP$^+$
Laurate
10-hydroxy-laurate
11-hydroxy-laurate
12-hydroxy-laurate
OH
HO
O
O$^-$

Figure 1.3. Reaction scheme for the biocatalyzed hydroxylation of sodium laurate (Laurate).

Regarding its possible industrial applications, hydroxylated fatty acids are widely used as starting materials for the synthesis of polymers or lactones (fragrances) and also as additives for the production of lubricants and emulsifiers. Furthermore, they can also exhibit antibiotic, anti-inflammatory and anticancer activities [101], [102].

1.6.2 Hydroxylation of α-isophorone

The hydroxylation of α-isophorone (ISO) is highly interesting due to the low cost of the substrate and the variety of different applications presented by the obtained products [103]–[105]. This was selected as the major target for the P450 BM3 and specially, for the P450 BM3 wild type. As it can be seen in Figure 1.3, the reaction consisted in a two steps oxidation conducted firstly by P450 BM3 and secondly by an alcohol dehydrogenase.

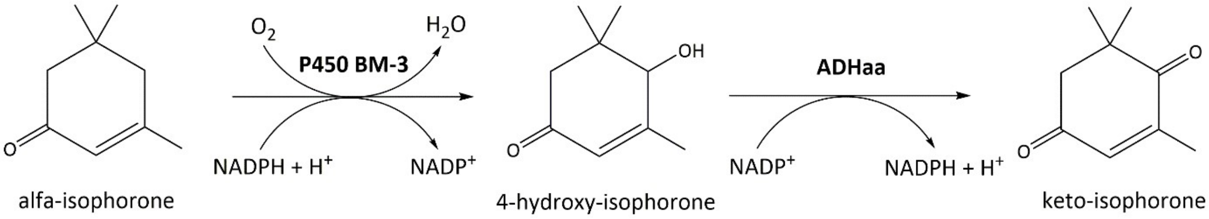
O$_2$
H$_2$O
P450 BM-3
NADPH + H$^+$
NADP$^+$
ADHaa
NADP$^+$
NADPH + H$^+$
alfa-isophorone
4-hydroxy-isophorone
keto-isophorone
OH
O

Figure 1.4. Reaction scheme for the biocatalyzed two step oxidation of α-isophorone.

α-isophorone can be isolated from biomass or obtained from the aldol condensation of acetone. Its main product, keto-isophorone (KET), can be converted to actinol for the production of carotenoids [106] or transformed to trimethylhidroquinone, a key intermediate for the synthesis of vitamin E [107]. Introduction to results section 6 covers the different features of this reaction in more detail.

1.6.3 Hydroxylation of diclofenac

Diclofenac (DIF) is a well-known and vastly prescribed anti-inflammatory drug. However, the uptake of this medicine is often associated with health disorders: gastrointestinal- and renal toxicity, cardiovascular alterations and idiosyncratic drug-induced liver injury. Even though all these symptoms are considered to be caused by multiple factors, an immune response triggered by the bio-activation of diclofenac is thought to be a main reason [108]. In this sense, the oxidation carried out by the cytochromes P450s is the second major route for diclofenac bio-activation in humans. Both 5' and 4'-hydroxy-diclofenac (HDI) are the primary intermediates in the processing of this molecule [109], [110].

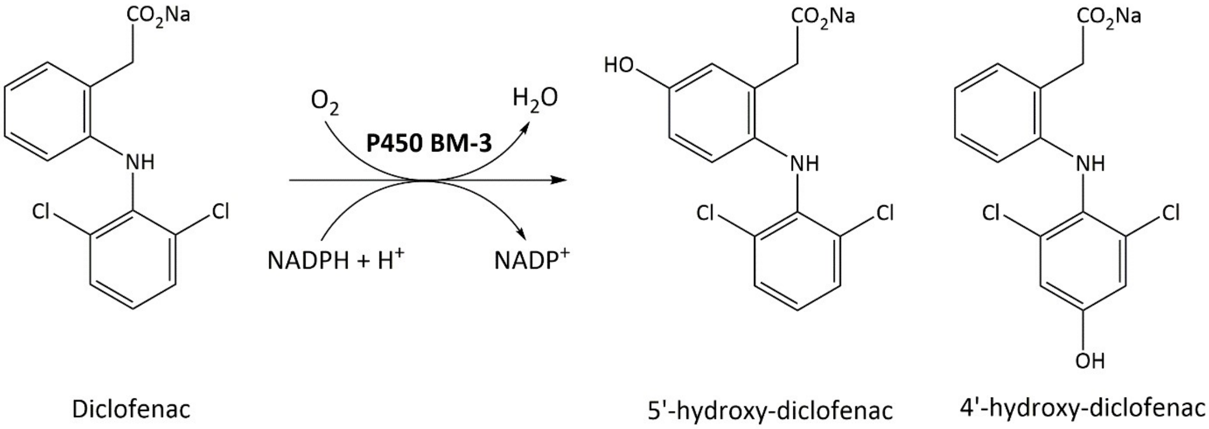

Figure 1.5. Reaction scheme for the biocatalyzed hydroxylation of diclofenac.

While going through the drug development trials, it is often mandatory to present metabolism studies. Authentic human metabolites are required for this purpose. Thus, all the molecules derived from the active pharmaceutical ingredient (API) are of special interest for pharmaceutical companies [111]. As aforementioned, in Phase I drug metabolism, cytochrome P450 and its products play a crucial role.

1.6.4 Baeyer-Villiger oxidation of 3,3,5-trimethylcyclohexanone

The substrate in this case was the hydrogenated form of α-isophorone, the 3,3,5-trimethylcyclohexanone (TMCH). A Baeyer-Villiger monooxygenase from *Thermocrispum municipale* was utilized for the synthesis of trimethyl-ε-caprolactone (CHL).

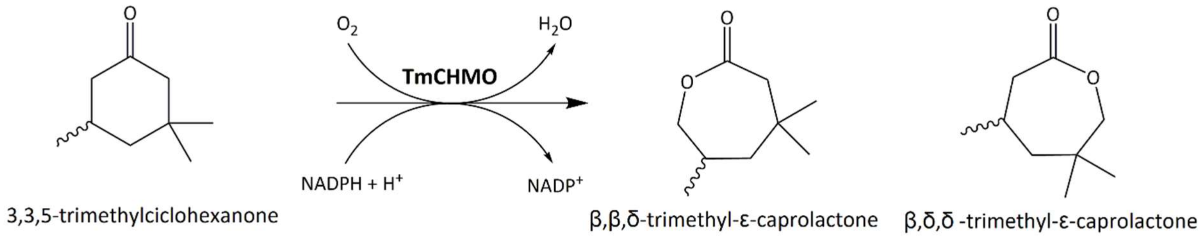
O
3,3,5-trimethylciclohexanone
O2
H2O
TmCHMO
NADPH + H+
NADP+
O
O
β,β,δ-trimethyl-ε-caprolactone
O
O
β,δ,δ -trimethyl-ε-caprolactone

Figure 1.6. Reaction scheme for the biocatalyzed Baeyer-Villiger oxygenation of 3,3,5-trimethylcyclohexanone.

The obtained product has gained interest in last years in the polymer industry. It can serve as a building block for the synthesis of aliphatic (co)polyesters [112]. Section 7 covers the process intensification and scale-up of this reaction while section 8 covers the immobilization of TmCHMO and its cofactor regeneration enzyme.

2. Objectives

The main objective of this thesis was the understanding and application of the main tools available to intensify a bio-catalyzed process. Centered in oxidoreductases, major part of the experimental work has focused on the utilization of the enzyme immobilization principles and their potential benefits. Another part of the research was focused on overcoming the limiting factors of unoptimized reactions and scale them up.

The specific objectives were:

- To characterize and immobilize the P450 BM3 wild type and the cofactor regenerator enzyme, the glucose dehydrogenase.
- To study the recycling capacity of both enzymes in a model reaction, the hydroxylation of sodium laurate.
- To optimize the main limiting factors in the hydroxylation of α-isophorone performed by P450 BM3 wild type and glucose dehydrogenase.
- To study the re-cycling capacity of both enzymes in the hydroxylation of α-isophorone.
- Immobilization of P450 BM3 M22C02 variant.
- To study the recycling capacity of P450 BM3 M22C02 mutant and glucose dehydrogenase in the hydroxylation of diclofenac.
- To characterize and immobilize of an alcohol dehydrogenase from *Artemisia annua*.
- To apply the alcohol dehydrogenase, either in its soluble form or immobilized, in the oxidation of 4-hydroxy-isophorone.
- To optimize and scale up the Baeyer-Villiger oxidation of 3,3,5-trimethylcyclohexanone performed by a cyclohexanone monooxygenase and a cofactor regeneration enzyme, the glucose dehydrogenase.
- To characterize and immobilize a novel and highly active glucose dehydrogenase (GDH-01).
- To study the recycling capacity of the immobilized cyclohexanone monooxygenase and the immobilized GDH-01 in the oxidation of 3,3,5-trimethylcyclohexanone.

3. Experimental: materials & methods

3.1 Materials and supports

Nicotinamide adenine dinucleotide phosphate sodium salts in its oxidized and reduced form (NADP+ disodium salt and NADPH tetrasodium salt) was purchased from BONTAC Bioengineering (Shenzhen, Guandong, China). D-(+)-glucose (> 97.5%) and ethyl acetate (> 99.9%) were purchased from VWR Chemicals (Radnor, PA, USA). 4-hydroxy-isophorone (> 98%) was enzymatically produced and further purified following the work described by Kaluzna *et al.* [113]. Dicalite 4208 was purchased from Dicalite Europe (Gent, Belgium). Distal and proximal trimethyl-ε-caprolactones (> 99%), that served as analytical standards, were provided by University of Maastricht and synthesized according to a chemical Baeyer-Villiger oxidation procedure reported in the literature [114]. All the other reagents were purchased from Sigma Aldrich® (St. Louis, MO, USA) and were of analytical grade if not stated otherwise. All solutions like buffers or stocks were prepared freshly prior to use.

Methacrylate/styrene resins were kindly donated by Purolite® Life Science (Bala Cynwyd, PA, USA) and stored at 4 – 6˚C.

The epoxy-agarose-SIGMA was purchased from Sigma-Aldrich®. According to the supplier's specifications it presented spherical shape, it had an activation degree of ≥ 20 µmol L^{-1} and 12 atoms spacer.

Non-functionalized agarose 4BCL (spherical beads Ø 50-150 µm) purchased from Agarose Bead Technologies® (ABT®, Madrid, Spain) was used to obtain epoxy-agarose-M1 and epoxy-agarose-M2 by support functionalization carried out as described by Axarli *et al.* [115] and Sundberg *et al*. [116] respectively. The quantification of the epoxy groups present on the supports was done following the method described by Gupta [117].

Amino functionalized agarose (Mana-agarose) presenting monoaminoethyl-*N*-aminoethyl linkers and aldehyde functionalized agarose (Glyoxyl-agarose), both with an extent of labelling of 40 - 60 µmol mL^{-1}, were purchased from ABT®. All this information was always according to the supplier's specifications.

Lentikats® polymer was purchased from GeniaLab® (Braunschweig, Germany) with composition consisting of a mixture of polyvinyl alcohol (10%), polyethylene glycol (6%) and demineralized water (84%).

3.2 Commercial enzymes

Bovine liver catalase was purchased from Sigma-Adrich (St. Louis, MO, USA) as a lyophilized powder. Glucose dehydrogenase GDH-105 was purchased from Codexis® (Redwood City, CA, USA) in powder form. Commercial glucose dehydrogenase GDH-01 was supplied by InnoSyn B.V. (Geleen, The Netherlands) as liquid enzyme formulation.

3.3 Recombinant expression of enzymes

The recombinant production of enzymes was performed by the project partners and co-workers working at InnoSyn B.V. (Geleen, The Netherlands).

P450 BM3 (CYP102A1 from *Bacillus megaterium* BM3) wild type (WT) and mutant M22C02 were recombinantly produced in *Escherichia coli* in a 20 L scale batch fermentation employing an *E. coli* K12 derivative and a pBAD/myc-HisC based expression vector. Glucose dehydrogenase (GDH) from *Thermoplasma acidophilum* (GDH-Tac) was co-expressed (in the cases of P450 BM3 WT/GDH-Tac and P450 BM3 M22C02/GDH-Tac lysates) from the same vector in a poly-cistronic arrangement of the GDH gene downstream of the P450 BM3 gene. A 500 mL pre-culture were used to inoculate 20 kg main culture medium with 100 µg mL^{-1} neomycin. The pre-culture was prepared in standard Luria-Bertani (LB) medium supplemented with 100 µg mL^{-1} neomycin. The fermentation was performed using terrific broth (TB) medium with glycerol. 2.5h after inoculation of the fermenter as inducer, pre-sterilized L-arabinose was added to the fermenter to final concentration 0.02% (w/v). Twenty-four hours after inoculation of the fermenter, the cell material was harvested by centrifugation.

Glucose dehydrogenase from *Thermoplasma acidophilum* (GDH-Tac) was recombinantly produced in *Escherichia coli* in a 10 L scale fed-batch, high cell-density fermentation with glucose a growth limiting C-source employing an *E. coli* K12 derivative and a pBR322 derived expression vector. A 500 ml pre-culture were used to inoculate 10 kg main culture medium with 100 µg mL^{-1} neomycin. The pre-culture was prepared in standard LB medium supplemented with 100 µg mL^{-1} neomycin. The fermentation was performed using mineral medium supplemented with 20 g L^{-1} yeast extract. 1.5 d after inoculation of the fermenter as inducer, pre-sterilized inducer was added to the fermenter to final concentration 0.02 % (w/w). After about 100h the biomass was harvested by centrifugation.

ADHaa from *Artemisia annua* and the NAD(P)H oxidase (NOX) variant from *Streptococcus mutans* were recombinantly produced in *Escherichia coli* in 10 L scale fed-batch, high cell-density fermentations with glucose as growth limiting carbon source employing an *E. coli* K12 derivative and a pBR322 derived expression vectors. 500 ml pre-cultures were used to inoculate 10 kg main culture medium with 100 µg mL^{-1} neomycin. The pre-cultures were prepared in standard LB medium supplemented with 5 g L^{-1} glycerol and 50 µg mL^{-1} neomycin. The fermentations were performed using mineral medium supplemented with 20 g L^{-1} yeast extract (25 g L^{-1} for NOX). Approximately 29h after inoculation (25h for NOX) of the fermenters as inducer, pre-sterilized L-rhamnose was added to the fermenters to final concentrations of 0.5% (w/w). After about 102 and 126h for ADHaa and NOX, respectively, the biomass was harvested by centrifugation.

Cyclohexanone monooxygenase from *T. municipale* (TmCHMO) was recombinantly produced in *Escherichia coli* in a 10 L scale fed-batch, high cell-density fermentations with glucose as growth limiting C-source employing an *E. coli* K12 derivative and a pBR322 derived expression vectors. 500 mL pre-culture was used to inoculate 10 kg main culture medium with 100 µg mL^{-1} neomycin. The pre-culture was prepared in standard Luria-Bertani medium supplemented with 100 µg mL^{-1} neomycin. The fermentation was performed using mineral medium supplemented with 20 g L^{-1} yeast extract. 1.5 d after inoculation of the fermenter as inducer, pre-sterilized L-arabinose was added to the fermenter to final concentration 0.02 % (w/w). After about 100h the biomass was harvested.

The fermentation broths were harvested either by centrifugation (wet cells) and the supernatant discarded or the fermentation broth was used as biocatalyst as such (**broth**). The **sonicated broth** was prepared by sonication of the broth with an ultrasound probe for 20 minutes (10 seconds on, 10 seconds off) with cooling on ice. **Whole cell** formulations were prepared by adding 2 weight equivalents of 100 mM potassium phosphate (KPi) buffer (pH 7.0) to 1 equivalent of *E. coli* wet cells (333.3 g_{cww} L^{-1}). **Cell free extracts** (CFE) were prepared by disrupting the whole cell formulation by homogenization using a Microfluidics M-110P (Westwood, MA, USA) homogenizer. **Liquid formulation** (LF) of fermentation was prepared by sonication of the whole cell formulation with an ultrasound probe for 20 minutes (10 seconds on, 10 seconds off) with cooling on ice.

3.4 Total protein and enzyme content

The cell lysates were pre-clarified by centrifugation (3220 g for 15 min.) and analyzed accounting for total protein content by means of Bradford Protein Assay Kit (Thermo Fisher Scientific, Waltham, MA, USA) using bovine serum albumin as standard [118].

Enzyme content was assessed using sodium dodecyl sulphate polyacrylamide gel electrophoresis (SDS-PAGE) (NuPage 12%, Invitrogen, USA) run in a Mini-PROTEAN II apparatus (BioRad, Hercules, CA, USA) following the protocol of Laemmli *et al.* [119]. Low range protein markers were used for molecular weight determination. Gels were stained using Coomassie G250 colloidal stain solution [34% (v/v) ethanol, 2% (v/v) H_3PO_4, 17% (w/v) NH_4SO_4 and 0.066% Coomassie G250] and the Image LAB^{TM} software (BioRad, Hercules, CA, USA) was used for image processing.

3.5 Active P450 BM3 content determination

P450 BM3 active form concentration was determined using the CO-differential spectra analysis described by Omura and Sato, using $\varepsilon = 91\ mM^{-1}\ cm^{-1}$ [120], [121].

3.6 Enzymes activity measurements

The activity presented by the lysates was measured spectrophotometrically ($\lambda = 340$ nm) following the consumption or production rate of NADPH ($\varepsilon = 6.22\ mM^{-1}\ cm^{-1}$). In the case of catalase, the activity was measured following the consumption of hydrogen peroxide ($\varepsilon = 0.0383\ mM^{-1}\ cm^{-1}$). One unit of activity (U) is defined as the enzyme required to convert 1 µmol of NADPH per minute at the given conditions. In all cases, 1 mL plastic micro cuvettes BRAND® UV (Sigma Aldrich®) were used for soluble enzymes and 3.5 mL quartz cuvettes HELLMA® 100-QS (Hellma Analytics, Mülheim, Germany) with magnetic stirring were used for the immobilized derivates. In the second case, with 3.5 mL cuvettes, the test amounts were 4-fold increased with respect to the soluble enzymes. The temperature was controlled and set at 30˚C for all lysates. The absorbance was recorded using a spectrophotometer Cary 50 Bio UV-visible (Palo Alto, USA). The background consumption or production of NADPH or by non-target enzymes present in the cell lysate was measured with the same test but avoiding the addition of substrate. The background consumption of NADPH by non-NOX enzymes present in the lysate was measured by bubbling nitrogen gas into the cuvette (2 – 4 min.) and so, stripping off the dissolved oxygen. The background activity was subtracted from the target measured activity. In the catalase case, the background activity could not be measured.

In all cases the linear range was found between 0.2 and 5 U mL^{-1} and the background activity never exceeded 5% of the total activity measured.

The amounts and concentrations used in every case with soluble enzymes are described below:

Table 3.1. P450 BM3 activity assay content.

Compound	Volume (500 µL)	[Stock]	[Final]
Sodium phosphate (NaPi) buffer, pH = 7.5	375 µL	50 mM	47.5 mM
Sodium laurate		1.75 mM	1.3 mM
NADPH (in NaPi, pH = 7.5)	100 µL	1 mM	200 µM
P450 BM3 sample	25 µL	ND	[Stock] x 1/20

Table 3.2. GDH-Tac, GDH-01 and GDH-105 activity assay content.

Compound	Volume (500 µL)	[Stock]	[Final]
NaPi buffer, pH = 8	425 µL	100 mM	95 mM
D-glucose		250 mM	212.5 mM.
NADP$^+$ (in NaPi buffer, pH = 8)	50 µL	4 mM	400 µM
GDH sample	25 µL	ND	[Stock] x 1/20

Table 3.3. Catalase activity assay content.

Compound	Volume (500 µL)	[Stock]	[Final]
H_2O_2	475 µL	20 mM	19 mM
NaPi buffer, pH = 7		50 mM	47.5 mM
Catalase sample	25 µL	ND	[Stock] x 1/20

Table 3.4. ADHaa activity assay content.

Compound	Volume (500 µL)	[Stock]	[Final]
NaPi buffer, pH = 7	350 µL	50 mM	47.5 mM
Cyclohexanone		14.5 mM	10.15 mM.
NADPH (in NaPi buffer, pH = 7)	125 µL	1 mM	250 µM
ADHaa sample	25 µL	ND	[Stock] x 1/20

Table 3.5. NOX activity assay content

Compound	Volume (500 µL)	[Stock]	[Final]
NaPi buffer, pH 6	300 µL	50 mM	47.5 mM
NADPH (in NaPi buffer, pH = 6)	175 µL	1 mM	350 µM
NOX sample	25µL	ND	[Stock] x 1/20

Table 3.6. TmCHMO activity assay content.

Compound	Volume (500µL)	[Stock]	[Final]
NaPi buffer, pH 8.5	425 µL	50 mM	47.5 mM
Cyclohexanone		0.6 mM	0.51 mM
NADPH (in NaPi buffer, pH = 8.5)	50 µL	1 mM	0.1 mM
TmCHMO sample	25 µL	ND	[Stock] x 1/20

3.7 Summary of the characterized lysates

As described in previous sections, the enzyme lysates were characterized accounting for protein concentration, enzyme content and specific activity.

Table 3.7. Summary of the characterization performed on all the lysates used

Lysate Construct	Supplier	Enzyme formulation†	Protein (mg mL^{-1})	Enzyme (mg enzyme mg^{-1} prot)	Activity (U mg^{-1} enz)
P450 BM3 WT/GDH-Tac	InnoSyn B.V.	CFE	45.4 ± 0.8	0.52 ± 0.01	5.4 ± 1.2
				0.14 ± 0.01	25.7 ± 2.9
GDH-Tac			63.4 ± 2.6	0.71 ± 0.02	1.4 ± 0.1
Catalase	Sigma Aldrich	Lyophilized powder	ND	0.59 ± 0.03	5610 ± 162*
P450 BM3 WT	InnoSyn B.V.	CFE	41.9 ± 1.3	0.44 ± 0.01	5.4 ± 0.3
GDH-01			47 ± 1.4	0.58 ± 0.04	311 ± 29
P450 BM3 M22C02/GDH-Tac	InnoSyn B.V.	CFE	55.1 ± 0.7	0.31 ± 0.0	0.91 ± 0.02
				0.3 ± 0.0	14.5 ± 1.6
ADHaa			34.8 ± 2.1	0.4 ± 0.03	13.1 ± 0.6
NOX			50.1 ± 2.3	0.61 ± 0.04	66.5 ± 0.8
TmCHMO			48 ± 4	0.55 ± 0.01	1.76 ± 0.06
GDH-105	Codexis®	Lyophilized powder	ND	ND	39.4 ± 3.5*

† Enzyme formulation used for the characterization of the lysates. The formulation in the reactions may change.

* Activity of the lyophilized powders. It is expressed as U mg^{-1} of lyophilized powder.

3.8 Stability studies

3.8.1 Substrates and products stability under reaction conditions

For every reaction studied, a negative control was performed to check for substrate and product/s stability as well as evaporation issues. For this purpose, the reaction conditions were mimicked and the target enzyme (P450 BM3, ADH or TmCHMO) was not included in the mixture. In case of substrates and/or products instabilities or loses, it was reported in the manuscript and the subsequent corrections were made when calculating, for example, the reaction conversion.

3.8.2 ADHaa and GDH-01 stability on different pH

The activity decay of four GDH-01 samples (0.8 U mL^{-1}) each one presenting a different pH value (5, 6, 7 and 8) was measured over time. The activity decay of ADHaa (1.8 – 2 U mL^{-1}) was studied in pH media 6, 7, 8 and 9 (NaPi, 50 mM). Both lysates were diluted in 50 mM phosphate buffer solutions and the pH was adjusted using either 1M HCl or 1M NaOH. The study was performed at 25˚C and mild agitation. Samples were taken periodically and measured using the activity test explained above.

Furthermore, the activity decay of three GDH-01 samples presenting different enzyme concentrations was measured after 1 hour incubation at pH 6, 7 or 8 each. The LF containing the over-expressed GDH-01 was diluted 100-fold, 1000-fold and 10000-fold containing 0.47, 0.047 and 0.0047 mg prot mL^{-1} respectively. Each of these solutions was then incubated for 1 hour at 30˚C in 50 mM phosphate buffer solutions (pH 6, 7 or 8).

3.9 Immobilization metrics

In every immobilization, a characterization was pursued in order to obtain the retained activity (RA) (equation 1) and immobilization yield (IY) (equation 2). Supernatant and suspension activities were analysed over time until a steady state was reached and in all cases the activity of a blank (no support) was also monitored to ensure that the enzyme activity was not affected by protocol's conditions. A 10% (w/v) relation between the support and the total volume was always established and small amounts of enzyme were loaded (1 - 5 U g^{-1} of support) so that diffusional limitations were minimized.

$$Retained\ activity\ (\%) = \frac{Suspension\ activity\left(\frac{U}{g}\right) - Supernatant\ activity\left(\frac{U}{g}\right)}{Initial\ offered\ activity\left(\frac{U}{g}\right)}\ x\ 100 \quad \textit{(Equation 1)}$$

$$Immobilization\ yield\ (\%) = \left(1 - \frac{Supernatant\ activity\ \left(\frac{U}{g}\right)}{Initial\ offered\ activity\ \left(\frac{U}{g}\right)}\right)\ x\ 100 \quad \textit{(Equation 2)}$$

For the assessment of the loading capacity the supports were saturated with enzyme and the activity was calculated taking into account that diffusional limitations do not allow the actual visualization of the activity in the support (equation 3) [122].

$$Loading\ capacity\ \left(\frac{U}{g}\right) = \left(Offered\ initial\ activity\ \left(\frac{U}{g}\right) - Supernatant\ activity\ \left(\frac{U}{g}\right)\right)\ x\ \frac{Retained\ activity\ (\%)}{Immobilization\ yield\ (\%)} \quad \textit{(Equation 3)}$$

In section 6, the loading capacity of ADHaa on epoxy-agarose-M2 (U g^{-1} support) is calculated using specific terms. First, the *Attached units* were calculated from the measured supernatant activity and the initial loaded activity. The Attached units (theoretical units attached to the support) equal to the units of activity missing from the supernatant (equation 4):

$$Attached\ units\ (U\ g^{-1}) = \frac{Activity\ loaded\ (U\ mL^{-1}) - Activity\ supernatant\ (U\ mL^{-1})}{Support\ loaded\ (g)}\ x\ Total\ volume\ (mL) \quad \textit{(Equation 4)}$$

Then, the *Multiplying factor* was calculated with the RA and IY values obtained in the characterization stage. The Multiplying factor results from dividing the retained activity by the immobilization yield at each given time. Finally, the *Specific activity* was obtained. It is the final theoretical specific activity (U g^{-1} support) of the immobilized derivate. It is the product of multiplying the Attached units by the Multiplying factor.

Moreover, the amount of protein per gram of support was also calculated in some cases, analysing the initial protein content and subtracting from it, the concentration still remaining in the supernatant at the end of the process. In all cases protein concentration was determined by means of Bradford Protein Assay Kit, as already described.

3.10 Immobilization studies

3.10.1 Methacrylate/styrene and epoxy-agarose supports from Purolite®

From Purolite®, a set of commercially available methacrylate/styrene resins presenting a variety of matrices, pore sizes, linker lengths, and functional groups (sections 4.2.2, 6.4 and 8.4) were tested for the immobilization of P450 BM3, ADHaa and GDH-01. The conditions in which immobilizations were carried out in each case were those specified by the supplier's protocols.

In all cases, the relation of 10% (w/v) between support and total volume was maintained. The immobilizations were done at 25°C and mild agitation. The incubation times ranged from 0.5 to 5 hours depending on the speed at which the enzymes were attached.

The epoxy functionalized methacrylates (ECR8204F, ECR8215F and ECR8285) were tested using 1 M potassium phosphate (KPi) buffer pH 8 to increase the ionic strength and favor the attachment. The amino functionalized carriers (ECR8309F, ECR8315F, ECR8409F and 8415F) were studied using 50 mM KPi buffer pH 7. The immobilization with amino functionalized supports is divided in three steps: i) ionic adsorption of the enzyme onto the support (0.5h) ii) addition of 10 mM *N*-(3-dimethylaminopropyl)-*N′*-ethylcarbodiimide (EDC) and incubation for 1.5 hours to promote the covalent binding and iii) addition of 0.5M NaCl to desorb all the protein attached non-covalently (0.5h). The non-functionalized supports (ECR8806F, ECR1061M and ECR1030M) were tested using 50 mM KPi pH 7. The amino resins were further functionalized with 2% w/v glutaraldehyde for 60 min at 25˚C leaving free aldehyde groups on the surface of the carrier. The immobilization was carried out using 50 mM KPi buffer pH 7. Finally, immobilizations using the epoxy agaroses (Praesto 45, 65 and 90) were performed in 1 M potassium phosphate buffer pH 8.

A criterion was set to consider a support as good candidate for further optimization, 90% immobilization yield and 20% retained activity.

3.10.2 Immobilization of enzymes on functionalized agaroses

For the other epoxy-agaroses (epoxy-agarose-SIGMA, epoxy-agarose-M1 and M2), the enzyme was dissolved in 1 M (pH 8 - 9) potassium phosphate buffer, mixed with the resin (10% (w/v)) and left at 25°C with mild agitation. The epoxy-agaroses M1 and M2 were incubated for 4 hours and epoxy-agarose-SIGMA was incubated for 0.5 h. At the end of the process, in order to eliminate the unreacted epoxy groups, the samples were incubated with 0.2 M β-mercaptoethanol for at least 2 h at 25°C.

For the immobilization using Glyoxyl-agarose different pH's were tested (6.5 – 8.5) using 50 mM sodium phosphate buffers. The immobilizations lasted 6 hours and were done at 25°C and mild agitation. For the reduction of the Schiff base, two different reducing agents were studied: sodium borohydride (1 mg mL^{-1}) added at the end of the immobilization and sodium cyanoborohydride (0.05 mg mL^{-1} for characterization and 0.4 mg mL^{-1} for high loads of enzyme) added at the beginning of the immobilization.

For Mana-agarose, 50mM sodium phosphate buffer (pH 6) was used to dissolve the enzymes and mix it with the support. The enzymes were left to ionically adsorb onto the support for 0.5h - 1h. After that, a 200mM stock solution of *N*-(3-Dimethylaminopropyl)-*N'*-ethylcarbodiimide (EDC) was prepared dissolving it in 50 mM phosphate buffer and adjusting to pH 6 with HCl. It was then added at different concentrations and incubated for 30 min. to activate the carboxyl groups and promote the covalent binding. In most cases the concentration of EDC was optimized in in the characterization phase (from 1 to 20 mM) and, with P450 BM3, it was also optimized when using high loads of enzyme (3, 6, 12, 30, 60 mM). Finally, 0.5 M NaCl was introduced to desorb all the protein attached non-covalently. The immobilization was carried out at 25°C with mild agitation.

With ADHaa no carnodiimide was added and so, no covalent bond was formed. The support was loaded with 12 – 13 U g^{-1} of support (0.9 – 1 mg of enzyme g^{-1} of support) and, three different pH values were tested: 6, 6.5 and 7 (NaPi, 50 mM).

3.10.3 Co-immobilization of P450 BM3 and GDH on Mana-agarose and epoxy-agarose M1

The conditions in which co-immobilizations were carried out were the same as the ones previously optimized for P450 BM3 WT. The activity of the GDH present in the lysate was also monitored in this stage together with the P450 BM3. Retained activities and immobilization yields were obtained for GDH and P450 BM3.

3.10.4 Co-Immobilization of P450 BM3 WT and GDH-Tac into polyvinyl alcohol lenses (Lentikats®)

Co-immobilization of GDH-Tac and P450 BM3 WT by entrapment was carried out using an organic polymer commercialized as Lentikats®. The solid mixture was heated to 95°C until it turned into a transparent liquid. Then it was cooled down to 40°C and 8 mL of the polymer were mixed with 2 mL of a suspension containing the desired amount of biocatalyst. Afterwards the mixture was poured on a petri dish and the lenses were printed using the LentiPrinter® (Lentikats®, Ralskem, Czech Republic). The resulting plates were left to dry at 25°C for 1 h until they lost 80% of their weight approximately. Once printed, the support adopted a lentil-like shape of 1 - 2 mm diameter and 200 - 300 µm wide where the proteins were entrapped inside.

3.11 Oxidoreductive reactions

3.11.1 Reactor configurations and pictures

Each reactor and set up was adapted to the reaction requirements. Furthermore, part of the experimental work was performed in two different labs. A summary of the specifications of each case is detailed in the table below. After this table, a scheme and a picture of each reactor is showed.

Table 3.8. The reactor configurations utilized throughout this thesis and their main features.

Results section	Reaction	Enzymes involved	Total reactor volume	Working volume	Stirring	Temperature control	pH control	Aeration	Dissolved oxygen sensor	Outlet oxygen sensor
4.2.6	Sodium laurate hydroxylation	P450 BM3 WT & GDH-Tac	8 mL	5 mL	Thermo-shaker	Thermoblock	No	No	No	No
5.2.2	α-isophorone hydroxylation	P450 BM3 WT/GDH-Tac & P450 BM3 WT & GDH-01 & catalase	80 mL	30 mL	Mechanical	Jacketed reactor	Biostat B	O_2	Biostat B	No
5.2.4-6			10 mL	5 mL	Magnetic	Thermostated vessel	Titrino 718	O_2	OX-NP Unisense	No
5.2.7-8			20 mL	10 mL						
5.2.11	Diclofenac hydroxylation	P450 BM3 M22C02/GDH-Tac	10 mL	5 mL	Magnetic	Thermostated vessel	Titrino 718	O_2	No	No
6.2.5	4-hydroxy-isophorone oxidation	ADHaa & NOX	20 mL	10 mL	Magnetic & Mechanical	Thermostated vessel	No	O_2	No	No
7.2.1 **8.2.4**	3,3,5-trimethylcyclohexanone oxygenation	TmCHMO & GDH-105 or GDH-01	80 mL	30 mL	Mechanical	Jacketed reactor	Titrino plus 877	Air	No	No
7.2.2			2 L	1 L				O_2	F4-Field Five Go Mettler	SDL 150 ExTech
7.2.3			200 L	100 L						

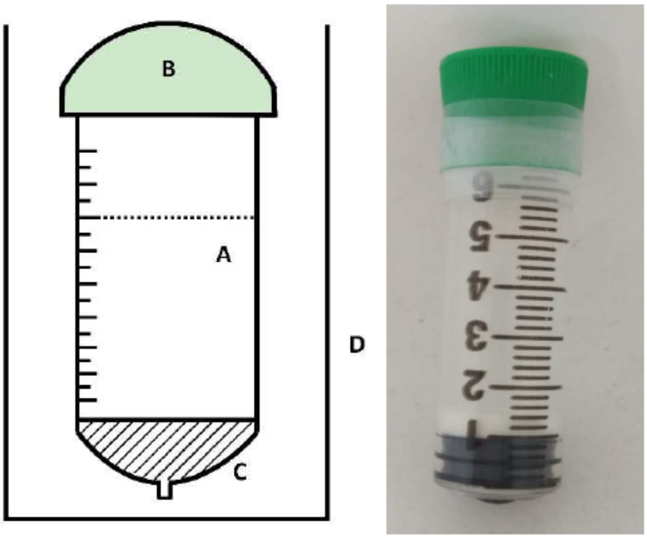

Figure 3.1. Sodium laurate hydroxylation 8 mL (V_T = 5 mL) reactor: scheme (left) and picture (right). Results section 4.2.6. A) syringe-like 8 mL reactor, B) reactor cap, C) porous plate and rubber plug and D) thermo-shaker.

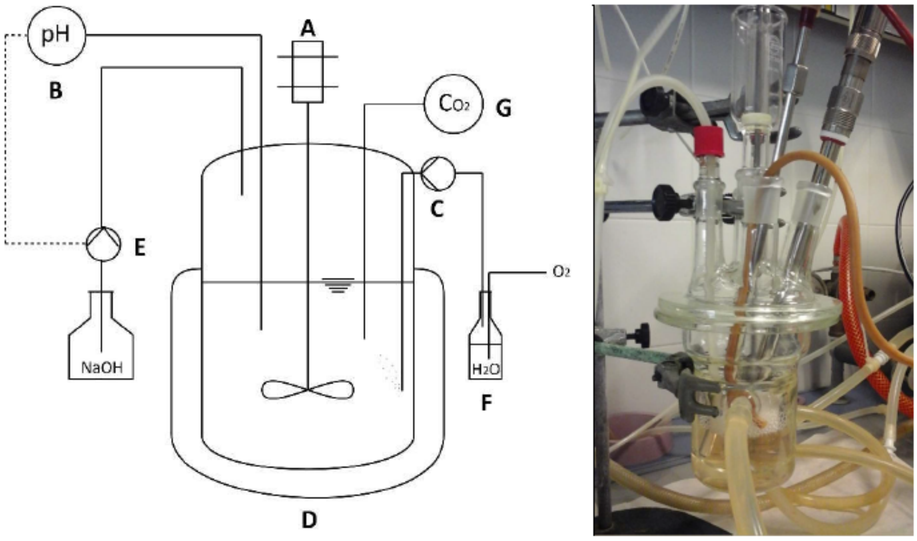

Figure 3.2. α-isophorone hydroxylation 80 mL (V_T = 30 mL) reactor: scheme (left) and picture (right). Results section 5.2.2. A) stirrer, B) pH electrode, C) air supply controller, D) jacketed 80mL reactor, E) automatic titration device, F) gas washing bottle and G) liquid phase oxygen probe.

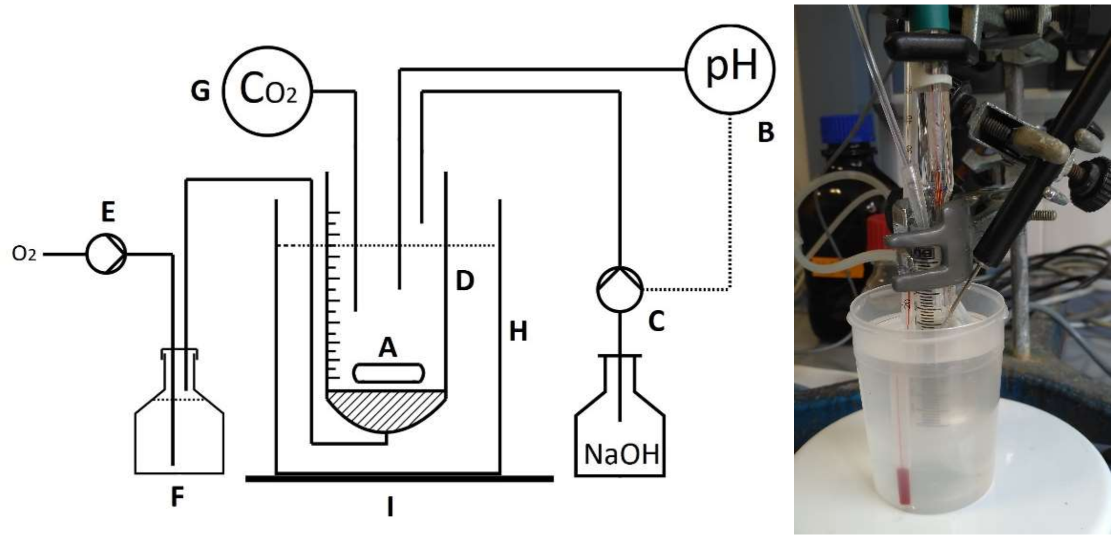

Figure 3.3. α-isophorone and diclofenac hydroxylation; and 4-hydroxy-isophorone oxidation 10 - 20 mL (V_T = 5 - 10 mL) reactor: scheme (left) and picture (right). Results section from 5.2.4 to 5.2.8 and 5.2.11 and 6.2.5. A) magnetic (or mechanic) stirrer, B) pH electrode, C) automatic titration device, D) 10 to 20 mL syringe-like reactor with a porous plate at the bottom, E) oxygen supply controller, F) gas washing bottle, G) liquid phase oxygen probe, H) thermostated plastic vessel and I) thermo-magnetic source of heat and stirring.

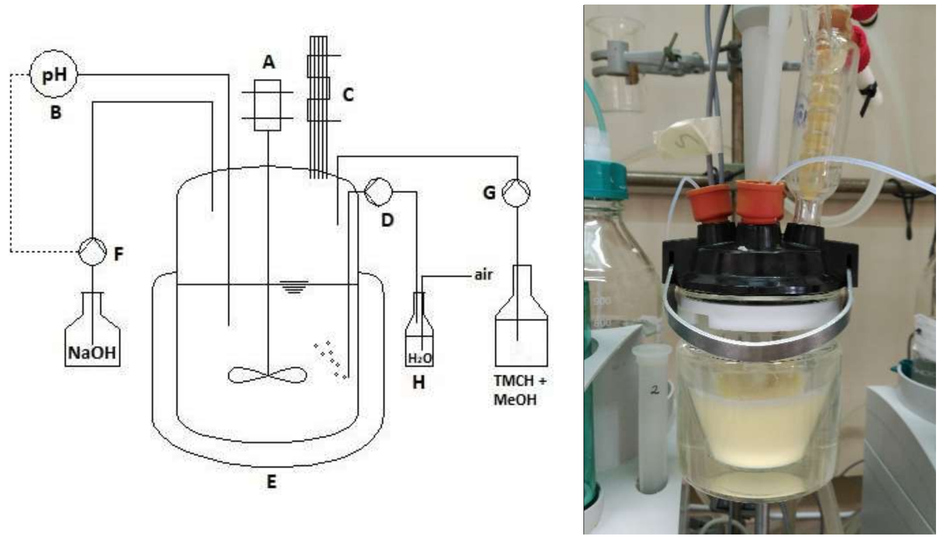

Figure 3.4. 3,3,5-Trymethylcyclohexanone oxidation using 80 mL (V_T = 30 mL) reactor: scheme (left) and picture (right). Results section 7.2.1 and 8.2.4. A) stirrer, B) pH electrode, C) reflux-condenser, D) air supply controller, E) jacketed 80mL reactor, F) automatic titration device, G) substrate dosing pump and H) gas washing bottle.

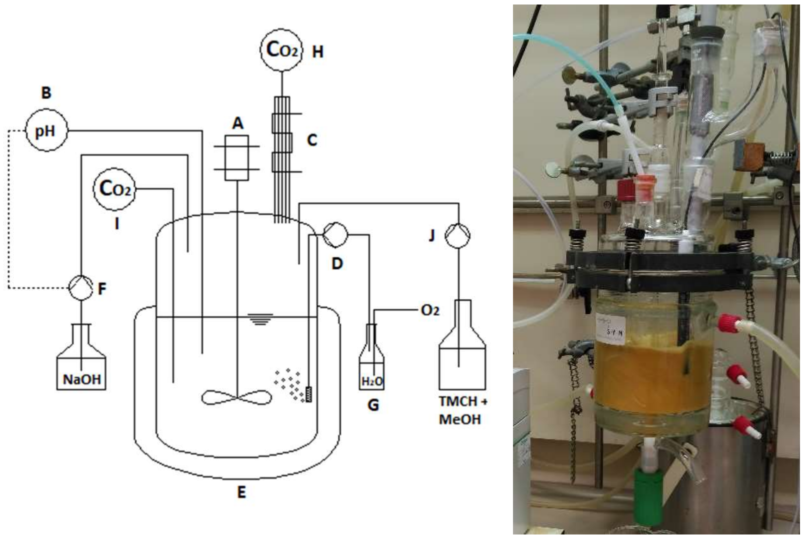

Figure 3.5. 3,3,5-Trymethylcyclohexanone oxidation using 2 L (V_T = 1 L) reactor: scheme (left) and picture (right). Results section 7.2.2. A) stirrer, B) pH electrode, C) reflux-condenser, D) oxygen supply controller, E) jacketed 2000 mL reactor, F) automatic titration device, G) gas washing bottle H) oxygen sensor in gas outlet I) oxygen sensor in reaction mixture and J) substrate dosing pump.

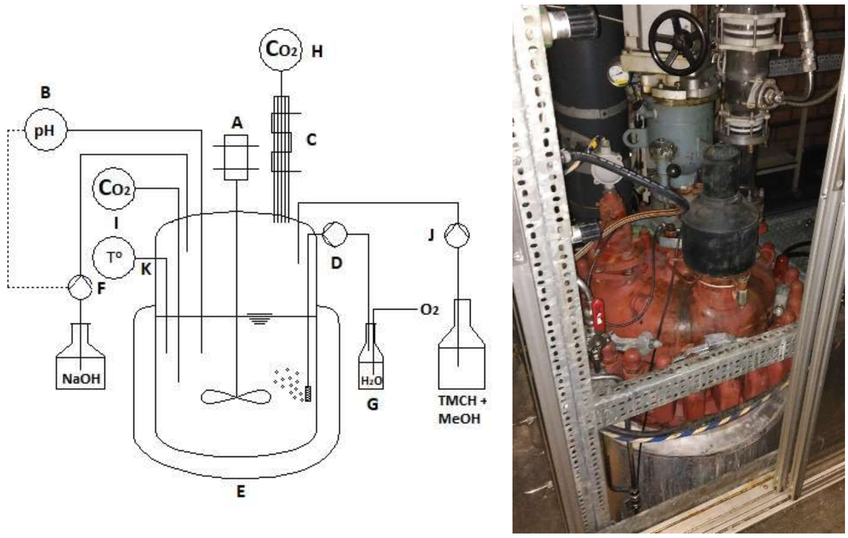

Figure 3.6. 3,3,5-Trymethylcyclohexanone oxidation using 200 L (V_T = 100 L) reactor: scheme (left) and picture (right). Results section 7.2.3. A) stirrer, B) pH electrode, C) reflux-condenser, D) oxygen supply controller, E) jacketed 2000 mL reactor, F) automatic titration device, G) gas washing bottle H) oxygen sensor in gas outlet I) oxygen sensor in reaction mixture J) substrate dosing pump and K) temperature probe.

3.11.2 Hydroxylation of sodium laurate catalyzed by P450 BM3 WT/GDH-Tac

The enzymes used in this case were the P450 BM3 WT and the GDH-Tac. The lysate used in this case was the co-expressed P450 BM3 WT/GDH-Tac and also the GDH-Tac solely expressed to ensure sufficient cofactor regeneration. The 8 mL reactor (V_T = 5 mL) contained 1.53 mM sodium laurate, 0.2 mM NADP$^+$ and 12.5 mM D-glucose. All dissolved in 50 mM sodium phosphate buffer pH 7.5. The enzyme added was the minimum necessary to convert at least 90% of the initial substrate in 1 hour [0.18 - 0.2 U P450 mL^{-1} (0.063 - 0.07 nmols mL^{-1})]. The reactors used were purchased from MultiSynTech (Witten, Germany) and consisted of 8 mL plastic syringe-like vessels with a porous plate at the bottom, a plastic cap on top and a rubber plug below the porous plate to avoid leaking. It allowed the extraction of the whole reactor liquid content by filtering with this same porous plate without losing any fraction of the immobilized derivative. The reactor was sealed and no aeration was applied. The reaction took place at 25°C and 1000 rpm using a Multi-Therm H5000-HC-E thermo-shaker (Benchmark Scientific Inc., Sayreville, NJ, USA). After each cycle, the immobilized enzymes were washed twice with sodium phosphate buffer 50 mM pH 7.5 then new reaction medium was added and substrate conversion was quantified.

3.11.3 Hydroxylation of α-isophorone catalyzed by P450 BM3 WT and GDH-Tac

The enzymes used in this case were the P450 BM3 WT and the GDH-Tac. In the 50 mM substrate concentration reaction (3.11.3.3) the commercial GDH-01 was used instead of the GDH-Tac. The lysates used were the co-expressed P450 BM3 WT/GDH-Tac for the sections 3.11.3.1 and 3.11.3.2; the solely expressed GDH-Tac for section 3.11.3.1 and 3.11.3.2; the solely expressed P450 BM3 WT for section 3.11.3.3; and the GDH-01 for the section 3.11.3.3.

3.11.3.1 Reactions with 2 mM substrate concentration and 30 mL total/working volume (V_T)

The first reactions performed were carried out in a 80 mL (V_T = 30 mL) jacketed glass reactor. The content was stirred with a stainless steel stirrer set at 500 rpm (Heidolph stirrer – RZR 1, Schwabach, Germany), the temperature was set at 30˚C and the pH was controlled with a 1 M NaOH solution. A bioreactor controller Biostat B – Braun Biotech (Sartorius, Gotinga, Germany) controlled both the temperature and the pH. Furthermore, this same equipment allowed the monitoring of dissolved oxygen. An oxygen inlet was placed at the bottom of the vessel and the flow was set at 100 mL min^{-1}; and controlled by a mass-flow controller F-201C-FAC-20-V (Bonkhorst HI-TEC BV, Ruurlo, The Netherlands). The conditions applied for this reactions were: enzyme load 3.5% (v/v) of P450 BM3 WT/GDH-Tac CFE (127.1 U of P450 mL^{-1} of CFE and 163.4 U of GDH-Tac mL^{-1} of CFE) and 3.5% (v/v) of GDH-Tac CFE (63 U mL^{-1} of CFE); [α-isophorone] 2 mM; [D-glucose] 40 or 500 mM; [NADP+] 0.4 mM; everything dissolved in 50 mM NaPi buffer pH 7.

3.11.3.2 Reactions with 10 mM substrate concentration and 5 mL total volume

The reactor used in this case was a 10 mL (5 mL working volume) plastic syringe-like reactor (MultiSynTech GmbH, Witten, Germany) with a porous plate disposed at the bottom. It was submerged in a 50 mL thermostated plastic vessel with the temperature set at 30 ˚C and controlled manually. The heat source as well as the magnetic stirring (1000 rpm) were provided by an MS-H-PRO agitator (DDBiolab, Barcelona, Spain). The pH was set at 7 and it was controlled with a Titrino 718 (Metrohm, Herisau, Switzerland) filled with a 0.5 M NaOH solution. The reactor's porous plate served as an oxygen diffusor as well as a filter for the immobilized derivates. An oxygen flow of 0.45 mL min^{-1} was applied and controlled by a mass-flow controller F-200CV-005-AAD-11-V (Bonkhorst HI-TEC BV, Ruurlo, The Netherlands) the dissolved oxygen was monitored by and Oxygen sensor [for needle piercing (NP)] (Unisense, Aarhus, Denmark).

This configuration was used in a series of experiments where both soluble and immobilized enzymes were utilized: results sections 5.2.4, 5.2.5 and 5.2.6. The enzyme loads used in the soluble reaction (no catalase) were: 7% (v/v) P450 BM3 WT/GDH-Tac (127.1 U of P450 mL^{-1} of CFE and 163.4 U of GDH-Tac mL^{-1} of CFE). The enzyme loads for the Mana-agarose immobilized enzymes were: 10% (w/v) immobilized P450 BM3 WT/GDH-Tac (53 U of P450 g^{-1} of support and 18 U of GDH-Tac g^{-1} of support). The enzyme loads for the epoxy-agarose immobilized enzymes were: 10% (w/v) immobilized P450 BM3 WT/GDH-Tac (30 U of P450 g^{-1} of support and 3 U of GDH-Tac g^{-1} of support). The enzyme loads used in the soluble reaction with catalase were: 7% (v/v) P450 BM3 WT/GDH-Tac (127.1 U of P450 mL^{-1} of CFE and 163.4 U of GDH-Tac mL^{-1} of CFE) and 0.1% (w/v) bovine liver catalase (5610 U mg^{-1} lyophilized powder). The enzyme loads for the epoxy-immobilized derivate with catalase were: 10% (w/v) immobilized P450 BM3 WT/GDH-Tac (30 U of P450 g^{-1} of support and 3 U of GDH-Tac g^{-1} of support) and 0.1% (w/v) bovine liver catalase (5610 U mg^{-1} lyophilized powder).

The rest of conditions applied in these reactions were: [α-isophorone] 10 mM; [D-glucose] 500 mM; [NADP$^+$] 0.4 mM; everything dissolved in 50 mM NaPi buffer pH 7.

3.11.3.3 Reactions with 50 mM substrate concentration and 10 mL total volume

The same configuration and conditions explained above were also used here to perform a set of reactions with 50 mM substrate concentration and soluble enzymes. In this case a 20 mL (10 mL working volume) syringe-like reactor was used. The lysates applied were also different. The P450 BM3 WT was not co-expressed with the GDH-Tac and the GDH utilized was the commercial GDH-01, supplied by InnoSyn B.V. (Geleen, The Netherlands).

The enzyme loads varied depending on the experiment. The P450 BM3 WT load changed from 5% (v/v) to 25% (v/v) and the GDH-01 load changed from 1.7% (v/v) to 5% (v/v). In the case of P450, the total load was divided in 3 and 5 pulses in the last two reactions (results section 5.2.8). In the last reaction, where the P450 load was divided in 5 pulses, 250 mM extra glucose was added after 6 hours of reaction.

3.11.4 Hydroxylation of diclofenac catalyzed by P450 BM3 M22C02 and GDH-Tac

The enzymes used here were the P450 BM3 M22C02 and the GDH-Tac. The lysates applied were the co-expressed P450 BM3 M22C02/GDH-Tac and the solely expressed GDH-Tac to ensure enough cofactor regeneration. The same reactor configuration explained in section 3.11.3.2 was used here for the hydroxylation of diclofenac. In this case, the oxygen was not monitored.

The loads for the reaction with soluble enzymes were 7% (v/v) of P450 BM3 M22C02/GDH-Tac lysate (15.5 U of P450 mL^{-1} of CFE and 239.7 U of GDH mL^{-1} of CFE). The loads for the reaction with immobilized enzymes on epoxy-agarose were 10% (w/v) of P450 BM3 M22C02/GDH-Tac derivate (5.8 U of P450 g^{-1} of support and 13.8 U of GDH g^{-1} of support).

The rest of applied conditions were: temperature 28˚C; agitation 1000 rpm; oxygen flow 0.45 mL min^{-1}; [diclofenac] 3.5 mM; [D-glucose] 500 mM; [$NADP^+$] 0.4 mM; [methanol] 3% (v/v) everything dissolved in NaPi buffer 50 mM pH 7.2

3.11.5 Oxidation of 4-hydroxy-isophorone catalyzed by ADHaa and NOX

The reactions were performed in a similar manner as explained for the hydroxylation of α-isophorone (3.11.3.3). In this case the reactor was stirred (1000 rpm) either magnetically with a MS-H-PRO agitator (DDBiolab, Barcelona, Spain) or mechanically with a stainless steel stirrer (Heidolph stirrer – RZR 1, Schwabach, Germany). Since no GDH was used here, the pH was checked at the beginning of the reaction but it was not controlled.

The conditions for both soluble and immobilized reactions were: 10 mL total volume, 50 mM NaPi buffer pH 7.2, 50 mM [4-hydroxy-isophorone], 1 mM [$NADP^+$] and 0.45 mL min^{-1} O_2 flow regulated with a mass-flow controller F-200CV-005-AAD-11-V (Bonkhorst HI-TEC BV, Ruurlo, The Netherlands).

The soluble reaction contained 5% (v/v) of ADHaa lysate (271.6 U mL^{-1} of CFE) and 3% (v/v) of NOX lysate (2032.2 U mL^{-1} of CFE) while the immobilized reactions contained 10% (w/v) of ADHaa immobilized derivate (106.4 or 132 U g^{-1} of support) and 3% (v/v) of NOX lysate (2032.2

U mL^{-1} of CFE). In the second case, at the end of each cycle of reaction, the reactor content was filtered and the support was washed gently with NaPi buffer 50 mM pH 7.2.

3.11.6 Baeyer-Villiger oxidation of trimethyl-ε-caprolactone catalyzed by TmCHMO and GDH

The enzymes used in this case were the TmCHMO , the GDH-105 and the GDH-01. Both the TmCHMO and GDH-01 were produced separately by InnoSyn B.V. The GDH-01 was obtained from Codexis® as a lyophilized powder. The biocatalytic reactions were performed in cylindrical jacketed reactors that consisted of a glass vessel (30 mL and 1 L) or glass-lined stainless steel vessel (100 L); a pH controller (Metrohm Titrino plus 877, Herisau, Switzerland) filled with 1 M NaOH solution (30 mL) or 5 M NaOH solution (1 L and 100 L); a propeller stirrer, a thermostat (MGW-LAUDA RC6, Lauda-Brinkmann, Delran, NJ, USA) set at 30˚C, a condenser at 6˚C, a compact mass flow regulator (GCR Red-y, Vögtlin Ins., Aesch, Switzerland) to keep a constant air/oxygen flow; and substrate dosing pump (Harvard Pump11, Harvard Apparatus, Holliston, MA, USA). For the 1 L and 100 L reactions, the reactors also contained an oxygen sensor (SDL 150 – Extech Instruments, Waltham, MA, USA) in the gas outlet, an oxygen sensor F4-Field Five Go (Mettler Toledo, Columbus, OH, USA) for the liquid phase and a constant nitrogen flow in the headspace to maintain the oxygen concentration below 8% and prevent the formation of potentially explosive mixtures.

For the reaction with soluble biocatalysts (broth, sonicated broth, whole cells or cell free extract) the following conditions were used: temperature 30°C; stirring rate 400 - 1200 rpm; air flow 16 mL min^{-1}; pH 6 - 8; [D-glucose] 375 mM; [$NADP^+$] 0.25 mM; titration solution 1 or 5 M NaOH. The enzyme loads, the substrate concentration, the substrate dosing rate, the oxygen flow, the methanol concentration and the methanol dosing rate varied depending on the experiment.

For the reactions catalyzed by immobilized enzymes the support loaded varied from 1.7% to 10% (w/v), the substrate dosing rate was 29 mM h^{-1} (132.5 mM final concentration) and the methanol dosing rate was 2.17% (v/v) h^{-1} [10% (v/v) final concentration]. The rest of conditions were the same as for the reaction with soluble biocatalysts.

3.12 Reaction progress determination - sampling

For sodium laurate reactions, samples were taken periodically (500 µL), heated up to 70˚C for 5 min to stop the reaction, filtered (Ø 0.22µm) and 50µL of hexanoic acid (2.8 mg mL^{-1}), that served as internal standard (IS), were added to 300 µL of sample. The mixture was then analyzed by means of a gas chromatograph (GC) equipped with a flame ionization detector (FID).

In the case of α-isophorone, 4-hydroxy-isophorone, keto-isophrone, glucose and diclofenac, samples (50 µL) were taken periodically to follow the reaction performance and, if necessary, were 10-fold diluted in buffer NaPi 50 mM pH 7 – 7.5. Then, samples were 40-fold diluted in acetonitrile. After centrifuging and filtering (Ø 0.45 µm) the samples were analysed by a high performing liquid chromatograph (HPLC) equipped with a ultra-violet detector (UV). In the case of glucose, the HPLC was equipped with a refractive index detector (RID). Replicates of glucose samples were also analysed using an YSI 2700D Select (Yellow Spring Instruments, Yellow Springs, OH, USA) instrument.

In the case of 3,3,5-trimethylcyclohexanone reactions, samples (150 µL) were taken periodically from the reactor, weighed and dissolved up to 10 mL with a solution of acetonitrile containing 0.5 g L^{-1} of hexadecane that served as internal standard. The mixture was centrifuged to remove insoluble biomass and the supernatant was analysed by means of GC-FID.

In all cases the concentration of substrate and products were determined using calibration curves.

3.13 Substrates and products analysis

3.13.1 Sodium laurate

Samples containing sodium laurate and its products were analysed using a 7890A gas chromatograph (Agilent Technologies, Santa Clara, CA, USA) equipped with a HP-INNOWAX 19095N-123 column (30 m, 0.53 mm, 1 µm, Agilent Technologies). The column temperature started at 150 °C, increased to 240°C at 24 °C min^{-1} and it was held at final temperature for 11 minutes. The injector temperature was kept at 300°C; for the flame ionization detector, the temperature was 320°C. Helium was used as a carrier gas at a flow rate of 8 mL min^{-1}.

3.13.2 α-isophorone, 4-hydroxy-isophorone and keto-isophorone

The samples were analyzed by a high performing liquid chromatograph HPLC Dionex UltiMate 3000 equipped with a Variable Wavelength detector (Thermo Fisher, Waltham, MA, USA) and a reverse-phase column CORTCS C18+ 2.7µm 4.6x150mm (Waters, Milford, MA, USA). To perform the analysis, 15 µL of sample were injected in a 0.7 mL min^{-1} mobile phase flow and the column was kept at 40˚C. The solvents consisted on: A) 0.1% trifluoroacetic acid in H_2O miliQ and B) 0.095% trifluoroacetic acid in acetonitrile/H_2O miliQ 4:1 (v/v). Samples were eluted using a gradient of solvents: 95% of A (5% of B) at the beginning, to 35% of A (65% of B) at 0.5 min. and down to 5% of A (95% of B) at 8 min.; then back to 95% of A (5% of B) at 8.1 min. and hold it as such until 13 min. Data was quantified by Chromeleon 6.80 Software (Dionex Corporation, Sunnyvale, CA, USA).

3.13.3 D-glucose

The glucose concentration was primary determined by HPLC with a HP 1050 liquid chromatograph (Dionex Corporation, Sunnyvale, CA, USA), equipped with a Refractive index detector (RID) Waters 2410 (Waters, Milford, MA, USA) and using an ICSep ICE COREGEL 87H3 column (Transgenomic Inc., Omaha, NE, USA). The isocratic mobile phase was 8 mM sulphuric acid in H_2O MilliQ. Injection volume was 20 µL.

The glucose concentration was also determined by means of an ISY 2700D Select (Yellow Spring Instruments). The sample was diluted in H_2O MilliQ.

3.13.4 Diclofenac and 4’/5’-hydroxy-diclofenac

These compounds were analysed using the same equipment and conditions as the ones used for α-isophorone. The only difference was that the samples were eluted using a gradient of solvents: 95% of A (5% of B) at the beginning, to 55% of A (45% of B) at 0.5 min. and down to 20% of A (80% of B) at 13 min.; then down to 0% of A (100% of B) at 13.5 min., hold it as such for 1.5 min. and back to 95% of A (5% of B) at 15.5 min. and hold it as such until 20 min.

3.13.5 3,3,5-trimethylcyclohexanone and trimethyl-ε-caprolactone

Samples containing 3,3,5-trimethylcyclohexanone and trimethyl-ε-caprolactones were analyzed using a 7890A gas chromatograph (Agilent Technologies) equipped with a HP-5 column (30 m, 0.32 mm, 0.25 µm df, Agilent Technologies). The column temperature was maintained at 60°C for 2 minutes, increased up to 300°C at 10°C min^{-1} and it was held at final temperature for 2 minutes. The injector temperature was kept at 200°C; for the flame ionization detector, the temperature was 300°C. Hydrogen was used as a carrier gas at a flow rate of 40 mL min^{-1} and air at 450 mL min^{-1}.

3.14 Isolation and purification of trimethyl-ε-caprolactone

The isolation and purification procedure followed here is a modified version of the protocol described by Delgove *et al.* [123]. Once the reaction was finished (100 L), 50 liters of ethyl acetate were added to the reactor and stirred at 40˚C overnight. After that, 6 kg Dicalite 4208 were added and the mixture was stirred for 0.5 h. Subsequently the whole reactor content was filtered and the two phases were separated. The filter was washed three times with 25 liters of ethyl acetate each. The ethyl acetate that was used to carry out the first washing of the filter cake was mixed with the aqueous phase, which had been separated from the first extraction, to perform a second extraction (40˚C and 0.5h). After that, a third extraction (40˚C and 0.5h) was carried out with the ethyl acetate resulting from the second and third washings of the filter. At the end all resulting organic phases were mixed and reintroduced into the reactor to start the distillation of the solvent. The distillation was carried out at 42˚C and 170 mbar.

4. Co-immobilization of P450 BM3 and glucose dehydrogenase on different supports for application as a self-sufficient oxidative biocatalyst

Abstract

The oxy-functionalization of non-activated carbon bonds by the bacterial cytochrome P450 BM3 from *Bacillus megaterium*, presents a promising field in biosynthesis and it has gained much interest in recent decades. Nevertheless, the need for the expensive cofactor NADPH, together with low operational stability of the enzyme have made the implementation of this biocatalyst unfeasible in most cases for industry.

P450 BM3 and glucose dehydrogenase (GDH), as a cofactor regeneration enzyme, were successfully co-immobilized obtaining a bi-functional self-sufficient oxidative biocatalyst. First, a broad screening on 13 different supports was carried out. Moreover, five selected agaroses with three different functionalities (epoxy, amine and aldehyde) were studied and their immobilization processes optimized. Finally, P450 BM3 and GDH, were co-immobilized on those supports showing the best performance for P450 BM3 immobilization: epoxy-agarose (epoxy-agarose-M1) presenting 83% and 20% retained activities respectively; Mana-agarose presenting 28% and 25%, and Lentikats® with which both enzymes retained 100% of the initial activity. Furthermore, the re-utilization of the self-sufficient immobilized derivatives was tested in five repeated cycles towards the hydroxylation of sodium laurate.

P450 BM3 and GDH have been successfully immobilized on three supports and their re-usability has been tested in a model reaction. It represents a step forward for future P450 BM3 industrial implementations.

4.1 Introduction

Cytochromes P450 (CYPs) are versatile monooxygenases able to hydroxylate non-activated carbon bonds with the only requirement being molecular oxygen and an electron donor. CYPs are found as: (i) double domain proteins, presenting a heme-containing oxidative part and a FAD-/FMN-containing reductase; as (ii) triple domain enzymes with a third Ferredoxin subunit and (iii) as fusion proteins with just one enzymatic unit [124]. These enzymes have been the focus of research in recent decades due to interest in their application as catalysts for the efficient production of fine chemicals, polymers, active pharmaceutical ingredients or nutritional supplements. They display a broad substrate range as well as the capability to catalyse a variety of oxidations including epoxidations, hydroxylation of aromatics, N-oxidation, deamination, dehalogenation and others [125].

P450 BM3 (EC 1.14.14.1) from *Bacillus megaterium* was discovered in 1986 and excels among CYPs because it presents the highest turnover numbers (17000 min^{-1} for arachidonic acid) [100], [126]. In contrast with eukaryotic CYPs, P450 BM3 is a self-sufficient soluble protein that contains both oxidative and reductase domains in the same polypeptide chain. Its natural substrates are medium to long chain fatty acids, however, as with other CYPs, P450 BM3 is a promiscuous enzyme. It accepts fatty amides and alcohols, hydroxylated fatty acids and ω-oxo fatty acids. It also displays, not only hydroxylating activity, but olefin epoxidation, ring expansion, heteroatom oxidation and dealkylation, and dehydrogenation across C-O, C-N and C-C bonds, as well as carbon-carbon bond formation and cleavage [98].

There are some limitations in the large-scale application of P450 BM3 such as, low operational stability, a dependence on the expensive NADPH electron donor and low retained activity in organic media [127]. Thus, there have been few cases where it has been attempted to use it industrially [113], [128]. In order to tackle these bottlenecks, protein engineering, cofactor recycling systems, surface modifications, reaction media engineering or immobilization are the main strategies usually followed in biocatalytic processes.

Regarding the low operational stability, immobilization has proven to be an efficient methodology for a broad type of oxidoreductases, not only for improving their stability but also for enhancing process metrics by biocatalyst recycling [60], [77]. In addition, immobilization can confer operational advantages such as the possibility to operate in continuous mode, reduction of foam formation, increased stability in organic solvents or simplified product purification [79], [129]. Immobilization of P450 BM3 has been pursued by other authors. For example, Maurer *et* *al.* tried to immobilize it on a variety of commercially available supports [130]. They succeeded using the positively charged resins DEAE and SuperQ; and a Sol-Gel, but only the last one was found suitable for bioconversions. Axarli *et al.* immobilized a triple mutant onto epoxy-sepharose, achieving retained activities of 81% and improved stabilities at 37°C [115]. Weber *et al.* entrapped the heme-domain of the P450 BM3 into mesoporous molecular sieves (MCM-41 and SBA-15) and found a correlation between the activity observed from the derivative and pore diameter [131]. Furthermore, Zhao *et al.* immobilized a mutant on DEAE-650S, further entrapped into k-carrageenan together with catalase and zinc dust (Zn/Co(III)sep) which served as electron source. They could operate the reactor over 10 batch cycles with continued conversions above 80% [132]. Other successful and more recent examples involved the fusion of the enzyme to linkers that enabled immobilization on solid surfaces [133]–[135]. From all the works present in the literature, there are few cases where P450 BM3 has been successfully immobilized covalently for bioconversion purposes. Many of the above works focused on bio-sensing, in which low amounts of enzyme are required, or on the electrochemical study of the enzyme [136]. For large scale applications, the attachment of large quantities of the enzyme to solid matrices by covalent bonds is a robust method that often confers novel properties to the enzyme and it does not present leaching.

With regard to electron donors, there have been attempts to substitute the expensive NADPH co-substrate for less costly products, *e.g.* NADH or H_2O_2 by protein engineering [137]–[139]. In a different way, electrochemical-driven catalysis has also proved a successful method to bypass the use of NADPH. In various works, the immobilization of P450s on electrode surfaces, that served as electrons sources, led to enzymatically catalyzed product formation [140]–[143]. Strategies for regenerating the expensive NADPH have also been studied both in enzymatic and non-enzymatic manners [30], [144], [145]. The use of whole cell biocatalyst expressing P450 has been considered as a suitable and much cheaper strategy by taking advantage of the cellular metabolism for NADPH regeneration [71], [146]. However, the use of whole cells entails several drawbacks such as secondary undesired reactions or low reaction rates due to substrate or product mass transfer limitation. Among the different strategies for cofactor regeneration, the utilization of secondary enzymes that make use of sacrificial substrates is one of the most attractive systems. The use of enzymatic NADPH regeneration systems in P450-catalyzed reactions has been reported by other authors. Different enzymes such as glucose dehydrogenase, formate dehydrogenase or phosphite dehydrogenase proved to be efficient and suitable biocatalysts for this purpose [95], [130], [147], [148].

In this work, a bi-functional self-sufficient oxidative biocatalyst is obtained by the successful co-immobilization of P450 BM3 and a GDH from *Thermoplasma acidophilum* as cofactor-regenerating enzyme (Figure 1.1). First, P450 immobilization was analysed prior to selection of the best co-immobilization strategy since P450 is a less robust enzyme compared with GDH. Thus, deeper understanding of P450 BM3 immobilization by two different enzyme-support interactions (adsorption or covalent attachment) is presented. In this sense, different supports presenting a broad range of features were tested to gain insight to the optimal immobilization procedure that should be followed. Finally, co-immobilization of P450 BM3 and GDH was performed by applying the best methodologies resulting for the P450 BM3. The encapsulation in polyvinyl alcohol particles (Lentikats®) was also studied for the confinement of both P450 BM3 and GDH as an alternative to adsorption and covalent attachment strategies.

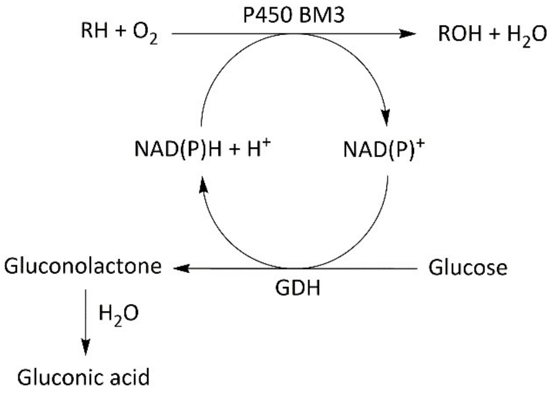

Figure 4.1 Scheme of the bi-functional self-sufficient oxidative biocatalyst obtained by the co-immobilization of P450 BM3 from *Bacillus megaterium* and a GDH from *Thermoplasma acidophilum* as cofactor-regenerating enzyme.

The resulting self-sufficient biocatalysts were tested in terms of operational stability in the hydroxylation of sodium laureate as a model reaction for proof-of-concept (Figure 1.2 and 4.1).

4.2 Results and discussion

4.2.1 Characterization of the *E. coli* lysate containing P450 BM3 and GDH

As already mentioned, P450s are enzymes that require a cofactor to perform the redox reactions they catalyse. One of the strategies widely used for overcoming the disadvantages of co-factor dependency is the use of an enzyme-coupled reaction for the regeneration of the expensive NADPH. In this work, GDH (EC 1.1.1.47) from the archaea *Thermoplasma acidophilum* was used as NADPH-recycling enzyme using glucose as sacrificial substrate (Figure 4.1). This robust and stable tetrameric protein is reported to be an efficient enzyme for NADPH regeneration [34], [95], [148].

In the present work, GDH was co-expressed with P450 BM3 in *E. coli* and both enzymes were present in the cell lysates utilized [113].

The characterization of the lysate was performed regarding protein content, enzyme content (SDS-PAGE, Figure 4.2), activity and P450 BM3 active form concentration and the results are shown in Table 4.1.

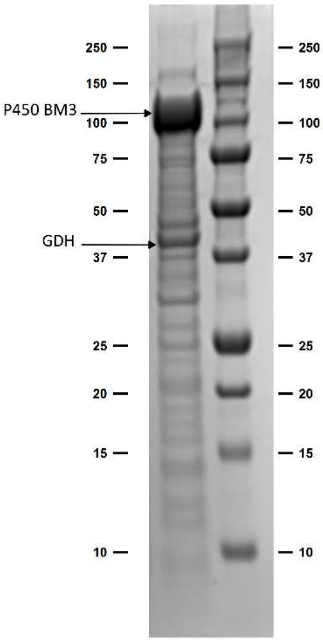

Figure 4.2 SDS-PAGE gel containing a lysate co-expressing P450 BM3 and GDH (left lane) and a molecular weight standard Bio-Rad Precision Plus (right lane). Numbers on both sides represent the molecular weight of the protein bands (kDa).

Table 4.1. Characterization of the cell free extract containing P450 BM3 and glucose dehydrogenase.

Enzyme	[Protein] (mg protein mL^{-1} lysate)	Specific Activity (U mg^{-1} protein)	Enzyme* (mg enzyme mg^{-1} protein)	[Enzyme] (mg enzyme mL^{-1} lysate)	P450 BM3 active form concentration† (μM)
P450 BM3	45.4 ± 0.8	2.8 ± 0.6	0.52 ± 0.01	23.8 ± 0.6	44.9 ± 2.1
GDH		3.6 ± 0.4	0.14 ± 0.01	6.64 ± 0.16	-

*Data obtained from SDS-PAGE analysis

†Data obtained from CO difference spectrum assay

The P450 BM3 was expressed at a higher level than the GDH, however, under the conditions in which the activity tests were performed, GDH gave higher specific activity. Table 4.1, also shows the correlation between activity units (Us) and concentration (nmols) of active enzyme; for the P450 BM3 case, 2.85 U nmol^{-1}.

4.2.2 Screening of supports for the immobilization of P450 BM3 – Purolite®

The main objective of the present work was to obtain a bi-functional self-sufficient oxidative biocatalyst by co-immobilization of P450 BM3 and GDH. To accomplish this, supports and immobilization conditions that were found to be most suitable for the P450 BM3 enzyme were prioritised, since cytochrome is the key enzyme performing the target reaction and it has been described as an unfavourable enzyme for immobilizing. GDH, on the contrary, has been described as a robust and more stable enzyme so difficulties in its immobilization were not anticipated [34]. In fact, successful immobilization of GDH on different kinds of support has been reported by several authors [149]. The results obtained for P450 BM3 imobilization, the materials tested and its features are summarized in Table 4.2. The supports purchased in the screening kits encompass a range of different particle sizes (45 to 710 μm), matrices (methacrylate, styrene and agarose), functional groups (amino, epoxy and aldehyde), enzyme-support interaction (covalent binding or hydrophobic adsorption) and linker lengths (2 to 18 carbon atoms). All of these properties have been identified as critical for successful enzyme immobilization [79].

Table 4.2. Main characteristics of the matrices tested and their results regarding immobilization and retained activity of P450 BM3. The criterion chosen to select a support for further studies sets a minimum for Immobilization yield at 90% and 20% for Retained activity.

Code	Functional group (Linker)	Matrix	Interaction	Pore diameter (Å)	Particle size (µm)	Immobilization Yield (%)	Retained activity (%)
ECR8204F	Epoxy	Methacrylate	Covalent	300 - 600	150 - 300	92 ± 4	0
ECR8215F	Epoxy	Methacrylate	Covalent	1200 - 1800	150 - 300	99 ± 1	2 ± 1
ECR8309F	Amino (C2)	Methacrylate	Ionic/Covalent	600 - 1200	150 - 300	95 ± 5	3 ± 2
ECR8315F	Amino (C2)	Methacrylate	Ionic/Covalent	1200 - 1800	150 - 300	97 ± 2	4 ± 2
ECR8409F	Amino (C6)	Methacrylate	Ionic/Covalent	600 - 1200	150 - 300	100	6 ± 3
ECR8415F	Amino (C6)	Methacrylate	Ionic/Covalent	1200 - 1800	150 - 300	98 ± 1	18 ± 1
ECR8285	Epoxy (C4)	Methacrylate	Covalent	400 - 600	300 - 710	100	3 ± 2
ECR8806F	None (C18)	Methacrylate	Hydrophobic	500 - 700	150 - 300	93 ± 2	0
ECR1061M	None	Styrene/Methacrylic	Hydrophobic	600 - 750	300 - 710	21 ± 6	0
ECR1030M	None	Styrene/Methacrylic	Hydrophobic	200 - 300	300 - 710	33 ± 1	7 ± 14
Praesto 45	Epoxy	Agarose	Covalent	ND	45	92 ± 6	63 ± 1
Praesto 65	Epoxy	Agarose	Covalent	ND	65	95 ± 1	68 ± 3
Praesto 90	Epoxy	Agarose	Covalent	ND	90	95 ± 1	60 ± 11

As shown in Table 4.2, the immobilization yields obtained were higher than 90% in all cases, except for the supports that interact with the enzyme by hydrophobic adsorption: ECR1061M and ECR1030M. In both cases the immobilization yields only reached 21 ± 6% and 33 ± 1% respectively. On the other hand, no retained activities or very low values (< 20%) were observed in all tested supports, except for Praesto 45, 65 and 90, all epoxy-agarose supports (Figure 4.3 A). According to the titration performed, Praesto 45, 65 and 90 contained an epoxide concentration of 9, 6 and 8 µmol per gram of support respectively and resulted in retained activities of 60 - 68% after 4h incubation. The maximum loading capacities of these epoxy-agarose resins ranged from 18 to 20 U g^{-1} and 7 to 8 mg protein g^{-1} of support. The immobilization profiles were very similar among the three supports and they did not show any significant correlation with the particle size or the initial epoxide concentration (Figure 4.3 A).

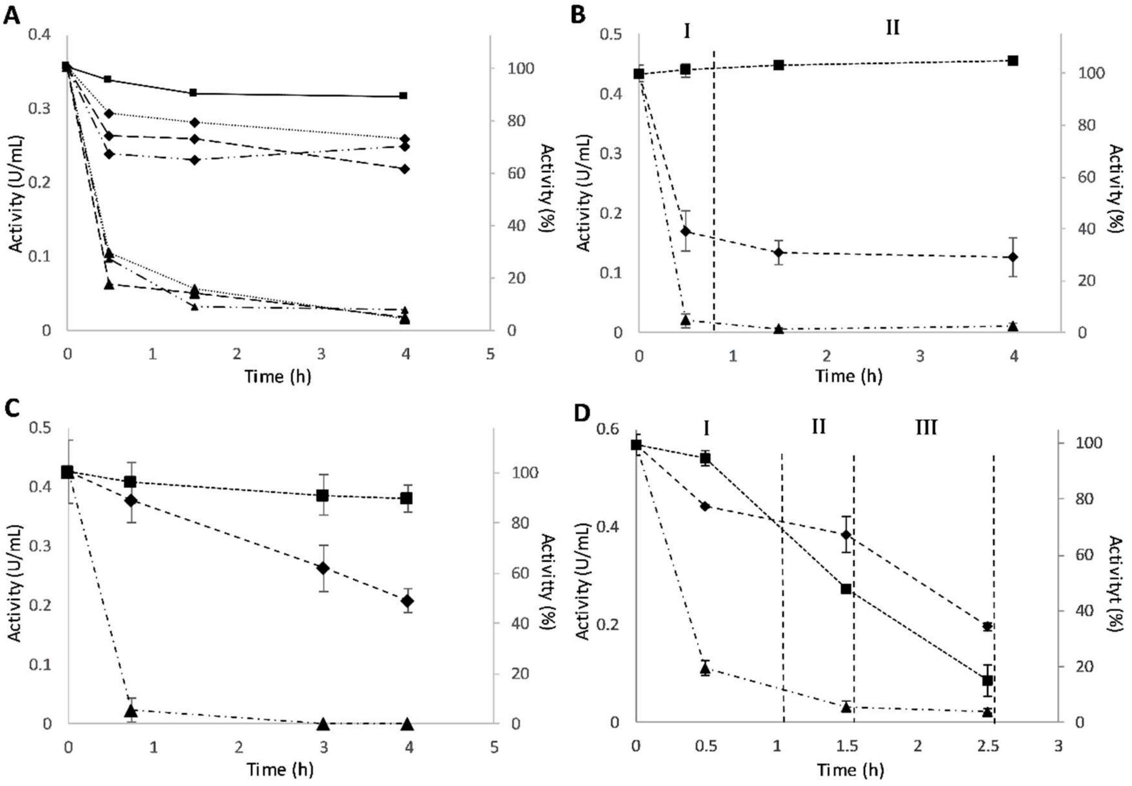

Figure 4.3. P450 BM3 immobilization onto: A) Praesto 45 [discontinued line (-----)], 65 [dotted line (·····)] and 90 [combined dotted and discontinued line (-···-··-)] [Sodium Phosphate Buffer 1 M pH 8] B) Epoxy-agarose-Sigma [Sodium Phosphate Buffer 1 M pH 8]; (I) the enzyme is bound to the support (II) β-mercaptoethanol 0.2 M final concentration is added to eliminate the unreacted epoxy groups, C) Epoxy-agarose-M1 [Sodium Phosphate Buffer 1 M pH 8] and D) Mana-agarose [Sodium phosphate buffer 0.05 M pH 6]; (I) adsorption of the enzyme to the support (II) incubation with certain amount of carbodiimide (EDC) (III) incubation with 0.5 M NaCl and desorption of the unattached protein. The activity offered always ranged from 3.5 to 6 U g^{-1} of resin. The activities of a blank (squares), the supernatant (rhombus) and the suspension (triangle) were continuously analysed. Error bars correspond to standard deviation (n=2).

Regarding the methacrylate and styrene matrices, even though different ionic strengths and pH values were assessed, none of the tested supports showed retained activities above 20%. P450 BM3 had adhered to the matrices in most cases, but did not remain active. Two methacrylate-based materials harbouring amino groups on six carbon chain linkers (ECR8409F and the ECR8415F) gave retained activities of 24 ± 4% and 22 ± 3% respectively when the enzyme was adsorbed onto the resins solely by ionic interactions, however once carbodiimide was added, to promote covalent bond formation, the activity was reduced to 6 ± 3% and 18 ± 1% respectively. Furthermore, following the supplier's protocol, the four amino methacrylate based supports were further functionalized with glutaraldehyde prior to enzyme binding, but none resulted in successful immobilization either.

It should also be mentioned that methacrylic matrices with the same functional groups as the epoxy-agarose support (ECR8204F, ECR8215F and ECR8285) did not lead to actively immobilized enzyme, as can be seen by the low retained activities obtained (0%, 2 ± 1% and 3 ± 2% respectively). These results could indicate that for P450 immobilization the hydrophilicity of the matrix is a key factor. The higher hydrophobicity of the methacrylate/styrene matrices, together with the flexible nature of the enzyme and the presence of two active sites, are probably the causes of the deactivation of the biocatalyst [99]. This hypothesis would also be in accordance with the low immobilization yields and retained activities obtained with the styrene matrices (ECR1061M and ECR1030M). The immobilization mechanism of these matrices is also based on hydrophobic adsorption and both the immobilization yield and retained activity are low. Other authors have also reported unsuccessful attempts to immobilize P450s by hydrophobic adsorption. Maurer *et al.* attempted to immobilize the P450 BM3 on hydrophobic supports such as EP100, MP1000, phenylsepharose, octylsepharose and nutylsepharose but none of them presented final retained activity [130].

Taking into account the results obtained in the screening which showed a strong effect of the hydrophilicity of the matrix on P450 immobilization, agarose was chosen to perform further studies.

4.2.3 Immobilization of P450 BM3 onto different functionalized agaroses

In addition to the epoxy resins already tested (Praesto 45, 65 and 90), two other agarose matrices with free epoxy groups and different epoxide concentrations were studied: a commercial lyophilized epoxy-agarose resin from Sigma-Aldrich® (epoxy-agarose-SIGMA) and an in-house functionalized agarose resin (epoxy-agarose-M1) prepared as shown in the experimental section. In addition, an agarose based matrices containing aldehyde (Glyoxyl-agarose) and primary amine (Mana-agarose) functional groups were tested.

The epoxy-agarose-SIGMA resin, according to the titration performed, contained an epoxide concentration of 110 ± 7 µmol g^{-1} of support and gave an immobilization yield greater than 95% after 0.5 h (Figure 4.3 B). However, a rapid decrease in activity of the suspended biocatalyst was noted during the immobilization procedure, indicating a strong deactivation of the enzyme after immobilization. Thus, after just half an hour, low retained activities (35 ± 8%) were observed from this support. These results could indicate that the utilization of an epoxy-agarose with high epoxide concentration, such as the epoxy-agarose-SIGMA, results in a progressive loss of activity over time due to the multipoint attachment of the enzyme to the support [150]. The explanation can be found in the reactivity of the epoxy groups which differs over time: firstly, reacting with the amines present on the surface of the enzyme and secondly reacting with the carboxyl and thiol groups [151]. At the end, if the incubation time is long enough, the protein can be attached by too many points and lose its whole catalytic activity. This issue can be stopped by adding a blocking agent that removes the unreacted epoxy groups once the protein is immobilized. In Figure 4.3 B, β-mercaptoethanol (0.2 M final concentration) was added after 0.5h and the suspension was incubated for 3.5h at 25°C. No significant loss of activity was observed during this period which validates the hypothesis of multipoint attachment as the main reason for enzyme deactivation. However, due to its elevated cost (118 € g^{-1}) and low retained activities, compared with the Praesto supports, the epoxy-agarose-SIGMA was discarded from further studies.

On the other hand, the epoxy-agarose-M1 displayed an epoxide concentration of 30 ± 3 µmol g^{-1} of support and gave more than a 95% immobilization yield and 83 ± 8% retained activity after 0.5h (Figure 4.3 C), with a maximum loading capacity of 30 ± 2 U g^{-1} of support (7.5 ± 0.8 mg protein/g of support). A decrease in retained activity can also be seen, reaching 50 ± 5% after 4h of incubation probably due to the excessive number of covalent bindings. In this case, as well as for Praesto supports (Figure 4.3 A), the agarose contains a lower epoxide concentration compared with epoxy-agarose-SIGMA. Therefore, the activity loss due to multipoint attachment is lower for the epoxy-agarose-M1 or even negligible for the Praesto compared with the epoxy-agarose-SIGMA. Thus, when choosing the right support, a consensus should be found. Higher epoxide concentration may imply higher loading capacity as is seen when comparing Praesto (18 to 20 U g^{-1} of support) and epoxy-agarose-M1 (30 ± 2 U g^{-1} of support); however, at the same time, higher epoxide concentration entails higher deactivation of the enzyme over time as it is the case comparing all three epoxy-agaroses: Praesto (32 - 40% activity lost), epoxy-agarose-SIGMA (75% activity lost) and epoxy-agarose-M1 (50% activity lost). In this sense, due to the loading capacity, the high retained activities reached and the low cost (2.5 € g^{-1}), the epoxy-agarose-M1 was considered the best candidate for the immobilization of P450 BM3 among epoxy-agaroses. This study represents a deeper insight into the work of Axarli *et al.* [115] in the understanding of the immobilization of P450 BM3 on epoxy-agaroses and sets the bases for an optimal process.

As mentioned before, other agarose-based supports with different functional groups were also tested such as Glyoxyl-agarose and Mana-agarose. The Glyoxyl-agarose (aldehyde activated) immobilization must be pursued in alkali media [152], however, P450 BM3 is not stable above pH 8.5 (data not shown). After screening a range of immobilization pH's (6.5 – 8.5), 7.5 was the best performing one resulting in 50 ± 2% retained activity after 6h incubation. For the reduction of the Schiff base formed between the aldehyde of the resin and the amine of the enzyme, two reducing agents were tested: (i) sodium borohydride (1 mg mL^{-1}) which is added at the end of the incubation and (ii) sodium cyanoborohydride (0.05 mg mL^{-1}) which has slower kinetics and can be added at the beginning of the immobilization. Sodium borohydride resulted in complete deactivation of the enzyme while the sodium cyanoborohydride strategy resulted in 36 ± 0.1% of retained activity. Thus, sodium cyanoborohydride was selected as the most suitable reducing agent. Regarding the studies on maximum loading capacity, the values previously obtained in the characterization (36 ± 0.1% retained activity) at low enzyme loadings were not extrapolated and a major inactivation occurred. This support has proved suitable for the immobilization of P450 BM3, nevertheless, since the covalent immobilization using high loading was not successful, it was discarded from further studies.

Regarding Mana-agarose, as for the other tested supports functionalized by amino groups (i.e. ECR8309F, ECR8315F, ECR8409F and ECR8415F) the immobilization is based on a three-stage process. In the first stage, the enzyme is adsorbed onto the support surface by ionic interaction of the amino groups of the support and the carboxyl groups of the enzyme, thus an ionic adsorption occurs. In the second stage, carbodiimide is added to the medium aiming to activate the carboxyl groups present on the enzyme making covalent bonding possible. Solutions with high ionic strength such as sodium chloride (0.5 M) can be finally added to desorb all the protein attached non-covalently (third stage). Ionic adsorption on Mana-agarose was performed at pH 6 and gave 58 ± 6% retained activity (Figure 4.3 D phase I). This value was 2.4 - 2.6-fold higher than the retained activities obtained during the ionic adsorption for the methacrylate based materials ECR8409F and ECR8415F harbouring the same functional group (24 ± 4% and 22 ± 3%), as previously discussed. The maximum loading capacity achieved was 112 ± 2 U g^{-1} of support (50 ± 4 mg protein g^{-1} of support) which represents the highest value among all the resins tested. Covalent binding of the amine and the carboxyl groups was carried out by adding EDC following ionic adsorption phase (Figure 4.3 D phase II). Since carbodiimide can lead to enzyme deactivation, different concentrations and incubation times were studied to determine the optimal conditions for the covalent binding phase. These studies showed optimal values of 3 mM EDC and 30 min reaction time respectively. Following covalent attachment, the biocatalyst was incubated with 0.5 M NaCl for 2 h (Figure 4.3 D, phase III) in order to increase the ionic strength of the media and release all the protein not adhered covalently. 28 ± 1% of the initial activity offered was covalently bound to the agarose, which represents 30% less activity than the value obtained for the ionic adsorption phase (Figure 4.3 D, phase I). On the other hand, compared with the methacrylate-based supports, the retained activity was 4.7-fold and 1.6-fold higher than the obtained with ECR8409F and ECR8415F respectively. Regarding the maximum load, 53 ± 2 U g^{-1} of resin was reached (47 ± 3 mg protein g^{-1} of support), representing a 52% decrease in immobilized activity compared with that obtained by ionic adsorption, likely due to enzyme deactivation caused by the carbodiimide. When testing for the maximum loading capacity the concentration of EDC was further optimized since more enzyme was added (Figure 4.4). It resulted in an optimal concentration between 6 and 12 mM. This second value was chosen due to the higher immobilization yield that it entailed. This support represents a step forward in comparison with the other tested agaroses and it is the first work reporting a successful covalent immobilization of P450 BM3 in an amino-based matrix.

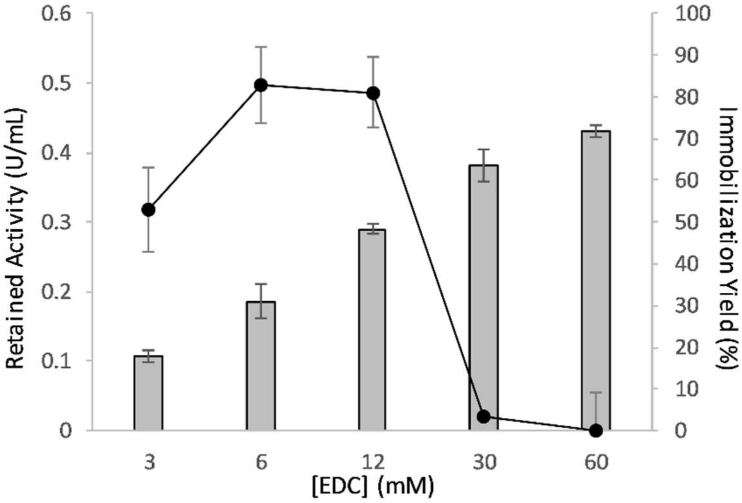

Figure 4.4. Optimization of the EDC concentration in Mana-agarose experiments using high loads. The immobilization was carried out using sodium phosphate buffer 50 mM pH 6 and offering 92 U g^{-1} of resin. Retained activity (black dots) and immobilization yield (grey bars) are represented. Error bars correspond to standard deviation (n=2).

Other authors have worked with P450s and agarose based matrices before. In 1988 King *et al.* obtained 100% immobilization yield and 66% retained activity using a cyanogen bormide-sepharose 4BCL and a P450 from *Saccharomyces cerevisiae*. Another example is the aforementioned case of Axarli *et al.* who immobilized the P450 BM3 on epoxy-agarose and obtained 81% retained activity [115].

4.2.4 Co-immobilization of P450 BM3 and glucose dehydrogenase

As has already been mentioned, for co-immobilization of both GDH and P450 BM3, it was decided to prioritize the supports and immobilization conditions that were found to be suitable for P450 BM3, i.e. epoxy-agarose-M1 and Mana-agarose.

The immobilization of GDH using epoxy-agarose-M1 resulted in poor affinity of the protein for the support with immobilization yields below 20%. However, of the enzyme that did adhere, a slight over-activation was observed compared with the same quantity of free enzyme. At the end of the incubation (4 h), retained activity of 20 ± 5% and a maximum loading capacity of 3 ± 0.1 U g^{-1} of support were achieved. Since the conditions were exactly the same as reported above for P450 BM3, the activity for the cytochrome was comparable and resulted in 50 ± 5% retained activity and 30 ± 2 U g^{-1} (7.5 ± 0.8 mg protein g^{-1} of support).

With Mana-agarose, GDH presented high affinity for the support and it also showed an over-activation effect when adhered to the matrix. It had better tolerance to the presence of EDC compared with P450 BM3, with 10 mM being the optimal concentration for this enzyme (57 ± 2% retained activity) in the characterization phase. Co-immobilization of both enzymes, initially using a low carbodiimide concentration of 3mM, resulted in a 25 ± 4% retained activity for GDH and 28 ± 1% for P450 BM3. Using a higher loading of EDC (12 mM) resulted in a loading capacity of 18 ± 1 U g^{-1} of support for GDH and 53 ± 2 U g^{-1} of support for P450 BM3. In summary, a self-sufficient oxidative biocatalyst was obtained.

There are several examples in the literature of the immobilization of GHD [149]. Regarding the immobilization on agarose based matrices, Anwar *et al.* immobilized a baker's yeast GDH on cyanogen bromide-sepharose obtaining a retained activity of 3% [153]. Persson *et al.* purified a GDH from *Bacillus subtilis* by immobilizing it on thiopropyl-sepharose and recovered up to 65% of the initial activity [154]. However, as far as the authors know, this is the first time that GDH has been covalently co-immobilized with P450 BM3.

4.2.5 Co-immobilization of P450 BM3 and GDH into polyvinyl alcohol particles - Entrapment

Finally, as an alternative to immobilization by adsorption or by covalent attachment, an entrapment strategy was also investigated for co-immobilization. Both P450 BM3 and GDH were successfully embedded into Lentikats® (polyvinyl matrix) as described in the experimental section. The analysis undertaken, showed maximum retained activities of 100 ± 0.1% for both P450 BM3 and GDH.

In the sense of the loading capacity employed, the activity and concentration of protein in the polymer was 1.8 ± 0.2 U g^{-1} of P450 BM3, 0.8 ± 0.1 U g^{-1} of GDH and 1.1 ± 0.1 mg protein g^{-1} of support respectively. It was not further increased due to operational issues. The capacity is limited by an aggregation effect observed when charging high concentrations of lysate with which the lenses form a compact mass that cannot be used in our reactions. This is a serious drawback when looking to industrial feasibility because the enzyme must be previously purified or the specific activity of the support would remain too low [71]. However, since the immobilization had been successful, albeit with low enzyme loading, and it is the first work that reports a successful entrapment of both P450 BM3 and GDH in Lentikats ®, it was decided to continue working with this immobilized derivative.

4.2.6 Reusability of the biocatalyst using sodium laurate as substrate

From all the supports tested, Mana-agarose, epoxy-agarose-M1 and Lentikats® were considered good candidates to be potential carriers in biocatalysis applications. It is well-known that uncoupling effects on P450s produce reactive oxygen species that inactivate the enzyme (uncoupling) [155]. This handicap is less relevant when working with native substrates such as sodium laureate and so this substrate was used as a model for studying the reusability of the self-sufficient biocatalyst. Firstly, the coupling efficiency of P450 towards this substrate was determined and then reusability studies were performed using the self-sufficient P450/GDH biocatalysts obtained with the aforementioned carriers.

Reactions using sodium laureate (1.3 mM) and NADPH (0.2 mM) were performed, monitoring and comparing substrates consumption by means of GC-FID. A coupling efficiency of 90.4 ± 8.3% was observed, which means that, 90.4% of the NADPH consumed was employed for sodium laurate hydroxylation, with the remainder directed towards uncoupled reactions. This substrate was considered adequate to assess the operational stability of the enzymes in repeated reaction cycles.

Total turnover number (mols of substrate consumed mols^{-1} of P450 BM3) (TTN) was chosen as the metric to evaluate the yield of the self-sufficient biocatalyst in comparison with the soluble lysate. To assess it, the immobilized P450 BM3/GDH (epoxy-agarose-M1, Mana-agarose and Lentikats®) biocatalysts were tested in sodium laurate reaction cycles of 1 hour each utilizing glucose as the sacrificial substrate and the cofactor in its oxidized form (NADP$^+$) thus forcing the cofactor regeneration to start before the P450-catalyzed reaction. Moreover, NADP$^+$ starting concentration was 6.5-fold lower than the sodium laureate. The amount of P450 BM3 required to convert > 90% of sodium laurate in 1 hour was found to be 0.18 - 0.2 U mL^{-1} (0.063 - 0.07 nmols mL^{-1}). GDH on the other hand, was always ensured to be present in excess so that it did not limit the hydroxylation reaction. The conversions obtained in each cycle for the immobilized systems are presented in Figure 4.5.

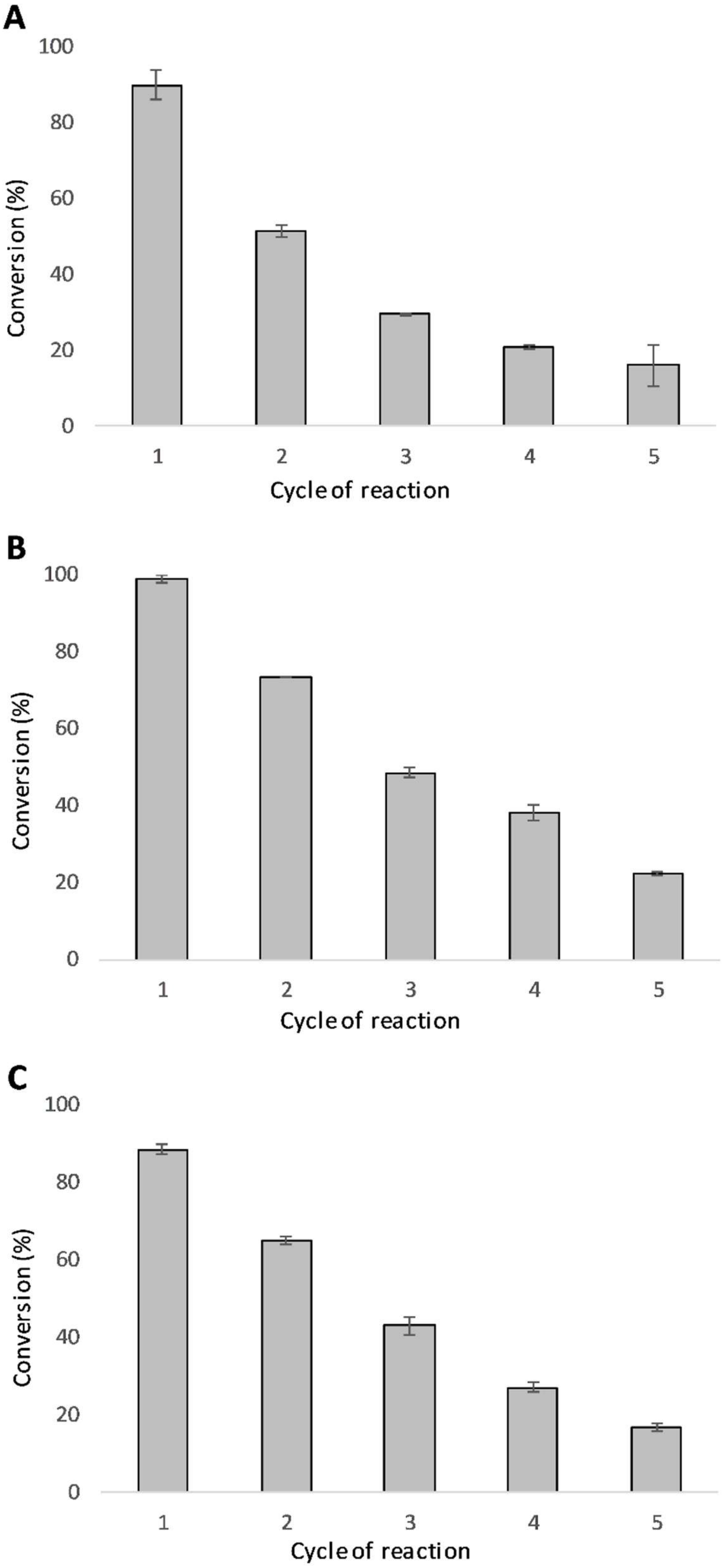

Figure 4.5. Reaction cycles using both P450 BM3 and GDH immobilized onto: A) Epoxy-agarose-M1 (10 mg of agarose mL^{-1}), B) Mana-agarose (10 mg of agarose mL^{-1}) and C) Lentikats® (50 mg of Lentikats mL^{-1}). Reactions were carried on in 5 mL scale adding 0.18 - 0.2 U of total activity and using sodium phosphate buffer 50 mM pH 7.5, 1.3 mM sodium laurate, 0.2 mM NADP$^+$, 12.5 mM D-glucose, temperature controlnatna at 25˚C and constant

1000 rpm agitation using a Multi-therm H5000-HC-E thermos shaker. Error bars correspond to standard deviation (n = 2).

The TTN for the soluble reaction was 21,500 ± 290 mols of sodium laurate consumed/mol of P450 BM3 in 1 hour of reaction. The immobilized derivatives allowed the re-utilisation of the self-sufficient biocatalyst boosting the TTN by 2.31-fold for the epoxy-agarose-M1, 2.98-fold for Mana-agarose and 2.3-fold for the enzymes immobilized into Lentikats®. As shown in Figure 4.5, the conversion dropped in an exponential manner for epoxy-agarose (Figure 4.5 A). On the contrary, with Mana-agarose and Lentikats® the decay was more linear (Figure 4.5 B and 4.5 C). At the end, all three derivatives could be re-used successfully, thus demonstrating a significant operational stability.

Some examples can be found in the literature about the reusability of P450s. Lee *et al.* immobilized a phasin fused P450 BM3 and re-used it 4 times with no loss of activity [133]. Zhao *et al.* were able to use a P450 BM3 mutein together with catalase in 10 batch cycles with conversions up to 80% [132]. Regarding GDH, different studies of re-usability have been reported. A recent example, Petrovicová *et al.* co-immobilized a ketoreductase and a GDH from *Bacillus megaterium* in polyvinyl alcohol particles and were able to use the derivate 18 times with minimal loss of activity [156].

4.3 Conclusions

P450 BM3 has gained much interest in recent years in biocatalysis for its oxy-functionalization characteristics, although, the implementation of this enzyme in industrial processes has lacked optimal metrics. Operational stability as well as its requirement for NADPH in stoichiometric amounts have been identified as the main bottlenecks. Aiming to overcome these two main drawbacks, P450 BM3 and GDH have been co-immobilized in the present work to obtain a robust bi-functional self-sufficient biocatalyst.

P450 BM3 and GDH were covalently co-immobilized on epoxy-functionalized agarose and amino-functionalized agarose. Both enzymes were also successfully co-immobilized by entrapment in a polyvinyl alcohol/polyethylen-glycol matrix named Lentikats®. From the five epoxy-agaroses tested, the optimal support (epoxy-agarose-M1) presented an epoxide concentration of 30 ± 3 µmol g^{-1} of support and retained activities of 83 ± 8% for P450 BM3 and 20 ± 5% for GDH. On the other hand, Mana-agarose showed retained activities of 28 ± 1% for P450 and 25 ± 4% for GDH. Finally, the entrapment of both enzymes in Lentikats ® lead to P450 BM3 and GDH co-immobilization maintaining 100% of the activity initially loaded.

P450 BM3 was also immobilized on aldehyde-functionalized agarose and presented 36 ± 0.1% retained activity. However, this support did not allow high enzyme loads required for reaction testing, thus making this support unattractive for further studies.

The operational stability of the obtained bi-functional self-sufficient biocatalysts (epoxy-agarose-M1, Mana-agarose and Lentikats®) was analysed in terms of re-usability for sodium laureate oxidation. All three derivatives showed successful reuse over five cycles, entailing an increment in the TTN of 2.31-fold the epoxy-agarose-M1, 2.98-fold for the Mana-agarose and 2.3-fold for the Lentikats® compared with the soluble enzymes.

The P450 BM3 wild type served as a model in the immobilization studies in this work. On the other hand, mutated P450 BM3s, usually required for oxidative reactions of non-natural substrates which entail high uncoupling effects, can follow the exact same principles reported here since the surface of the enzyme is usually unaffected [98], [124], [127], [157]. In this sense, immobilization can be an added value to the process, for these new enzymes, due to the many advantages that it confers.

5. Immobilized and soluble P450 BM3-mediated reactions of industrial interest: hydroxylation of α-isophorone and diclofenac

Abstract

Biocatalyst immobilization is a powerful tool to improve both enzyme and process performance. The benefits are numerous and it is often the case that industrial implementation is linked to the immobilization success. In this sense, in order to prove the industrial feasibility of an immobilized enzyme, this has to be tested towards reactions with market output. The hydroxylation of the highly available and cost-efficient α-isophorone together with the hydroxylation of diclofenac were studied. Both soluble and immobilized enzymes were utilized. In the first case, the product 4-hydroxy-isophorone, serves as an intermediate for the synthesis of polymers, carotenoids, vitamins, etc. In the second case, the 4'/5'-hydroxy-diclofenac, serves as a human metabolite for clinical trials.

Regarding the hydroxylation of α-isophorone, using an initial substrate concentration of 10 mM (5 mL) and soluble enzymes, 78 ± 6% conversion and 53 ± 3% yield could be reached. The co-immobilization of P450 BM3 WT and GDH-Tac (3 cycles of reaction) did not improve the final reaction metrics and the biocatalyst yield obtained previously with soluble enzymes (0.65 g ISO g^{-1} enzyme) could not be increased. The addition of catalase was beneficial and the yield in the second cycle was 2.05-fold higher, however, the P450 BM3 still presented poor operational stability (no re-cycling possible). Finally, when 50 mM (10 mL) substrate concentration was applied, the P450 BM3 WT lysate had to be added in pulses. At the end 86.2% conversion and 71.4% yield could be achieved.

Regarding the hydroxylation of diclofenac, a P450 BM3 mutant (M22C02) was used and the reaction conditions were previously optimized by the project partners. The immobilization of this new mutant proved to be similar to the wild type and 25 ± 2% retained activity was obtained with Mana-agarose and 73.9 ± 2.8% retained activity resulted from the immobilization on epoxy-agarose. Since the reaction suffered from substrate inhibition, the initial substrate concentration was limited to 3.5 mM. Total conversion was obtained with soluble enzymes after 0.25h. When co-immobilization on epoxy-agarose was implemented and the derivate was used in the target reaction, full conversion was reached in the first cycle. However, as it happened with α-isophorone, the conversion dropped in the second cycle to 18 ± 2%. In both reaction, P450 BM3 proved to be the enzyme deactivated and so, the limiting factor.

As a conclusion, immobilization of P450 BM3 does not entail significant operational benefits for the reactions studied. Uncoupling is seen as a major cause of enzyme deactivation against whom immobilization can not counteract.

5.1 Introduction

Cytochrome P450s are ubiquitous enzymes present in most organisms. They are named after the absorption peak that they exhibit on ligation with carbon monoxide at λ = 450 nm. The iron ion present in the Fe-protoporphyrin IX (heme group) is responsible for this effect. The most common reaction catalyzed by these families of enzymes is the hydroxylation of non-activated carbon atoms [158]. For this purpose, molecular oxygen and an electron donor, usually NADH/NADPH, are required. In humans, P450s are in charge of the detoxification of the xenobiotics ingested. Its structure comprises a heme-containing domain and a FMN-/FAD-containing reductase domain [159]. Both parts can be found as two separate units, as in humans, or linked in the same polypeptide chain. This last is the case of the P450 discovered by Fulco *et al.* in 1986 in *Bacillus megaterium* (P450 BM3; EC 1.14.14.1) and utilized in this research [160]. P450 BM3 is currently one of the best candidates for industrial applications since it has been recombinantly produced in high densities, it can be used in soluble form and its structure and amino-acid composition and function has been extensively studied [161]. However, some drawbacks still hamper the implementation of the P450 BM3 system. On one side, the low operational stability exhibited by this enzyme and on the other side, the stoichiometric use of the expensive NADPH cofactor. Both downsides have been covered in this research.

It is often the case that enzymes are deactivated by an alteration produced on its quaternary structure. With P450 BM3 this is not the only limitation to reach high biocatalyst yields. This enzyme, as many other oxidoreductases, suffer from uncoupling. It is the unproductive use of NADPH and oxygen to produce by-products rather than the target molecule [162]. Hydrogen peroxide, superoxide or simply water are the main species described. The uncoupling effect has also been called “self-suicide” because these same reactive oxygen species (ROS) are responsible for the heme destruction and so, the deactivation of the P450 [163]. One approach in order to tackle this drawback is the use of ROS scavengers, such as catalase or superoxide dismutase.

As aforementioned, the biocatalyst loss of activity is also a consequence of the protein structure instability. In the case of P450 BM3, dimerization of the two domains into an inactive monomer, when the enzyme is placed in solution (low concentrations), has been described as a cause for sharp activity decrease [164]. Furthermore, between the two domains, the reductase subunit is known to present the weakest structure and it denaturizes under the application of 9.9 kcal mol^{-1}, equivalent to a few hydrogen bonds [165]. Immobilization of enzymes often confers and extra rigidity to the enzyme’s conformation and so it improves the biocatalyst stability [68].

The research covered here comprises the optimization of the reaction main limiting factors and it makes use of enzyme immobilization as a method for process intensification. The best results obtained in the previous chapter regarding P450 BM3/GDH-Tac co-immobilization, were replicated here and the immobilized derivates were used to catalyse reactions with industrial interest. Regarding the NADPH cofactor regeneration, as it was the case with sodium laurate (section 4), different GDHs were employed. The GDH-Tac from *Thermoplasma acidophillum* and a commercial GDH-01 from InnoSyn B.V. Moreover, catalase was applied in one case in order to get rid of the maximum amount of peroxide possible.

The reactions studied comprised the hydroxylation of α-isophorone (ISO) (Figure 5.1) and the hydroxylation of diclofenac (Figure 5.8). In the first case, the widely available and cost-efficient substrate is converted into 4-hydroxy-isophorone (HID) which is an intermediate for the synthesis of carotenoids and Vitamin E [106], [107]. In the second case, the anti-inflammatory drug is converted into the human metabolites 4’/5’-hydroxy-diclofenac [166]. Both reactions have been chosen due to the high difficulties and costs burdened by the classical chemical routes and the good profitabilities they could entail if successful.

5.2 Results and discussion

5.2.1 Hydroxylation of α-isophorone

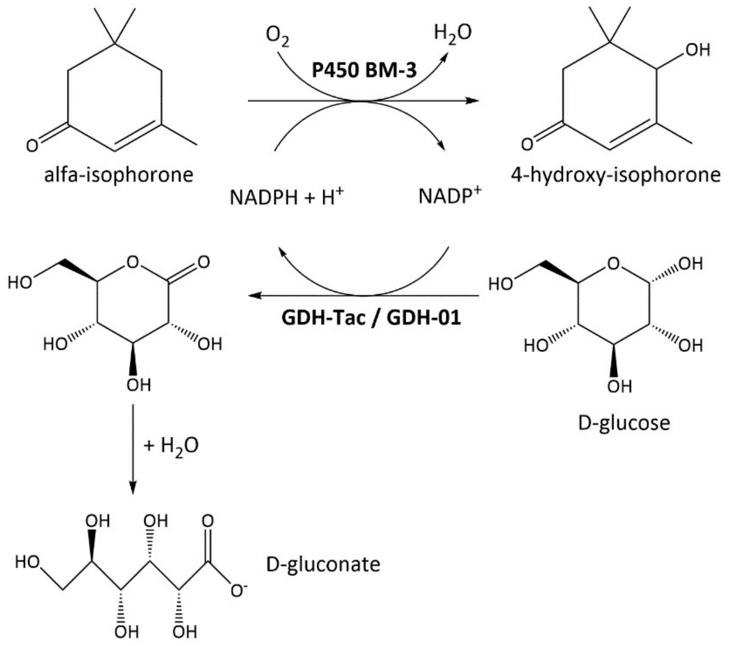

Figure 5.1. Biocatalyzed oxidation of alfa-isophorone (ISO) to 4-hydroxy-isophorone (HID) with a two-enzyme system using a P450 BM3 wild type (WT) and a glucose dehydrogenase (GDH-Tac or GDH-01) to regenerate the $NADP^+$ using glucose as a sacrificial substrate.

In order to start studying the hydroxylation of α-isophorone, the optimization of the main limiting factors was firstly tackled. This was performed at a substrate concentration of 2 mM. As a second step, the reactor configuration changed (lower volume) and the substrate concentration was raised up to 10 mM, where the optimization proceeded. With this set up, immobilized enzymes as well as catalase were tested. Finally, some experiments were run with a substrate concentration of 50 mM applying the enzymes in pulses, in its soluble form.

5.2.2 Reactions with low substrate concentration ($[S]_0$ = 2 mM, V_T = 30 mL)

As mentioned, the aim of this first part was to overcome the major constrains that the reaction presented and get some insight in the reaction variables. Exhaustive optimization of the reaction conditions was not intended. At the beginning, the knowledge about the hydroxylation of α-isophorone conducted by P450 BM3 was scarce. Thus, the first set of experiments was designed taking into account the conditions applied for the hydroxylation of sodium laurate (section 4.2.6).

The initial substrate concentration was kept low, 2 mM, due to the uncoupling effect exhibited by P450s in non-native reactions, such as the α-isophorone. As a consequence of this uncoupling, the total turnover number of P450s in these reactions is highly reduced compared with the native ones (e.g. sodium laurate) [155]. Keeping the substrate concentration low, was an easy way to ensure high conversions for a relatively low amount of enzyme. The rest of conditions were maintained almost the same as section 4.2.6 with laurate.

Some primary attempts conducted in the same reactor configuration as in section 4.2.6, resulted unsuccessful. Even though the enzyme loads, the glucose concentration or the reactor's headspace were varied, no conversion was observed (data not shown). It could be concluded that it was the lack of aeration that did not allow the reaction to proceed.

A new experiment was performed in an aerated reactor (100 mL min^{-1} of pure oxygen) whose results can be seen in Figure 5.2 A. In order to ensure proper cofactor regeneration, apart from the lysate co-expressing the P450 BM3 WT and the GDH-Tac, an extra 3.5% (v/v) portion of lysate containing only the GDH-Tac was added. After 4 hours of reaction, the whole glucose content (40 mM) had been consumed and 49 ± 4% of the initial 2 mM of α-isophorone had been transformed. At the same time, 0.6 mM of 4-hydroxy-isophorone (30 ± 6% yield) were obtained. The presence of keto-isophorone was practically zero. As a conclusion, on one hand, it could be demonstrated that the reaction was 97.5% uncoupled and on the other, it was evidenced that the mass balance only reached 80%.

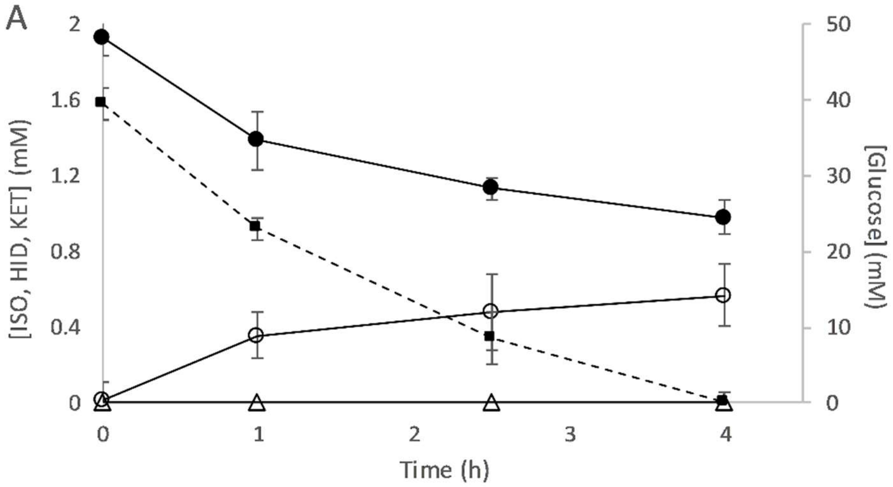

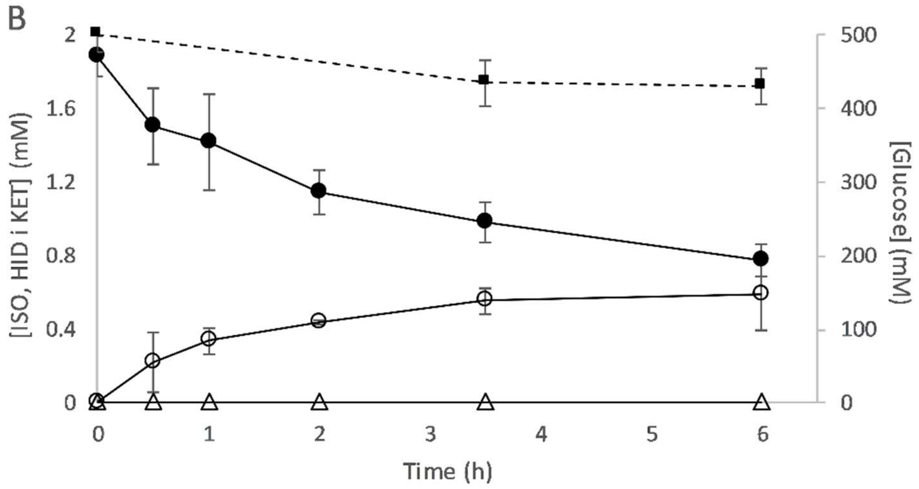

Figure 5.2. Hydroxylation reactions (30 mL) of α-isophorone using P450 BM3 wild type and glucose dehydrogenase (GDH-Tac) as the cofactor regenerating enzyme. A) Reaction using an initial glucose concentration of 40 mM and B) reaction using an initial glucose concentration of 500 mM. The graph shows the concentration along time of ISO (black spots), HID (white spots), KET (white triangles) and glucose (black squares and discontinuous line). Conditions: enzyme load 3.5% (v/v) of P450 BM3 WT/GDH-Tac CFE (127.1 U of P450 mL^{-1} of CFE and 163.4 U of GDH-Tac mL^{-1} of CFE) and 3.5% (v/v) of GDH-Tac CFE (63 U mL^{-1} of CFE); pH control solution 1 M NaOH; temperature 30˚C; stirring rate 500 rpm; O_2 flow 100 mL min^{-1}; [α-isophorone] 2 mM; [D-Glucose] 40 or 500 mM; [NADP+] 0.4 mM; everything dissolved in 50 mM NaPi buffer pH 7. The error bars correspond to the standard deviation of at least two replicates.

Another reaction was performed (Figure 5.2 B). Since the glucose amount proved to be insufficient in the previous reaction, the glucose content was increased up to 500 mM and the oxygen dissolved in the reactor was monitored. By following the dissolved oxygen concentration, the oxygen availability could be confirmed or discarded as a limiting factor. After 6 hours of reaction, the conversion was 59 ± 3% and the reaction yield was 31 ± 7% (72% mass balance). In this case, the glucose consumption was around 70 mM, however, the higher concentrations applied (500 mM) did not allow proper analysis. The oxygen concentration in the liquid phase started at 60% with respect to an air saturated buffered solution. After 7 minutes it raised up to 90% and after 14 minutes it went up to 120%. The signal was stabilized after 30 minutes at 160 – 165%. It could be concluded that neither the glucose nor the oxygen were limiting factors.

5.2.3 Tackling the mass imbalance

In order to address the mass imbalance observed in the previous reactions (Figure 5.2 A and 5.2 B), the stability of the substrate (ISO) and the products (HID and KET) was analysed in reaction conditions with no aeration. The ISO and the HID concentrations were not altered whatsoever. However, the KET concentration, sharply decreased over time. In order to try to discern which was the reason for this KET consumption, 2 mM of KET were incubated in four different conditions (Figure 5.3).

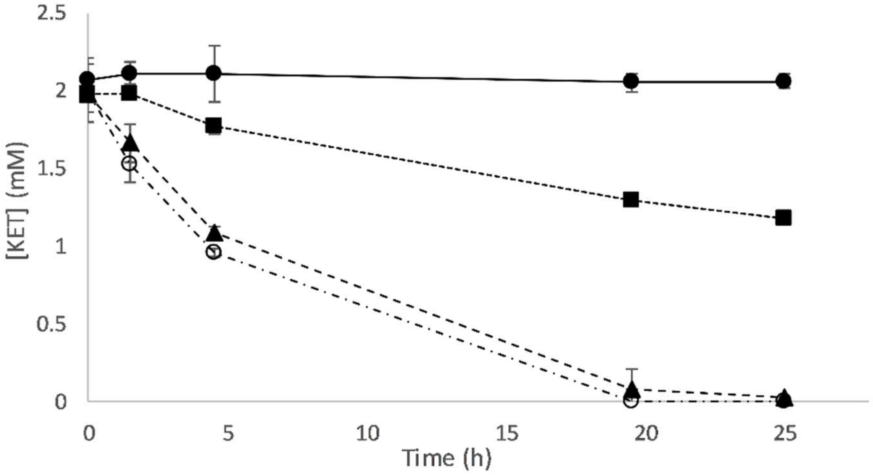

Figure 5.3. Stability of 2 mM keto-isophorone (500 µL) in the presence of: i) 50 mM NaPi buffer solution pH 7 (black spots and continuous line), ii) 3.5% (v/v) GDH-Tac lysate, [NADP$^+$] 0.4 mM and [D-glucose] 40 mM (black squares and dotted line), iii) 3.5% (v/v) P450 BM3 WT/GDH CFE, [NADP+] 0.4 mM and [D-glucose] 40 mM (black triangles and discontinuous line) and iv) 3.5% (v/v) P450 BM3 WT/GDH CFE, 3.5% (v/v) GDH-Tac lysate, [NADP+] 0.4 mM and [D-glucose] 40 mM (white spots and combined discontinuous line-dot-line). Conditions: temperature 30˚C and agitation 500 rpm. All samples dissolved in a 50 mM NaPi buffered solution pH 7. The error bars correspond to the standard deviation of at least two replicates.

Depending on the sample, the two lysates were used solely or mixed together. As it is shown in Figure 5.3, when 2 mM of KET were placed in a 50 mM NaPi pH 7 buffer solution, the amount did not change during the 25 h experiment. On the contrary, when the KET was mixed with a solution containing GDH-Tac CFE, the amount was reduced 41 ± 0%. Finally, when the KET was mixed with a P450 BM3 WT/GDH-Tac CFE or when it was mixed with a P450 BM3 WT/GHD-Tac plus GDH-Tac, it was totally consumed after 25 h. The conversion of HID to KET by P450s and the subsequent degradation of KET has been previously described in the literature by Shaghayegh *et al.* [167]. An ene reductase present in the *E. Coli* extracts was identified as the enzyme responsible for the KET reduction to levodione. It could be concluded that the instability of KET was the cause, or one of the causes, for the mass imbalance observed.

Another potential factor that could be involved, is the oxidation of the substrate and/or products by the reactive oxygen species produced by the uncoupled P450 reactions.

5.2.4 Reactions with 10 mM substrate concentration and soluble enzymes (V_T = 5 mL)

Once it could be demonstrated that neither the glucose nor the oxygen were limiting factors, the substrate concentration was increased up to 10 mM. The aim of this part was to run a reaction with the enzymes on its soluble form and compare it with reactions on which both P450 BM3 and GDH-Tac were immobilized (Mana-agarose and epoxy-agarose-M1).

The reaction set up was changed at this point, firstly, because the reactor configuration used so far did not allow a direct filtration of the content. When using immobilized enzymes, which was the final aim, filtering in a separate porous plate always entails losses of support. In this case, a syringe-like reactor with a porous plate disposed at the bottom, allowed the oxygen income to be properly dispersed and the reactor content to be filtered straight ahead (Figure 3.3). Furthermore, the pH control was conducted in this case by a Titrino 718 instead of a Biostat B used so far. The NaOH added could be rigorously quantified and so, the amount of glucose consumed.

The oxygen income was drastically reduced from 3.3 vvm (100 mL min^{-1} in the 30 mL reactor) to 0.09 vvm (0.45 mL min^{-1} in the 5 mL reactor). As it was demonstrated in the previous reaction, the oxygen dissolved outcompeted the requirements of the reaction by far. In this sense, by reducing the oxygen availability, the uncoupling effect could as well be reduced [168], [169].

The amount of P450 BM3 WT/GDH-Tac CFE was increased from 3.5% (v/v) to 7% (v/v) and the amount of GDH-Tac was reduced. In this case, no additional GDH-Tac CFE was added at the beginning of the reaction. On its turn, an additional 7% (v/v) GHD-Tac CFE were added at the end of the reaction in order to determine if either the GDH or the P450 had been deactivated.

As it can be seen in Figure 5.4 A, after 6 h of reaction, 78 ± 6% conversion and 53 ± 3% yield were reached. Significant higher values compared with the 59 ± 3% conversion and 31 ± 7% yield obtained in Figure 5.2 B. The mass balance in this case was 75%, similar to those balances obtained in the previous reactions (80% and 72%). When the additional pulse of GDH was added (7% (v/v) GDH-Tac CFE), the reaction did no further proceed, meaning that it was the P450 indeed, the enzyme deactivated. Regarding the titration, 0.479 ± 0.1 mL of 0.5 M NaOH were added after 6 h of reaction. Meaning that, 47.9 mM of glucose had been consumed. This equals to 83.7% uncoupling, a lower value than the previously obtained (97.5%), but still high enough to significantly deactivate the P450. Finally, the oxygen dissolved was also monitored here and it abruptly increased as soon as the bubbling started. Before 0.5 h, the concentration reached 100% saturation (against an air saturated buffered solution) and went up to 250 – 330% saturation where it stayed steady. Further decrease of the oxygen income was not possible because on one hand, the mass flow controller did not allow it and on the other hand, when air was used instead of oxygen, the foam formed was practically impossible to eliminate. This foam issue was presented by DSM as a major drawback for this reaction in OxyZymes 2016 conference.

As a conclusion, the conditions applied were considered a good starting point to compare the soluble enzymes with the immobilized ones.

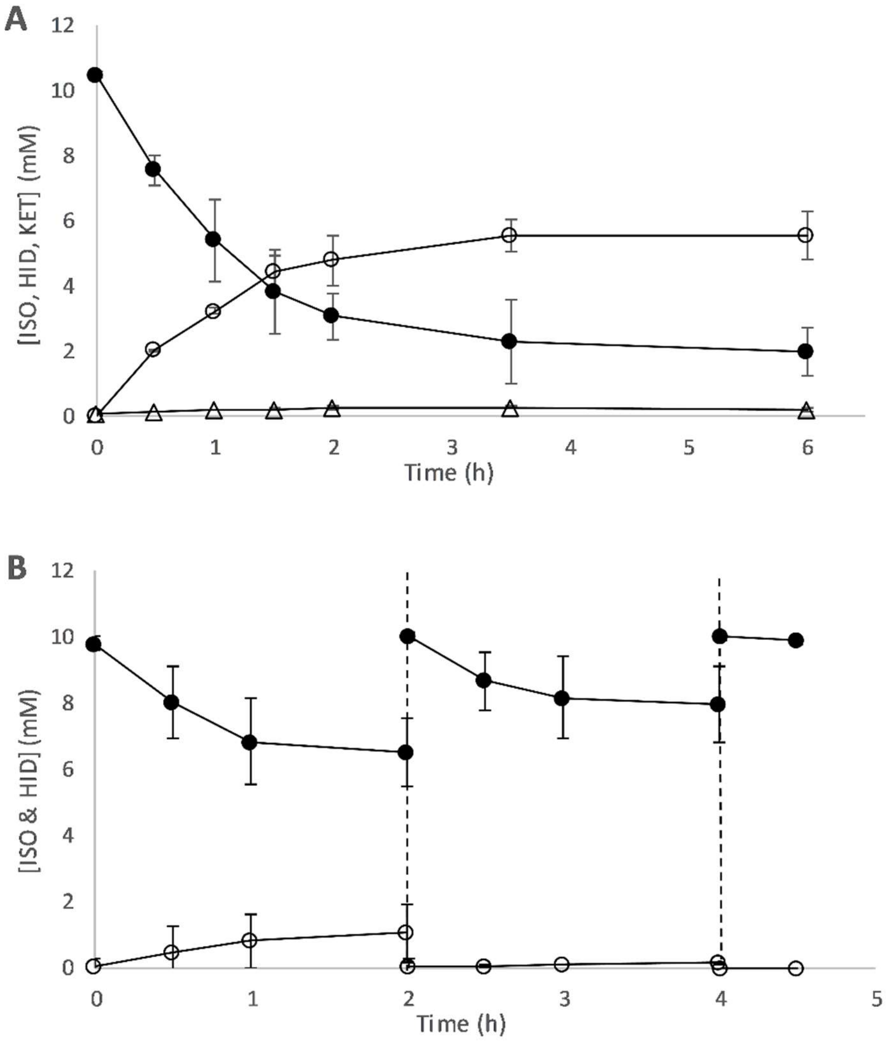

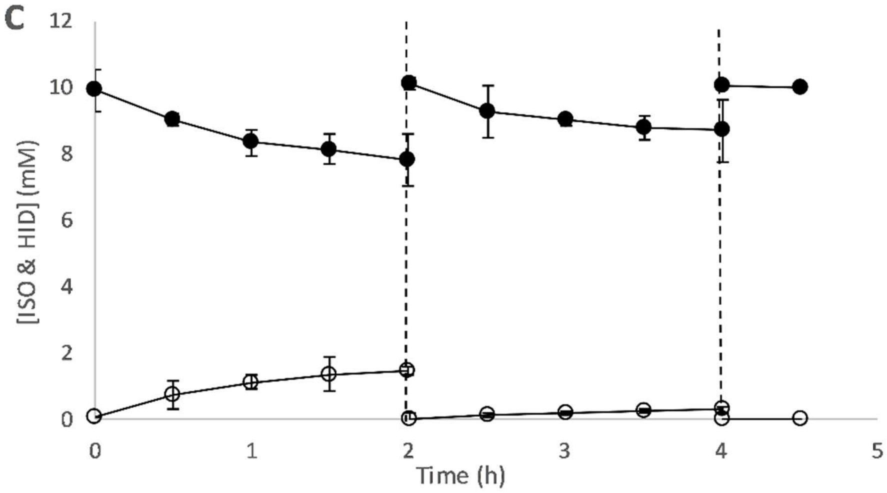

Figure 5.4. Reaction progress for the hydroxylation of α-isophorone in 5 mL reactor. A) Reaction with soluble enzymes containing: 7% (v/v) P450 BM3 WT/GDH-Tac (127.1 U of P450 mL^{-1} of CFE and 163.4 U of GDH-Tac mL^{-1} of CFE) B) Reaction with co-immobilized enzymes onto Mana-agarose containing: 10% (w/v) immobilized P450 BM3 WT/GDH-Tac (53 U of P450 g^{-1} of support and 18 U of GDH-Tac g^{-1} of support) and C) Reaction with co-immobilized enzymes onto epoxy-agarose containing: 10% (w/v) immobilized P450 BM3 WT/GDH-Tac (30 U of P450 g^{-1} of support and 3 U of GDH-Tac g^{-1} of support). The graph shows the concentration along time of ISO (black spots), HID (white spots) and KET (white triangles). Conditions: pH control solution 0.5 M NaOH; temperature 30˚C; agitation rate 1000 rpm; O_2 flow 0.45 mL min^{-1}; [α-isophorone] 10 mM; [D-glucose] 500 mM; [$NADP^+$] 0.4 mM; everything dissolved in 50 mM NaPi buffer pH 7. The error bars correspond to the standard deviation of at least two replicates.

5.2.5 Reactions with Mana- and epoxy-agarose immobilized enzymes ($[S]_0$ = 10 mM, V_T = 5 mL)

The reaction conditions used in the previous section (Figure 5.4 A) had proven successful and reached 78 ± 6% conversion and 53 ± 3% yield. In that trial 7% (v/v) P450 BM3/GDH-Tac CFE was loaded. The goal here was to compare those results with reactions performed with the P450 BM3 and the GDH-Tac co-immobilized on Mana-agarose and epoxy-agarose.

The optimized conditions used in section 4.2.4 for the co-immobilization of P450 BM3 WT and GDH-Tac were applied here and the derivates were tested in the target reaction. The aim was to reach similar yields as those obtained with the soluble enzymes and at the same time, be able to re-use the biocatalyst in repetitive reaction cycles. The amount of support that can be added into the reactor is limited to 10% (w/v), to ensure good dispersion of the particles. In this same line, the amount of units of activity that can be loaded are limited by the carrier's loading capacity. When higher amounts of resin were tested (15% (w/v)), the agarose was packed on top of the liquid phase provoking an accumulation of NaOH and so, a sudden change of pH.

The results with Mana-agarose can be seen in Figure 5.4 B. The conversion in the first cycle was 33 ± 7% and the yield 11 ± 2% while in the second, the conversion was 20 ± 8% and the yield 1 ± 0%.

The results with epoxy-agarose can be seen in Figure 5.4 C. The conversion in the first cycle was 21 ± 6% and the yield 15 ± 1% while in the second, the conversion was 14 ± 7% and the yield 3 ± 1%.

In the two immobilized cases, both conversion and yield were lower than the soluble and no activity was observed in the third cycle. However, it must be noticed that, due to the 10% (w/v) limitation, the activity loaded in these two reactions, was significantly lower compared with the soluble reaction. In Figure 5.4 B, 5.3 U mL^{-1} of P450 and 1.8 U mL^{-1} of GDH were loaded and in Figure 5.4 C, 3 U mL^{-1} of P450 and 0.2 U mL^{-1} of GDH. Meanwhile, with soluble enzymes (Figure 5.4 A), 8.9 U mL^{-1} of P450 and 11.4 U mL^{-1} of GDH were loaded. If the biocatalyst yield (g of consumed ISO per g of enzyme loaded) is calculated for the limiting enzyme, the P450, the soluble reaction resulted in 0.65 g ISO g^{-1} enzyme; the Mana-agarose resulted in 0.47 g ISO g^{-1} enzyme and the epoxy-agarose resulted in 0.52 g ISO g^{-1} enzyme. It could be concluded that immobilization does not entail an improvement of operational stability. Re-cycling was possible and the derivates maintained certain activity in the second cycle, albeit the immobilization costs would be higher than the benefits in this case.

Regarding the GDH, after the third cycle, the activity of the immobilized biocatalysts was measured showing from 70% to 80% of the initial activity (diffusional limitations probably present). It could be finally assured that it was the P450 BM3 indeed, the limiting enzyme.

5.2.6 Addition of catalase as a hydrogen peroxide scavenger

It is well known that hydrogen peroxide, one of the major exponents of the reactive oxygen species produced by the uncoupling of P450, destroys the heme-group and deactivates the enzyme [155], [162], [170], [171]. Thus, the continuous elimination of this oxidative agent from the reaction medium would theoretically improve the enzyme's operational stability. This task is commonly carried out, by sodium pyruvate, N,N'-dimethylthiourea, sodium sulfite or catalase. The enzymatic pathway was chosen for this study due to its availability, previous knowledge and environmental considerations.

According to Zhao L et al., the immobilization of a P450 BM3 mutant on DEAE-650S together with catalase, allowed the re-cycling of the enzyme up to 10 cycles, maintaining 80% of the initial activity [132].

The same soluble reaction presented previously (Figure 5.4 A), as well as the reaction with epoxy-agarose (Figure 5.4 C), were repeated here with the addition of bovine liver catalase (5 mg, 28000 U). In the first case, there was no improvement of the enzyme performance (Figure 5.5 A) while in the second case (Figure 5.5 B), the results showed that: in the first cycle the conversion increased 1.54-fold while the yield increased 1.19-fold; and in the second cycle the conversion increased 1.06-fold while the yield increased 2.05-fold. Even though, the HID production was even doubled in the second cycle, the final conversions were still low in both cycles, 31.5% and 14.8% respectively (16.9% and 6% yields). Thus, it could be concluded that the addition of catalase did improve the reaction metrics but it did not overcome the low biocatalyst yield presented by P450 BM3 towards α-isophorone. Considering the price of the catalase employed (11.5 – 46.2 € g^{-1}; Sigma Aldrich), it was discarded for future experiments.

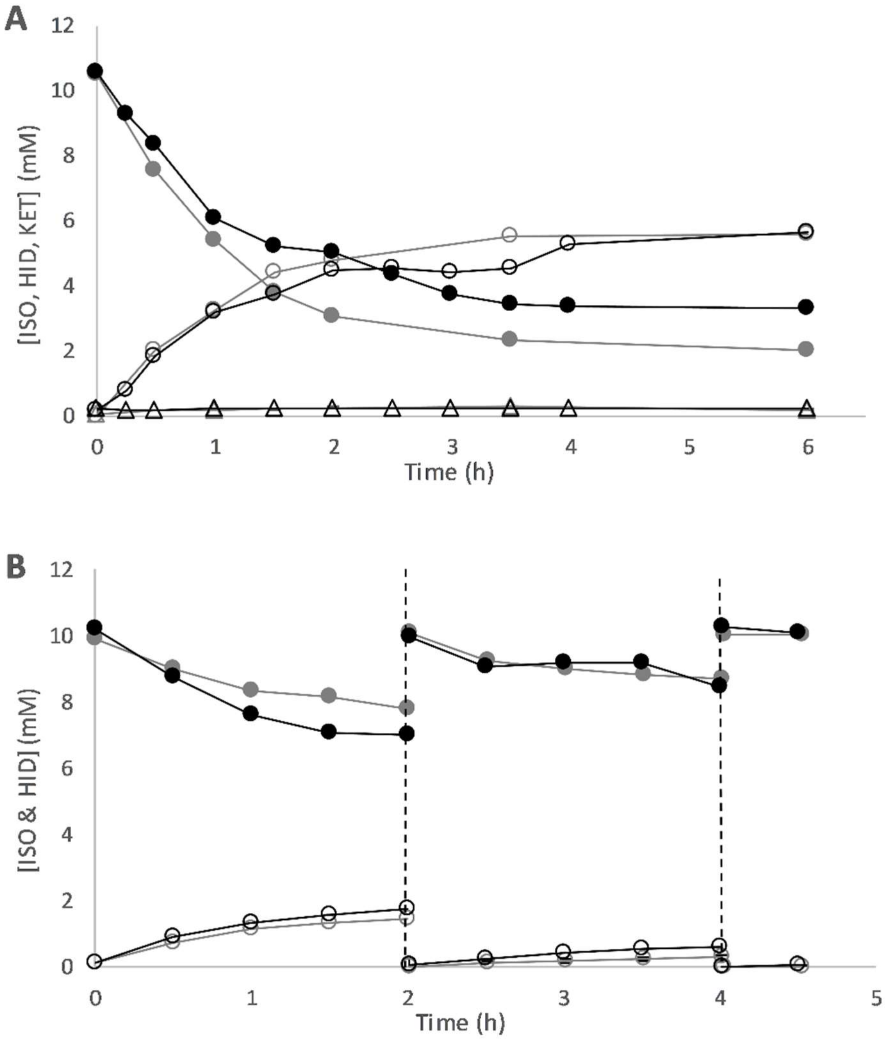

Figure 5.5. Reaction progress for the hydroxylation of α-isophorone in 5 mL reactor with the addition of 0.1% (w/v) bovine liver catalase. **A)** Reaction with soluble enzymes containing: 7% (v/v) P450 BM3 WT/GDH-Tac (127.1 U of P450 mL^{-1} of CFE and 163.4 U of GDH-Tac mL^{-1} of CFE) and **B)** Reaction with co-immobilized enzymes onto epoxy-agarose containing: 10% (w/v) immobilized P450 BM3 WT/GDH-Tac (30 U of P450 g^{-1} of support and 3 U of GDH-Tac g^{-1} of support). The graph shows the concentration along time of ISO (black spots), HID (white spots) and KET (white triangles). The graph **A)** also shows the Figure 5.4 A as overlaid grey dots and the graph **B)** also

shows the Figure 5.4 C as overlaid grey dots. Conditions: 0.1% (w/v) bovine liver catalase (5610 U mg^{-1} lyophilized powder), pH control solution 0.5 M NaOH; temperature 30˚C; agitation rate 1000 rpm; O_2 flow 0.45 mL min^{-1}; [α-isophorone] 10 mM; [D-glucose] 500 mM; [$NADP^+$] 0.4 mM; everything dissolved in 50 mM NaPi buffer pH 7.

It must to be taken into account that the relatively high k_M (28.6 – 33.3 mM) of catalase does not allow a proper in-situ removal of hydrogen peroxide from the medium. An unknown portion of it, is present during the whole reaction. At the same time, the hydrogen peroxide is formed in the active centre of the cytochrome. Meaning that, the deactivation could occur prior to the catalase action. Finally, there are other species that could also be formed as by-products of the uncoupling and deactivate the enzyme (e.g. superoxide). Future experiments should be focused on the complete elimination of these species from the medium. Mutants with lower uncoupling effects would also improve the performance and final metrics.

5.2.7 Reactions with 50 mM substrate concentration and soluble enzymes (V_T = 10 mL)

Once it was demonstrated that immobilization did not solve the operational stability issue presented by P450 BM3, the aim was to optimize the reaction from a process perspective using soluble biocatalysts. In this sense, new reactor sizes were acquired and the reactor volume was doubled (10 mL). The substrate concentration was 5-fold increased reaching values close to industrial requirements. The cofactor regeneration enzyme used in this case was GDH-01 instead of GDH-Tac, a novel and highly active glucose dehydrogenase (310.6 ± 28.5 U mg^{-1} enzyme) that, in principle, could be used in lower amounts compared with GDH-Tac.

Taking into account the previous results obtained, the first limitation tackled was the enzyme loading of both P450 and GDH. As it is shown in Figure 5.6, increasing the P450 BM3 WT CFE load from 5% to 15% (v/v) did not increase neither the conversion nor the yield. On its turn, it increased the uncoupling and the glucose was totally consumed (5 mmol). As it can be seen in Figure 5.7 A (15% P450 : 5% GDH), the glucose consumption rate stayed steady until the whole content was consumed (≈ 9 h). On the contrary, the ISO consumption and the HID production rates drastically dropped after 2 hours of reaction.

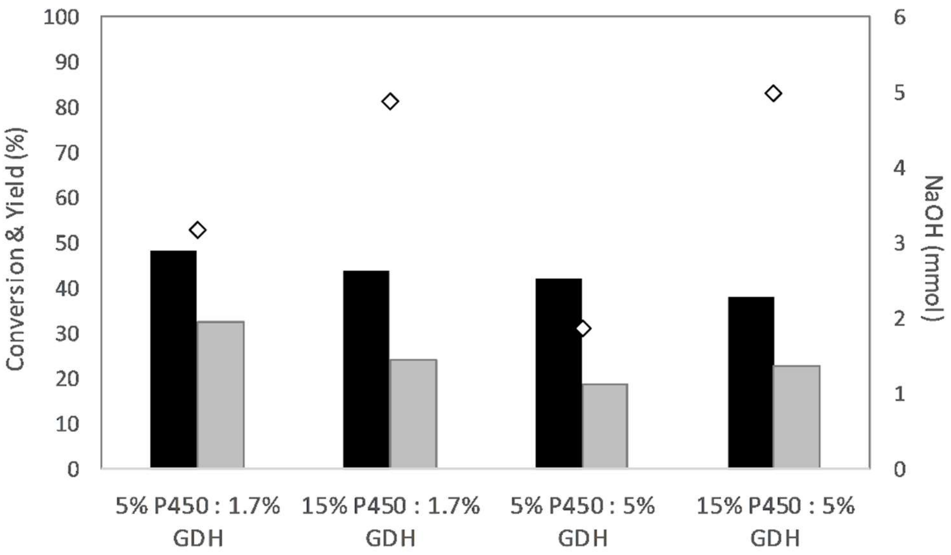

Figure 5.6. Results for the hydroxylation of α-isophorone in 10 mL reactor using P450 BM3 WT and GDH-01 in its soluble form. The amount of P450 BM3 WT lysate and GDH-01 was varied as it is described on the horizontal axes. The graph shows the conversion (black bars), the yield (grey bars) and the NaOH added (white rhombus) for each of the four different reactions. Conditions: P450 BM3 WT (98.9 U of P450 mL^{-1} of CFE) and GDH-01 LF (8467 U of GDH-01 mL^{-1} of LF), pH control solution 1 M NaOH; temperature 30˚C; agitation rate 1000 rpm; O_2 flow 0.45 mL min^{-1}; [α-isophorone] 50 mM; [D-glucose] 500 mM; [NADP+] 0.4 mM; everything dissolved in 50 mM NaPi buffer pH 7.

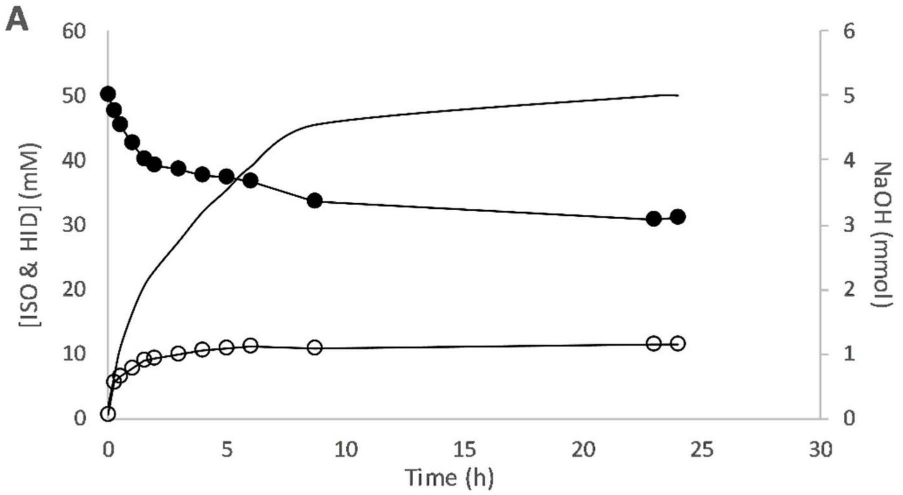

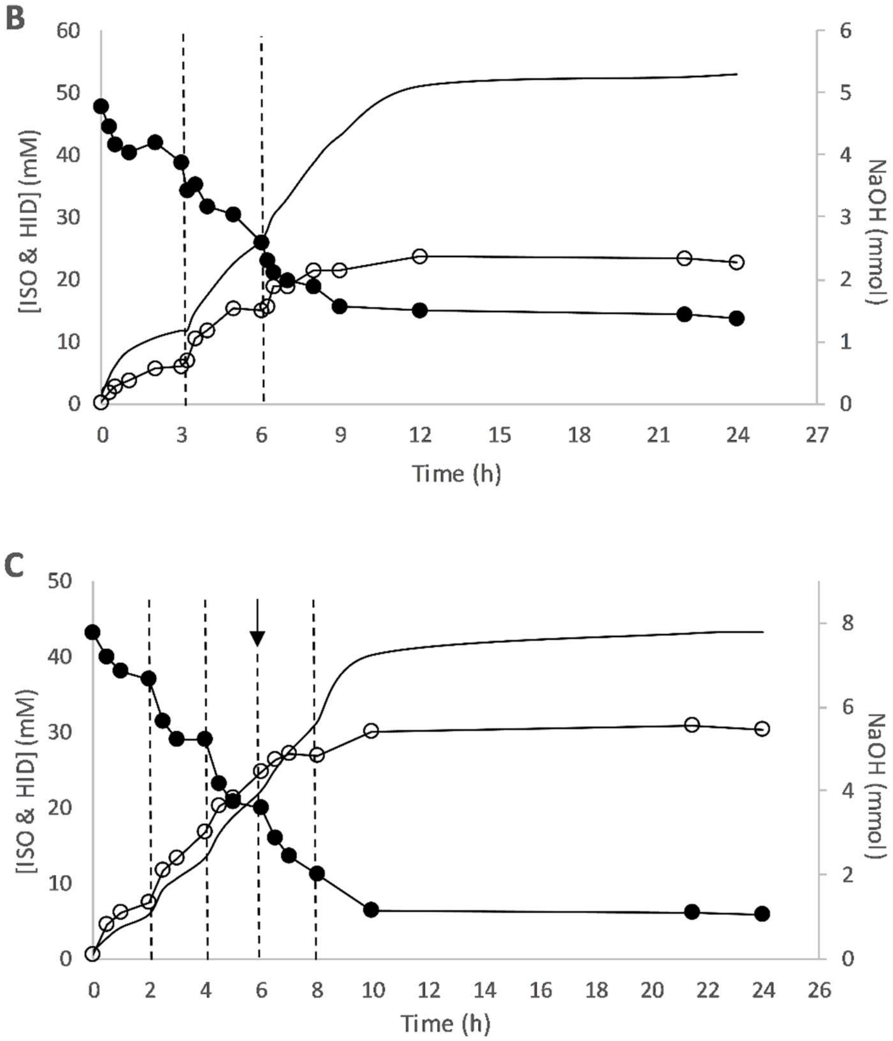

Figure 5.7. Reaction progress for the hydroxylation of α-isophorone in 10 mL reactor using P450 BM3 WT and GDH-01. A) Reaction adding 15% (v/v) P450 BM3 WT CFE and 5% (v/v) GDH-01 LF, B) reaction adding two additional pulses (discontinuous lines) of 5% (v/v) P450 BM3 WT CFE and C) reaction adding four additional pulses (discontinuous lines) of 5% (v/v) P450 BM3 WT CFE and one additional pulse (black arrow) of 250 mM of glucose. The graph shows the concentration along time of ISO (black spots), HID (white spots) and NaOH added (black continuous line). Conditions: enzyme load 5% (v/v) of P450 BM3 WT CFE (98.9 U of P450 mL^{-1} of CFE) and 5% (v/v) of GDH-01 LF (8467 U mL^{-1} of LF); pH control solution 1 M NaOH; temperature 30˚C; agitation rate 1000 rpm; O_2 flow 0.45 mL min^{-1}; [α-isophorone] 50 mM; [D-glucose] 500 mM; [$NADP^+$] 0.4 mM; everything dissolved in 50 mM NaPi buffer pH 7.

Increasing the GDH-01 LF load from 1.7% to 5% (v/v) did not result in any significant change meaning that, the cofactor regeneration was not limiting the reaction. Two other parameters were checked as well: the $NADP^+$ concentration was varied from 0.4 to 1 mM and the oxygen flow was increased from 0.45 to 1.8 mL min^{-1}, but no appreciable changes were observed (data not shown).

5.2.8 Reactions with additional pulses of 5% (v/v) P450 BM3 WT CFE ($[S]_0$ = 50 mM, V_T = 10 mL)

The presence of higher P450 concentrations was demonstrated not to improve the final reaction conversion nor yield (Figure 5.6). However, the fact that the pH controller kept adding NaOH even when the reaction stopped (Figure 5.7 A), is an indication that the P450 remains active and completely uncoupled. At the same time, all the other reaction parameters (GDH, O_2, $NADP^+$ and glucose) were studied and proved to be non-limiting. A strong product inhibition could be the cause for the reaction to stop, however, previous works published, reported reaction yields of 81 ± 1% ([S] = 63 mM; V_T = 100 L), with no apparent reduction of the reaction rate until 60% yield was achieved [113]. Permeabilized whole cells were used there instead of the cell free extract used in this case.

In order to disclose the reason behind the reaction stopping, an experiment was performed adding 5% (v/v) of P450 BM3 WT CFE from the beginning, and two additional pulses of 5% (v/v) after 3 and 6 hours respectively (Figure 5.7 B). As it can be seen, the reaction rate boosted after each addition of CFE, demonstrating that the P450 BM3 WT was the enzyme deactivated and the reason why the reaction stopped after 2 hours of operation. In this case, after 24 hours, the conversion reached 71.5% and the yield 49.3%. In the last best case scenario, when 5% (v/v) P450 and 1.7% (v/v) GDH (Figure 5.6 – left columns) were added, the conversion was 48.4% and the yield 32.8%. As it happened previously, in this case (Figure 5.7 B) the reaction almost stopped after 9 hours, however, the NaOH addition rate stayed constant until the whole glucose content was consumed (5 mmol).

A second reaction was performed adding four additional pulses of 5% (v/v) P450 BM3 WT CFE, every two hours (Figure 5.7 C). As expected, the reaction rate increased after each pulse and at the end, 86.2% conversion and 71.4% yield were obtained. After 6 hours of reaction a second pulse of glucose (2.5 mmol) was necessary and after 10 hours, the whole content had been consumed (7.5 mmol). A third addition of glucose could have helped improve the metrics since the reaction was still going between 8 and 10 hours of operation.

As a conclusion, it was proved that the P450 BM3 WT was the limiting factor of the reaction as a consequence of its complete deactivation after 2 – 3 hours. The addition of the cytochrome CFE in different pulses, demonstrated to re-activate the reaction rate and up to 30.4 mM of HID (71.4% yield) could be synthesized (Figure 5.7 C). On the other hand, the over-titration effect provoked when 15% (v/v) P450 BM3 WT CFE were added, could not be clarified. Two main hypothesis were considered: i) the P450 stops catalysing the target reaction after 2 – 3 hours but it keeps performing the uncoupled ones or ii) the background activity from the P450 BM3 WT CFE is responsible for the NADPH consumption and so, the over-titration.

Considering the biomass concentration of the CFE employed to be 333.3 g_{cww} L^{-1}, the biocatalyst yield achieved in the last reaction was 0.062 g ISO consumed g^{-1}_{cww}. This value represents a 2.67-fold increase compared with the aforementioned publication where permeabilized whole cells were used, added all from the beginning. Taking into account that the reaction stopped after 10h of operation, the space time yield obtained was 0.48 g HID L^{-1} h^{-1}.

5.2.9 Hydroxylation of diclofenac

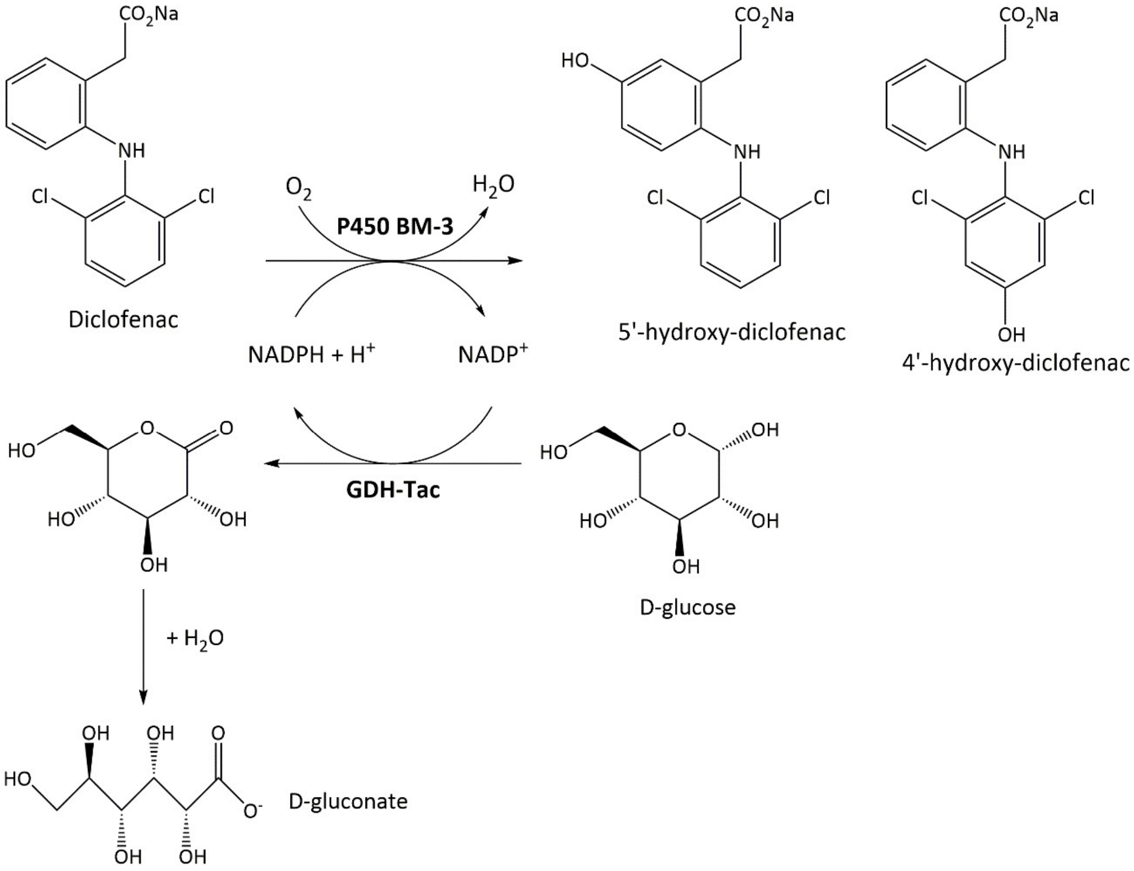

Figure 5.8. Biocatalyzed oxidation of diclofenac to 4’/5’-hydroxy-diclofenac with a two-enzyme system using a P450 BM3 (M22C02 mutant) and a glucose dehydrogenase (GDH-Tac) to regenerate the NADP+ using glucose as a sacrificial substrate.

As a second reaction with industrial interest, the hydroxylation of diclofenac was studied (Figure 5.8). In this case though, compared with α-isophorone, the conditions were previously optimized by the project partners [172]. The enzyme employed in this case was also the P450 BM3, however, the variant utilized was a mutant named P450 BM3 M22C02. The cofactor regeneration was carried out by the co-expressed GDH-Tac. The aim of this part was to compare the reaction performance using the enzymes in its soluble and immobilized forms. As it happened in the previous section, the P450 BM3 M22C02 together with the GDH-Tac were co-immobilized onto Mana-agarose and epoxy-agarose. The immobilization conditions were optimized de novo for both P450 BM3 M22C02 and GDH-Tac.

5.2.10 Immobilization of a P450 BM3 mutant (M22C02) onto Mana-agarose and epoxy-agarose

In principle, the immobilization of P450 BM3 WT sets the basis for the immobilization of any P450 BM3 variant. When muting an enzyme, the modifications usually occur in the active centre, thus, the surface aminoacids, involved in the protein-support interactions, are not altered. In this sense, in order to prove this statement, the immobilization of a P450 BM3 variant was studied, P450 BM3 M22C02. The matrices that proved success sful for the wild type were also tested here, Mana-agarose and epoxy-agarose.

The immobilization of P450 BM3 M22C02 onto Mana-agarose (Table 5.1) resulted in 25 ± 2% retained activity when 1 mM of EDC was employed. Similar value to the 28 ± 1% achieved with P450 BM3 WT (section 4.2.3). In that case though, the optimum EDC concentration was 3 mM. Regarding the GDH-Tac, 38 ± 4% retained activity was obtained when using 5 mM EDC concentration. This value is 19 percent points lower than that achieved with 10 mM EDC and 10 percent points higher than that obtained with 3 mM EDC (P450 BM3 WT, section 4.2.3). In summary, the results obtained do not allow the co-immobilization of the P450 BM3 M22C02 and the GDH-Tac due to the big difference in the EDC optimum concentration. However, the final retained activities of both enzymes are similar to those obtained previously for the P450 BM3 WT/GDH-Tac.

Table 5.1. Co-immobilization of P450 BM3 M22C02 and GDH-Tac onto Mana-Agarose with distinct EDC concentrations. The experiments were performed loading the support with low amounts of enzyme (4.7 U of P450 g^{-1} and 71.9 U of GDH g^{-1}). The standard error (± %) was calculated from at least two replicates.

Enzyme	Bond	[EDC] (mM)	Immobilization Yield (%)	Retained Activity (%)
P450	Covalent	1	63 ± 6	25 ± 2
		2	72 ± 4	15 ± 3
		3	82 ± 3	10 ± 5
		4	86 ± 2	7 ± 5
		5	88 ± 2	8 ± 2
GDH	Covalent	1	24 ± 5	11 ± 1
		2	31 ± 7	4 ± 1
		3	48 ± 3	0 ± 0
		4	60 ± 2	22 ± 5
		5	55 ± 3	38 ± 4

The immobilization onto epoxy-agarose was performed only with the in-lab functionalized support that presented an epoxide content of 30 ± 3 µmol g^{-1} of resin (epoxy-agarose-M1). Among the five different epoxy-agaroses previously tested with the P450 BM3 WT, this one resulted in the highest performance. As it can be seen in Figure 5.9, the overall suspension activity decay was lower compared with the WT (section 4.2.3) and the final retained activity was 73.9 ± 2.8%, 1.48-fold higher than the WT. On the other hand, the supernatant activity did not drop to zero after 4 hours of incubation. Meaning that, the affinity of the enzyme for the support was lower compared with the WT. These differences might be associated with the higher amounts of CFE that had to be loaded due to the lower enzyme content of the lysate (31 ± 0%) and the lower specific activity (0.91 ± 0.02 Us mg^{-1} enzyme) of the P450 variant. As it happened with the P450 BM3 WT/GDH-Tac lysate, the affinity of the GDH-Tac for the epoxy-functionalized agarose was poor. At the end of the immobilization, 23 ± 2% retained activity and 23 ± 1% immobilization yield were obtained. This support was selected to perform a model reaction of industrial interest, the hydroxylation of diclofenac to 4'/5'-hydroxy-diclofenac. Furthermore, re-cycling of the derivate was also intended.

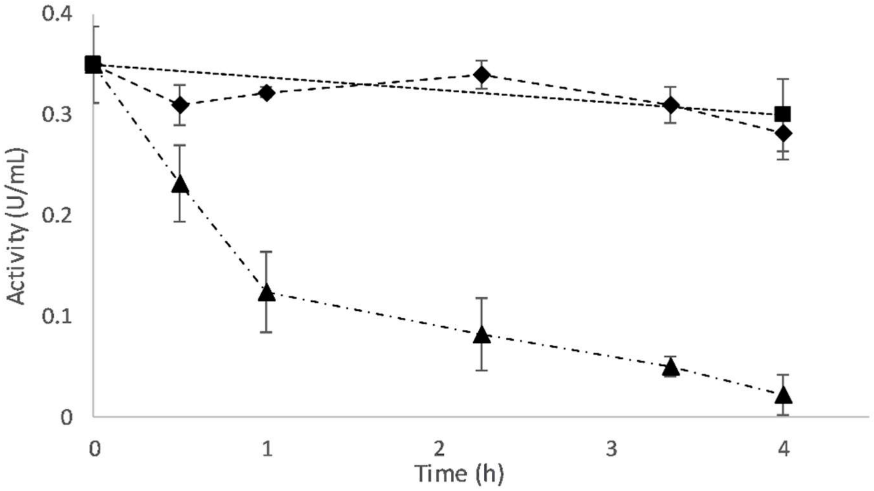

Figure 5.9. Immobilization of P450 BM3 M22C02 onto epoxy-Agarose. The experiment was performed loading the support with low amounts of enzyme (3.5 U g^{-1}) in order to characterize the enzyme-support interaction. The graph shows the activity of the blank (black squares), the supernatant (black triangles) and the suspension (black rhombus) along time. The error bars correspond to standard deviation of at least two replicates.

It could be concluded that the immobilization results of the P450 BM3 WT and the P450 BM3 M22C02 are similar but not exactly the same. The first results obtained served as a good guidance for the mutants in order to chose the right support.

5.2.11 Hydroxylation of diclofenac with P450 BM3 M22C02 ($[S]_0$ = 3.5 mM, V_T = 5 mL)

The conditions for the hydroxylation of diclofenac catalyzed by P450s were optimized by the project partners and did not differ much from the ones applied so far (isophorone). A major change though, was the initial substrate concertation. This reaction highly suffers from substrate inhibition and only 3.5 mM of diclofenac were added to the reactor. In this section, re-cycling of the biocatalyst was proposed as an alternative to a fed-batch strategy, usually implemented in these cases.

As a proof of concept, a first reaction using the P450 BM3 M22C02/GDH-Tac lysate in its soluble form was run (Figure 5.10 A). As it can be seen, full conversion with 100% mass balance was reached after 0.25 h. Regarding the glucose consumption, 0.29 ± 0.09 mmol of NaOH were added, which represents an uncoupling of 94 ± 2%.

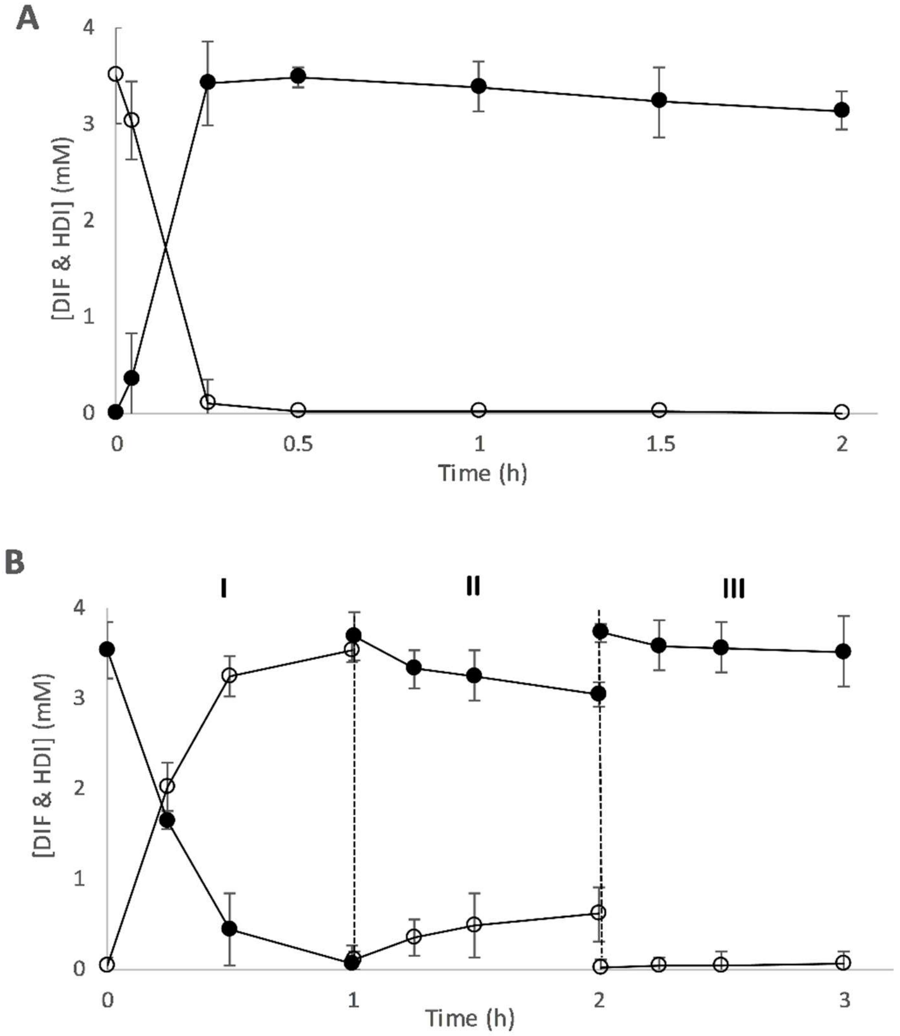

Figure 5.10. Hydroxylation of diclofenac on 5 mL reactor with P450 BM3 M22C02/GDH-Tac in its soluble and immobilized form. The graph shows the reaction course of diclofenac (white spots) and 4'/5'-hydroxydiclofenac (black spots). A) Reaction using the enzymes on its soluble form: 7% (v/v) of P450 BM3 M22C02/GDH-Tac lysate (15.5 U of P450 mL^{-1} of CFE and 239.7 U of GDH mL^{-1} of CFE) and B) reaction using the enzymes co-immobilized on epoxy-agarose: 10% (w/v) of P450 BM3 M22C02/GDH-Tac derivate (5.8 U of P450 g^{-1} of support and 13.8 U of GDH g^{-1} of support). Conditions: temperature 28˚C; agitation 1000 rpm; oxygen flow 0.45 mL min^{-1}; [diclofenac] 3.5 mM; [D-glucose] 500 mM; [$NADP^+$] 0.4 mM; [methanol] 3% (v/v) everything dissolved in NaPi buffer 50 mM pH 7.2. The error bars correspond to the standard deviation of at least two replicates.

For the co-immobilization of P450 BM3 M22C02/GDH-Tac on epoxy-agarose-M1, in this case, high loads of enzyme were used in order to obtain a derivate as active as possible. In this sense, 0.8 mL of

CFE were loaded per gram of resin (44.1 mg of protein g^{-1}). After 4 hours of incubation, the final derivate contained 5.8 ± 0.2 U of P450 g^{-1} and 13.8 ± 3.8 U of GDH g^{-1} with a protein content of 11.6 mg g^{-1}.

The reaction performed with both enzymes co-immobilized can be seen in Figure 5.10 B. As it happened with α-isophrone, 10% (w/v) of resin was loaded in order to ensure proper dispersion of the support. This amount represents 1.87-fold less P450 activity and 12.16-fold less GDH activity, compared with the soluble reaction. Even with this limitation, in the first cycle, full conversion with 100% mass balance was reached after 1 hour. In the second cycle, 18 ± 2% conversion and 17 ± 5% yield were achieved, while in the third cycle, 6 ± 4% conversion and 2 ± 1% yield were obtained. The addition of soluble GDH-Tac did not produce any difference. In this target reaction it could be demonstrated, as it happened with α-isophorone, that re-usability of P450 for more than two cycles, is not possible on the given conditions.

Future research should primary address the uncoupling issue presented by P450s. While the deactivation of the enzyme is a matter of the heme-group destruction rather than a structural weakness, immobilization will barely serve as a process benefit.

5.3 Conclusions

Immobilization can offer many benefits to a biocatalyzed process, not only an improved operational stability. However, the costs involved in the immobilization must be overcome by these added improvements. For example, better storage stability, better pH spectrum tolerance or easier product purification do not usually entail enough process upturn to compensate for the immobilization costs. On the contrary, biocatalyst re-utilization implies a direct and often substantial expense reduction. Depending on the production cost of the enzyme, the amount of reaction cycles necessary will vary.

In this sense, the research performed in this chapter, has been focused on the optimization of the main limiting factors affecting each target reaction but most of all, in the re-utilization trials of the immobilized enzymes. Both target reactions studied were selected due to their industrial interest. On one hand, the hydroxylation of α-isophorone and on the other hand, the hydroxylation of diclofenac.

In the first case, the P450 BM3 WT co-expressed with a GDH-Tac were studied both soluble and immobilized. However, the re-utilization of the immobilized derivate was not possible and no conversion was observed in the third reaction cycle ($[S]_0$ = 10 mM; 5 mL). Not even with the addition of catalase, as a hydrogen peroxide scavenger, product could be measured after the second cycle. P450

BM3 WT was identified as the enzyme deactivated. The best results were obtained with both enzymes soluble and adding the P450 BM3 WT in pulses. Using an initial substrate concentration of 50 mM (10 mL), the final conversion achieved was 86.2% and the final yield was 71.4%. The biocatalyst yield was 0.062 g ISO consumed g^{-1}_{cww} and the STY after 10h was 0.48 g of HID L^{-1} h^{-1}.

Regarding the hydroxylation of diclofenac, the reaction had been previously optimized by the project partners. Because of that, the research was only focused on the immobilization of the P450 BM3 mutant (M22C02) selected for this target molecule and the re-cycling capacitiy of the derivate. The conversion in the first cycle ($[S]_0$ = 3.5 mM; 5 mL) was complete, however, as it happened with α-isophorone, re-utilization was not possible. In the second cycle 18 ± 2% conversion was obtained while in the third, only 6 ± 4%.

As a conclusion, immobilization proved to be successful for both enzymes (P450 BM3 and GDH-Tac) in terms of retained activity but the operational stability of the cytochrome did not improve. The deactivation of P450 BM3 is probably a consequence of the ROS species produced from the uncoupling. Future experiments should be addressed to reduce this negative effect, for example, by reducing the oxygen availability. Finally, the addition of P450 BM3 in pulses, served to increase the final conversion for the hydroxylation of α-isophorone.

6. Synthesis of keto-isophorone with an immobilized alcohol dehydrogenase

Abstract

The monoterpenoid α-isophorone is sourced from the widely available and renewable plant dry matter, as well as a waste recovery operation from acetone. This compound, can then be hydroxylated to 4-hydroxy-isophorone which is the main precursor for the synthesis of keto-isophorone. On its turn, keto-isophorone is a key intermediate for the production of carotenoids (zeaxanthin, cryptoxanthin and xanthoxin) and α-tocopherol (Vitamin E).

Here, the enzymatic oxidation of 4-hydroxy-isophorone to keto-isophorone is demonstrated employing an alcohol dehydrogenase (ADHaa) from *Artemisia annua* and a NADPH oxidase (NOX), as a cofactor regeneration enzyme. After 24h of reaction and an initial substrate concentration of 50 mM, 95.7% yield and a space time yield of 6.52 g L^{-1} day^{-1} could be obtained.

Furthermore, the immobilization of the alcohol dehydrogenase was studied on 17 different supports covering different carrier's features. An epoxy-agarose with an activation grade of 106 ± 1 µmol g^{-1} resulted in the highest metrics, 100 ± 0% immobilization yield and 58.2 ± 3.5% retained activity.

Finally, the immobilized ADHaa was successfully implemented in 4 reaction cycles (96h operation) presenting a biocatalyst yield of 23.4 g product g^{-1} of enzyme. It represents 2.5-fold increase compared with the reaction where both enzymes were used in its soluble form.

6.1 Introduction

The combination of environmental consciousness and legislation is paving the way towards a steeply increasing bio-based economy. However, the petro-alternative, still remains as the major carbon source worldwide [173]. To revert this, the scientific knowledge is playing an important role, offering a continuously updated portfolio of highly competitive processes and products. As a result, the industry and in turn, the society, is becoming more sustainable and eco-friendly [103].

One of the most prominent and highly energetic resources on earth, apart from petroleum, is lignocellulose. Defined as "plant dry matter", this raw material is accessible, renewable, recyclable and vastly abundant [3]. All sorts of products such as poly-saccharides, lignin, oils, fragrances, phenolic compounds or building block chemicals can be obtained from lignocellulose[174], [175]. Among them, α-isophorone (3,5,5-trimethyl-2-cyclohexen-1-one) (ISO) is a monoterpenoid that can be converted into intermediates for the production of poly-urethans [176], pharmaceuticals [177], fragrances [178], *etc.* The chemical route towards some of these compounds comprises the isomerization of α-isophorone to β-isophorone and the further oxidation of this, to keto-isophorone (KET) [107]. However, the first step (isomerization) requires the use of high temperatures and the equilibrium is shifted towards the substrate, only 2% yield is commonly obtained [179]. The direct selective allylic oxidation of ISO to KET has also been demonstrated, nevertheless, it makes use of toxic heavy metals, yields undesired by-products and/or requires harsh conditions [180]–[182]. Apart from its biomass origin, α-isophorone is also produced at large scale as a waste recovery operation from industry. An aldol condensation is run using potassium hydroxide and the acetone obtained as by-product from the synthesis of phenol [183].

Once the KET has been synthesized, it can then be reduced to (4*R*, 6*R*)-actinol which is an intermediate for the production of zeaxanthin, cryptoxanthin and xanthoxin [106]. Furthermore, keto-isophorone can also be converted to trimethylhydroquinone, a key intermediate for the synthesis of α-tocopherol (vitamin E) [184].

A greener and more sustainable strategy to obtain KET is the enzyme catalyzed hydroxylation of α-isophorone to 4-hydroxy-isophorone (HID) and the further oxidation of this to obtain the desired product (KET). Tavanti *et al.* co-expressed a self-sufficient P450 together with an alcohol dehydrogenase from *Candida magnoliae* to run the reaction as one-pot two step oxidation and obtained a space time yield of 1.4 g L^{-1} day^{-1} [185]. In this same line, Shaghayegh *et al.* compared the performance of two P450 (CYP102A1 and CYP101A1) for the hydroxylation of ISO, however, background activity from the *E. coli* host cells converted the recently formed KET to levodione [167].

Another recent example is from Aranda *et al.* that used an unspecific peroxygenase from *Humicola insolens* to fully convert 10 mM ISO in a 1:1 ratio (HIP:KET) [104].

As previously reported by Kaluza *et al.,* the first oxidation step, the hydroxylation of ISO to 4-hydroxy-isophorone is feasible and it was demonstrated at pilot plant scale [113], [186]. The biocatalyst utilized consisted of *E. coli* whole cells over-expressing a P450 BM3 and a glucose dehydrogenase, that served as the cofactor regeneration enzyme. The 100 L reactions performed, resulted in 80 – 82% conversion of the initial 6.3 mol of ISO, with a space time yield of 1 g L^{-1} h^{-1}. The present work has been focused on the subsequent oxidation step, the conversion of HID to KET.

In order to study the enzyme-mediated oxidation of HID, an alcohol dehydrogenase from *Artemisia annua* (ADHaa) (EC 1.1.1.1) was used as biocatalyst. Furthermore, immobilization of ADHaa on different supports was investigated in order to re-use the enzyme in various cycles of reaction. In this sense, immobilization often results in an increased stability of the catalyst and allows an ease separation of the enzymes from the reactor content [76], [79], [112]. Numerous are the examples in literature about immobilized alcohol dehydrogenases [187]–[190], however, this is the first time that immobilization has been studied on *Artemisia annua*'s ADH.

Regarding the NADPH, since the cofactor dependence is a drawback that hampers the use of alcohol dehydrogenases at large scale, an engineered NADPH oxidase from *Streptococcus mutans* (NOX) (EC 1.6.3.4) was used as a cofactor regeneration enzyme (Figure 6.1) [35], [93]. Previous results obtained in the group about the immobilization of NOX did not show any operational stability improvement. That is why NOX was utilized in its soluble form in all cases.

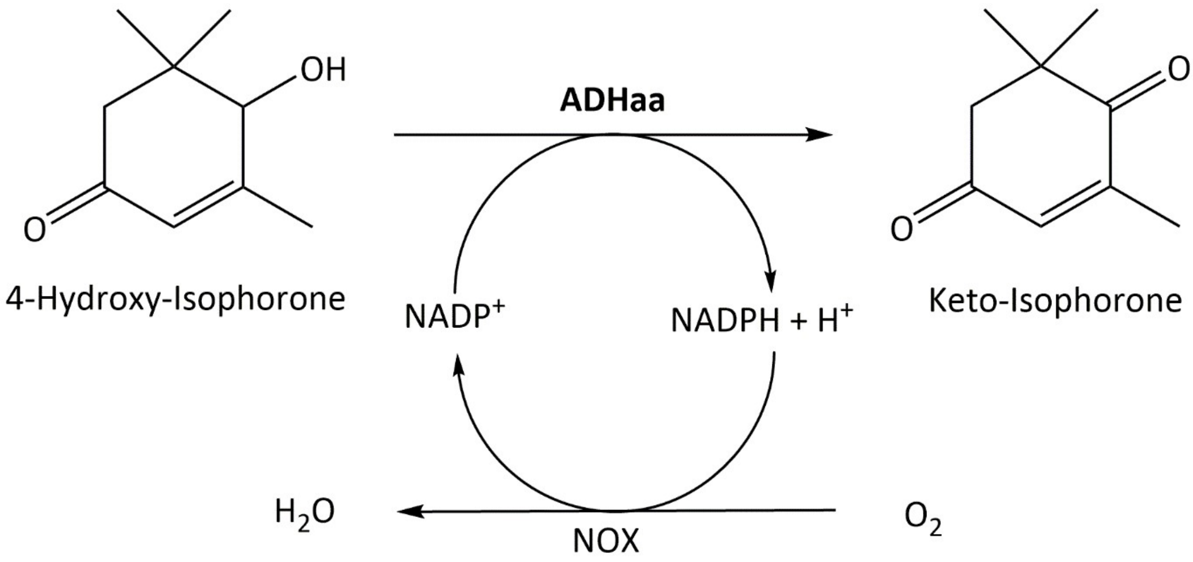

Figure 6.1. Biocatalyzed oxidation of 4-hydroxy-isophorone (HID) to keto-isophorone (KET) with a two-enzyme system using an alcohol dehydrogenase (ADHaa) and NADPH oxidase (NOX) to regenerate the NADPH using oxygen as a sacrificial substrate.

6.2 Results and discussion

6.2.1 Characterization of the cell lysates

Prior to any immobilization or operational study, the cell lysates with over-expressed ADHaa and NOX were characterized accounting for total protein content, target enzyme content and activity.

The obtained results are shown in Table 6.1. As it can be observed, ADHaa lysate contained lower amounts of protein and the enzyme was present in a lower ratio to the *E. coli* background proteins, compared with the NOX extract. In terms of specific activity, ADHaa was 5.1-fold less active than the cofactor regeneration enzyme, towards the substrates and conditions of these activity tests.

Table 6.1. Characterization of the *E. coli* cell free extracts overexpressing the ADHaa and NOX. The standard error (± %) was calculated from at least two replicates.

Enzyme	[Protein] (mg mL^{-1})	Enzyme content (%)	Specific activity (U mg^{-1} enz)
ADHaa	34.8 ± 2.1	39.6 ± 1.2	13.1 ± 0.6
NOX	50.1 ± 2.3	61.0 ± 1.2	66.5 ± 0.8

Aiming to select the most suitable strategies for ADHaa immobilization, its stability at different pH values (6, 7, 8 and 9) was assessed. It is known that the activity decay of the enzyme at certain pH, partially determines the immobilization method to be used [152]. As it can be seen in Figure 6.2, ADHaa maintained more than 80% of the initial activity after 2 hours at pH 7, 8 and 9. Under pH 6 ADHaa showed to be less stable, reaching 30% of the initial activity after 1 hour. Theoretically, alkaline media are more suitable for epoxy and/or aldehyde functionalized supports and, on the other hand, pH 6 is more appropriate for amino functionalized carriers [191]. Anyhow, a screening set of supports presenting different features and all three functionalizations was studied.

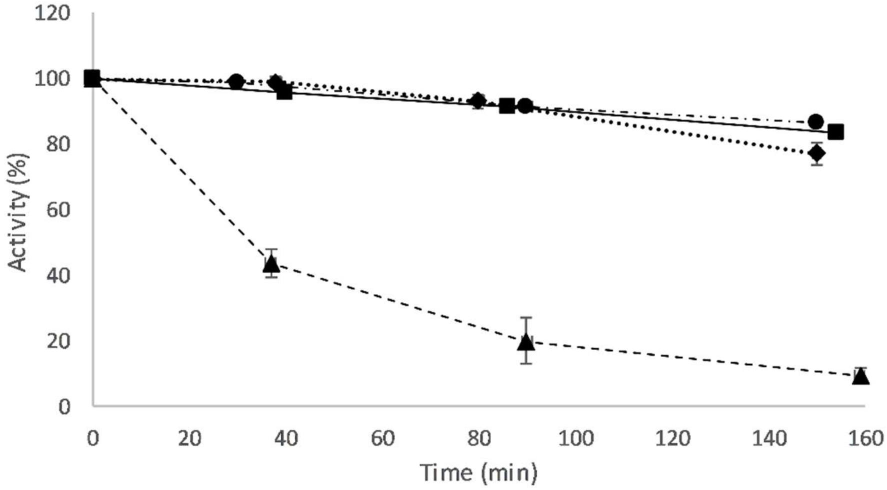

Figure 6.2. ADHaa relative activity over time measured at different pH values (of KPi buffers): pH 6 (black triangles and discontinuous line), pH 7 (black squares and continuous line), pH 8 (black rhombus and dotted line) and pH 9 (black circles and combined discontinuous spot-line-spot). The initial activity of the samples was 1.8 - 2 U mL^{-1}; 100-fold dilution of the initial lysate. Samples were maintained at 25˚C and mild agitation. The error bars correspond to the standard error calculated from at least two replicates.

6.2.2 Immobilization of ADHaa onto methacrylate/styrene supports

As explained in the introduction, immobilization can confer added benefits to industrial biocatalysts. By improving stability or allowing its re-cycling, an immobilized biocatalyst can reduce the overall cost of the process. In this sense, commercial carriers as the ones used in this study, are a good primary choice due to the ease of large-scale supply.

A commercial screening set of methacrylate/styrene materials presenting different features was studied. The carriers had different pore diameters (300 - 1800 Å), enzyme-carrier interactions (ionic, covalent and hydrophobic), functional groups (epoxy, amino and aldehyde), linker lengths (C2 - C18), material matrices (methacrylate and/or styrene) and particle sizes (150 - 710µm).

Only those supports presenting at least 90% immobilization yield and 20% retained activity are presented in Table 6.2. All the other trials are presented in Table 6.1S (Supporting information). As it can be seen (Table 6.2), two carriers fulfilled this criterion: an epoxy-functionalized (ECR8215F) and an amino-functionalized (ECR8409F) methacrylate. In both cases, even though the immobilization yield (IY) almost reached 100%, the retained activity (RA) was low (≈ 20%).

Table 6.2. Results regarding the immobilization of ADHaa onto Methacrylate/Styrene (Purolite®) resins and description of the support's features. The experiments were performed loading the support with low amounts of enzyme (12 U g-1 support) in order to characterize the enzyme-support interaction behaviour. Only those experiments with at least 90% immobilization yield and 20% retained activity are presented. Further information regarding other supports screened can be found in Supporting information, Table 6.1S. The standard error (± %) was calculated from at least two replicates.

Code	Functional group (Linker)	Matrix	Interaction	Pore diameter (Å)	Particle size (µm)	Immobilization yield (%)	Retained acitivty (%)
ECR8215F	Epoxy	Methacrylate	Covalent	1200-1800	150-300	99.9 ± 0.1	23.1 ± 1.9
ECR8409F	Amino (C6)	Methacrylate	Ionic/Covalent	600-1200	150-300	99.3 ± 0.1	20.2 ± 2.1

In the immobilization on the epoxy-functionalized methacrylate (ECR8215F), the ADHaa showed good affinity for the support. All the offered activity was attached to the resin after 0.5h incubation (99.9 ± 0.1 % IY). The final RA and IY values were obtained after 2 hours incubation. In the case of the amino-functionalized methacrylate (ECR8409F), the immobilization occurs in different phases. The ionic adsorption of the enzyme to the carrier (0.5h), which is the first step, resulted in 98.3 ± 0.1% immobilization yield and 24.2 ± 5.2% retained activity. However, being 7.2 the optimum pH for the target reaction, this method was not considered adequate. When 10 mM EDC was added to promote the covalent binding, the retained activity was reduced to 20.2 ± 2.1% (2.5h).

The functionalization of the carrier turned out to be not excluding, since each support presented a different functional group (epoxy or amino). Before trying to optimize the immobilization of the ADHaa on the methacrylate-based supports presented so far (ECR8215F an ECR8409F), a more hydrophilic matrix harboring the same functional groups (epoxy and amino) was also tested.

6.2.3 Immobilization of ADHaa onto epoxy and amino functionalized agaroses

The common feature that all methacrylate/styrene materials share is the higher hydrophobicity and rigidity that they present compared with, for instance, a hydrogel such as agarose [151], [191], [192].

Therefore, as already mentioned, an agarose matrix was considered to be tested aiming to study if higher retained activities could be achieved. Three agaroses were tested: an amino-functionalized (Mana) and two epoxy-functionalized with different activation grades: M1 (30 ± 3 µmol g^{-1}) and M2 (106 ± 1 µmol g^{-1}).

Table 6.3. Immobilization of ADHaa onto Mana-agarose and Epoxy-agarose-M1 and M2. The experiments were performed loading the support with low amounts of enzyme (12 U g^{-1} support). The standard error (± %) was calculated from at least two replicates.

Support	Activation grade (µmol g^{-1} support)	Kind of interaction	pH	[KPi] (M)	Immobilization Yield (%)	Retained Activity (%)
Mana-agarose	40 - 60	Ionic	6	0.05	88.2 ± 0.7	13.7 ± 2.3
			6.5		76.1 ± 2.3	4.8 ± 1.0
			7		14.3 ± 3.3	4.7 ± 1.2
Epoxy-agarose-M1	30 ± 3	Covalent	8	1	40.6 ± 4.8	33.9 ± 3.7
			9		93.2 ± 2.4	36.6 ± 2.5
Epoxy-agarose-M2	106 ± 1	Covalent	9		100 ± 0.0	58.2 ± 3.5

The results are presented in Table 6.3. Regarding Mana-agarose, three pH values were tested (6, 6.5 and 7). It can be seen that the immobilization yield was very low (14.3 ± 3.3 %) when the immobilization was performed at pH 7. This result could be related to the pKa of the primary amine of Mana-agarose. When the pH is higher than the pKa (6.8) the amino-groups are deprotonated and, therefore, the first step of the immobilization, i.e. the ionic adsorption of the enzyme towards the support, is not favored. On the other hand, when the immobilization with Mana-agarose was pursued at pH 6.0 or 6.5, even though the immobilization yields were higher than the pH 7 case, the final retained activities were lower due to the high instability of ADHaa at pH < 7. Regarding the Epoxy-agaroses, when the immobilization occurs at pH close to 10, it favors the epoxy-ring opening and so the covalent bond formation with the amino groups of the enzyme [151]. The first studies were carried out with Epoxy-agarose-M1 by testing two pH values, 8 and 9. In this line, pH 9 (Figure 6.3 A) significantly improved the results by increasing the immobilization yield 2.3-fold, compared to pH 8. Therefore, pH 9 was selected to test the Epoxy-agarose-M2 which presents a 3.5-fold higher activation grade compared with M1. , The utilization of Epoxy-agarose-M2 (Table 6.3), resulted in 1.6-fold higher retained activity compared with the less activated Epoxy-agarose-M1. As it can be seen in Figures 6.3 A and B, the suspension activity profile is similar in both cases, a gradual drop of the suspension activity over time. The reason behind this behavior can be the progressive multi-point attachment of the enzyme to the support [150]. The epoxy groups of the carrier initially react with the amino groups of the enzyme creating a first binding. Over time though, the epoxy groups start reacting with the carboxyl and thiol groups of the enzyme generating a second multipoint binding that can partially deactivate the ADHaa. Comparing the two figures, in the second case, the decrease is less pronounced and it levels off after 3 hours of incubation. This different behavior could be attributed to the enzyme's nature and its specific interaction with the differently distributed epoxy groups. When using other enzymes such as the cytochrome P450 BM3 (CYP102A1), the opposite effect has been reported [193].

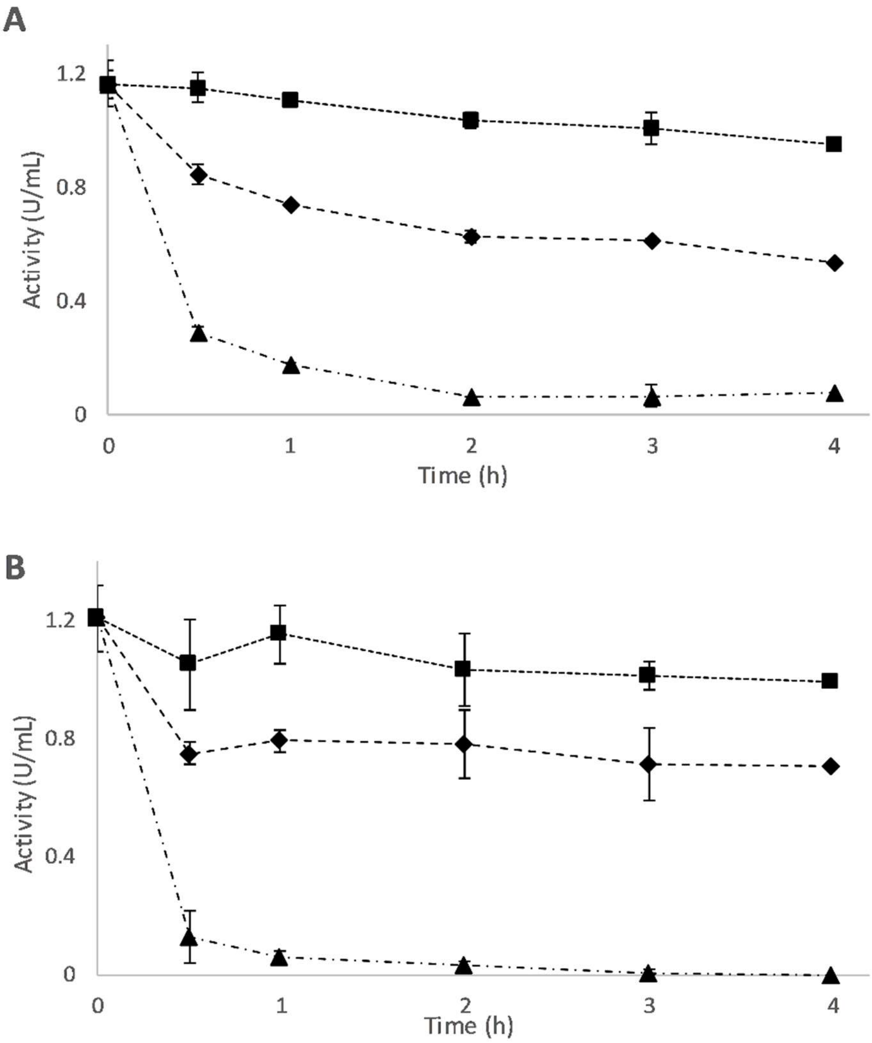

Figure 6.3. Immobilization course of ADHaa onto: A) Epoxy-agarose-M1 and B) Epoxy-agarose-M2. The experiments were performed loading the supports with low amounts of enzyme (12 U g^{-1} support). The immobilization was carried out using 1 M KPi buffer pH 9. Samples were maintained at 25˚C and mild agitation. The graph shows the activity of the blank (black squares), the supernatant (black triangles) and the suspension (black rhombus) over time. The error bars correspond to standard error of at least two replicates.

The Epoxy-agarose-M2 resulted in the highest immobilization metrics achieved so far, presenting 100% immobilization yield and 58.2 ± 3.5% retained activity. It should be highlighted that this is the first time that an alcohol dehydrogenase from *Artemisia annua* has been successfully immobilized.

6.2.4 Immobilization of ADHaa on Epoxy-agarose-M1 and M2 applying high loads of enzyme

The immobilizations presented in Table 6.2, 6.3 and Figure 6.3 were carried out loading the supports with low amounts of enzyme, minimizing the possible diffusional limitations. Thus, it allows the characterization of the immobilization processes. However, in order to ideally study an immobilized biocatalyst in an industrial target reaction, the support should contain the highest number of units of activity possible [112]. To do so, the two best performing carriers, according to the IY and RA obtained during characterization, were chosen: Epoxy-agarose-M1 and Epoxy-agarose-M2 (pH 9).

In Figure 6.3 A and B, as aforementioned, it can be observed that the suspension activity slightly decreases over time, especially in Figure 6.3 A, reducing like this the retained activity and also the multiplying factor (Table 6.4). At the same time, the longer the immobilization time, the higher is the amount of enzyme that can be attached to the support (Attached units). Therefore, in order to generate an immobilized derivate with the highest activity possible (Specific activity), a compromise must be found between the amount of units attached to the support (longer immobilization times) and the multiplying factor (shorter immobilization times).

Table 6.4. Immobilization of ADHaa onto Epoxy-agarose-M1 and M2 using maximum loads of enzyme per gram of support. In both cases the offered activity was 476.6 U g^{-1} of support (36.4 mg enzyme g^{-1} of support). The immobilization was carried out using 1 M KPi buffer pH 9. Samples were maintained at 25˚C and mild agitation.

	Epoxy-agarose-M1			**Epoxy-agarose-M2**		
Time (h)	Attached units (U g^{-1} support)	Multiplying factor (RA/IY)	Specific activity (U g^{-1} support)	Attached units (U g^{-1} support)	Multiplying factor (RA/IY)	Specific activity (U g^{-1} support)
1	189.2	0.57	108.4	222.8	0.64	142.0
2	207.8	0.51	106.4	266.5	0.64	169.5
3	236.9	0.51	119.9	301.0	0.59	177.4
4	261.9	0.42	109.9	336.4	0.58	195.7

As it can be observed in Table 6.4, the optimum immobilization time for Epoxy-agarose-M1 was 3 hours leading to 119.9 U g^{-1} of support, and for epoxy-agarose-M2 it was 4 hours with 195.7 U g^{-1} of support. This second immobilization leaves room for improvement since longer immobilization times could result in higher specific activities. Anyhow, epoxy-agarose-M2 (pH 9 and 4h) was chosen as the best carrier to be studied in the target reaction.

6.2.5 Oxidation of 4-hydroxy-isophorone to keto-isophorone: soluble and immobilized biocatalysts

The target reaction was primary studied using both the ADHaa and NOX in its soluble form, as cell free extracts. The results obtained can be seen in Figure 6.4 A. As the graph shows, the reaction time was set at 24 hours and the ADHaa load was adjusted so that at least 90% conversion was reached [5% ADHaa lysate (v/v)]. The cofactor regeneration enzyme (NOX), as well as the oxygen supply, were assured to be non-limiting.

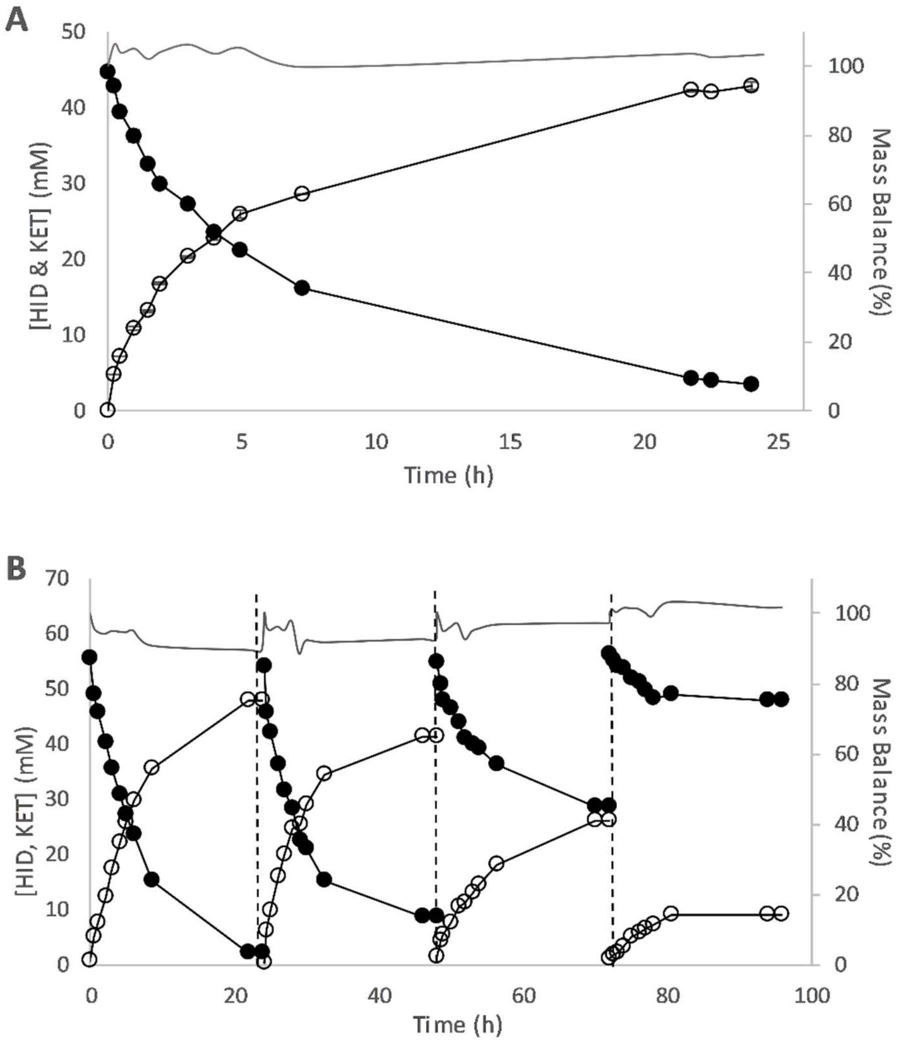

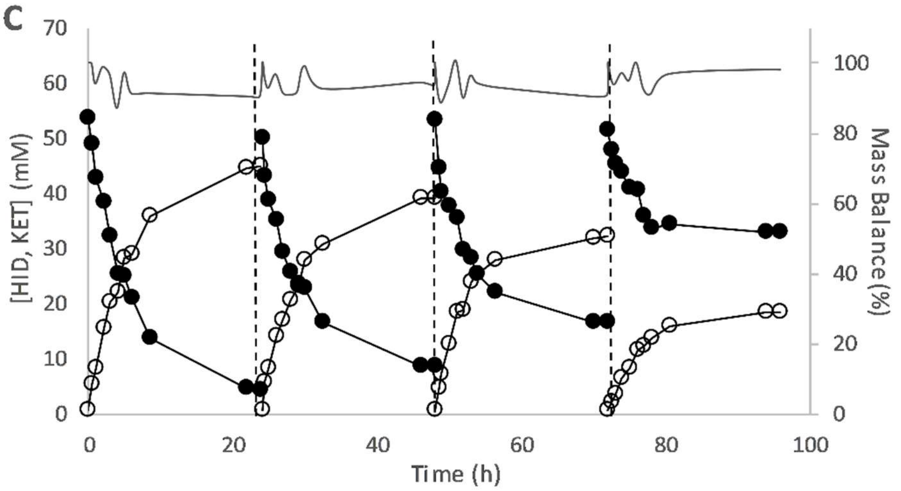

Figure 6.4. Oxidation of 4-hydroxy-isophorone to keto-isophorone on 10 mL reactor with ADHaa and NOX as the cofactor regeneration enzyme. The graphs show the reaction course of KET (white spots), HID (black spots) and mass balance (continuous grey line with no spots). A) Reaction using the enzymes on its soluble form: 5% (v/v) of ADHaa lysate (180.9 U mL^{-1} of CFE) and 3% (v/v) of NOX lysate (2032.2 U mL^{-1} of CFE); B) Reaction cycles with magnetic stirring and immobilized ADHaa and soluble NOX lysate: 10% (w/v) of ADHaa immobilized derivate (106.4 U g^{-1} of support) and 3% (v/v) of NOX lysate (2032.2 U mL^{-1} of CFE) and C) Reaction cycles with mechanical stirring and immobilized ADHaa and soluble NOX lysate: 10% (w/v) of ADHaa immobilized derivate (131.6 U g^{-1} of support) and 3% (v/v) of NOX lysate (2032.2 U mL^{-1} of CFE). Conditions: temperature 30°C; stirring rate 1000 rpm; oxygen flow 0.45 mL min^{-1}; pH 7.2; [HID] 50 mM and [NADP$^+$] 1 mM.

As the Figure 6.4 A shows, the final conversion was 92.2% and the yield was 95.7% indicating a slight mass balance gap of 3.5%. Even though the oxygen gas was hydrated prior to be introduced in the reactor, certain evaporation could have occurred. Thus, a slight reduction of the reaction volume could increase both substrate and product concentration, causing the mass imbalance. The final metrics of the reaction can be seen on Table 6.5. The space time yield obtained after 24h of reaction was 6.52 g L^{-1} day^{-1}.

Once the soluble reaction was performed, the ADHaa was immobilized on epoxy-agarose-M2 in order to be applied in the target reaction. Regarding NOX, at the beginning of each cycle, it was added freshly as cell free extract.

The results regarding the re-utilization of the immobilized ADHaa are shown in Figure 6.4 B and C. In the first case (Figure 6.4 B), magnetic stirring was employed, causing an observable grinding of the agarose particles. This caused an obturation of the porous plate during filtration. In order to solve this issue, in the second case (Figure 6.4 C), mechanic stirring was used allowing a rapid and efficient filtration every cycle. In this case no particle breakdown was observed.

As it can be seen, when the ADHaa was immobilized, the biocatalyst could be re-used up to 4 times. However, the conversion decreased from cycle to cycle in Figure 6.4 B: 1) 95.4% conversion and 85.6% yield, 2) 83.8% conversion and 76.4% yield, 3) 46.6% conversion and 46.4% yield and 4) 14.1% conversion and 15.8% yield; and also in Figure 6.4 C: 90.4% conversion and 82.1% yield, 2) 81.7% conversion and 76.8% yield, 3) 67.9% conversion and 59.8% yield and 4) 36.0% conversion and 35.1% yield. The mass balance varied from 87.0 to 101.7% in both cases.

In Table 6.5 a final summary of the reaction metrics can be found. When immobilized ADHaa was used, the biocatalyst yield (g KET g^{-1} enzyme) obtained for this enzyme was improved compared with the soluble enzyme. The reactions performed under magnetic stirring and mechanical stirring led to similar biocatalyst yields (23.4 g KET g^{-1} enzyme and 20.2 g KET g^{-1} enzyme) representing among 2.5 and 2.1-fold improvement, respectively. Regarding NOX, it should be taken into account that, while ADHaa is used immobilized and recycled, NOX is added freshly in each reaction cycle. That is why, the biocatalyst yield of NOX is lower when compared with the reaction with soluble ADHaa (Table 6.5, grey values).

Table 6.5. Final summary of the performed reactions, Figure 4 A, B and C. The conditions are the same as the ones reported before for those figures.

Figure	**Enzyme**	**Immob**	**Soluble**	**Activity in the reactor (U mL^{-1})**	**Enzyme loaded in the reactor (mg)**	**Total KET formed (mg)**	**Biocatalyst yield (g KET g^{-1} enzyme)**	**Improvement factor**
Figure 4 A)	ADHaa		X	9.1	6.9	65.2	9.5	-
	NOX		X	61.0	9.2		7.1	-
Figure 4 B)	**ADHaa**	**X**		**10.6**	**8.1**	189.1	**23.4**	**2.5**
	NOX		X	61.0 x 4	9.2 x 4		5.1	0.7
Figure 4 C)	**ADHaa**	**X**		**13.2**	**10.1**	204.5	**20.2**	**2.1**
	NOX		X	61.0 x 4	9.2 x 4		5.6	0.8

6.3 Conclusions

The enzymatic production of chemical compounds offers a greener alternative to the traditional routes in which often harsh conditions and reagents or expensive catalysts are employed [81]. When the synthesized compound is meant for nutritional purposes, biocatalysis also adds the possibility to include the “natural” label to the final product [194]. In this sense, the enzymatic oxidation of 4-hydroxy-isophorone is in this same situation. The product obtained, keto-isophorone, is a key intermediate for the synthesis of carotenoids and Vitamin E, among others.

The synthesis of keto-isophorone catalyzed by an alcohol dehydrogenase has proven successful. Moreover, in order to avoid the addition of stoichiometric amounts of $NADP^+$, a NADPH oxidase was added as a cofactor regeneration enzyme. In 24h, up to 95.7% of the initial 50 mM substrate concentration could be converted into the desired product. The reaction showed a space time yield of 6.52 g L^{-1} day^{-1} and good mass balances (96.5%).

Immobilization of ADHaa was also studied as a strategy to improve the final metrics of the reaction. For the first time, an alcohol dehydrogenase from *Artemisia annua* could be successfully immobilized on four different supports showing immobilization yields above 40% and retained activities above 20%. In this sense, an epoxy-agarose excelled among the four showing 100 ± 0% immobilization yield and 58.2 ± 3.5% retained activity.

The immobilized ADHaa was used in 4 consecutive reaction cycles, that lasted 24h each. Two sets of 4 reaction cycles were performed comparing magnetic and mechanical stirring. As expected, the magnetic stirring significantly grinded the agarose particles and hampered the filtration. However, the breakdown of the particles did not entail a significant loss of activity when compared with the reaction mechanically stirred. At the end, the re-utilization of ADHaa implied from 2.1 to 2.5-fold increase in biocatalyst yield (20.2 to 23.4 g KET g^{-1} enzyme).

These promising results on the use of immobilized enzymes open new possibilities to implement novel reactor configurations (e.g. plug flow design), facilitate the product purification and allow the re-utilization of the enzyme.

6.4 Supporting information

Table 6.1S. Methacrylate/styrene (Purolite®) screening set of resins and the immobilization results (immobilization yield and retained activity) for the ADHaa. The experiments were performed loading the supports with low amounts of enzyme (12 U g^{-1} support). The standard error (± %) was calculated from at least two replicates.

Code	Functional group (Linker)	Matrix	Interaction	Pore diameter (Å)	Particle size (µm)	Immobilization (%)	Retained acitivty (%)
ECR8204F	Epoxy	Methacrylate	Covalent	300-600	150-300	100 ± 0	19.4 ± 2.0
ECR8215F	Epoxy	Methacrylate	Covalent	1200-1800	150-300	99.9 ± 0.1	23.1 ± 1.9
ECR8309F	Amino (C2)	Methacrylate	Ionic/Covalent	600-1200	150-300	99.6 ± 0.4	7.9 ± 1.0
ECR8315F	Amino (C2)	Methacrylate	Ionic/Covalent	1200-1800	150-300	99.7 ± 0.3	11.0 ± 1.0
ECR8409F	Amino (C6)	Methacrylate	Ionic/Covalent	600-1200	150-300	99.3 ± 0.1	20.2 ± 2.1
ECR8415F	Amino (C6)	Methacrylate	Ionic/Covalent	1200-1800	150-300	99.1 ± 0.0	19.2 ± 2.6
ECR8285	Epoxy (C4)	Methacrylate	Covalent	400-600	300-710	99.5 ± 0.5	13.0 ± 1.5
ECR8806F	None (C18)	Methacrylate	Hydrophobic	500-700	150-300	99.4 ± 0.1	3.7 ± 0.8
ECR1061M	None	Styrene/Methacrylic	Hydrophobic	600-750	300-710	40.8 ± 0.7	0 ± 0
ECR1030M	None	Styrene/Methacrylic	Hydrophobic	200-300	300-710	59.9 ± 1.9	0 ± 0
ECR8309F	Aldehyde (C7)	Methacrylate	Ionic/Covalent	600-1200	150-300	99.4 ± 0.6	1.8 ± 1.8
ECR8315F	Aldehyde (C7)	Methacrylate	Ionic/Covalent	1200-1800	150-300	99.6 ± 0.4	4.7 ± 1.6
ECR8409F	Aldehyde (C11)	Methacrylate	Ionic/Covalent	600-1200	150-300	100 ± 0.0	8.2 ± 1.5
ECR8415F	Aldehyde (C11)	Methacrylate	Ionic/Covalent	1200-1800	150-300	99.2 ± 0.8	15.2 ± 2.9

I-N-N-O
S-Y-N
Tomorrow's chemistry. Today.

The research explained in the following chapters was mostly performed in InnoSyn B.V.'s facilities (Geleen, The Netherlands) under the supervision of Dr. Jan Brummund and Dr. Martin Schürmann as part of an international internship.

7. Enzymatic synthesis of trimethyl-ε-caprolactone: process intensification and demonstration at 100 liter scale

Abstract

The optimization and scale up of the Baeyer-Villiger oxidation of 3,3,5-trimethylcyclohexanone to trimethyl-ε-caprolactones (CHL) was studied in order to demonstrate this technology on 100 L pilot plant scale. The reaction was catalyzed by a cyclohexanone monooxygenase from *Thermocrispum municipale* (TmCHMO). This enzyme utilizes the costly redox cofactor NADPH which was regenerated by a glucose dehydrogenase (GDH).

As a first stage, different cyclohexanone monooxygenase formulations were tested: cell free extract, whole cells, fermentation broth and sonicated fermentation broth. Using the broth resulted in the highest yield and required the least biocatalyst preparation effort: 63% yield instead of 39% obtained with a cell free extract or 59% obtained with whole cells. Two glucose dehydrogenases were evaluated and the selection was made for the enzyme with a pH optimum in application of 7.0 (GDH-01) instead of 8.0 (GDH-105) to minimize the risk of base catalyzed lactone hydrolysis.

The substrate dosing rate and the biocatalyst loadings were optimized. At 30 mL scale, the best conditions were found when 30 mM h^{-1} dosing rate, 10% (v/v) cyclohexanone monooxygenase broth and 0.05% (v/v) of glucose dehydrogenase (GDH-01) liquid enzyme formulation were applied. These same conditions (with oxygen instead of air) were applied at 1 liter scale with 92% conversion, achieving a specific activity of 13.3 U g^{-1} cell wet weight (cww), a space time yield of 3.4 g CHL L^{-1} h^{-1} and a biocatalyst yield of 0.83 g CHL g^{-1}_{cww}.

A final 100 liter demonstration was performed in a pilot plant facility. After 9 hours, the reaction reached 85% conversion, 12.8 U g^{-1}_{cww}, a space time yield of 2.7 g L^{-1} h^{-1} and a biocatalyst yield of 0.60 g CHL g^{-1}_{cww}. The extraction of the product was accomplished with ethyl acetate that, once evaporated, resulted in 2.58 kg isolated final product. It contained 11.9% of remaining substrate and 84.5% of the CHL isomers. The overall isolated CHL yield was 76% (distal lactone 47% and proximal lactone 53%).

7.1 Introduction

Historically, the chemical pathway followed for the production of aliphatic polyesters comprises the Baeyer-Villiger oxidation of (branched) cyclic ketones to obtain (branched) lactones that serve as the monomer building blocks. This route presents several drawbacks: limited regioselectivity, use of pollutant organic solvents, halogenated oxidants and formation of undesired by-products [195].

The biocatalytic alternative, on the other hand, overcomes most of these disadvantages. Baeyer-Villiger monooxygenases operate in mild aqueous conditions, make use of molecular oxygen as the oxidant molecule and frequently present high regioselectivity [81], [196]. Different examples of large scale applications of these enzymes can be found in the literature [197], [198]. For example, Hilker *et al.* scaled up the oxidative reaction of *rac*-bicyclo[3.2.0]hept-2-en-6one to kilogram scale using a resin-based *in situ* substrate-feeding/product-removal (SFPR) strategy [199]. The main disadvantages of these biocatalysts though, are its low stability, poor organic solvent tolerance, substrate and product inhibition and the use of the costly and unstable NADPH cofactor [200]–[202].

In 2016, a cyclohexanone monooxygenase from *Thermocrispum municipale* DSM 44069 (TmCHMO; EC 1.14.13.22) was discovered [97]. It exhibits an improved thermostability with a melting temperature of 48˚C, improved organic solvent tolerance and a broad scope towards branched cyclic ketones compared to other CHMOs. Furthermore, two different fusion constructs have been obtained in order to enable *in situ* regeneration of the cofactor. First, the TmCHMO was fused to an alcohol dehydrogenase and it was used to oxidize cyclohexanol to ε-caprolactone [203]. Second, the TmCHMO was fused to a phosphite dehydrogenase that utilizes phosphite as a sacrificial substrate [204], [205].

In this work, the TmCHMO was investigated in combination with a Glucose dehydrogenase (GDH), as the cofactor regeneration enzyme [34], for the oxidation of 3,3,5-trimethylcyclohexanone (TMCH) to produce trimethyl-ε-caprolactone (CHL) (Figure 7.1). The GDH uses glucose (Glc) as a sacrificial substrate forming gluconolactone which spontaneously hydrolyses to gluconic acid that causes an acidification of the reaction medium. Therefore the pH was controlled by addition of base and the amount of base added, provided a good indication of the reaction course.

The combination of TmCHMO and a commercial GDH-105 to synthesize trimethyl-ε-caprolactones from 3,3,5-trimethylcyclohexanone was recently studied and published by Delgove *et al.* [123]. In that work, reaction engineering regarding biocatalyst loading, air flow, stirring rate, substrate dosing rate and methanol concentration was performed up to 500 mL scale and conversions >99% were achieved with 240 mM substrate concentration. Since the reaction suffers from substrate inhibition, a constant substrate feeding strategy was applied.

This work has been focused on further optimization of the main limiting parameters of the biotransformation to finally scale up the optimized reaction to 100 liter reaction volume in the 200 L pilot plant reactor of InnoSyn B.V.

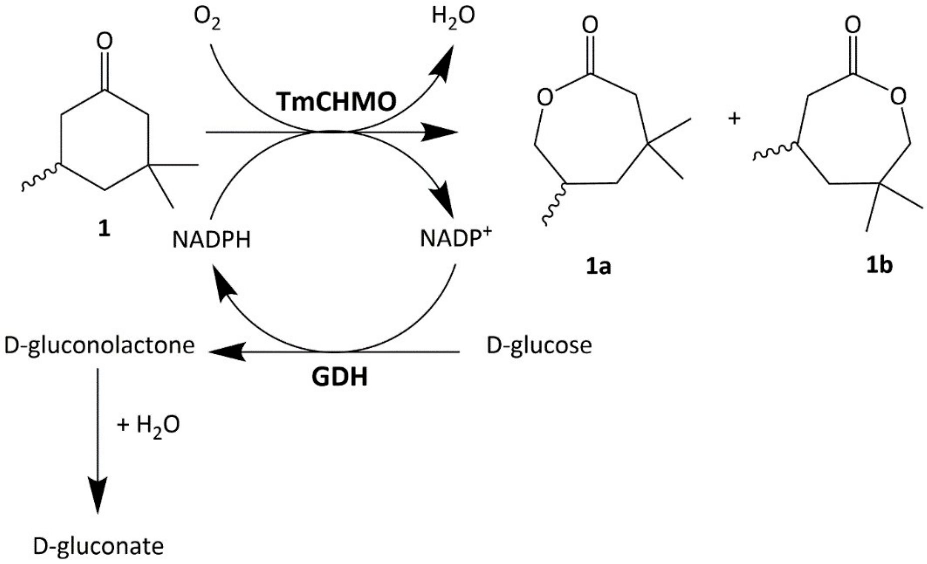

Figure 7.1. Biocatalyzed oxidation of the branched substrate 3,3,5-trimethylcyclohexanone (**1**) to a mixture of β,β,δ-trimethyl-ε-caprolactone (**1a**) and β,δ,δ-trimethyl-ε-caprolactone (**1b**) with the two-enzyme system consisting of cyclohexanone monooxygenase (TmCHMO) and glucose dehydrogenase (GDH) to regenerate the NADPH using D-glucose as a sacrificial substrate.

7.2 Results and discussion

7.2.1 Process development on 30 mL scale

7.2.1.1 Control experiments for substrate and product solubility and background titration

Before starting to optimize the reaction, some tests were performed to assess the substrate and product solubility and the background titration of the system.

To study the substrate solubility, 240 mM TMCH were added to the reactor in presence of 25 mM KPi buffer and 10% (v/v) methanol. The final substrate and methanol concentrations were set based on the previous work of Delgove *et al.* [123]. The measured TMCH concentration was between 100 and 130 mM. Apart from this, even when the substrate was dosed, the analyzed concentration over time was always below the added concentration, leading to the conclusion that the substrate required some additional time after dosing to dissolve in the reaction system completely.

Regarding the results for the analyzed product concentration, CHL was considered to be rather insoluble even in presence of 10% (v/v) methanol. The same conditions of the following reaction were mimicked, 25 mM KPi pH 8, 5% (v/v) TmCHMO CFE and 0.1 mg mL^{-1} GDH-105. The analyzed CHL concentration did not exceed a 200 mM threshold. The addition of an extra 5% (v/v) portion of methanol, however, allowed the product to be analyzed up to the added 240 mM.

Moreover, control experiments were carried out to study a potential NaOH titration by the pH controller without any target reaction taking place (background acidification and titration). Among these background acidification effects, the most important considered were: 1) the by-products of potential bacterial growth, 2) the by-products of enzymes present in the TmCHMO cell-free extracts (CFEs) and 3) the spontaneous degradation of NADPH to NADP$^+$. All of them were studied; the first by using broth of an *E. coli* strain expressing a non-target enzyme, the second by using only the TmCHMO CFE and the third, by using only the cofactor regenerating GDH liquid enzyme formulation without TmCHMO. The titration values were: 10.9%, 0.5% and 1.8%, respectively (percentages expressed with respect to the total substrate added). As a conclusion, the NaOH added by the pH controller was considered to be as a good estimation of the total CHL produced.

7.2.1.2 Variation of the applied TmCHMO enzyme formulation

The reaction conditions, which were published recently, served as starting point for further investigation [123]. The reactor contained 240 mM final substrate concentration which was dosed as stock solution in methanol at a dosing rate of 15 mM h^{-1}, finally 10% (v/v) methanol, 375 mM of D-glucose, 0.25 mM of NADP$^+$, 25 mM KPi buffer, pH 8.0, stirring at 500 rpm, 16 mL min^{-1} air flow, 5% (v/v) TmCHMO CFE and 0.1 mg mL^{-1} GDH-105. The only implemented changes were the stirring rate (1200 rpm instead of 500 rpm); and the co-solvent methanol that was dosed together with the substrate instead of adding it to the reactor from the beginning.

The obtained results can be seen in the graph below (Figure 7.2, left columns, CFE). 40% CHL yield was obtained. The ratio of product regio-isomers, 45 ± 2% distal lactone and 55 ± 2% proximal lactone, was sustained in all reactions. The difference between the three presented values (conversion, yield and titration) can be attributed to the poor solubility of the components and the lack of a proper work up procedure for the reactor content once the reaction was finished. For the following reactions, to obtain a final representative sample, the whole reaction volume was dissolved in acetonitrile at the end of the reaction. The results that were obtained from the analysis of this final dilution are the ones presented in all bar charts in this article.

The first parameter that has been investigated was the TmCHMO formulation (Figure 7.2). Apart from the cell free extract, also whole cells (WC), fermentation broth and sonicated fermentation broth were tested. The results showed that the application of broth and sonicated broth resulted in highest yields and highest rates. The difference to the results that were achieved with the other two TmCHMO formulations can be explained by the higher biomass that these two formulations contained (413 g cww equivalents L^{-1}) in contrast to the CFE and WC (333 g cww equivalents L^{-1}). Nevertheless, fermentation broth requires the least unit operations for its production (no cell disruption, centrifugation and/or washing steps). Therefore, it was selected as optimal formulation for further process development studies.

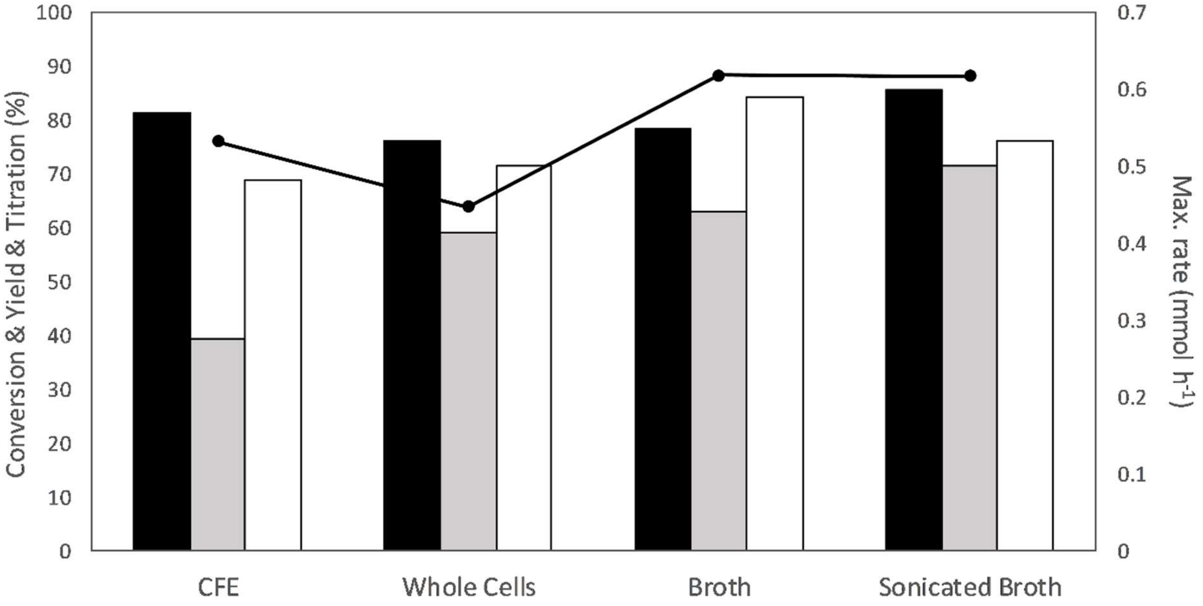

Figure 7.2. Comparison between four different formulations of TmCHMO regarding conversion (black bar), yield (grey bar), titration (white bar) and maximum rate (black circles, right axis). The rate was calculated by linear regression on the reaction kinetics (from 1 to 4 hours). Reactions were performed in 30 mL reactors with an enzyme load of 5% (v/v) of the respective TmCHMO formulation and 0.1 mg mL^{-1} of GDH-105; temperature 30°C; stirring rate 1200 rpm; air flow 16 mL min^{-1}; pH 8; [TMCH] 15 mM h^{-1} (240 mM final); Methanol 0.625% (v/v) h^{-1} (10% (v/v) final); [D-glucose] 375 mM; [$NADP^+$] 0.25 mM; titration solution 1 M NaOH.

7.2.1.3 Variation of the applied GDH source for cofactor regeneration

The second implemented change consisted in the substitution of GDH-105 (Codexis) for GDH-01, produced by InnoSyn. GDH-01 has its operational stability optimum in the neutral pH range. Therefore, two other pH values were tested using GDH-01 in 30 mL reactions, namely pH 6 and 7 (Figure 7.3). The yield at pH 7 was similar to that obtained with the GDH-105 at pH 8, 63% and 67% respectively. Regarding the maximum reaction rate achieved, pH 7 was significantly higher than the other two tested conditions. Working at neutral pH came with the advantage of a reduced risk of base catalyzed lactone hydrolysis which preferentially occurs at more basic pH.

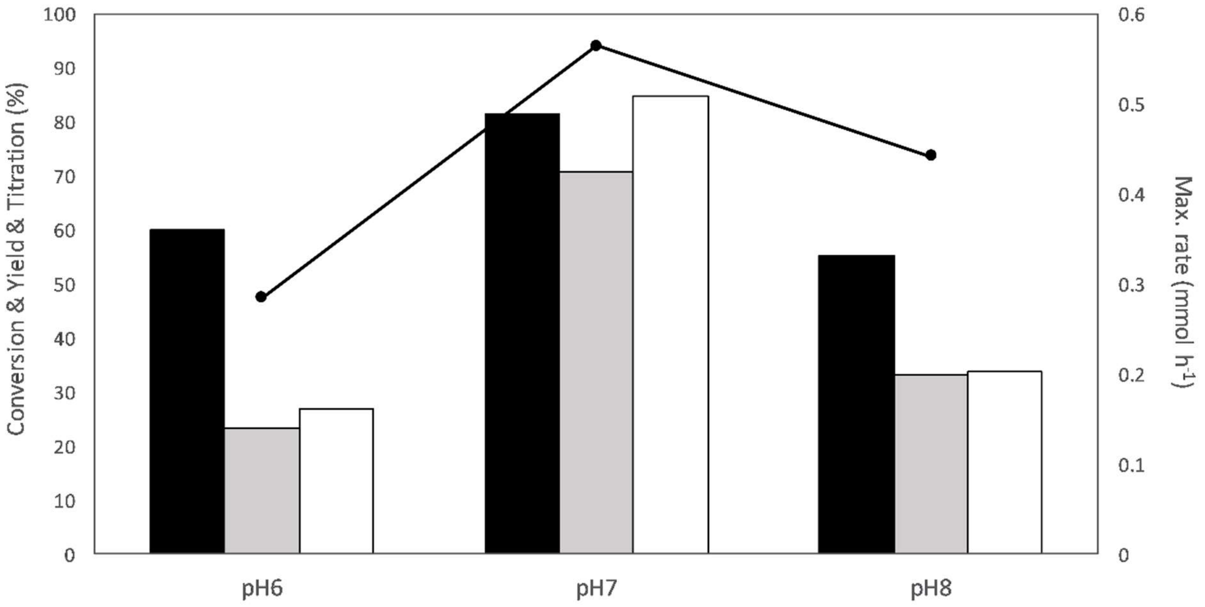

Figure 7.3. Comparison between three different pH set points for the application of GDH-01 regarding conversion (black bar), yield (grey bar), titration (white bar) and maximum rate (black circles, right axis). The rate was calculated by linear regression on the reaction kinetics (from 1 to 4 hours). Reactions in 30 mL reactors with a biocatalyst load of 5% (v/v) TmCHMO Broth and 0.5% (v/v) GDH-01; temperature 30°C; stirring rate 1200 rpm; air flow 16 mL min^{-1}; [TMCH] 15 mM h^{-1} (240 mM final); Methanol 0.625% (v/v) h^{-1} (10% (v/v) final); [D-glucose] 375 mM; [NADP$^+$] 0.25 mM; titration solution 1 M NaOH.

7.2.1.4 Variation of the applied substrate dosing rate

The substrate availability in the reactor was a limiting factor for the first 6 hours of reaction (Figure 7.4, left). As it can be observed, at the beginning of the reaction, there was no substrate accumulation (dosing rate 15 mM h^{-1}). Increasing the dosing rate could result in higher reaction rates that in turn would represent shorter reaction times for constant total substrate amounts. With shorter reaction times, the enzyme deactivation as well as product degradation (e.g. potential hydrolysis or methyl-ester formation) would be reduced. As a result, the reaction yield would increase.

Doubling the dosing rate to 30 mM h^{-1} (Figure 7.4, right) reduced the reaction time from 18.2 h to 13.5 h (according to the titration progress), it increased the maximum rate from 0.54 mmol h^{-1} to 0.68 mmol h^{-1} and the yield from 67% to 79%. However, the substrate accumulation is detrimental for the reaction since the BVMO suffers from substrate inhibition. That is why the following experiments were aimed at the reduction of the limiting factors provoking this accumulation. The final mass balance, on the other hand, did not change and stayed around 90% in both cases.

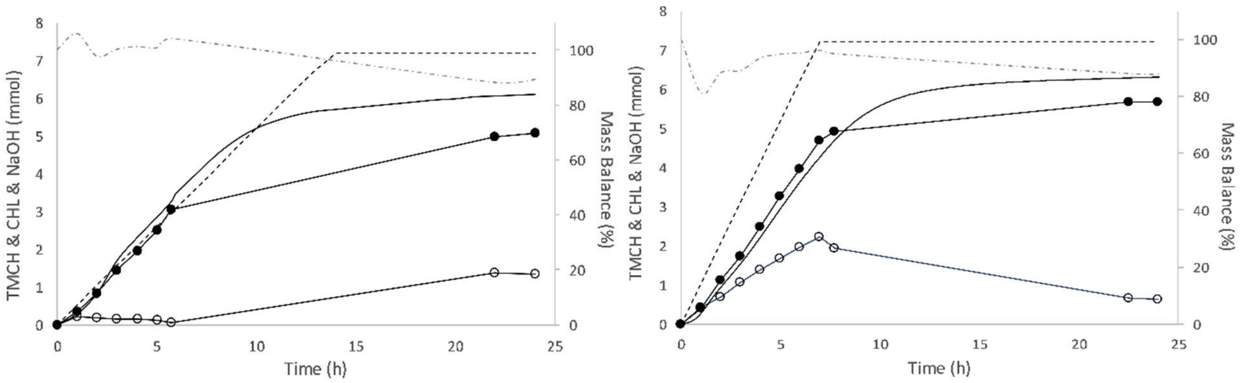

Figure 7.4. Reaction in 30 mL reactor with 15 mM h^1 substrate dosing rate (left graph) and 30 mM h^{-1} (right graph). The graphs show the reaction course of TMCH (white circles), CHL (black circles), NaOH addition (black line), substrate dosing (discontinuous line) and mass balance (combined discontinuous spot-line-spot). Conditions: biocatalyst load of 5% (v/v) of TmCHMO Broth and 0.5% (v/v) of GDH-01; temperature 30°C; stirring rate 1200 rpm; air flow 16 mL min^{-1}; pH 7; 240 mM final TMCH concentration; Methanol 0.625% (v/v) h^{-1} (10% (v/v) final); [D-glucose] 375 mM; [$NADP^+$] 0.25 mM; titration solution 1 M NaOH.

7.2.1.5 Variation of the applied TmCHMO loading

Once the substrate dosing rate was increased, the considered limiting factors were: the TmCHMO loading, the GDH loading and the oxygen supply rate. Using pure oxygen instead of pressurized air was the feasible change to overcome oxygen limitations in the reaction. However, this change was not possible at 30 mL scale due to safety issues (nitrogen purge has to be installed to keep the oxygen levels in a sufficiently low range) [206]. Regarding the GDH, on the other hand, a 0.5% (v/v) load of GDH-01 represents 9.6-fold more Units of activity compared to the experiments with GDH-105 (0.1 mg mL^{-1}). Therefore, GDH was most probably not limiting the reaction. For these reasons, the first investigated process parameter was the TmCHMO load using a variation from 5.0% (v/v) to 7.5% (v/v) and up to 10% (v/v) (Figure 7.5).

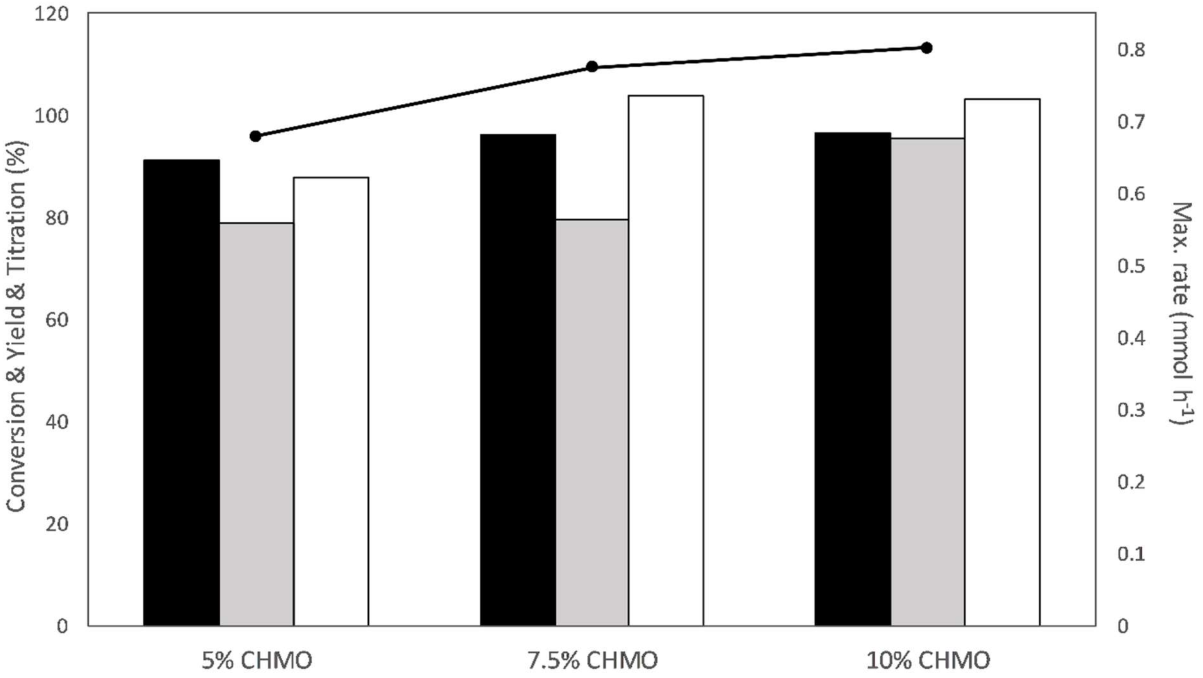

Figure 7.5. Comparison between three different TmCHMO loads regarding conversion (black bar), yield (grey bar), titration (white bar) and maximum rate (black circles, right axis). The rate was calculated by linear regression on the reaction kinetics (from 1 to 4 hours). Reactions in 30 mL reactors with an enzyme load of 5%; 7.5% and 10% (v/v) of TmCHMO Broth and 0.5% (v/v) of GDH-01; temperature 30°C; stirring rate 1200 rpm; air flow 16 mL min^{-1}; pH 7; [TMCH] 30 mM h^{-1} (240 mM final); Methanol 1.25% (v/v) h^{-1} (10% (v/v) final); [D-glucose] 375 mM; [NADP$^+$] 0.25 mM; titration solution 1 M NaOH.

The maximum rate achieved by the 10% (v/v) TmCHMO load reaction was not twice as high as by using the 5% (v/v) load which meant that other factors were also limiting the reaction. Thus, oxygen was most probably the cause. If the biocatalyst yield was taken into account, 5% (v/v) load should be used. It presented 79% yield, only 17% less than with the 10% (v/v) TmCHMO load. However, the goal was to get as close as possible to full conversion to facilitate an efficient down-stream processing to isolate the product. Finally, 10% (v/v) TmCHMO broth was selected as biocatalyst loading for further investigations.

7.2.1.6 Variation of the applied GDH loading

As aforementioned, the GDH was most probably not limiting the reaction. However, the added amount of 0.5% (v/v) liquid enzyme formulation had not been optimized. A broad range of GDH-01 loadings, from 1% (v/v) to 0.01% (v/v) was screened (Figure 7.6). As it can be seen in the graph below, the maximum rate was maintained and full conversion was achieved with 0.05% (v/v) loading. This load represents 3.8 U mL^{-1} in the reactor, similar activity as offered with 0.1 mg mL^{-1} of GDH-105 (3.9 U mL^{-1}). It could be concluded that the GDH-01 is as stable as the GDH-105 under the applied conditions.

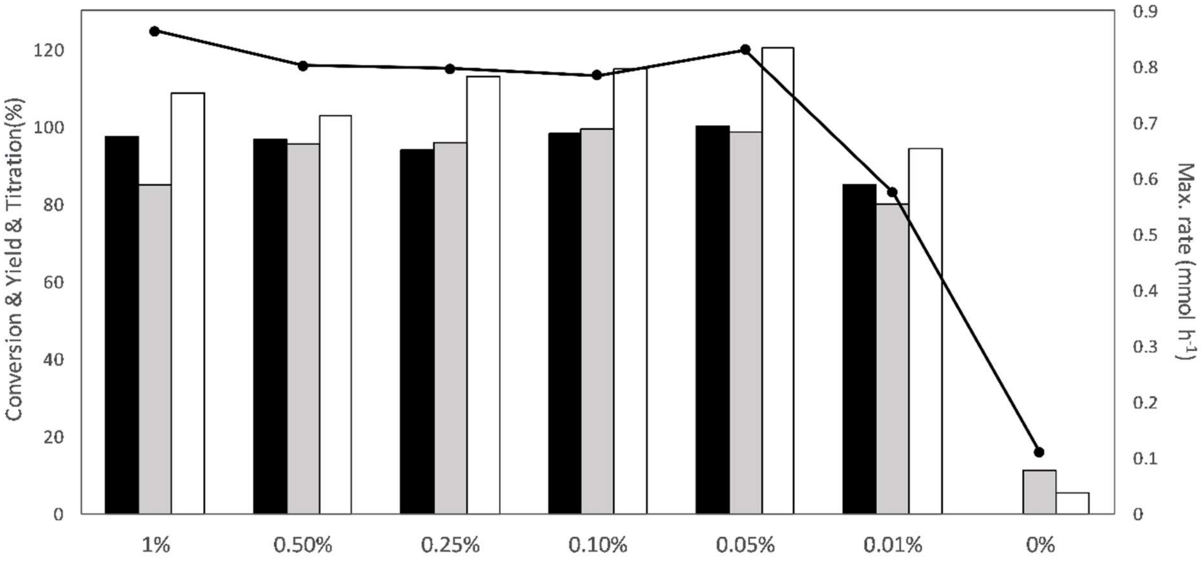

Figure 7.6. Comparison between seven different GDH loads regarding conversion (black bar), yield (grey bar), titration (white bar) and maximum rate (black circles, right axis). The rate was calculated by linear regression on the reaction kinetics (from 1 to 4 hours). Reactions in 30 mL reactors with and enzyme load of 10% (v/v) of TmCHMO Broth and 1%, 0.5%, 0.25%, 0.1%, 0.05%, 0.01% or 0% (v/v) of GDH-01 liquid enzyme formulation; temperature 30°C; stirring rate 1200 rpm; air flow 16 mL min^{-1}; pH 7; [TMCH] 30 mM h^{-1} (240 mM final); Methanol 1.25% (v/v) h^{-1} (10% (v/v) final); [D-glucose] 375 mM; [NADP^{+}] 0.25 mM; titration solution 1 M NaOH.

The results for the reaction with 0.01% (v/v) load were: 0.14 mg of total protein (0.08 mg of GDH-01) added and 6.4 mmol (1153.6 mg) D-glucose consumed (NaOH added). Even though this reaction did not result in full conversion, it presented the highest biocatalyst yield, 13970 g Glu g^{-1} GDH-01. It must be taken into account though, that part of the total titration, is a consequence of bacterial growth.

When no GDH-01 was added (right columns), 11.2% yield and 5.3% titration were still obtained. The NADPH regeneration system from the *E. Coli* cells present, probably allowed certain biotransformation of the TMCH. Regarding the substrate consumption, since the TMCH solubility (100 to 130 mM) did not allow reliable measurements of its concentration, the conversion value was misleading and it was obviated in this case.

The GDH-01 load that was selected for the subsequent studies did not change, it remained at 0.5% (v/v). It was not advisable to go too low with GDH concentration, because this could lead to a decreased reaction performance if other critical process parameters are further optimized.

7.2.1.7 Variation of the applied methanol amount

The methanol serves as a co-solvent in this reaction increasing the solubility of both substrate and product in the liquid phase. Increasing its concentration could allow to obtain more reliable samples during the reaction. Moreover, increasing the solubility and/or the solubilization rate of the substrate could make it more accessible for the TmCHMO. Recent publications state that the TmCHMO is stable up to 30% (v/v) of methanol [97] hence, increasing the methanol above 10% (v/v) should not represent an issue.

The effect of methanol was studied at 30 mL scale (Table 7.1). Two different concentrations of methanol, apart from the standard conditions of 10% (v/v), were tested: 5% and 15% (v/v). The results can be seen in the table below. The best concentration was 5% (v/v) methanol, however, the samples analyzed during the reaction showed that both substrate and product presented poor solubility (mass balance of 65%). Besides this, the reaction time was the highest observed reaching 16h in contrast with the 10% (v/v) of methanol that lasted 13h until the reaction was finalized. 10% (v/v) was chosen as the best co-solvent concentration for further studies. The reason why the reaction with 15% (v/v) methanol did not reach similar yields was most probably due to the inactivation of the GDH-01 and the difference between storage and operational stability.

Table 7.1. Results of the experiments at 30 mL scale regarding different methanol concentrations. Enzyme load 5% or 10% (v/v) of TmCHMO Broth and 0.5% (v/v) of GDH-Bam; temperature 30°C; stirring rate 1200 rpm; air flow 16 mL min^{-1}; pH 7; [TMCH] 30 mM h^{-1} (240 mM final); Methanol 0.73% or 1.44% or 2.173% (v/v) h^{-1} (10% or 15% (v/v) final); [D-glucose] 375 mM; [NADP$^+$] 0.25 mM; titration solution 1 M NaOH.

Methanol (% v/v)	TmCHMO (% v/v)	Conversion (%)	Yield (%)	Titration (%)	Max. rate (mmol h^{-1})	Reaction time (h)
5	5	98	94	103	0.58	16
10	5	91	79	88	0.68	13
10	10	96	95	103	0.8	13
15	10	73	73	84	0.77	11

7.2.2 Scale-up to 1 L scale

7.2.2.1 Scale-up of the optimized conditions and application of pure oxygen

As explained before, in order to use pure oxygen instead of air, a nitrogen flow had to be constantly applied in the headspace of the reactor to keep the oxygen concentration below 8% (to avoid a potentially explosive atmosphere). This installation was applied in a 1 liter set up where the previously optimized conditions were applied. 10% (v/v) load of TmCHMO Broth, 0.5% (v/v) load of GDH-01 liquid enzyme formulation, 30 mM h^{-1} substrate dosing rate and 20 mL min^{-1} oxygen flow were selected for the initial experiment. The oxygen measurements enabled certain oxygen control for the operator, assuring that oxygen was always available in the reactor by adaption of the oxygen supply rate respectively the nitrogen purge. Furthermore, the oxygen mass balance (oxygen consumption) served as a good estimation of the reaction progress together with the NaOH titration.

The reaction course graph can be seen below (Figure 7.7). No substrate accumulation was observed until the fifth hour, meaning that the substrate feed rate of 30 mM h^{-1} was dominating the reaction rate, which increased around 20% compared with the 30 mL reaction. The graph shows that the added NaOH that was required to keep the pH stable increased until 260 mmol while the product stayed at 182 mmol, close to the solubility limit of CHL. The oxygen consumption, on the other hand, is well aligned with the substrate consumption. 99% of the oxygen uptake was utilized in the substrate conversion.

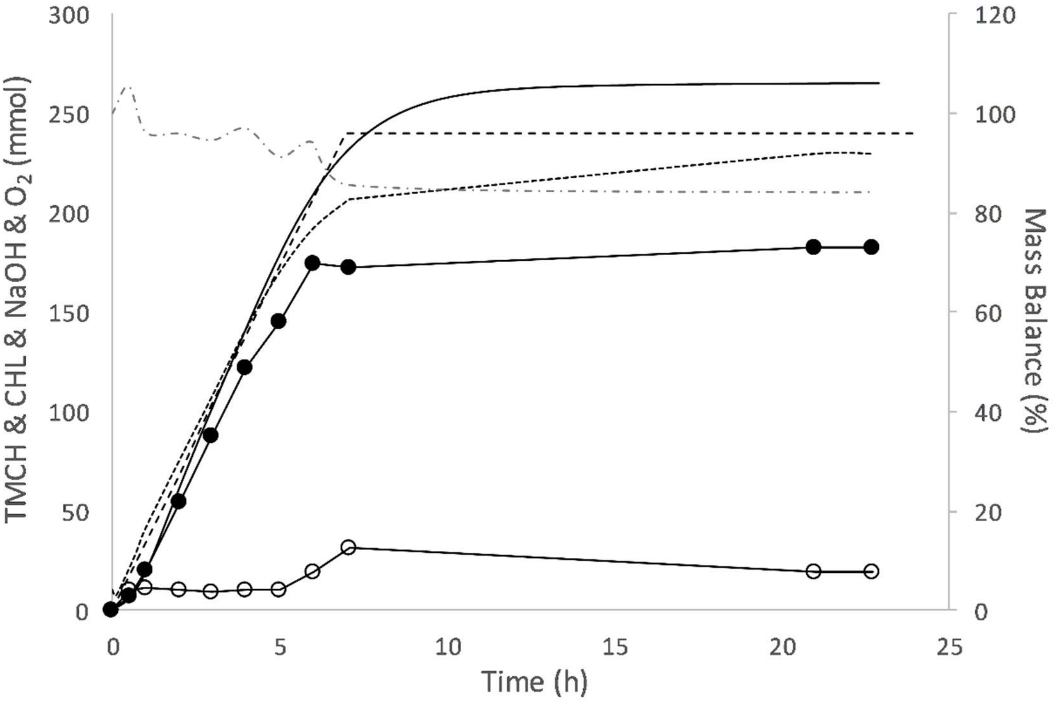

Figure 7.7. Reaction in 1 liter reactor. The graphs show the reaction course of TMCH (white circles), CHL (black circles), NaOH addition (black line), substrate dosing (discontinuous line), mass balance (combined discontinuous spot-line-spot) and oxygen consumption (dotted line). Enzyme load of 10% (v/v) of TmCHMO Broth B97 and 0.5% (v/v) of GDH-01 liquid enzyme formulation; temperature 30°C; stirring rate 400 rpm; O_2 flow 20 mL min^{-1}; pH 7; [TMCH] 30 mM h^{-1} (240 mM final); Methanol 1.43% (v/v) h^{-1} (10% (v/v) final); [D-glucose] 375 mM; [$NADP^+$] 0.25 mM; titration solution 5 M NaOH.

Without a proper workup of the reaction mixture an adequate product analysis was not possible. This is why the product yield in the course of the reaction was not taken into account at this stage. At the end, 92% conversion and 111% titration were reached, both values close to those obtained at 30 mL

(93% and 101% respectively). The reaction time was slightly reduced compared with the 30 mL reaction, from 12 h to 10 h, according to the titration curve.

The utilization of pure oxygen instead of air allowed the reaction to proceed as fast as the applied substrate dosing rate of 30 mM h^{-1}. It confirmed the hypothesis that the oxygen supply rate was limiting the reaction at 30 mL scale. At the same time, the fact that no substrate accumulation was observed, enabled further increase of the substrate dosing rate in the following experiments.

7.2.2.2 Final conditions under application of the fermented material for the demonstration

In order to obtain sufficient biocatalyst material for the planned reaction on 100 L demonstration scale, a new 15 L TmCHMO fermentation batch was performed. The characterization and comparison of the two batches was carried out at 30 mL scale using 5% (v/v) load of the TmCHMO broths. A comparative table of the new (B153) and the old (B97) batch, can be found below (Table 7.2).

Table 7.2. Comparative table of the results obtained with the different batches of TmCHMO. Enzyme load 5% (v/v) of TmCHMO Broth 0.5% (v/v) of GDH-01; temperature 30°C; stirring rate 1200 rpm; air flow 16 mL min^{-1}; pH 7; [TMCH] 30 mM h^{-1} (240mM final); Methanol 1.44% (v/v) h^{-1} (10% (v/v) final); [D-glucose] 375 mM; [$NADP^+$] 0.25 mM; titration solution 1 M NaOH.

Batch	Biomass (g_{cww} L^{-1})	Biomass added (mg_{cww})	CHL (mmol)	CHL (mg)	Biocatalyst yield (g CHL g^{-1}_{cww})
97	412.7	619.1	6.33	989.2	1.60
153	361.9	542.9	5.10	798.5	1.47

TmCHMO fermentation Batch 97, used in all the experiments discussed in the previous sections, was the most productive one, presenting the highest biocatalyst yield and the highest biomass concentration. However, due to lack of sufficient material to perform larger scale reactions the TmCHMO material of batch 153 was used in further experiments.

A final reaction at 1 liter scale with TmCHMO fermentation batch 153 was performed (Figure 7.8) adding 0.2% (v/v) GDH-01 instead of 0.5% (v/v). The broth used in this reaction, as well as in the pilot plant, was γ-ray radiated, which enabled the demonstration of this reaction in a pilot plant set-up without GMO permit [207].

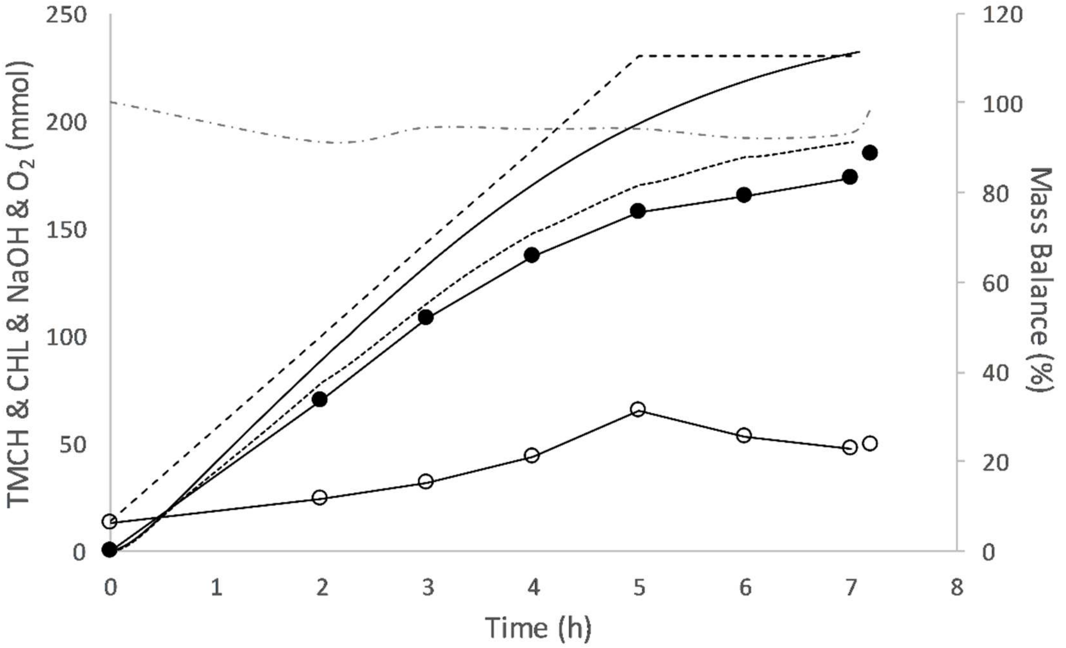

Figure 7.8. Reaction in 1 liter reactor using TmCHMO fermentation batch 153. The graphs show the reaction course of TMCH (white spots), CHL (black spots), NaOH addition (black line), substrate dosing (discontinuous line), mass balance (combined discontinuous spot-line-spot) and oxygen consumption (dotted line). Conditions: enzyme load 10% (v/v) of TmCHMO Broth and 0.2% (v/v) of GDH-01; temperature 30°C; stirring rate 400 rpm; O_2 flow 30 mL min^{-1}; pH 7; [TMCH] 48 mM h^{-1} (237 mM final); Methanol 2.47% (v/v) h^{-1} (10% (v/v) final); [D-glucose] 375 mM; [NADP$^+$] 0.25 mM; titration solution 5 M NaOH.

The yield after 7 h was 78% and 184 mmol of product were generated. Additional GDH-01 liquid enzyme formulation was added to make sure this enzyme was not limiting the reaction. The lower yield could then be attributed to the lower productivity of the TmCHMO fermentation broth that had been observed in the characterization (Table 7.2). The uncoupling (unproductive use of NADPH equivalents from glucose, observed via NaOH consumption) was in line with the previous reaction at 1 liter scale: 20% over-titration with batch 153. The cause, as previously explained, could be found on the acidification caused by remaining bacterial growth or resting metabolism. The oxygen consumed, in contrast to titration, was well aligned with the product synthesis. At the end, 98% of the totally consumed oxygen was used for the target reaction.

Once the reaction was finished, 50 mL of methanol were added to solubilize the whole substrate and product amount. After stirring for 10 minutes, a final sample was taken. The analyzed amounts are represented as the two last isolated points in the graph. As it can be observed, the mass balance of those samples is close to 100%, demonstrating a solubility issue of the reaction components when only 10% (v/v) methanol was used.

For the pilot plant run (100 L scale), full conversion was prioritized over higher product concentrations and substrate accumulation was to be avoided due to the substrate inhibition that the TmCHMO suffers. Furthermore, low substrate concentration in the final mixture would facilitate the separation of the formed CHL from the remaining TMCH. Therefore the applied substrate concentration was reduced to 180 mM and the dosing rate was decreased to 36 mM h^{-1}.

7.2.2.3 Development of an adequate downstream processing procedure

In order to isolate and concentrate the finally obtained product, an extraction procedure was required. n-Heptane and ethyl acetate were tested as organic solvents. 10 mL of the reaction were mixed with 10 mL of the corresponding organic solvent. n-Heptane presented good phase separation but a low extraction coefficient (EC = 4). The mixture containing ethyl acetate, on the other hand, formed an interlayer that did not allow proper analysis in first instance. A pre-filtration step was required before phase separation could occur in this case.

For the extraction, filtration and phase separation tests using ethyl acetate, 1 liter of the final reaction mixture was mixed with 500 mL of ethyl acetate. The combination was stirred for a defined time and temperature. Two conditions were tested for this purpose: a) 33˚C for 0.5 h and b) 40˚C for 15 h. Afterwards 50 g of Dicalite 4208 were added and the container was gently mixed for 15 minutes. A glass filter, pre-coated with 1 cm layer of Dicalite 4028, was used to filter all the content under vacuum. The resulting filtrate, separated from Dicalite 4028 and biomass, could be separated in two phases. The obtained extraction coefficients for the two different conditions were: a) 27.4 and b) 54.1. The conditions for the first extraction of the 100 L reaction were set to 40˚C and stirring for 15 h.

7.2.3 Demonstration on 100 L pilot plant scale

7.2.3.1 Reaction

The 200 liter reactor (100 L working volume) presented the same configuration and sensors as the 1 liter reactor, plus one temperature probe inside the reactor. As stated above the final substrate concentration was reduced to 180 mM and the substrate dosing rate was lowered to 36 mM h^{-1}.

As it can be seen in Figure 7.9, the reaction course was similar to that obtained at 1 liter scale with the same TmCHMO batch (B153). Nevertheless, the reaction almost stopped after approximately 7 hours at a yield of 82% (15.12 mol). This equals about 15% less product concentration compared to the 1 liter reaction. A second portion of both enzymes was added aiming to increase the final conversion. At the end (9 h), 85% of the substrate was converted to trimethyl-ε-caprolactones. Meaning a total product amount of 15.6 mol and a concentration of 24.4 g L^{-1}. The uncoupling was higher compared to the 1 liter experiment of TmCHMO batch 153 (Figure 7.8). In this case 47% over-titration was obtained. An excess of oxygen in the reactor could have contributed to this higher NaOH addition [168]. The oxygen efficiency was lower in this reaction, 81% of the consumed oxygen was used in the target reaction.

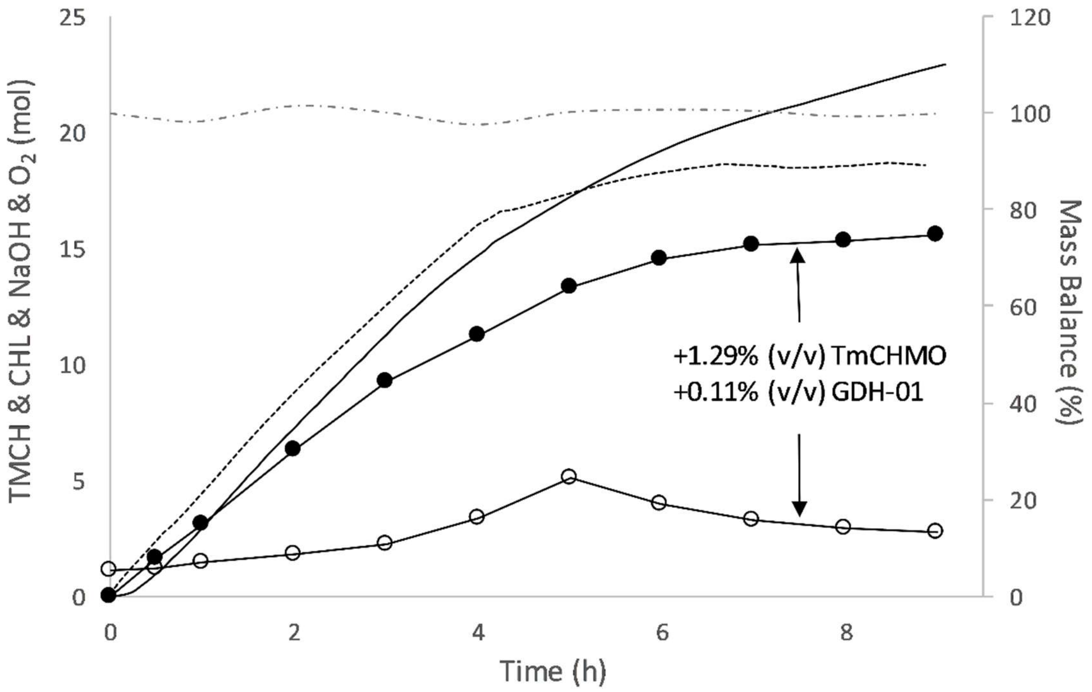

Figure 7.9. Reaction in 100 liter reactor. The graphs show the reaction course of TMCH (white spots), CHL (black spots), NaOH addition (black line), substrate dosing (discontinuous line), mass balance (combined discontinuous spot-line-spot) and oxygen consumption (dotted line). Conditions: enzyme load 10% (v/v) of TmCHMO Broth Batch 153 and 0.2% (v/v) of GDH-01; temperature 30°C; stirring rate 150 rpm; O_2 flow 3 L min^{-1}; pH 7; [TMCH] 34.4 mM h^{-1} (183.35 mM final); Methanol 2.47% (v/v) h^{-1} (10% (v/v) final); [D-glucose] 375 mM; [NADP$^+$] 0.5 mM; titration solution 5 M NaOH.

A comparative summary of the different reactions that were carried out with the TmCHMO batches can be seen below (Table 7.3).

Table 7.3. Comparative table of the reactions performed at 1 liter scale using the enzyme material of two different TmCHMO batches and the 100 liter reaction using TmCHMO fermentation batch 153. The substrate dosing rate and oxygen flow were the only conditions that differed between reactions. The dosing rate was 30 mM h^{-1} for Batch 97, 48 mM h^{-1} for Batch 153 (1 L) and 34.4 mM h^{-1} for Batch 153 (100 L). The oxygen flow was 20 mL min^{-1} for Batch 97, 30 mL min^{-1} for Batch 153 (1 L) and 3 L min^{-1} for Batch 153 (100 L).

*due to the lack of reliable product analysis, these values correspond to consumed substrate (conversion) and the space time yield was calculated as if the reaction was stopped after 10 hours.

Ferm. batch no.	Reaction volume (L)	Biocatalyst yield (kg_{CHL} kg^{-1}_{cww})	Yield (%)	Space time yield (g L^{-1} h^{-1})	[Product] (g L^{-1})	Specific activity (µmol min^{-1} g^{-1}_{cww})
97*	1	0.83	92	3.4	34.4	13.3
153	1	0.79	78	4.1	28.8	16.5
153	100	0.60	85	2.7	24.4	12.8

The reaction with TmCHMO batch 97 resulted in the highest biocatalyst yield, as on 30 mL scale. However, since the dosing rate was only 30 mM h^{-1}, the reaction lasted 10 hours (according to the titration) and the substrate addition dominated the reaction rate. That is why both, the space time yield and the specific activity, were lower compared to the other experiments. On the other hand, batch 153 (1 L) presented two significant variations: a dosing rate of 48 mM h^{-1} and an oxygen supply of 30 mL min^{-1}. These implementations allowed the reaction to proceed at higher rate compared with batch 97 and that is why it resulted in the highest space time yield and specific activity among the three. Comparing the two reactions with TmCHMO batch 153, a decrease in activity and yield can be observed at 100 liter scale. This can mainly be explained by the lower substrate dosing rate as well as a poorer temperature control (less surface area with respect to total volume) and the inefficiency of the pH controller which could not dose fast enough to maintain a stable pH (variation of ± 0.15).

7.2.3.2 Downstream processing

Once the reaction was finished, the procedure described before was followed to extract all the remaining substrate and product from the aqueous phase.

The final organic phase contained 2.55 kg (16.6 mol) of substrate and product, in the same ratio as it was analyzed at the end of the reaction, 85% CHL product and 15% remaining TMCH substrate. However, when the reaction was finished, 18.3 mol (CHL + TMCH) were present, meaning that around 9.3% yield was lost during the whole downstream procedure. The final water phase analyzed only contained 0.2% of the compounds. Therefore, the filter cake was also analyzed and the samples taken retained 15 g kg^{-1} (30.7 kg total cake weight) of the substrate and product, even after the applied three washing steps. Hence, the 9.1% yield loss was related to the filtration step. The washing steps were not as effective as anticipated due to small cracks in the filter cake.

Finally, the final organic phase containing all the extracted material, was re-introduced in the reactor and heated up to 42°C. The applied pressure from the top of the condenser was 170 mbar. The ethyl acetate could be evaporated at approximately 25 L h^{-1} and it did not contain any traces of substrate or product. The concentrated final material (2.58 kg) contained 84.5% CHL (47% **1a** and 53% **1b**), 11.9% TMCH and 3.6% impurities. The overall isolated CHL yield of the reaction was 76%.

7.3 Conclusions

Optimization and scale up has been conducted in the Baeyer-Villiger oxidation of 3,3,5-timethylcyclohexanone resulting in a final reaction that fulfills most of the target metrics evaluated in the project for industrial feasibility: 95 - 100% conversion, 10-20 g L^{-1} of product concentration and 0.26 - 1.9 g g^{-1}_{cww} biocatalyst yield.

The TmCHMO biocatalyst formulation did not require any further down-stream operation units after fermentation. The GDH-01 can be produced in *E. coli* in high cell density fed-batch fermentations (InnoSyn B.V.) and the required amount for an efficient process is comparatively low (0.05% (v/v) liquid enzyme formulation).

The scale up of the reaction to 1 liter allowed the use of pure oxygen. The oxygen supply rate proved to be a limiting factor for the reaction when air was used at 30 mL scale. The substrate dosing rate was increased 4-fold, which in consequence reduced the reaction time to 25% of the initially required time. All the other parameters were not affected by the scale-up.

The biomass concentration of the TmCHMO broth and the enzyme content (activity) of this biomass were crucial parameters to be taken into account. The use of a different TmCHMO batch (B153) reduced the yield from 92% to 78% at 1 L scale. The fermentation processes had variable activity yields (not discussed in this publication) and requires further work to determine whether the high activity of fermentation #97 or the lower one of fermentation #153 represent the rule or the exception of the average lies in the middle. This will result in a higher reproducibility and predictability of the biocatalytic reaction batches and thus an improved reproducibility of the overall process.

The feasibility of an industrial application of this reaction system was successfully demonstrated, even though the final conversion at 100 liter scale was slightly lower. Major constraints, arising if larger scales were considered, are not expected. As a conclusion, the BVMO oxidation of cyclic ketones of medium ring size such as cyclohexanone derivatives were demonstrated on pilot plant scale and are ready for replication in industrial environments.

8. Synthesis of trimethyl-ε-caprolactone with a novel immobilized glucose dehydrogenase and an immobilized thermostable cyclohexanone monooxygenase

Abstract

An often associated drawback with Baeyer-Villiger monooxygenases, that hinders its application in industrial synthesis, is its poor operational stability. Furthermore, these biocatalysts frequently suffer from substrate/product inhibition and require from the costly NADPH cofactor.

In this work, a thermostable cyclohexanone monooxygenase (TmCHMO) was immobilized and used in the synthesis of trimethyl-ε-caprolactone (CHL). As a cofactor regeneration enzyme, a novel and highly active glucose dehydrogenase (GDH-01) was successfully immobilized for the first time on four different methacrylate supports and on amino-functionalized agarose. This last matrix was chosen to study the recyclability potential of GDH-01 in the target reaction as it presented an immobilization yield of 76.3 ± 0.7% and a retained activity of 62.6 ± 2.3%, the highest metrics among the supports tested.

Both immobilized enzymes were studied either separately or together in six reaction cycles (30 mL; [substrate] = 132.5 mM). When both enzymes were used in its immobilized formulation, 2.8 g of CHL could be synthesized. The reaction yield reached almost completion in the first two cycles and slightly dropped from the third cycle reaching 57.2% in the sixth. A biocatalyst yield of 37.3 g CHL g^{-1} of TmCHMO and 474.2 g CHL g^{-1} of GDH-01 were obtained. These values represent a 3.6-fold and 1.9-fold increase respectively, compared with a model reaction where both enzymes were used in its soluble form.

8.1 Introduction

Process chemists have long considered biocatalysis as a good alternative to the conventional routes in chemical manufacturing [81]. The use of whole cells, isolated enzymes or immobilized enzymes has often proven to be a greener, sustainable and more profitable way to catalyze such chemical reactions [208]. The industry has already adopted bioconversions, for example, for the production of amino-acids [209], lactic acid, succinic acid or 3-hydroxypropionic acid [210] among many others [6], [211].

In the case of the concerned reaction, Baeyer-Villiger oxidations are well known since their discovery in 1899 [212]. The chemical route though, usually implies a limited regio-selectivity (to the sterically more hindered side), the use of hazardous and pollutant solvents and halogenated oxidants [213]–[215]. At the same time, the transformation of ketones into esters or cyclic ketones into lactones can also be accomplished by the so called Baeyer-Villiger monooxygenases (BVMOs) [195], [200], [201]. The first evidence was provided by Fired *et al.* in 1953 with the conversion of progesterone to testololactone [216]. The enzymatic alternative is often associated with milder aqueous conditions, the use of oxygen as oxidant and higher selectivity [217]. However, their implementation is hindered by some drawbacks that may come with biocatalysts and specially with monooxygenases [36], [159]. BVMOs have been suffering from low operational stability, substrate and product inhibition and the use of the costly NADPH cofactor [200], [201], [205].

These limitations can be tackled mainly by three strategies: protein engineering [218], reaction engineering [84] and immobilization [82], [219]. There are many are the examples of BVMOs that had been engineered either by means of directed evolution or rational design [217], [220]. For example, a recent work by Kathleen *et al.* demonstrated that certain conserved residues in the active site of BVMOs, when altered, lead to modified regioselectivity [221], [222]. At the same time, the substrate and product inhibition can be overcome using a different approach [223], [224]. The substrate feeding and product removal strategy (SFPR) has been applied for BVMOs processes using resins like Optipore L-493 or Lewatit VPOC 1163 [225], [226]. Finally, immobilization of enzymes is a well-known procedure that often confers improved operational and storage stability, allows the possibility to operate in continuous mode, facilitates the isolation and purification of the product and allows the re-utilization of the biocatalyst [60], [227], [228].

In this sense, one of the first contributions was from Walsh *et al.* who immobilized a cyclohexanone monooxygenase (CHMO) together with a glucose dehydrogenase (GDH), as a cofactor regeneration enzyme, onto polyacrylamide gel and used it in 1 liter reactions for 10 days [229]. Interestingly, the covalent immobilization of BVMOs together with a GDH is one of the most widely used combinations in the literature [201]. In this work, this same strategy was applied for the production of the two regio-isomers of trimethyl-ε-caprolactone (CHL) from 3,3,5-trimethylcyclohexanone (TMCH). Two novel enzymes were used for this purpose, the thermostable CHMO from *Thermocrispum municipale* DSM 44069 (TmCHMO; EC 1.14.13.22) [97] and the highly active GDH-01 (EC 1.1.1.47) (Figure 8.1).

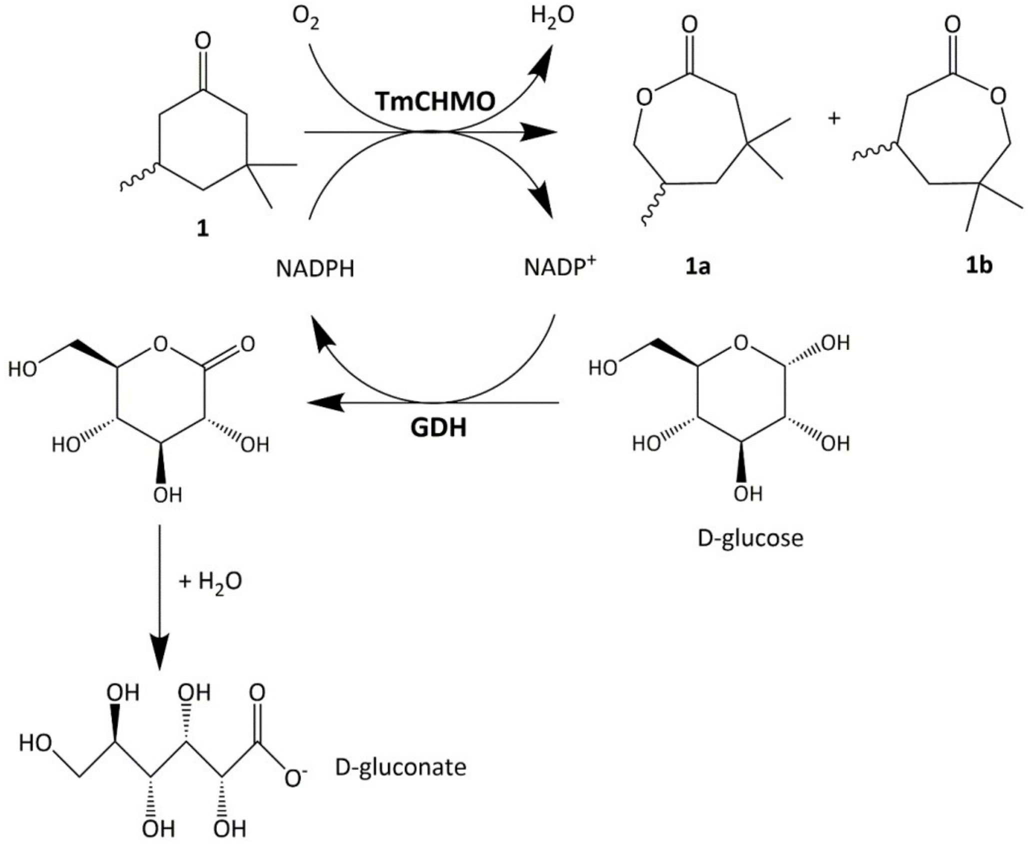

Figure 8.1. Biocatalyzed oxidation of the branched substrate 3,3,5-trimethylcyclohexanone (**1**) (TMCH) to a mixture of β,β,δ-trimethyl-ε-caprolactone (**1a**) and β,δ,δ-trimethyl-ε-caprolactone (**1b**) (CHL) with a two-enzyme system using glucose dehydrogenase (GDH) to regenerate the NADPH using D-(+)-glucose as a sacrificial substrate.

Immobilization of TmCHMO has been previously conducted by Delgove *et al.* and the derivate was also used for the synthesis of CHL [112]. In order to regenerate the cofactor, an immobilized GDH from *Thermoplasma acidophilum* was used in that case.

In the present work, in contrast, the immobilization of the novel GDH-01 has been studied for the first time on a broad variety of supports presenting different functional groups and characteristics [79]. The immobilized derivate served as biocatalyst together with the immobilized TmCHMO in the target reaction and they were re-used for six cycles. The substrate was continuously dosed, in order to avoid substrate inhibition, until 132.5 mM were reached. This substrate concentration represents a more than 13-fold increase compared with the previous work aforementioned.

8.2 Results and discussion

8.2.1 Stability of GDH-01 in different pH values and concentrations

As introduced previously, the aim of this work was the immobilization of the novel GDH-01 and the re-utilization of this enzyme together with the TmCHMO in the synthesis of trimethyl-ε-caprolactone. As opposite to the TmCHMO, the GDH-01 has never been immobilized before, that is why characterization regarding its stability was required. When immobilizing, the media pH must be chosen taking into account the support utilized and the activity decay of the enzyme at that certain pH. The results obtained are represented in Figure 8.2 A.

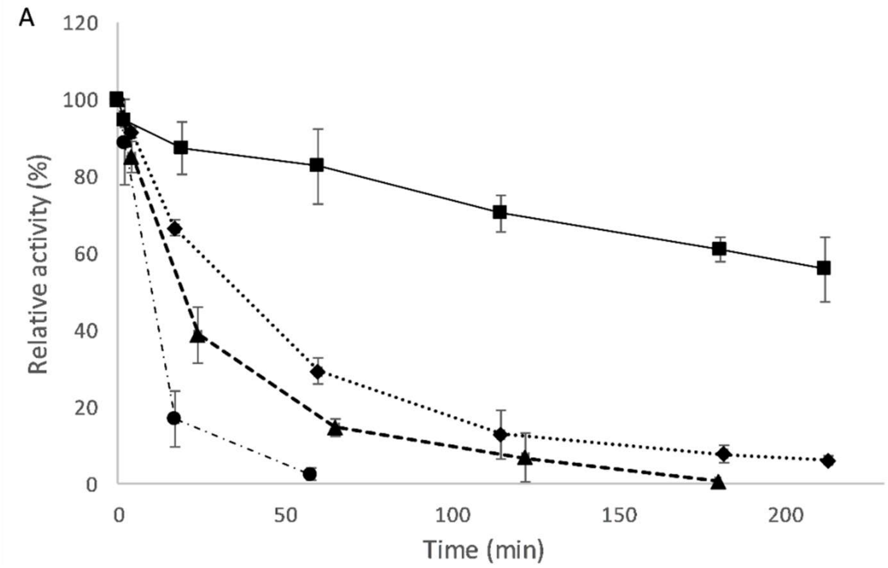

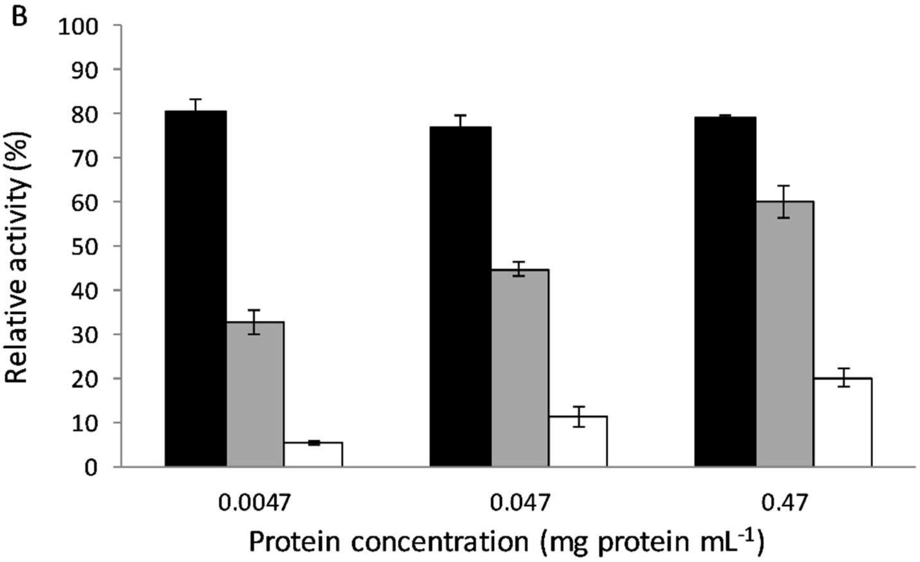

Figure 8.2. GDH-01 stability studies. A) GDH-01 relative activity along time measured at different pH values (of KPi buffers): pH 5 (black triangles and discontinuous line), pH 6 (black squares and continuous line), pH 7 (black rhombus and dotted line) and pH 8 (black circles and combined discontinuous spot-line-spot). The initial activity of the samples was 0.8 U mL^{-1}; 10000-fold dilution of the initial liquid formulation. B) GDH-01 relative activity after 1 hour incubation at three different pHs: pH 6 (black bars), pH 7 (grey bars) and pH 8 (white bars); and three different protein concentrations. The initial activities of the samples were 0.8 U mL^{-1}, 8 U mL^{-1} and 80 U mL^{-1} for the 0.0047, 0.047 and 0.47 mg protein mL^{-1} respectively. The error bars of both figures, A and B, correspond to the standard error calculated from at least two replicates.

As it can be observed in Figure 8.2 A, when GDH-01 was diluted in pH 8 buffer, it was almost completely deactivated after one hour. On the other hand, pH 6 turned out to be the most favorable for this enzyme which maintained 50% of the activity after 3.5 hours. In Figure 8.2 B, the LF containing GDH-01 was incubated for 1 hour at three different pHs (6, 7 and 8) and three different protein concentrations were applied for each pH. The graph shows that, at pH 7 and 8, the enzyme is deactivated to different extent depending on the concentration it is in. The lowest concentrated sample suffers the highest loss of activity. At pH 6 though, the relative activity after 1 hour is almost the same for the three enzyme concentrations. Diluting the GDH-01 LF in a solution containing 5 mg mL^{-1} of Bovine Serum Albumin (BSA) or pre-coating the vial with BSA did not improve the GDH-01 stability at pHs different from 6.

The stability dependency on the enzyme concentration has also been observed previously on other biocatalysts but not with GDH-01. The dilution of the enzyme below the concentration of the binding constant of its subunits or prosthetic groups can provoke the loss of the protein quaternary structure or the loss of the essential prosthetic group [1].

The TmCHMO stability was not measured due to the existence of previous works about its immobilization [112].

8.2.2 Immobilization of GDH-01. Characterization of different supports.

8.2.2.1 Methacrylate/styrene based supports

Glucose dehydrogenase is used in this target reaction as a cofactor regeneration enzyme. In the case of the novel GDH-01, the GDH studied in this work, no publications exist regarding its immobilization as far as the authors know. Once the stability of the enzyme at different pHs was known, the goal was finding a suitable support for immobilization.

A set of 14 different methacrylate/styrene resins covering a broad range of enzyme carrier features were obtained from Purolite® Technologies. The materials supplied had different: pore diameters (300 - 1800 Å), enzyme-carrier interactions (ionic, covalent and hydrophobic), functional groups (epoxy, amino and aldehyde), linker lengths (C2 - C18), material matrices (methacrylate and styrene) and particle sizes (150 – 710 µm). A detailed description of each carrier and the results obtained for the immobilization of GDH-01 can be found in the Supporting information (Table 8.1S).

The supports that resulted in at least 90% immobilization yield (with the exception of ECR8415F) and 20% retained activity are presented in the table below (Table 8.1). As can be seen, only four supports fulfilled the aforementioned criterion: one amino functionalized support (ECR8415F) and three aldehyde-functionalized supports (ECR8315F, ECR8409F and ECR8415F).

Table 8.1. Results regarding the immobilization of GDH-01 onto Methacrylate/Styrene (Purolite®) resins and description of the support's features. Only those experiments with at least 90% immobilization yield (with the exception of ECR8415F) and 20% retained activity are presented. Further information regarding other supports screened can be found in Supporting information, Table 8.1S. The standard error (± %) was calculated from at least two replicates.

Code	Functional group (Linker)	Matrix	Interaction	Pore diameter (Å)	Particle size (µm)	Immobilization Yield (%)	Retained acitivty (%)
ECR8415F	Amino (C6)	Methacrylate	Ionic/Covalent	1200 - 1800	150 - 300	40.8 ± 2.2	21.3 ± 3.5
ECR8315F	Aldehyde (C7)	Methacrylate	Ionic/Covalent	1200 - 1800	150 - 300	99.9 ± 0.1	23.9 ± 3.4
ECR8409F	Aldehyde (C11)	Methacrylate	Ionic/Covalent	600 - 1200	150 - 300	100 ± 0.0	22.5 ± 2.6
ECR8415F	Aldehyde (C11)	Methacrylate	Ionic/Covalent	1200 - 1800	150 - 300	100 ± 0.0	28.0 ± 5.1

When working with amino functionalized resins, as is the case of ECR8415F, the immobilization is carried out in three steps. First, an ionic interaction between the positively charged amino groups of the support and the negatively charged carboxyl groups of the enzyme occurs. In this first binding, 99.1 ± 0.1% immobilization yield and 60.0 ± 4.1% retained activity were obtained with ECR8415F. However, the optimized pH for the target reaction is 7, which changes the positive charge of the resin's amino groups, desorbing the enzyme from the carrier. Thus, an agent promoting a covalent bond formation is required for its use in the target reaction. *N*-(3-dimethylaminopropyl)-*N*'-ethylcarbodiimide (EDC) was chosen due to its high solubility in water. The immobilization yield and retained activity obtained were 40.8 ± 2.2% and 21.3 ± 3.5%, respectively. The EDC is often associated with enzyme deactivation, however, in this case, the low immobilization yield indicates that the amount of EDC added was not enough to covalently bind all the enzyme offered and a major part of the initially attached GDH-01 was desorbed when the NaCl was introduced.

Regarding glutaraldehyde functionalized supports (ECR8315F, ECR8409F and 8415F), the results are similar between the three, even though the supports differ in linker lengths and pore diameters. In the three cases, the GDH-01 showed immobilization yields close to 100% meaning that the enzyme presents high affinity for the carrier. However, either due to miss-orientation, unfolding or stacking, the enzyme attached was significantly deactivated (low retained activities) showing less than 30% of retained activity in all cases.

The methacrylate/styrene resins are rather hydrophobic which can contribute to enzyme deactivation during immobilization. Taking into account that all the supports tested so far had different functionalizations but similar matrices, new materials made out of more hydrophilic materials were to be tested. In this sense, agaroses were the first choice for further investigation, aiming to obtain immobilized derivatives with higher retained activities [191].

8.2.2.2 Agarose based matrices: epoxy- and Mana-agarose

As mentioned before, more hydrophilic matrices were tested presenting two different functionalizations. An epoxy functionalized agarose and an amino functionalized agarose (Mana-agarose) were studied as potential immobilization supports for GDH-01.

The epoxy-agarose immobilization is usually pursued at alkaline pH. However, the studies performed with GDH-01 showed a very poor stability of the enzyme at pH 8 (Figure 8.2 A). The immobilization was therefore conducted at pH 6 and 0.5 M of NaCl were added in order to increase the ionic strength of the medium to promote the binding. The results showed low affinity of the enzyme for the support and a slight over-activation. At the end, 29.5 ± 7.3% retained activity were obtained.

The amino functionalized agarose (Mana-agarose) immobilization proceeds like the amino functionalized resins from Purolite®. The immobilization takes place in three steps: i) ionic adsorption, ii) covalent binding and iii) desorption with 0.5 M NaCl (Figure 8.3).

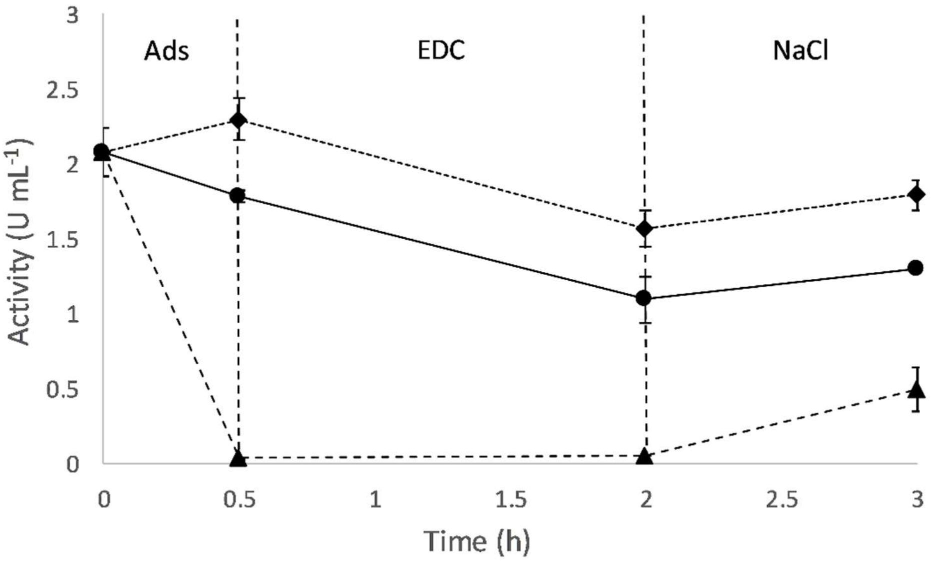

Figure 8.3. Immobilization course of the GDH-01 onto amino functionalized agarose (Mana-agarose) using 10 mM EDC concentration and offering 20 units of GDH-01 activity (64.4 µg of enzyme) per gram of agarose. The graph shows the activity of the blank (black circles and continuous line), the supernatant (black triangles and discontinuous line) and the suspension (black rhombus and dotted line) along time. The immobilization is divided in the three different phases: i) ionic adsorption of the enzyme to the carrier (Ads), ii) incubation with the covalent bond promoter, EDC (EDC) and iii) desorption of the unattached enzyme with 0.5 M NaCl (NaCl).

The results regarding the Mana-agarose immobilization are presented in Table 8.2. As it can be observed in the second and third columns, 98.4 ± 0.2% of the initial GDH-01 bound to the agarose by ionic interaction and a slight over-activation occurred (retained activity 105.5 ± 3.8%). As explained for the amino-methacrylate supports though, the pH of the reaction (pH 7) does not allow an ionic immobilization to be used. Results obtained after covalent binding formation reached 76.3 ± 0.7 % and 62.6 ± 2.3% of immobilization yield and retained activity, respectively (Figure 8.3), which represents a high significant improvement compared to the results obtained with the methacrylate/styrene matrices.

Table 8.2. Immobilization of GDH-01 onto amino functionalized agarose (Mana-agarose) using three different EDC concentrations. 20 units of GDH-01 activity (64.4 µg of enzyme) were offered per gram of agarose. The standard error (± %) was calculated from at least two replicates.

	Ionic Adsorption		**Covalent binding**	
[EDC]	Immobilization Yield (%)	Retained Activity (%)	Immobilization Yield (%)	Retained Activity (%)
10	98.4 ± 0.2	105.5 ± 3.8	76.3 ± 0.7	62.6 ± 2.3
20			94.1 ± 0.1	47.2 ± 3.3
30			98.2 ± 0.1	44.2 ± 0.2

Due to the promising results obtained with Mana-agarose, in addition to the use of 10 mM of EDC, two different concentrations were also tested (20 mM and 30 mM) aiming to obtain an immobilized derivate with the highest activity possible (Table 8.2). However, even though when using higher concentrations of EDC the immobilization yield increased more than 1.2-fold, the enzyme got deactivated and the retained activity dropped to 15.4% and 18.4%, respectively. That is why 10 mM of EDC was chosen as the best condition albeit 23.7% of the initial activity remained in the supernatant. The immobilization onto Mana-agarose represents a step forward compared to the methacrylate/styrene (Purolite®) supports. The retained activity in this case is 2.94-fold higher than the amino functionalized methacrylate (ECR8415F) and 2.24-fold higher than the aldehyde functionalized methacrylate (ECR8415F), the best candidates from the previous trials. As it happened with the other resins, this is the first time that the successful immobilization of GDH-01 onto Mana-agarose is reported. This support was chosen to study the re-cyclability capacity of GDH-01 in the synthesis of trimethyl-ε-caprolactone.

8.2.3 Immobilization of GDH-01 and TmCHMO on Mana-agarose. Maximum loading capacity

The maximum quantity of GDH-01 and TmCHMO that can be attached to Mana-agarose was studied. Different amounts of enzyme were immobilized onto the support in order to determine this value. Since mass transfer limitation could occur at high enzyme loads, retained activities obtained during the immobilization characterization at low loads were used here to calculate the theoretical maximum loading capacity in terms of activity units [Table 8.3, Final activity (U g^{-1} support)].

Table 8.3. Immobilization of GDH-01 onto Mana-agarose using maximum loads of enzyme per gram of support. The covalent immobilization of GDH-01 was carried out using 10 mM EDC for 1.5 hours while the TmCHMO was incubated for 2 hours with 35 mM of EDC.

Enzyme	Activity offered (U g^{-1} support)	Final activity (U g^{-1} support)	Retained protein (mg protein g^{-1} support)
GDH	11061.6	3692.5	23.1
TmCHMO	86.5	53.2	67.7

The immobilization of TmCHMO was carried out using the optimized conditions published recently by Delgove *et at.* [112]. The amino-functionalized agarose was used as a carrier and 35 mM of EDC were applied as a covalent bond promoter. The obtained retained activity at low loads in that study was 62.4 ± 2.1%. The results obtained regarding the immobilization of TmCHMO using high loads of enzyme, are shown in Table 8.3. The maximum loading capacity of TmCHMO resulted in 67.7 mg protein g^{-1} support and 53.2 U g^{-1} support.

Regarding the GDH-01, 23.1 mg protein g^{-1} support were immobilized using 10 mM EDC concentration. According to the retained activity obtained during the characterization (62.6 ± 2.3%), 3692.5 U g^{-1} support could be loaded onto Mana-agarose (Table 8.3).

8.2.4 Synthesis of trimethyl-ε-caprolactone

8.2.4.1 Soluble enzymes

Aiming to compare the performance of the immobilized derivatives with the soluble enzyme, a reaction was run firstly using non-immobilized TmCHMO and GDH-01. Different metrics such as biocatalyst yield and total product synthesized were used for comparison. The conditions published recently [123] and further optimized by the authors (data not shown) were mimicked in this study at 30 mL scale using 10% (v/v) load of TmCHMO fermentation broth and 0.5% (v/v) GDH-01 LF.

The reaction course can be seen in Figure 8.4. A continuous substrate feeding strategy was used in order to avoid substrate inhibition which has been observed for this enzyme [123], [205]. Even though the substrate was continuously added, certain amount of it was accumulated at the beginning of the reaction. At the same time, as it can be seen in the graph, the amount of NaOH added to control the pH is well aligned with the product formed and it serves as good indicator of the reaction performance. At the end though, after 24 h, a gap exists between the titration and the product analyzed. This can be associated with product solubility limitations [123]. In order to obtain reliable values for conversion and yield at the end of the reaction the reactor was worked up by adding acetonitrile which solubilized the whole substrate and product content.

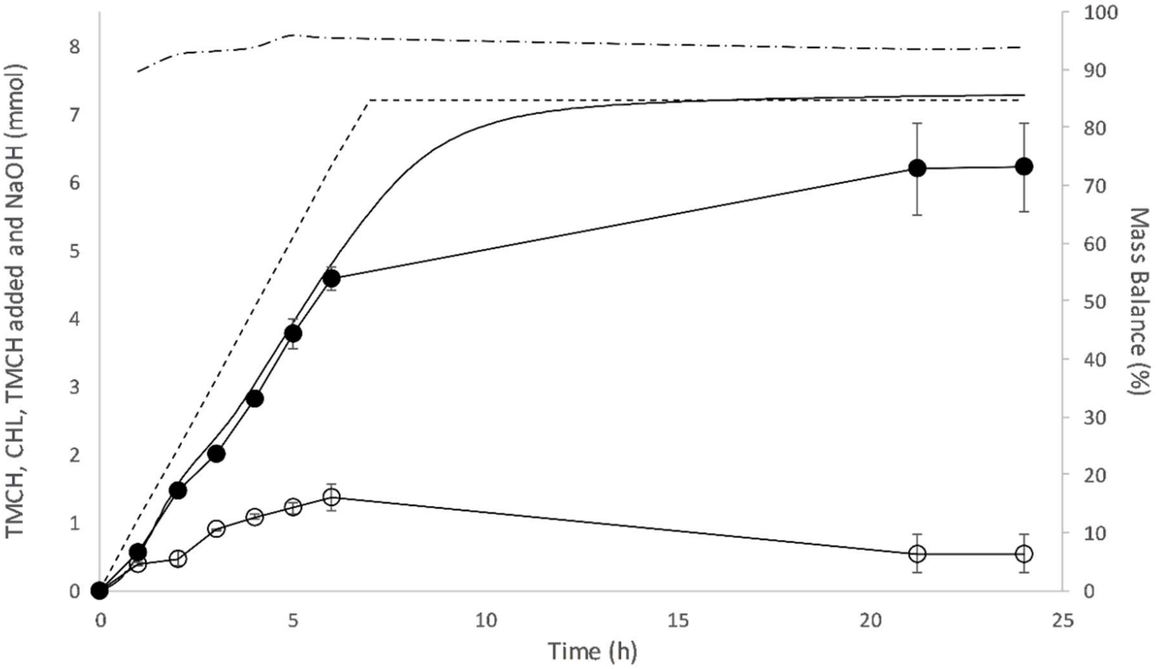

Figure 8.4. Synthesis of trimethyl-ε-caprolactone (30 mL) using the enzymes in its soluble forms: the TmCHMO broth and GDH-01 LF. The graph shows the reaction course of TMCH (white circles), CHL (black circles), NaOH addition (black line), substrate dosing (discontinuous line) and mass balance (combined discontinuous spot-line-spot). Conditions: enzyme load 10% (v/v) of TmCHMO broth (57.8 U mL^{-1} of Broth) and 0.5% (v/v) of GDH-01 LF (8408.8 U mL^{-1} of LF); temperature 30°C; stirring rate 1200 rpm; air flow 16 mL min^{-1}; pH 7; [TMCH] 30 mM h^{-1}(240 mM final); Methanol 1.25% (v/v) h^{-1} [10% (v/v) final]; [D-glucose] 375mM; [NADP+] 0.25mM; titration solution 1M NaOH.

The conversion and yield of the reaction after 24 h were 92.1 ± 4.5% and 92.0 ± 3.3% respectively. The amount of NaOH added was 101.2 ± 1.9% of the final substrate dosed (on molar basis). The product concentration reached was 34.5 ± 1.2 g L^{-1} and the biocatalyst yield was 10.5 ± 2 g CHL g^{-1} TmCHMO and 255.0 ± 9.2 g CHL g^{-1} GDH-01.

8.2.4.2 Immobilized enzymes

From an industrial point of view, the possibility of re-using enzymes in various reaction cycles can significantly improve the process throughput. For example, when re-cycling, the required enzyme decreases and it facilitates the product isolation and purification among others.

Three sets of reactions were performed using one of the two enzymes immobilized and the other in its soluble form or both enzymes immobilized. Several disadvantages are sometimes observed when working with immobilized enzymes: substrates/product mass transfer limitations, lower oxygen transfer rates, poor distribution of the carrier in the reactor, enzyme selectivity alterations, etc.

The reaction time was reduced (6 h), total conversion was prioritized over high product concentrations and substrate accumulation was to be avoided. For these reasons, the initial substrate concentration was reduced, compared to the reaction with soluble biocatalysts. In each set of reactions, re-cycling of the immobilized enzyme/s was intended up to 6 cycles. The results can be seen in the graphs below (Figure 8.5, A, B and C) and a final summary is presented in Table 8.4.

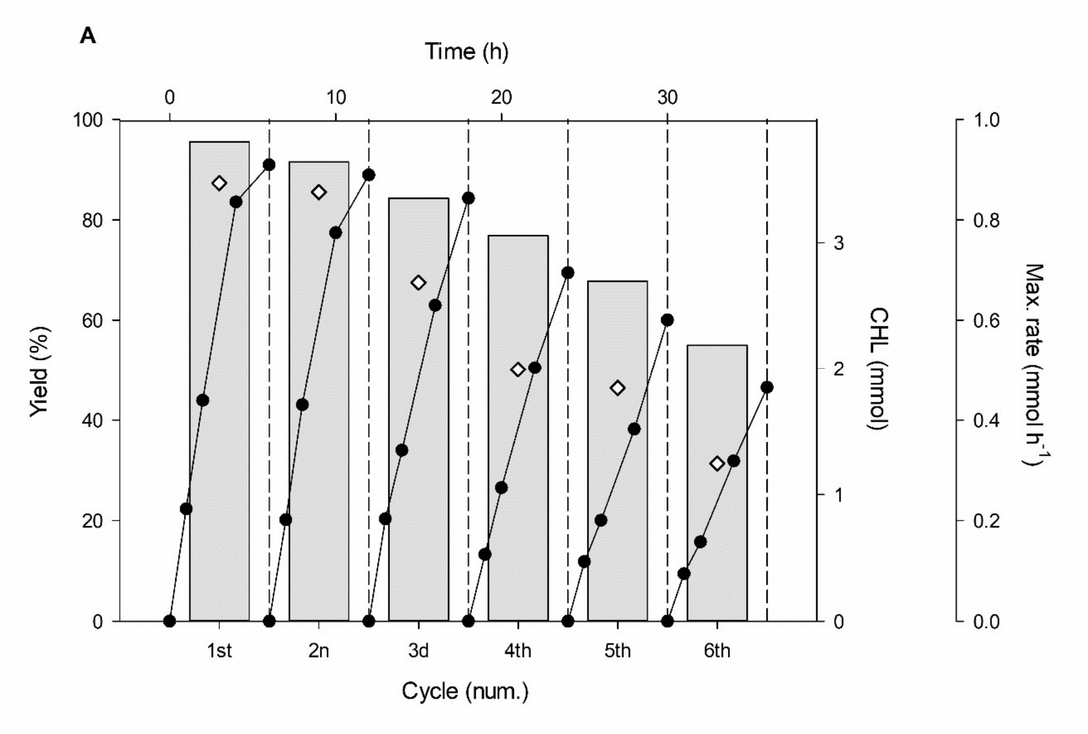

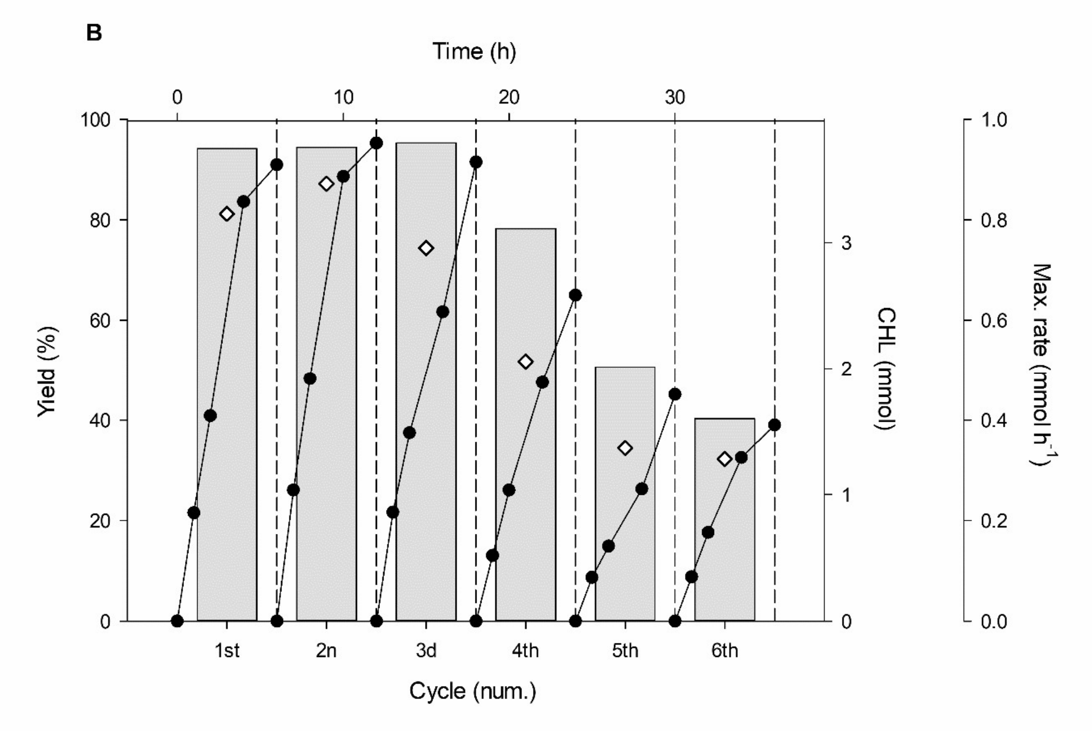

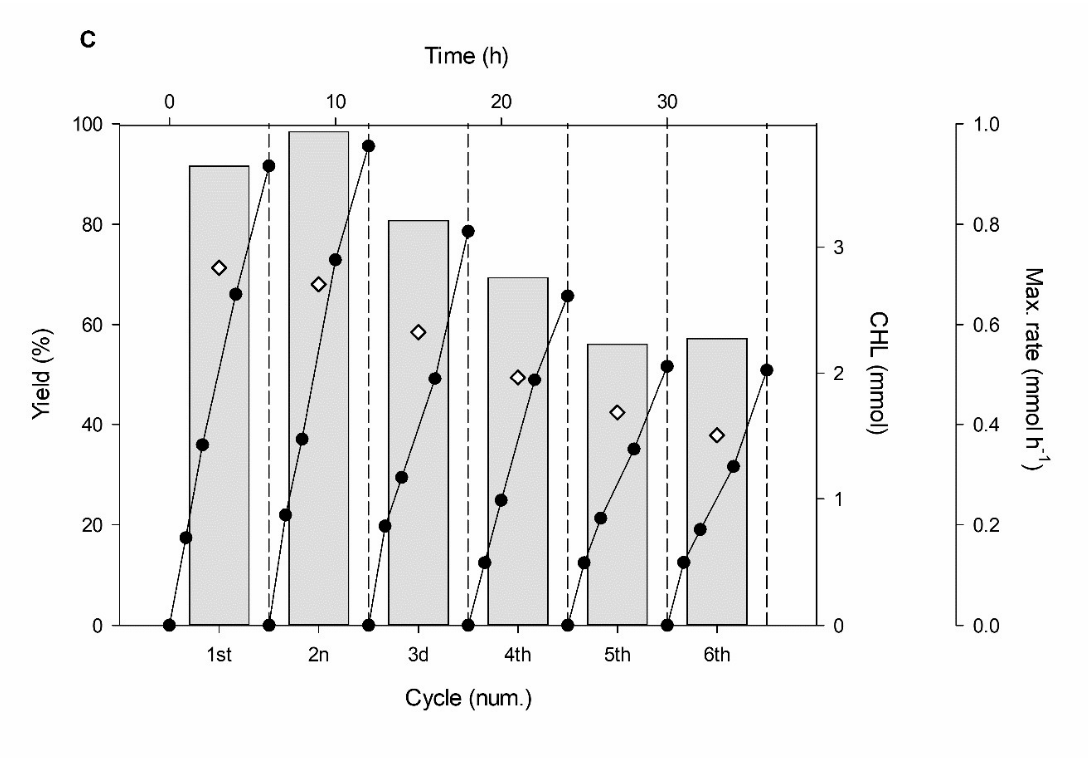

Figure 8.5. Reaction cycles using either one or both enzymes immobilized (30 mL). Each graph shows the reaction yield (grey bars), the CHL formation (black circles and continuous line) and the maximum reaction rate (white rhombus). A) TmCHMO immobilized [3 g of support loaded (53.2 U g^{-1} of support)] and 0.5% (v/v) of GDH-01 LF (8408.8 U mL^{-1} of LF), B) GDH-01 immobilized [1.5 g of support loaded (1624.9 U g^{-1} of support)] and 10% TmCHMO LF (46.7 U mL^{-1} of LF) and C) TmCHMO immobilized [2.5 g of support loaded (53.2U g^{-1} of support)] and GDH-01 immobilized [0.5 g of support loaded (3692.5 U g^{-1} of support)]. Conditions: temperature 30°C; stirring rate 1200 rpm; Air flow 16mL min^{-1}; pH 7; [TMCH] 29 mM h^{-1}(132.5 mM final); Methanol 2.17% (v/v) h^{-1} [10% (v/v) final]; [D-glucose] 375mM; [NADP+] 0.25mM; titration solution 1 M NaOH.

Table 8.4. Final summary of the reaction with soluble biocatalysts and the reactions where either one or both of the enzymes were immobilized.

Figure	**Enzyme**	**Immob**	**Soluble**	**Activity in the reactor (U mL^{-1})**	**Enzyme loaded in the reactor (mg)**	**CHL formed (mg)**	**Biocatalyst yield (g CHL g^{-1} enzyme)**	**Improvement factor**
Figure 8.4	TmCHMO		X	5.8	98.5	1033.8	10.5	
	GDH-01		X	42.0	4.1		254.6	
Figure 8.5 A	**TmCHMO**	**X**		**5.3**	**90.7**	2927.9	**32.3**	**3.1**
	GDH-01		X	42.0	24.4		120.2	0.5
Figure 8.5 B	TmCHMO		X	4.7	477.6	2816.5	5.9	0.6
	GDH-01	**X**		**81.2**	**7.8**		**358.9**	**1.4**
Figure 8.5 C	**TmCHMO**	**X**		**4.4**	**75.6**	2818.6	**37.3**	**3.6**
	GDH-01	**X**		**61.5**	**5.9**		**474.2**	**1.9**

The reaction containing immobilized TmCHMO and soluble GDH-01 LF showed good recyclability capacity of the derivate presenting 55% yield in the sixth cycle (Figure 8.5 A). The maximum rate of the reaction decreased from cycle to cycle as did the final yield. The titration, on the other hand, was higher than the product formation. In the first cycle 150.3% NaOH was added compared with the final added substrate concentration. This over-titration effect decreased along the cycles and even reverted in the last two. The titration in the fifth and sixth cycles was 59.5% and 39.4% whilst the yield was 67.8% and 55.0%. A possible explanation for this behavior could be found in the support's nature. The free and positively charged amino groups present on the surface of the carrier at the end of the immobilization, lose their proton when placed in pH 7 medium, causing an extra acidification, which was compensated by the auto-titration of NaOH base.

The reaction where GDH-01 was used in its immobilized form and the TmCHMO was added as LF is represented in Figure 8.5 B. The results show that the yield was maintained during the first three cycles (94 - 95%) and then continuously dropped until it reached 40.2% in the sixth. Over-titration was also observed in this case (142.6% in the 1st cycle) and the maximum rate decay of the reaction was well aligned with the yield, as it happened with the immobilized TmCHMO. It should be noticed that the GDH-01 immobilized derivate used in this case was loaded with lower amount of enzyme (2765.4 U g^{-1} support) and so it presented lower final activity (1624.9 U g^{-1} support) compared with the derivate previously reported (Table 8.3, 3692.5 U g^{-1} support). At the same time, in order to ensure proper recovery of the resin in the filtration and washing operations, 5% (w/v) support load was considered to be the minimum required. At the end, the GDH-01 activity offered was higher compared to the soluble reaction (42.0 U mL^{-1} compared to 81.2 U mL^{-1}).

The last reaction was performed with both TmCHMO and GDH-01 immobilized (Figure 8.5 C). The course of the reaction cycles was similar to the previous experiments. Both enzymes could be recycled and 57.2% yield was reached in the sixth cycle. The yield in the first two cycles was almost complete reaching 91.6 and 98.4%, while in the third cycle the yield dropped to 80.7%. The over-titration effect observed in the previous sets of reactions (Figure 8.5 A and B), was less prominent in this one. In the first cycle 107% titration and 91.6% yield were obtained. Regarding the maximum rate, no significant differences were observed and the rate decay was well aligned with the yield. The activity offered of each enzyme differed from the previous reactions with immobilized enzymes: 17% less TmCHMO Units and 24.3% less GDH-01 Units. This was due to the maximum support amount that can be loaded to ensure a proper mixing [10% (w/v)] and the GDH-01/TmCHMO activities of the immobilized derivatives. Furthermore, when comparing the three reactions, the reaction with immobilized GDH-01 and soluble TmCHMO maintained almost full yield for the first three cycles (Figure 8.5 B) while the reaction with immobilized TmCHMO and soluble GDH-01 (Figure 8.5 A) presented 91.5% in the second cycle and 84.3% in the third. For this reason, TmCHMO was considered to be, most probably, the enzyme limiting the reaction cycles.

A comparative table with the final metrics is presented (Table 8.4). Two parameters are shown for comparative purposes: the total CHL formed (mg) and the biocatalyst yield (mg CHL mg^{-1} of enzyme). Biocatalyst yield was used as the most suitable process metric to compare all the reactions settings since it takes into account the grams of enzymes loaded in the reaction which, as already mentioned, could not be maintained constant in all experiments performed.

The improvement factor refers to the biocatalyst yield obtained in each immobilized set of reactions compared with the biocatalyst yield of the soluble reaction. When looking at the three reactions with immobilized derivates (Figure 8.5 A, B and C) the amount of CHL formed almost triples the amount obtained in the soluble reaction. At the same time, the amount of immobilized GDH-01 added is also higher. As it can be seen, when immobilized, the TmCHMO improves the amount of product that the enzyme is able to catalyze by a factor of 3.1 (Figure 8.5 A) and 3.6 (Figure 8.5 C). On the other hand, the immobilized GDH-01 is able to regenerate the NADPH cofactor until 1.4 and 1.9 times more CHL is synthesized by the soluble TmCHMO LF or immobilized one, respectively.

This work represents a step forward in the utilization of the immobilized TmCHMO compared with a previous publication [112]. The amount of CHL synthesized with both enzymes immobilized was increased by a factor of 5.2 and the biocatalyst yield obtained was improved by a factor of 2.2 and 14, for the TmCHMO and the GDH-01 respectively. In the above mentioned work, a GDH from *Thermoplasma acidophilum* (GDH-Tac) was used instead of GDH-01.

Regarding the cofactor regeneration enzyme, it is the first time that the GDH-01 has been repetitively used in six reaction cycles in the synthesis of a product with industrial interest at high substrate and product concentrations.

8.3 Conclusions

The immobilization of the novel and highly active (310.6 ± 28.5 U mg^{-1} enzyme) glucose dehydrogenase GDH-01 has proven successful for the first time. The enzyme presented acceptable retained activities (>20%) in four out of the fourteen supports that were tested from Purolite®. Furthermore, the GDH-01 was adsorbed onto amino functionalized agarose presenting significantly improved metrics, an immobilization yield of 98.4 ± 0.2% and a slight over-activation with 105.5 ± 3.8% retained activity.

When the adsorbed derivate was further treated with a covalent bond promoter (EDC), the immobilization yield obtained was 76.3 ± 0.7% and the retained activity 62.6 ± 2.3%. A final derivate could be obtained presenting 3692.5 U g^{-1} of support.

The immobilization of TmCHMO performed previously by Delgove *et al.* [112] could be mimicked in this study and highly loaded and active derivates (53.2 U g^{-1} of support) were obtained for its application in the synthesis of trimethyl-ε-caprolactone. At the same time, the immobilized GDH-01 could be used as cofactor regeneration enzyme. A set of five reactions with 6 reaction recycles were carried out using either one or both of the enzymes in its immobilized forms. The biocatalyst yield obtained in each case for the immobilized enzymes was compared with a model reaction where both enzymes were in its soluble form. The best results were obtained with both enzymes immobilized. The total CHL produced in 6 different reaction cycles (30 mL, [TMCH] = 132.5 mM each cycle) was 2818.6 mg. The biocatalyst yields obtained were 3.6 times and 1.9 times higher for the TmCHMO and the GDH-01 respectively, compared with the soluble reaction.

This work represents a step forward compared with the previous research regarding the immobilization of TmCHMO and synthesis of CHL. When both enzymes were used immobilized, the total product formed was increased 5.2-fold and the TmCHMO biocatalyst yield was increased 2.2-fold compared with the aforementioned publication [112]. Although the most significant improvement was observed in the biocatalyst yield of GDH-01 compared with the GDH used in the previous work, GDH-Tac. The biocatalyst yield as gram product obtained per gram (immobilised) enzyme was increased 14-fold.

As it happens with any biochemical process, there are parameters that could be better adjusted and higher yields could potentially be achieved. The first parameters that the authors would work on would be the variation of the immobilized GDH-01:TmCHMO ratio, and the increase of the final substrate concentration. Comparing the soluble and immobilized reactions, the amount of enzyme offered does not differ much, however, the final substrate concentration was 1.8 times lower with the immobilized derivates.

In conclusion, this work represents a new input for the potential implementation of TmCHMO and GDH-01 in the industrial production of ε-caprolactone derivatives and other lactones.

8.4 Supporting information

Table 8.1S. Methacrylate/styrene (Purolite®) screening set of resins and the immobilization results (immobilization yield and retained activity) for the GDH-01.

Code	Functional group (Linker)	Matrix	Interaction	Pore diameter (Å)	Particle size (µm)	Immobilization (%)	Retained acitivty (%)
ECR8204F	Epoxy	Methacrylate	Covalent	300-600	150-300	0 ± 2.9	21.9 ± 4.9
ECR8215F	Epoxy	Methacrylate	Covalent	1200-1800	150-300	15.8 ± 2.8	23.6 ± 1.3
ECR8309F	Amino (C2)	Methacrylate	Ionic/Covalent	600-1200	150-300	66.9 ± 1.1	19.1 ± 0.9
ECR8315F	Amino (C2)	Methacrylate	Ionic/Covalent	1200-1800	150-300	76.1 ± 0.7	18.9 ± 0.2
ECR8409F	Amino (C6)	Methacrylate	Ionic/Covalent	600-1200	150-300	36.9 ± 2.1	11.9 ± 4.4
ECR8415F	Amino (C6)	Methacrylate	Ionic/Covalent	1200-1800	150-300	40.8 ± 2.2	21.3 ± 3.5
ECR8285	Epoxy (C4)	Methacrylate	Ionic/Covalent	400-600	300-710	100 ± 0.0	9.7 ± 1.1
ECR8806F	None (C18)	Methacrylate	Hydrophobic	500-700	150-300	99.7 ± 0.1	6.5 ± 0.5
ECR1061M	None	Styrene/Methacrylic	Hydrophobic	600-750	300-710	95.9 ± 0.3	3.1 ± 0.6
ECR1030M	None	Styrene/Methacrylic	Hydrophobic	200-300	300-710	93.7 ± 1.8	3.1 ± 0.8
ECR8309F	Aldehyde (C7)	Methacrylate	Ionic/Covalent	600-1200	150-300	99.5 ± 0.0	16.2 ± 1.1
ECR8315F	Aldehyde (C7)	Methacrylate	Ionic/Covalent	1200-1800	150-300	99.9 ± 0.1	23.9 ± 3.4
ECR8409F	Aldehyde (C11)	Methacrylate	Ionic/Covalent	600-1200	150-300	100 ± 0.0	22.5±2.6
ECR8415F	Aldehyde (C11)	Methacrylate	Ionic/Covalent	1200-1800	150-300	100 ± 0.0	28 ± 5.1

9. Overall conclusions

The feasibility of four biocatalyzed oxidoreductive reactions has been studied in this thesis. For this purpose, three target enzymes were tested in reaction conditions and their immobilization was studied on a wide variety of supports. Furthermore, two additional enzymes were employed as cofactor (NADPH) regenerators. The set of biocatalysts used consisted on the P450 BM3 (wild type and M22C02), different glucose dehydrogenases, an alcohol dehydrogenase, a NADPH oxidase and a cyclohexanone monooxygenase.

With the exception of the NOX which had been previously immobilized and it did not show any additional improvement, all the enzymes were successfully bound onto solid matrices and retained more than 20% of the initial loaded activity. The supports that best performed were always agarose based and presented either amino or epoxy functional groups. When the immobilized derivates were used to catalyze target reactions, with the exception of P450 BM3, all of them entailed an increase in the biocatalyst yield. Always compared with the soluble enzymes.

Regarding the target reactions, in the case of the hydroxylation of α-isophorone, the addition of the P450 BM3 WT CFE in 5 sequential pulses, proved to be beneficial. Rather than adding the whole enzyme load from the beginning. For the hydroxylation of diclofenac, even though 100% conversion could be reached, a strong substrate inhibition did not allow high initial substrate concentrations. In both cases, re-cycling of the P450 BM3 was intended and resulted unsuccessful.

For the oxidation of 4-hydroxy-isophorone, the hydroxylated form of α-isophorone, an ADH was used together with the NOX. The conversion after 24h of reaction reached 92.2% with soluble enzymes (50 mM initial). When the immobilized ADH was applied, the biocatalyst yield could be improved 2.5-fold.

Finally, the Baeyer-Villiger oxygenation of the 3,3,5-trimethylcyclohexanone, was first optimized and scaled up to 100 L using soluble enzymes. After 9h of reaction, 85% conversion and 2.7 g L^{-1} h^{-1} space time yield could be obtained (183.35 mM initial). The industrial feasibility of this reaction could be demonstrated. Moreover, as a second part, the reaction was also studied using both enzymes immobilized onto Mana-agarose. The biocatalyst yield could be improved 3.6-fold and 1.9-fold for the CHMO and the GDH respectively.

As a final conclusion, this thesis has added some additional value to the enzymes and reactions studied and it has contributed to broaden the potential implementation of these oxidoreductive biocatalyzed bioprocesses.

10. Acknowledgements

The research for this work has received funding from the European Union project ROBOX (grant agreement n° 635734) under EU’s Horizon 2020 Programme Research and Innovation actions H2020-LEIT BIO-2014-1. This document reflects only the author's view and the Agency is not responsible for any use that may be made of the information it contains. The Department of Chemical, Biological and Environmental Engineering of Universitat Autònoma de Barcelona constitutes the Biochemical Engineering Unit of the Reference Network in Biotechnology and the research group 2017 SGR 1462, Generalitat de Catalunya. Authors also thank COST Action CM 1303–Systems Biocatalysis for financial support. Jordi Solé acknowledges also UAB for funding his Ph.D. grant.

ROBOX

This project is funded by the European Union (grant agreement 635734) under EU's Horizon 2020 Programme Research and Innovation actions H2020-LEIT BIO-2014-1

11. Scientific contributions

- **Co-immobilization of P450 BM3 and glucose dehydrogenase on different supports for application as a self-sufficient oxidative biocatalyst**
  J. Solé, G. Caminal, M. Schürmann, G. Álvaro and M. Guillén
  J Chem Technol Biotechnol, vol. 94, no. 1, pp 244-255, 2018

- **High performing immobilized Baeyer-Villiger monooxygenase and glucose dehydrogenase for the synthesis of ε-caprolactone derivative**
  M. A. F. Deglove, D. Valencia, J. Solé, K. V. Bernaerts, S. M. A. De Wildeman, M. Guillen and G. Álvaro
  Appl. Catal. A, Gen., vol. 572, pp. 134-141, 2019

- **Keto-isophorone synthesis with an immobilized alcohol dehydrogenase**
  J. Solé, J. Brummund, G. Caminal, M. Schürman, G. Álvaro and M. Guillén
  ChemCatChem, accepted with minor revisions at the moment of the deposit (25/07/2019)

- **Enzymatic synthesis of trimethyl-ε-caprolactone: process intensification and demonstration at 100 liter scale**
  J. Solé, J. Brummund, G. Caminal, M. Schürman, G. Álvaro and M. Guillén
  *Organic Process Research & Develop*ment, accepted with major revisions at the moment of the deposit (25/07/2019)

- **Trimethyl-ε-caprolactone synthesis with a novel immobilized glucose dehydrogenase and an immobilized thermostable cyclohexanone monooxygenase**
  J. Solé, J. Brummund, G. Caminal, M. Schürman, G. Álvaro and M. Guillén
  Applied Catalysis A: General, returned with major revisions at the moment of the deposit (25/07/2019)

12. References

[1] A. Illanes, *Enzyme biocatalysis: Principles and applications*, First edit. Springer, 2008.

[2] D. E. Koshland, “Application of a Theory of Enzyme Specificity to Protein Synthesis,” *Proc. Natl. Acad. Sci.*, vol. 44, no. 2, pp. 98–104, Feb. 1958.

[3] M. S. Yousef, S. A. Clark, P. K. Pruett, T. Somasundaram, W. R. Ellington, and M. S. Chapman, “Induced fit in guanidino kinases--comparison of substrate-free and transition state analog structures of arginine kinase,” *Protein Sci.*, vol. 12, no. 1, pp. 103–111, Jan. 2003.

[4] R. Eisenthal, M. E. Peterson, R. M. Daniel, and M. J. Danson, “The thermal behaviour of enzyme activity: implications for biotechnology,” *Trends Biotechnol.*, vol. 24, no. 7, pp. 289–292, Jul. 2006.

[5] V. G. H. Eijsink, A. Bjørk, S. Gåseidnes, R. Sirevåg, B. Synstad, B. van den Burg, and G. Vriend, “Rational engineering of enzyme stability,” *J. Biotechnol.*, vol. 113, no. 1–3, pp. 105–120, Sep. 2004.

[6] C. W. A. Liese, K. Seelbach, *Industrial Biotransformations*, Second edi. WILEY-VCH, 2006.

[7] A. N. Glaser and H. Nikaido, *Microbial biotechnology. Fundamentals of Applied Microbiology, Second Edition*. 2007.

[8] R. Singh, M. Kumar, A. Mittal, and P. K. Mehta, “Microbial enzymes: industrial progress in 21st century,” *3 Biotech*, vol. 6, no. 2, pp. 1–15, 2016.

[9] B. McNeil and L. M. Harvey, *Practical fermentation technology*, First edit. Strathclyde University, UK: John Wiley & Sons, Ltd, 2008.

[10] Howard Gest, “The Discovery of Microorganisms by Robert Hooke and Antoni van Leeuwenhoek, Fellows of the Royal Society on JSTOR,” *Notes Rec. R. Soc.*, vol. 58, no. 2, pp. 187–201, 2004.

[11] M. J. Schleiden, “Beiträge zur phytogenesis,” *Arch. für Anat. Physiol. und Wissenschaftliche Med.*, pp. 137–176, 1839.

[12] T. Schwann, *Mikroskopische Untersuchungen über die Uebereinstimmung in der Struktur und dem Wachsthum der Thiere und Pflanzen*, 1 auflage. Berlin: Sander, 1839.

[13] A. Payen, “Mémoire sur la diastase, les principaux produits de ses réactions et leurs applications aux arts industriels&quot;,” *J. Ann. Chem. Phys.*, pp. 73–93, 1833.

[14] L. Pasteur, “Suite à une précédente communication sur les mycodermes; Nouveau procéde industriel de fabrication du vinaigre,” *Compt. Rend.*, vol. 55, pp. 28–32, 1862.

[15] W. Kühne, “Über das Verhalten verschiedener organisirter und sog. ungeformter Fermente. Über das Trypsin (Enzym des Pankreas),” 1876.

[16] E. Buchner, “Alkoholische Gärung ohne Hefezellen,” *Berichte der Dtsch. Chem. Gesellschaft*, vol. 30, no. 1, pp. 1110–1113, Jan. 1897.

[17] L. Michaelis, M. Mand, and L. Menten, “Die Kinetik der Invertiiiwirkulig,” *Biochem. Z.*, vol. 49, pp. 333–369, 1913.

[18] James B. Sumner, “The isolation and crystallization of the enzyme urease,” *J. Biol. Chem.*, vol. 69, pp. 435–441, 1926.

[19] D. C. Phillips, “The Hen Egg-White Lysozyme Molecule,” *Proc. Natl. Acad. Sci. U. S. A.*, vol. 57, no. 3, pp. 483–495, 1967.

[20] J. D. Watson and F. H. Crick, “Molecular Structure of Nucleic Acids: A Structure for Deoxyribose Nucleic

Acid," *Nature*, vol. 171, no. 4356, pp. 737–738, Apr. 1953.

[21] G. W. Beadle and E. L. Tatum, "Genetic Control of Biochemical Reactions in Neurospora," *Proc. Natl. Acad. Sci.*, vol. 27, no. 11, pp. 499–506, Nov. 1941.

[22] S. N. Cohen, A. C. Y. Chang, H. W. Boyer, and R. B. Helling, "Construction of Biologically Functional Bacterial Plasmids In Vitro," *Proc. Natl. Acad. Sci.*, vol. 70, no. 11, pp. 3240–3244, Nov. 1973.

[23] B. D. Ensley, B. J. Ratzkin, T. D. Osslund, M. J. Simon, L. P. Wackett, and D. T. Gibson, "Expression of naphthalene oxidation genes in Escherichia coli results in the biosynthesis of indigo.," *Science*, vol. 222, no. 4620, pp. 167–9, Oct. 1983.

[24] "NOVOZYMES — Driven by research and scientists," *Nature*, vol. 409, no. 6817, pp. 268–268, Jan. 2001.

[25] V. Kumar, P. Sangwan, and D. Singh, "Global scenario of industrial enzyme market Hexavalent Chromium Phytotoxicity View project Biofortification of wheat for micronutrients through conventional and molecular approaches-Phase II View project," no. January 2016, 2014.

[26] J.-M. Choi, S.-S. Han, and H.-S. Kim, "Industrial applications of enzyme biocatalysis: Current status and future aspects.," *Biotechnol. Adv.*, vol. 33, no. 7, pp. 1443–54, 2015.

[27] BCC Research Staff, "Enzymes in Industrial Applications," *Code-BIO030K*, 2018. [Online]. Available: https://www.bccresearch.com/market-research/biotechnology/global-markets-for-enzymes-in-industrial-applications.html. [Accessed: 04-Jun-2019].

[28] "Report of the comission of enzymes of the international Union of Biochemistry," *J. Biol. Chem.*, vol. 237, pp. 979–980, 1962.

[29] A. T. Martínez, F. J. Ruiz-Dueñas, S. Camarero, A. Serrano, D. Linde, H. Lund, J. Vind, M. Tovborg, O. M. Herold-Majumdar, M. Hofrichter, C. Liers, R. Ullrich, K. Scheibner, G. Sannia, A. Piscitelli, C. Pezzella, M. E. Sener, S. Kılıç, W. J. H. van Berkel, V. Guallar, M. F. Lucas, R. Zuhse, R. Ludwig, F. Hollmann, E. Fernández-Fueyo, E. Record, C. B. Faulds, M. Tortajada, I. Winckelmann, J. A. Rasmussen, M. Gelo-Pujic, A. Gutiérrez, J. C. del Río, J. Rencoret, and M. Alcalde, "Oxidoreductases on their way to industrial biotransformations," *Biotechnol. Adv.*, vol. 35, no. 6, pp. 815–831, 2017.

[30] H. K. Chenault, E. S. Simon, and G. M. Whitesides, "Cofactor regeneration for enzyme- catalysed synthesis," *Biotechnology and Genetic Engineering Reviews*, vol. 6, no. 1. pp. 221–270, 1988.

[31] M. A. Noble, C. S. Miles, S. K. Chapman, D. A. Lysek, A. C. MacKay, G. A. Reid, R. P. Hanzlik, and A. W. Munro, "Roles of key active-site residues in flavocytochrome P450 BM3.," *Biochem. J.*, vol. 339 (Pt 2, pp. 371–379, 1999.

[32] R. Devaux-Basseguy, A. Bergel, and M. Comtat, "Potential applications of NAD(P)-dependent oxidoreductases in synthesis: A survey," *Enzyme Microb. Technol.*, vol. 20, no. 4, pp. 248–258, 1997.

[33] L. Sellés Vidal, C. L. Kelly, P. M. Mordaka, and J. T. Heap, "Review of NAD(P)H-dependent oxidoreductases: Properties, engineering and application," *Biochim. Biophys. Acta - Proteins Proteomics*, vol. 1866, no. 2, pp. 327–347, 2018.

[34] A. Weckbecker and W. Hummel, "Glucose Dehydrogenase for the Regeneration of NADPH and NADH," *Microb. Enzym. Biotransformations*, vol. 17, no. 8, pp. 225–238, 2005.

[35] B. Petschacher, N. Staunig, M. Müller, M. Schürmann, D. Mink, S. De Wildeman, K. Gruber, and A. Glieder, "Cofactor Specificity Engineering of Streptococcus Mutans Nadh Oxidase 2 for Nad(P) + Regeneration in Biocatalytic Oxidations," *Comput. Struct. Biotechnol. J.*, vol. 9, no. 14, 2014.

[36] D. E. Torres Pazmiño, M. Winkler, A. Glieder, and M. W. Fraaije, "Monooxygenases as biocatalysts: Classification, mechanistic aspects and biotechnological applications," *J. Biotechnol.*, vol. 146, no. 1–2, pp. 9–24, Mar. 2010.

[37] M. A. Wegman, M. H. A. Janssen, F. van Rantwijk, and R. A. Sheldon, “Towards Biocatalytic Synthesis of β-Lactam Antibiotics,” *Adv. Synth. Catal.*, vol. 343, no. 6–7, pp. 559–576, Aug. 2001.

[38] A. S. Bommarius and J. M. Broering, “Established and novel tools to investigate biocatalyst stability,” *Biocatal. Biotransformation*, vol. 23, no. 3–4, pp. 125–139, Jan. 2005.

[39] A. Illanes and Andrés, “Stability of biocatalysts,” *Electron. J. Biotechnol.*, vol. 2, no. 1, pp. 0–0, Apr. 1999.

[40] P. Kaul and Y. Asano, “Strategies for discovery and improvement of enzyme function: State of the art and opportunities,” *Microb. Biotechnol.*, vol. 5, no. 1, pp. 18–33, 2012.

[41] B. S. Nield, R. D. Willows, A. E. Torda, M. R. Gillings, A. J. Holmes, K. M. H. Nevalainen, H. W. Stokes, and B. C. Mabbutt, “New enzymes from environmental cassette arrays: functional attributes of a phosphotransferase and an RNA-methyltransferase.,” *Protein Sci.*, vol. 13, no. 6, pp. 1651–9, Jun. 2004.

[42] H. A. Bunzel, X. Garrabou, M. Pott, and D. Hilvert, “Speeding up enzyme discovery and engineering with ultrahigh-throughput methods,” *Curr. Opin. Struct. Biol.*, vol. 48, pp. 149–156, 2018.

[43] G. Yang and S. G. Withers, “Ultrahigh-Throughput FACS-Based Screening for Directed Enzyme Evolution,” *ChemBioChem*, vol. 10, no. 17, pp. 2704–2715, Nov. 2009.

[44] N. Varadarajan, J. R. Cantor, G. Georgiou, and B. L. Iverson, “Construction and flow cytometric screening of targeted enzyme libraries,” *Nat. Protoc.*, vol. 4, no. 6, pp. 893–901, Jun. 2009.

[45] S. Lim, B. Chen, M. S. Kariolis, I. K. Dimov, T. M. Baer, and J. R. Cochran, “Engineering High Affinity Protein–Protein Interactions Using a High-Throughput Microcapillary Array Platform,” *ACS Chem. Biol.*, vol. 12, no. 2, pp. 336–341, Feb. 2017.

[46] C. J. Ingham, A. Sprenkels, J. Bomer, D. Molenaar, A. van den Berg, J. E. T. van Hylckama Vlieg, and W. M. de Vos, “The micro-Petri dish, a million-well growth chip for the culture and high-throughput screening of microorganisms,” *Proc. Natl. Acad. Sci.*, vol. 104, no. 46, pp. 18217–18222, Nov. 2007.

[47] D. S. Tawfik and A. D. Griffiths, “Man-made cell-like compartments for molecular evolution,” *Nat. Biotechnol.*, vol. 16, no. 7, pp. 652–656, Jul. 1998.

[48] M. S. Packer and D. R. Liu, “Methods for the directed evolution of proteins.,” *Nat. Rev. Genet.*, vol. 16, no. 7, pp. 379–94, 2015.

[49] X. Li, Z. Zhang, and J. Song, “Computational enzyme design approaches with significant biological outcomes : progress and challenges,” *Comput. Struct. Biotechnol. J.*, vol. 2, no. 3, 2012.

[50] A. Muhammad Nazif, “Maximizing Stability in Industrial Enzymes: Rational Design Approach – A Review,” *Am. J. Chem. Eng.*, vol. 5, no. 6, p. 135, 2018.

[51] K. Steiner and H. Schwab, “Recent Advances in Rational Approaches for Enzyme Engineering,” *Comput. Struct. Biotechnol. J.*, vol. 2, no. 3, p. e201209010, 2012.

[52] O. Abian, V. Grazú, J. Hermoso, R. González, J. L. García, R. Fernández-Lafuente, and J. M. Guisán, “Stabilization of penicillin G acylase from Escherichia coli: site-directed mutagenesis of the protein surface to increase multipoint covalent attachment.,” *Appl. Environ. Microbiol.*, vol. 70, no. 2, pp. 1249–51, Feb. 2004.

[53] M. G. Roig and J. F. Kennedy, “Perspectives for Chemical Modifications of Enzymes,” *Crit. Rev. Biotechnol.*, vol. 12, no. 5–6, pp. 391–412, Jan. 1992.

[54] D. Mislovičová, J. Masárová, M. Bučko, and P. Gemeiner, “Stability of penicillin G acylase modified with various polysaccharides,” *Enzyme Microb. Technol.*, vol. 39, no. 4, pp. 579–585, Aug. 2006.

[55] L. Cao, L. van Langen, and R. A. Sheldon, “Immobilised enzymes: carrier-bound or carrier-free?,” *Curr.*

Opin. Biotechnol., vol. 14, no. 4, pp. 387–394, Aug. 2003.

[56] C. Mateo, J. M. Palomo, L. M. van Langen, F. van Rantwijk, and R. A. Sheldon, “A new, mild cross-linking methodology to prepare cross-linked enzyme aggregates,” *Biotechnol. Bioeng.*, vol. 86, no. 3, pp. 273–276, May 2004.

[57] D. Häring and P. Schreier, “Cross-linked enzyme crystals,” *Curr. Opin. Chem. Biol.*, vol. 3, no. 1, pp. 35–38, Feb. 1999.

[58] J. J. Roy and T. E. Abraham, “Preparation and characterization of cross-linked enzyme crystals of laccase,” *J. Mol. Catal. B Enzym.*, vol. 38, no. 1, pp. 31–36, Jan. 2006.

[59] A. Manuscript, “Use of chemical auxiliaries to control P450 enzymes for predictable oxidations at unactivated C-H bonds of substrates,” pp. 209–228, 2016.

[60] W. Tischer and F. Wedekind, “Immobilized Enzymes: Methods and Applications,” *Top. Curr. Chem.*, vol. 200, pp. 95–126, 1999.

[61] J. M. Walker and S. E. E. Ditor, “Immobilization of enzymes and cells [electronic resource],” *Food Microbiol.*, 2006.

[62] L. Cao, *Carrier-bound Immobilized Enzymes: Principles, Application and Design*, First edit. John Wiley & Sons, Ltd, 2006.

[63] R. H. Ringborg and J. M. Woodley, “The application of reaction engineering to biocatalysis,” *React. Chem. Eng.*, vol. 1, no. 1, pp. 10–22, 2016.

[64] M. T. Lundemo, *Bioprocess Engineering for the Application of P450s Bioprocess Engineering for the Application of P450s*. 2015.

[65] J. M. Nelson and E. G. Griffin, “Adsorption of invertase,” *J. Am. Chem. Soc.*, vol. 38, no. 5, pp. 1109–1115, May 1916.

[66] T. Godfrey and S. West, *Industrial enzymology*, 2nd ed. London: Stockton Press, 1996.

[67] J. M. Bolivar, L. Wilson, S. A. Ferrarotti, J. M. Guisan, R. Fern??ndez-Lafuente, and C. Mateo, “Improvement of the stability of alcohol dehydrogenase by covalent immobilization on glyoxyl-agarose,” *J. Biotechnol.*, vol. 125, no. 1, pp. 85–94, 2006.

[68] C. Mateo, J. M. Palomo, G. Fernandez-Lorente, J. M. Guisan, and R. Fernandez-Lafuente, “Improvement of enzyme activity, stability and selectivity via immobilization techniques,” *Enzyme Microb. Technol.*, vol. 40, no. 6, pp. 1451–1463, 2007.

[69] W. Neto, M. Schürmann, L. Panella, A. Vogel, and J. M. Woodley, “Immobilisation of omega-transaminase for industrial application: Screening and characterisation of commercial ready to use enzyme carriers,” *J. Mol. Catal. B Enzym.*, vol. 117, pp. 54–61, 2015.

[70] M. Persson, L. Bülow, and K. Mosbach, “Purification and site-specific immobilization of genetically engineered glucose dehydrogenase on thiopropyl-sepharose,” *FEBS Lett.*, vol. 270, no. 1–2, pp. 41–44, 1990.

[71] M. T. Lundemo and J. M. Woodley, “Guidelines for development and implementation of biocatalytic P450 processes,” *Appl. Microbiol. Biotechnol.*, vol. 99, no. 6, pp. 2465–2483, 2015.

[72] A. T. Pedersen, T. M. Carvalho, E. Sutherland, G. Rehn, R. Ashe, and J. M. Woodley, “Characterization of a continuous agitated cell reactor for oxygen dependent biocatalysis,” *Biotechnol. Bioeng.*, vol. 114, no. 6, pp. 1222–1230, 2017.

[73] R. Nicoli, M. Bartolini, S. Rudaz, V. Andrisano, and J. L. Veuthey, “Development of immobilized enzyme reactors based on human recombinant cytochrome P450 enzymes for phase I drug metabolism

studies," *J. Chromatogr. A*, vol. 1206, no. 1, pp. 2–10, 2008.

[74] M. Cárdenas-Fernández, C. López, G. Á lvaro, and J. López-Santín, "Immobilized L-aspartate ammoniα-lyase from Bacillus sp. YM55-1 as biocatalyst for highly concentrated L-aspartate synthesis," *Bioprocess Biosyst. Eng.*, vol. 35, no. 8, pp. 1437–1444, 2012.

[75] M. Cárdenas-Fernández, C. López, G. Álvaro, and J. López-Santín, "L-Phenylalanine synthesis catalyzed by immobilized aspartate aminotransferase," *Biochem. Eng. J.*, vol. 63, pp. 15–21, 2012.

[76] R. A. Sheldon and S. van Pelt, "Enzyme immobilisation in biocatalysis: why, what and how," *Chem. Soc. Rev.*, vol. 42, pp. 6223–6235, 2013.

[77] U. Guzik and K. Hupert-kocurek, "Immobilization as a Strategy for Improving Enzyme Properties-Application to Oxidoreductases," pp. 8995–9018, 2014.

[78] O. Barbosa, R. Torres, C. Ortiz, Á. Berenguer-Murcia, R. C. Rodrigues, and R. Fernandez-Lafuente, "Heterofunctional supports in enzyme immobilization: From traditional immobilization protocols to opportunities in tuning enzyme properties," *Biomacromolecules*, vol. 14, no. 8, pp. 2433–2462, 2013.

[79] J. C. S. D. Santos, O. Barbosa, C. Ortiz, A. Berenguer-Murcia, R. C. Rodrigues, and R. Fernandez-Lafuente, "Importance of the Support Properties for Immobilization or Purification of Enzymes," *ChemCatChem*, vol. 7, no. 16, pp. 2413–2432, 2015.

[80] S. Datta and L. R. Christena, "Enzyme immobilization : an overview on techniques and support materials," *3 Biotech*, vol. 3, pp. 1–9, 2013.

[81] R. A. Sheldon and J. M. Woodley, "Role of Biocatalysis in Sustainable Chemistry," *Chem. Rev.*, vol. 118, no. 2, pp. 801–838, 2018.

[82] R. A. Sheldon and P. C. Pereira, "Biocatalysis engineering: the big picture," *Chem. Soc. Rev.*, vol. 46, no. 10, pp. 2678–2691, 2017.

[83] C. Ratledge and B. Kristiansen, *Basic biotechnology*, Third. Cambridge: Cambridge university press, 2006.

[84] R. Kratzer, J. M. Woodley, and B. Nidetzky, "Rules for biocatalyst and reaction engineering to implement effective , NAD (P) H-dependent , whole cell bioreductions," *Biotechnol. Adv.*, vol. 33, no. 8, pp. 1641–1652, 2015.

[85] E. Seibert and T. S. Tracy, "Different Enzyme Kinetic Models," in *Methods in molecular biology (Clifton, N.J.)*, vol. 1113, 2014, pp. 23–35.

[86] J. Brummund, M. Müller, T. Schmitges, I. Kaluzna, D. Mink, L. Hilterhaus, and A. Liese, "Process development for oxidations of hydrophobic compounds applying cytochrome P450 monooxygenases in-vitro," *J. Biotechnol.*, vol. 233, pp. 143–150, 2016.

[87] J. S. Alford, "Bioprocess control: Advances and challenges," *Comput. Chem. Eng.*, vol. 30, no. 10–12, pp. 1464–1475, 2006.

[88] G. D. Najafpour and G. D. Najafpour, "Downstream Processing," *Biochem. Eng. Biotechnol.*, pp. 170–198, Jan. 2007.

[89] J. Conner, D. Wuchterl, M. Lopez, B. Minshall, R. Prusti, D. Boclair, J. Peterson, and C. Allen, "The Biomanufacturing of Biotechnology Products," *Biotechnol. Entrep.*, pp. 351–385, Jan. 2014.

[90] K. Schmölzer, K. Mädje, B. Nidetzky, and R. Kratzer, "Bioprocess design guided by in situ substrate supply and product removal: Process intensification for synthesis of (S)-1-(2-chlorophenyl)ethanol," *Bioresour. Technol.*, vol. 108, no. C, p. 216, Mar. 2012.

[91] J. Nielsen, J. Villadsen, and G. Lidén, "Scale-up of bioprocesses," in *Bioreaction Engineering Principles*,

Boston, MA: Springer US, 2003, pp. 477–518.

[92] J. Xia, G. Wang, J. Lin, Y. Wang, J. Chu, Y. Zhuang, and S. Zhang, “Advances and Practices of Bioprocess Scale-up,” in *Advances in biochemical engineering/biotechnology*, vol. 152, 2015, pp. 137–151.

[93] J. Brummund, T. Sonke, and M. Müller, “Process Development for Biocatalytic Oxidations Applying Alcohol Dehydrogenases,” *Org. Process Res. Dev.*, vol. 19, no. 11, pp. 1590–1595, 2015.

[94] T. Pongtharangkul, P. Chuekitkumchorn, N. Suwanampa, P. Payongsri, K. Honda, and W. Panbangred, “Kinetic properties and stability of glucose dehydrogenase from Bacillus amyloliquefaciens SB5 and its potential for cofactor regeneration,” *AMB Express*, vol. 5, no. 1, pp. 1–12, 2015.

[95] Y. Lu and L. Mei, “Co-expression of P450 BM3 and glucose dehydrogenase by recombinant Escherichia coli and its application in an NADPH-dependent indigo production system,” *J. Ind. Microbiol. Biotechnol.*, vol. 34, no. 3, pp. 247–253, 2007.

[96] H. N. Kirkman and G. F. Gaetani, “Catalase: a tetrameric enzyme with four tightly bound molecules of NADPH.,” *Proc. Natl. Acad. Sci. U. S. A.*, vol. 81, no. July, pp. 4343–4347, 1984.

[97] E. Romero, J. Ø. Rub, A. Mattevi, and M. W. Fraaije, “Characterization and Crystal Structure of a Robust Cyclohexanone Monooxygenase,” *Angew. Chemie - Int. Ed.*, vol. 55, pp. 15852–15855, 2016.

[98] C. J. C. Whitehouse, S. G. Bell, and L.-L. Wong, “P450 $_{\text{BM3}}$ (CYP102A1): connecting the dots,” *Chem. Soc. Rev.*, vol. 41, no. 3, pp. 1218–1260, 2012.

[99] A. W. Munro, D. G. Leys, K. J. Mclean, K. R. Marshall, T. W. B. Ost, S. Daff, C. S. Miles, S. K. Chapman, D. A. Lysek, C. C. Moser, C. C. Page, L. Dutton, D. G. Leys, K. R. Marshall, C. S. Miles, S. K. Chapman, C. C. Page, and L. Dutton, “P450 BM3 : the very model of a modern flavocytochrome,” vol. 27, no. 5, pp. 250–257, 2002.

[100] A. J. Warman, O. Roitel, R. Neeli, H. M. Girvan, H. E. Seward, S. A. Murray, K. J. McLean, M. G. Joyce, H. Toogood, R. A. Holt, D. Leys, N. S. Scrutton, and A. W. Munro, “Flavocytochrome P450 BM3: an update on structure and mechanism of a biotechnologically important enzyme,” *Biochem. Soc. Trans.*, vol. 33, no. 4, pp. 747–753, 2005.

[101] M. Wada, A. Yoshizumi, Y. Noda, S. Shimizu, H. Takagi, M. Kataoka, and S. Nakamori, “Production of a Doubly Chiral Compound , by Two-Step Enzymatic Asymmetric Reduction Production of a Doubly Chiral Compound , Enzymatic Asymmetric Reduction,” vol. 69, no. 2, pp. 933–937, 2003.

[102] K. R. Kim and D. K. Oh, “Production of hydroxy fatty acids by microbial fatty acid-hydroxylation enzymes,” *Biotechnology Advances*, vol. 31, no. 8. pp. 1473–1485, 2013.

[103] L. A. Lucia, “Lignocellulosic biomass: a potential feedstock to replace petroleum,” *BioResources*, vol. 3 (4), pp. 981–982, 2008.

[104] C. Aranda, M. Municoy, V. Guallar, J. Kiebist, K. Scheibner, R. Ullrich, J. C. Del Río, M. Hofrichter, A. T. Martínez, and A. Gutiérrez, “Selective synthesis of 4-hydroxyisophorone and 4-ketoisophorone by fungal peroxygenases,” *Catal. Sci. Technol.*, vol. 9, no. 6, pp. 1398–1405, 2019.

[105] Y. Mdcami, Y. Fukunaga, M. Arita, Y. Obi, and T. Kisaki, “Preparation of aroma compounds by microbial transformation of isophorone with aspergillus niger,” *Agric. Biol. Chem.*, vol. 45, no. 3, pp. 791–793, 1981.

[106] O. Isler and P. Zeller, “Total Syntheses of Carotenoids,” *Vitam. Horm.*, vol. 15, pp. 31–71, Jan. 1957.

[107] W. Bonrath and T. Netscher, “Catalytic processes in vitamins synthesis and production,” *Appl. Catal. A Gen.*, vol. 280, no. 1, pp. 55–73, Feb. 2005.

[108] R. Bort, X. Ponsoda, R. Jover, M. J. Gomez-Lechon, and J. V Castell, “Diclofenac Toxicity to Hepatocytes: A Role for Drug Metabolism in Cell Toxicity,” *J. Pharmacol. Exp. Ther.*, vol. 288, no. 1, pp. 65–72, 1998.

[109] H. Bouju, P. Nastold, B. Beck, J. Hollender, P. F. X. Corvini, and T. Wintgens, “Elucidation of biotransformation of diclofenac and 4’hydroxydiclofenac during biological wastewater treatment,” *J. Hazard. Mater.*, vol. 301, pp. 443–452, 2016.

[110] M. C. Damsten, B. M. A. van Vugt-Lussenburg, T. Zeldenthuis, J. S. B. de Vlieger, J. N. M. Commandeur, and N. P. E. Vermeulen, “Application of drug metabolising mutants of cytochrome P450 BM3 (CYP102A1) as biocatalysts for the generation of reactive metabolites,” *Chem. Biol. Interact.*, vol. 171, no. 1, pp. 96–107, 2008.

[111] M. W. den Braver, S. P. den Braver-Sewradj, N. P. E. Vermeulen, and J. N. M. Commandeur, “Characterization of cytochrome P450 isoforms involved in sequential two-step bioactivation of diclofenac to reactive p-benzoquinone imines,” *Toxicol. Lett.*, vol. 253, pp. 46–54, 2016.

[112] M. A. F. Delgove, D. Valencia, J. Solé, K. V Bernaerts, S. M. A. De Wildeman, M. Guillén, and G. Álvaro, “High performing immobilized Baeyer-Villiger monooxygenase and glucose dehydrogenase for the synthesis of ε -caprolactone derivative,” *Appl. Catal. A, Gen.*, vol. 572, no. October 2018, pp. 134–141, 2019.

[113] I. Kaluzna, T. Schmitges, H. Straatman, D. Van Tegelen, M. Müller, M. Schürmann, and D. Mink, “Enabling Selective and Sustainable P450 Oxygenation Technology. Production of 4-Hydroxy-??-isophorone on Kilogram Scale,” *Org. Process Res. Dev.*, vol. 20, no. 4, pp. 814–819, 2016.

[114] M. A. F. Delgove, J. Luchies, I. Wauters, G. G. P. Deroover, S. M. A. De Wildeman, and K. V Bernaerts, “Increasing the solubility range of polyesters by tuning their microstructure with comonomers †,” *Polym. Chem.*, vol. 8, pp. 4696–4706, 2017.

[115] I. Axarli, A. Prigipaki, and N. E. Labrou, “Engineering the substrate specificity of cytochrome P450 CYP102A2 by directed evolution: Production of an efficient enzyme for bioconversion of fine chemicals,” *Biomol. Eng.*, vol. 22, no. 1–3, pp. 81–88, 2005.

[116] L. Sundberg and J. Porath, “Preparation of adsorbents for biospecific affinity chromatography. I. Attachment of group-containing ligands to insoluble polymers by means of bifunctional oxiranes,” *J. Chromatogr. A*, vol. 90, no. 1, pp. 87–98, Mar. 1974.

[117] N. G. Munishwar, *Methods for Affinity Based Separations for Enzymes and Proteins*. Birkhäuser, 2002.

[118] M. M. Bradford, “A rapid and sensitive method for the quantitation of microgram quantities of protein utilizing the principle of protein-dye binding,” *Anal. Biochem.*, vol. 72, no. 1–2, pp. 248–254, 1976.

[119] U. K. Laemmli, “Cleavage of structural proteins during the assembly of the head of bacteriophage T4,” *Nature*, vol. 227, no. 5259, pp. 680–685, 1970.

[120] R. Omura, Tsuneo; Sato, “The Carbon Monoxide-biding pigment of Liver Microsomes,” *J. Biol. Chem.*, vol. 239, no. 7, pp. 2370–2378, 1964.

[121] F. P. Guengerich, M. V Martin, C. D. Sohl, and Q. Cheng, “Measurement of cytochrome P450 and NADPH – cytochrome P450 reductase,” vol. 4, no. 9, pp. 1245–1252, 2009.

[122] D. Valencia, M. Guillén, J. L. J. Fürst, J. López-santín, and G. Álvaro, “An immobilized and highly stabilized self-sufficient monooxygenase as biocatalyst for oxidative biotransformations,” *J. Chem. Technol. Biotechnol.*, vol. 93, no. 4, pp. 985–993, 2017.

[123] M. A. F. Delgove, M. T. Elford, K. V Bernaerts, and S. M. A. De Wildeman, “Toward Upscaled Biocatalytic Preparation of Lactone Building Blocks for Polymer Applications,” *Org. Process Res. Dev.*, vol. 22, no. 7, pp. 803–812, 2018.

[124] V. B. Urlacher and M. Girhard, “Cytochrome P450 monooxygenases: An update on perspectives for synthetic application,” *Trends Biotechnol.*, vol. 30, no. 1, pp. 26–36, 2012.

[125] F. P. Guengerich, “Common and Uncommon Cytochrome P450 Reactions Related to Metabolism and

Chemical Toxicity," *Chem. Res. Toxicol.*, vol. 14, no. 6, pp. 611–650, 2001.

[126] L. O. Narhi and A. J. Fulco, "Characterization of a catalytically self-sufficient 119,000-dalton cytochrome P-450 monooxygenase induced by barbiturates in Bacillus megaterium," *J. Biol. Chem.*, vol. 261, no. 16, pp. 7160–7169, 1986.

[127] R. Bernhardt and V. B. Urlacher, "Cytochromes P450 as promising catalysts for biotechnological application: Chances and limitations," *Appl. Microbiol. Biotechnol.*, vol. 98, no. 14, pp. 6185–6203, 2014.

[128] C. J. Paddon, P. J. Westfall, D. J. Pitera, K. Benjamin, K. Fisher, D. McPhee, M. D. Leavell, A. Tai, A. Main, D. Eng, D. R. Polichuk, K. H. Teoh, D. W. Reed, T. Treynor, J. Lenihan, H. Jiang, M. Fleck, S. Bajad, G. Dang, D. Dengrove, D. Diola, G. Dorin, K. W. Ellens, S. Fickes, J. Galazzo, S. P. Gaucher, T. Geistlinger, R. Henry, M. Hepp, T. Horning, T. Iqbal, L. Kizer, B. Lieu, D. Melis, N. Moss, R. Regentin, S. Secrest, H. Tsuruta, R. Vazquez, L. F. Westblade, L. Xu, M. Yu, Y. Zhang, L. Zhao, J. Lievense, P. S. Covello, J. D. Keasling, K. K. Reiling, N. S. Renninger, and J. D. Newman, "High-level semi-synthetic production of the potent antimalarial artemisinin," *Nature*, vol. 496, no. 7446, pp. 528–532, 2013.

[129] R. DiCosimo, J. McAuliffe, A. J. Poulose, and G. Bohlmann, "Industrial use of immobilized enzymes," *Chem. Soc. Rev.*, vol. 42, no. 15, p. 6437, 2013.

[130] S. C. Maurer, H. Schulze, R. D. Schmid, and V. Urlacher, "Immobilisation of P450BM-3 and an NADP(+) cofactor recycling system: Towards a technical application of heme-containing monooxygenases in fine chemical synthesis," *Adv. Synth. Catal.*, vol. 345, no. 6–7, pp. 802–810, 2003.

[131] E. Weber, D. Sirim, T. Schreiber, B. Thomas, J. Pleiss, M. Hunger, R. Gläser, and V. B. Urlacher, "Immobilization of P450 BM-3 monooxygenase on mesoporous molecular sieves with different pore diameters," *J. Mol. Catal. B Enzym.*, vol. 64, no. 1–2, pp. 29–37, 2010.

[132] L. Zhao, G. Güven, Y. Li, and U. Schwaneberg, "First steps towards a Zn/Co(III)sep-driven P450 BM3 reactor," *Appl. Microbiol. Biotechnol.*, vol. 91, no. 4, pp. 989–999, 2011.

[133] J. H. Lee, D. H. Nam, S. H. Lee, J. H. Park, S. J. Park, S. H. Lee, C. B. Park, and K. J. Jeong, "New platform for cytochrome P450 reaction combining in situ immobilization on biopolymer," *Bioconjug. Chem.*, vol. 25, no. 12, pp. 2101–2104, 2014.

[134] S. Zernia, F. Ott, K. Bellmann-Sickert, R. Frank, M. Klenner, H.-G. Jahnke, A. Prager, B. Abel, A. Robitzki, and A. G. Beck-Sickinger, "Peptide-Mediated Specific Immobilization of Catalytically Active Cytochrome P450 BM3 Variant.," *Bioconjug. Chem.*, vol. 27, no. 4, pp. 1090–7, 2016.

[135] C. Y. Tan, H. Hirakawa, R. Suzuki, T. Haga, and F. Iwata, "Immobilization of a Bacterial Cytochrome P450 Monooxygenase System on a Solid Support," pp. 1–6, 2016.

[136] V. E. V Ferrero, L. Andolfi, G. Di Nardo, S. J. Sadeghi, A. Fantuzzi, S. Cannistraro, and G. Gilardi, "Protein and electrode engineering for the covalent immobilization of P450 BMP on gold," *Anal. Chem.*, vol. 80, no. 22, pp. 8438–8446, 2008.

[137] R. Neeli, O. Roitel, N. S. Scrutton, and A. W. Munro, "Switching pyridine nucleotide specificity in P450 BM3: Mechanistic analysis of the W1046H and W1046A enzymes," *J. Biol. Chem.*, vol. 280, no. 18, pp. 17634–17644, 2005.

[138] P. C. Cirino and F. H. Arnold, "A self-sufficient peroxide-driven hydroxylation biocatalyst," *Angew. Chemie - Int. Ed.*, vol. 42, no. 28, pp. 3299–3301, 2003.

[139] A. Vidal-Limón, S. Águila, M. Ayala, C. V. Batista, and R. Vazquez-Duhalt, "Peroxidase activity stabilization of cytochrome P450BM3 by rational analysis of intramolecular electron transfer," *J. Inorg. Biochem.*, vol. 122, pp. 18–26, 2013.

[140] S. J. Sadeghi, A. Fantuzzi, and G. Gilardi, "Breakthrough in P450 bioelectrochemistry and future perspectives," *Biochim. Biophys. Acta - Proteins Proteomics*, vol. 1814, no. 1, pp. 237–248, 2011.

[141] D. Holtmann, K. M. Mangold, and J. Schrader, “Entrapment of cytochrome P450 BM-3 in polypyrrole for electrochemically- driven biocatalysis,” *Biotechnol. Lett.*, vol. 31, no. 5, pp. 765–770, 2009.

[142] N. Sugihara, Y. Ogoma, K. Abe, Y. Kondo, and T. Akaike, “Immobilization of cytochrome P-450 and electrochemical control of its activity,” *Polym. Adv. Technol.*, vol. 9, no. 5, pp. 307–313, 1998.

[143] B. Munge, C. Estavillo, J. B. Schenkman, and J. F. Rusling, “Optimization of electrochemical and peroxide-driven oxidation of styrene with ultrathin polyion films containing cytochrome p450cam and myoglobin,” *ChemBioChem*, vol. 4, no. 1, pp. 82–89, 2003.

[144] F. Hollmann, K. Hofstetter, and A. Schmid, “Non-enzymatic regeneration of nicotinamide and flavin cofactors for monooxygenase catalysis,” *Trends Biotechnol.*, vol. 24, no. 4, pp. 163–171, 2006.

[145] W. Liu and P. Wang, “Cofactor regeneration for sustainable enzymatic biosynthesis,” *Biotechnol. Adv.*, vol. 25, no. 4, pp. 369–384, 2007.

[146] H. Schewe, B. A. Kaup, and J. Schrader, “Improvement of P450BM-3 whole-cell biocatalysis by integrating heterologous cofactor regeneration combining glucose facilitator and dehydrogenase in E. coli,” *Appl. Microbiol. Biotechnol.*, vol. 78, no. 1, pp. 55–65, 2008.

[147] N. Beyer, J. K. Kulig, A. Bartsch, M. A. Hayes, D. B. Janssen, and M. W. Fraaije, “P450 BM3 fused to phosphite dehydrogenase allows phosphite-driven selective oxidations,” *Appl. Microbiol. Biotechnol.*, 2016.

[148] L. D. Smith, N. Budgen, S. J. Bungard, M. J. Danson, and D. W. Hough, “Purification and characterization of glucose dehydrogenase from the thermoacidophilic archaebacterium *Thermoplasma acidophilum*.,” *Biochem. J.*, vol. 261, no. 3, pp. 973–7, 1989.

[149] P. K. Srivastava and S. Singh, “Immobilization and Applications of Glucose-6-Phosphate Dehydrogenase: a Review,” *Prep. Biochem. Biotechnol.*, vol. 43, no. 4, pp. 376–384, 2013.

[150] G. Alvaro, R. Fernandez-Lafuente, R. M. Blanco, and J. M. Guisán, “Immobilization-stabilization of Penicillin G acylase from Escherichia coli,” *Applied Biochemistry and Biotechnology*, vol. 26, no. 2. Applied Microbiology and Biotechnology, pp. 181–195, 1990.

[151] E. Katchalski-Katzir and D. M. Kraemer, “Eupergit® C, a carrier for immobilization of enzymes of industrial potential,” *J. Mol. Catal. - B Enzym.*, vol. 10, no. 1–3, pp. 157–176, 2000.

[152] C. Mateo, J. M. Palomo, M. Fuentes, L. Betancor, V. Grazu, F. Lopez-Gallego, B. C. C. Pessela, A. Hidalgo, G. Fernendez-Lorente, R. Fernandez-Lafuente, and J. M. Guisan, “Glyoxyl agarose: A fully inert and hydrophilic support for immobilization and high stabilization of proteins,” *Enzyme Microb. Technol.*, vol. 39, no. 2, pp. 274–280, 2006.

[153] M. A. Goheer, B. J. Gould, and D. V Parke, “Preparation of immobilized baker’s-yeast glucose 6-phosphate dehydrogenase attached to modified sepharose and sephadex and a comparison of the properties of these preparations with those of the soluble enzyme,” *Biochem. J.*, vol. 157, no. 2, pp. 289–294, 2015.

[154] M. Persson, L. Bülow, and K. Mosbach, “Purification and site-specific immobilization of genetically engineered glucose dehydrogenase on thiopropyl-sepharose,” *FEBS Lett.*, vol. 270, no. 1–2, pp. 41–44, 1990.

[155] I. I. Karuzina and A. I. Archakov, “The oxidative inactivation of cytochrome P450 in monooxygenase reactions,” *Free Radic. Biol. Med.*, vol. 16, no. 1, pp. 73–97, 1994.

[156] T. Petrovičová, K. Markošová, Z. Hegyi, I. Smonou, M. Rosenberg, and M. Rebroš, “Co-Immobilization of Ketoreductase and Glucose Dehydrogenase,” *Catalysts*, vol. 8, no. 4, p. 168, 2018.

[157] V. B. Urlacher and M. Girhard, “Cytochrome P450 monooxygenases: perspectives for synthetic application,” *Trends Biotechnol.*, vol. 24, no. 7, pp. 324–330, 2006.

[158] F. P. Guengerich, “Common and Uncommon Cytochrome P450 Reactions Related to Metabolism and Chemical Toxicity,” *Chem. Res. Toxicol.*, vol. 14, no. 6, pp. 611–650, 2001.

[159] M. M. E. Huijbers, S. Montersino, A. H. Westphal, D. Tischler, and W. J. H. Van Berkel, “Flavin dependent monooxygenases,” *Arch. Biochem. Biophys.*, vol. 544, pp. 2–17, 2014.

[160] D. Roccatano, “Structure, dynamics, and function of the monooxygenase P450 BM-3: Insights from computer simulations studies,” *J. Phys. Condens. Matter*, vol. 27, no. 27, p. 273102, 2015.

[161] A. Chefson and K. Auclair, “Progress towards the easier use of P450 enzymes,” pp. 462–469, 2006.

[162] I. I. Karuzina and A. I. Archakov, “Hydrogen peroxide-mediated inactivation of microsomal cytochrome P450 during monooxygenase reactions,” *Free Radic. Biol. Med.*, vol. 17, no. 6, pp. 557–567, 1994.

[163] E. NAGABABU and J. M. RIFKIND, “Heme degradation by reactive oxygen species,” *Antioxid. Redox Signal.*, vol. 6, no. 6, pp. 967–978, 2004.

[164] R. Neeli, H. M. Girvan, A. Lawrence, M. J. Warren, D. Leys, N. S. Scrutton, and A. W. Munro, “The dimeric form of flavocytochrome P450 BM3 is catalytically functional as a fatty acid hydroxylase,” vol. 579, pp. 5582–5588, 2005.

[165] A. P. Jamakhandi, B. C. Jeffus, V. R. Dass, and G. P. Miller, “Thermal inactivation of the reductase domain,” *Arch Biochem Biophys*, vol. 439, no. 2, pp. 165–174, 2013.

[166] G. Di Nardo and G. Gilardi, “Optimization of the bacterial cytochrome P450 BM3 system for the production of human drug metabolites,” *Int. J. Mol. Sci.*, vol. 13, no. 12, pp. 15901–15924, 2012.

[167] S. Dezvarei, J. H. Z. Lee, and S. G. Bell, “Stereoselective hydroxylation of isophorone by variants of the cytochromes P450 CYP102A1 and CYP101A1,” *Enzyme Microb. Technol.*, vol. 111, no. May 2017, pp. 29–37, 2018.

[168] D. Holtmann, M. W. Fraaije, I. W. C. E. Arends, J. Opperman, and F. Hollmann, “The taming of oxygen : biocatalytic oxyfunctionalisations,” *Chem. Commun.*, vol. 50, pp. 13180–13200, 2014.

[169] D. Holtmann and F. Hollmann, “The Oxygen Dilemma : A Severe Challenge for the Application of Monooxygenases ?,” pp. 1391–1398, 2016.

[170] A. Ozcan and M. Ogun, “Biochemistry of Reactive Oxygen and Nitrogen Species,” *Basic Princ. Clin. Significance Oxidative Stress*, pp. 37–58, 2015.

[171] W. H. Schaefer, T. M. Harris, and F. P. Guengerich, “Characterization of the enzymatic and nonenzymatic peroxidative degradation of iron porphyrins and cytochrome P-450 heme.,” *Biochemistry*, vol. 24, pp. 3254–3263, 1985.

[172] I. Kaluzna, J. Brummund, and M. Schuerman, “Production of diclofenac metabolites by applying cytochrome P450 technology,” *Chim. oggi- Chem. Today*, vol. 35, no. 6, 2017.

[173] J. C. Serrano-Ruiz, R. Luque, and A. Sepúlveda-Escribano, “Transformations of biomass-derived platform molecules: from high added-value chemicals to fuels via aqueous-phase processing,” *Chem. Soc. Rev.*, vol. 40, no. 11, p. 5266, Oct. 2011.

[174] A. Arevalo-Gallegos, Z. Ahmad, M. Asgher, R. Parra-Saldivar, and H. M. N. Iqbal, “Lignocellulose: A sustainable material to produce value-added products with a zero waste approach—A review,” *Int. J. Biol. Macromol.*, vol. 99, pp. 308–318, 2017.

[175] F. H. Isikgor and C. R. Becer, “Lignocellulosic biomass: a sustainable platform for the production of bio-based chemicals and polymers,” *Polym. Chem.*, vol. 6, pp. 4497–4559, 2015.

[176] F. Zia, K. M. Zia, M. Zuber, S. Kamal, and N. Aslam, “Starch based polyurethanes: A critical review updating recent literature,” *Carbohydr. Polym.*, vol. 134, pp. 784–798, Dec. 2015.

[177] J. Mao, X. Hu, H. Li, Y. Sun, C. Wang, and Z. Chen, "Iron chloride supported on pyridine-modified mesoporous silica: an efficient and reusable catalyst for the allylic oxidation of olefins with molecular oxygen," *Green Chem.*, vol. 10, no. 8, p. 827, Aug. 2008.

[178] S. Paganelli, F. Battois, M. Marchetti, R. Lazzaroni, R. Settambolo, and S. Rocchiccioli, "Rhodium catalyzed hydroformylation of β-isophorone: An unexpected result," *J. Mol. Catal. A Chem.*, vol. 246, no. 1–2, pp. 195–199, Mar. 2006.

[179] C. Beck, T. Mallat, and A. Baiker, "Oxidation–Isomerization of an Olefin to Allylic Alcohol Using Titania–Silica and a Base Co-catalyst," *J. Catal.*, vol. 195, no. 1, pp. 79–87, Oct. 2000.

[180] E. F. Murphy and A. Baiker, "Advances in homogeneous and heterogeneous catalytic aerobic oxidation of isophorone to ketoisophorone," *J. Mol. Catal. A Chem.*, vol. 179, no. 1–2, pp. 233–241, Feb. 2002.

[181] C. Wang, G. Wang, J. Mao, Z. Yao, and H. Li, "Metal and solvent-free oxidation of α-isophorone to ketoisophorone by molecular oxygen," *Catal. Commun.*, vol. 11, no. 8, pp. 758–762, Mar. 2010.

[182] W. Zhong, L. Mao, Q. Xu, Z. Fu, G. Zou, Y. Li, D. Yin, H. Luo, and S. R. Kirk, "Allylic oxidation of α-isophorone to keto-isophorone with molecular oxygen catalyzed by copper chloride in acetylacetone," *Appl. Catal. A Gen.*, vol. 486, pp. 193–200, Sep. 2014.

[183] "Autocondensation of acetone," U.S. Patent 3,497,558 A, 27-Dec-1965.

[184] M. Eggersdorfer, D. Laudert, U. Létinois, T. McClymont, J. Medlock, T. Netscher, and W. Bonrath, "One Hundred Years of Vitamins-A Success Story of the Natural Sciences," *Angew. Chemie Int. Ed.*, vol. 51, no. 52, pp. 12960–12990, Dec. 2012.

[185] M. Tavanti, F. Parmeggiani, J. R. G. Castellanos, A. Mattevi, and N. J. Turner, "One-Pot Biocatalytic Double Oxidation of α-Isophorone for the Synthesis of Ketoisophorone," *ChemCatChem*, vol. 9, no. 17, pp. 3338–3348, 2017.

[186] I. Kaluzna, A. De Vries, and D. Mink, "A sustainable P450 oxygenation technology for the selective synthesis of oxygenated intermediates and APIs," *Chim. Oggi-Chemistry Today*, vol. 33, no. 2, pp. 54–57, 2015.

[187] S. Soni, J. D. Desai, and S. Devi, "Immobilization of yeast alcohol dehydrogenase by entrapment and covalent binding to polymeric supports," *J. Appl. Polym. Sci.*, vol. 82, no. 5, pp. 1299–1305, 2001.

[188] M. Uygun, "Dye-attached cryogels for reversible alcohol dehydrogenase immobilization," *J. Chromatogr. B Anal. Technol. Biomed. Life Sci.*, vol. 959, pp. 42–48, 2014.

[189] S. B. Jadhav, S. B. Bankar, T. Granström, H. Ojamo, R. S. Singhal, and S. A. Survase, "Enhanced stability of alcohol dehydrogenase by non-covalent interaction with polysaccharides," *Appl. Microbiol. Biotechnol.*, vol. 98, no. 14, pp. 6307–6316, 2014.

[190] M. F. Alam, A. A. Laskar, M. Zubair, U. Baig, and H. Younus, "Immobilization of yeast alcohol dehydrogenase on polyaniline coated silver nanoparticles formed by green synthesis," *J. Mol. Catal. B Enzym.*, vol. 119, pp. 78–84, 2015.

[191] P. Zucca, R. Fernandez-Lafuente, and E. Sanjust, "Agarose and its derivatives as supports for enzyme immobilization," *Molecules*, vol. 21, no. 11, pp. 1–25, 2016.

[192] R. Fernandez-Lafuente, C. M. Rosell, V. Rodriguez, C. Santana, G. Soler, A. Bastida, and J. M. Guisán, "Preparation of activated supports containing low pK amino groups. A new tool for protein immobilization via the carboxyl coupling method," *Enzyme Microb. Technol.*, vol. 15, no. 7, pp. 546–550, 1993.

[193] J. Solé, G. Caminal, M. Schürmann, M. Guillén, and G. Alvaro, "Co-immobilization of P450 BM3 and glucose dehydrogenase on different supports for application as a self-sufficient oxidative biocatalyst," *J. Chem. Technol. Biotechnol.*, vol. 94, no. 1, pp. 244–255, 2018.

[194] T. Li and J. P. N. Rosazza, "Biocatalytic Synthesis of Vanillin," *Appl. Environ. Microbiol.*, vol. 66, no. 2, pp. 684–687, 2000.

[195] G.-J. ten Brink, I. W. C. E. Arends, and R. A. Sheldon, "The Baeyer−Villiger Reaction: New Developments toward Greener Procedures," *Chem. Rev.*, vol. 104, no. 9, pp. 4105–4124, 2004.

[196] F. Hollmann, I. W. C. E. Arends, K. Buehler, A. Schallmey, and B. Bühler, "Enzyme-mediated oxidations for the chemist," *Green Chem.*, vol. 13, no. 2, pp. 226–265, 2011.

[197] V. Alphand, G. Carrea, R. Wohlgemuth, R. Furstoss, and J. M. Woodley, "Towards large-scale synthetic applications of Baeyer-Villiger monooxygenases," *Trends Biotechnol.*, vol. 21, no. 7, pp. 318–323, 2003.

[198] C. V. F. Baldwin, R. Wohlgemuth, and J. M. Woodley, "The first 200-L scale asymmetric Baeyer-Villiger oxidation using a whole-cell biocatalyst," *Org. Process Res. Dev.*, vol. 12, no. 4, pp. 660–665, 2008.

[199] I. Hilker, R. Wohlgemuth, V. Alphand, and R. Furstoss, "Microbial transformations 59: First kilogram scale asymmetric microbial Baeyer-Villiger oxidation with optimized productivity using a resin-based in situ SFPR strategy," *Biotechnol. Bioeng.*, vol. 92, no. 6, pp. 702–710, 2005.

[200] H. Leisch, K. Morley, P. C. K. Lau, and P. Monooxygenase, "Baeyer À Villiger Monooxygenases : More Than Just Green Chemistry," *Chem. Rev.*, vol. 111, pp. 4165–4222, 2011.

[201] M. Bučko, P. Gemeiner, A. Schenkmayerová, T. Krajčovič, F. Rudroff, and M. D. Mihovilovič, "Baeyer-Villiger oxidations: biotechnological approach," *Appl. Microbiol. Biotechnol.*, vol. 100, no. 15, pp. 6585–6599, 2016.

[202] J. T. Wu, L. H. Wu, and J. A. Knight, "Stabilityof NADPH: Effectof VariousFactorson the Kineticsof Degradation," *Clin. Chem.*, vol. 32, no. 2, pp. 314–319, 1986.

[203] F. S. Aalbers and M. W. Fraaije, "Coupled reactions by coupled enzymes : alcohol to lactone cascade with alcohol dehydrogenase – cyclohexanone monooxygenase fusions," *Appl. Microbiol. Biotechnol.*, vol. 101, pp. 7557–7565, 2017.

[204] D. E. T. Pazmiæo, R. Snajdrova, B. Baas, M. Ghobrial, M. D. Mihovilovic, and M. W. Fraaije, "Self-Sufficient Baeyer – Villiger Monooxygenases : Effective Coenzyme Regeneration for Biooxygenation by Fusion Engineering **," *Angew. Chemie - Int. Ed.*, vol. 47, pp. 2275–2278, 2008.

[205] M. A. F. Delgove, M. T. Elford, K. V Bernaerts, and S. M. A. De, "Application of a thermostable Baeyer – Villiger monooxygenase for the synthesis of branched polyester precursors," *J. Chem. Technol. Biotechnol.*, vol. 93, no. 8, pp. 2131–2140, 2018.

[206] I. A. Zlochower and G. M. Green, "The limiting oxygen concentration and flammability limits of gases and gas mixtures," *J. Loss Prev. Process Ind.*, vol. 22, no. 4, pp. 499–505, 2009.

[207] A. Schmid, J. S. Dordick, B. Hauer, A. Kiener, M. Wubbolts, and B. Witholt, "Industrial biocatalysis today and tomorrow," *Nature*, vol. 409, no. January, pp. 258–268, 2001.

[208] B. M. Nestl, S. C. Hammer, B. A. Nebel, and B. Hauer, "New Generation of Biocatalysts for Organic Synthesis ** Angewandte," pp. 3070–3095, 2014.

[209] W. Leuchtenberger and K. Huthmacher, "Biotechnological production of amino acids and derivatives : current status and prospects," *Appl. Microbiol. Biotechnol.*, no. 69, pp. 1–8, 2005.

[210] Y. Chen and J. Nielsen, "Biobased organic acids production by metabolically engineered microorganisms," *Curr. Opin. Biotechnol.*, vol. 37, pp. 165–172, 2016.

[211] J. Becker, A. Lange, J. Fabarius, and C. Wittmann, "Top value platform chemicals: Bio-based production of organic acids," *Curr. Opin. Biotechnol.*, vol. 36, no. Figure 1, pp. 168–175, 2015.

[212] A. Baeyer and V. Villiger, "Einwirkung des Caro'schen Reagens auf Ketone," *Berichte der Dtsch. Chem.*

Gesellschaft, vol. 32, no. 3, pp. 3625–3633, Oct. 1899.

[213] M. M. Kayser, "'Designer reagents' recombinant microorganisms: new and powerful tools for organic synthesis," *Tetrahedron*, vol. 65, no. 5, pp. 947–974, Jan. 2009.

[214] R. H. Crabtree, *Handbook of Green Catalysis: Biocatalysis*. Wiley-VCH, 2009.

[215] M. Mihovilovic, F. Rudroff, and B. Grotzl, "Enantioselective Baeyer-Villiger Oxidations," *Curr. Org. Chem.*, vol. 8, no. 12, pp. 1057–1069, Aug. 2005.

[216] J. Fried, R. W. Thoma, and A. Klingsberg, "Oxidation of steroids by microörganisms. III. side chain degradation, ring d-cleavage and dehydrogenation in ring A," *J. Am. Chem. Soc.*, vol. 75, no. 22, pp. 5764–5765, Nov. 1953.

[217] K. Balke, M. Kadow, H. Mallin, S. Saß, and U. T. Bornscheuer, "Discovery , application and protein engineering of Baeyer – Villiger monooxygenases for organic synthesis," *Org. Biomol. Chem.*, no. 10, pp. 6249–6265, 2012.

[218] R. K. Singh, M. K. Tiwari, R. Singh, and J. Lee, "From Protein Engineering to Immobilization : Promising Strategies for the Upgrade of Industrial Enzymes," *Int. J. Mol. Sci.*, no. 14, pp. 1232–1277, 2013.

[219] M. Adamczak and S. H. Krishna, "Strategies for Improving Enzymes for Efficient Biocatalysis," *Food Technol. Biotechnol.*, vol. 42, no. 4, pp. 251–264, 2004.

[220] K. Balke, A. Beier, and U. T. Bornscheuer, "Hot spots for the protein engineering of Baeyer-Villiger monooxygenases," *Biotechnol. Adv.*, vol. 36, no. 1, pp. 247–263, Jan. 2018.

[221] K. Balke, B. Marcus, and U. T. Bornscheuer, "Controlling the Regioselectivity of Baeyer – Villiger Monooxygenases by Mutation of Active-Site Residues," *ChemBioChem*, no. 18, pp. 1627–1638, 2017.

[222] G. Li, M. Garcia-Borràs, M. J. L. J. Fürst, A. Ilie, M. W. Fraaije, K. N. Houk, and M. T. Reetz, "Overriding Traditional Electronic Effects in Biocatalytic Baeyer-Villiger Reactions by Directed Evolution," *J. Am. Chem. Soc.*, vol. 140, no. 33, pp. 10464–10472, Aug. 2018.

[223] J. T. Vicenzi, M. J. Zmijewski, M. R. Reinhard, B. E. Landen, W. L. Muth, and P. G. Marler, "Large-scale stereoselective enzymatic ketone reduction with in situ product removal via polymeric adsorbent resins," *Enzyme Microb. Technol.*, vol. 20, no. 7, pp. 494–499, May 1997.

[224] G. J. A. Conceição, P. J. S. Moran, and J. A. R. Rodrigues, "Highly efficient extractive biocatalysis in the asymmetric reduction of an acyclic enone by the yeast Pichia stipitis," *Tetrahedron Asymmetry*, vol. 14, no. 1, pp. 43–45, Jan. 2003.

[225] I. Hilker, M. C. Gutiérrez, R. Furstoss, J. Ward, R. Wohlgemuth, and V. Alphand, "Preparative scale Baeyer-Villiger biooxidation at high concentration using recombinant Escherichia coliand in situ substrate feeding and product removal process," *Nat. Protoc.*, vol. 3, no. 3, pp. 546–554, Mar. 2008.

[226] A. R. Haight, S. Z. Ariman, D. M. Barnes, N. J. Benz, F. X. Gueffier, R. F. Henry, M. C. Hsu, E. C. Lee, L. Morin, K. B. Pearl, M. J. Peterson, D. J. Plata, and D. R. Willcox, "Synthesis of the quinolone ABT-492: Crystallizations for optimal processing," *Org. Process Res. Dev.*, vol. 10, no. 4, pp. 751–756, 2006.

[227] R. C. Rodrigues, C. Ortiz, Á. Berenguer-Murcia, R. Torres, and R. Fernández-Lafuente, "Modifying enzyme activity and selectivity by immobilization," *Chem. Soc. Rev.*, vol. 42, no. 15, pp. 6290–6307, 2013.

[228] B. Brena, P. Gonzalez-Pombo, and F. Batista-Viera, "Immobilization of enzymes: A literature survey," *Immobil. Enzym. Cells Third Ed.*, vol. 1051, pp. 15–31, 2013.

[229] O. Abril, C. C. Ryerson, C. Walsh, and G. M. Whitesides, "Enzymatic Baeyer-Villiger type oxidations of ketones catalyzed by cyclohexanone oxygenase," *Bioorg. Chem.*, vol. 17, no. 1, pp. 41–52, Mar. 1989.